A Laser Doppler Anemometry Study of the Development of an Initially Turbulent Flow in a Horizontal Tube

by

Majed Samhan Mohammed

A Thesis Presented to the

FACULTY OF THE COLLEGE OF GRADUATE STUDIES

KING FAHD UNIVERSITY OF PETROLEUM & MINERALS

DHAHRAN, SAUDI ARABIA

In Partial Fulfillment of the
Requirements for the Degree of

MASTER OF SCIENCE

In

PHYSICS

July, 1991

Order Number 1354110

A Laser Doppler Anemometry study of the development of an initially turbulent flow in a horizontal tube

Mohammed, Majed Samhan, M.S.

King Fahd University of Petroleum and Minerals (Saudi Arabia), 1991

U·M·I
300 N. Zeeb Rd.
Ann Arbor, MI 48106

A LASER DOPPLER ANEMOMETRY STUDY OF THE DEVELOPMENT OF AN INITIALLY TURBULENT FLOW IN A HORIZONTAL TUBE

BY

Majed Samhan Mohammed

A Thesis Presented to the

FACULTY OF THE COLLEGE OF GRADUATE STUDIES

KING FAHD UNIVERSITY OF PETROLEUM & MINERALS

DHAHRAN, SAUDI ARABIA

In Partial Fulfillment of the

Requirements for the Degree of

MASTER OF SCIENCE

In

PHYSICS

July 1991

KING FAHD UNIVERSITY OF PETROLEUM & MINERALS

DHAHRAN, SAUDI ARABIA

COLLEGE OF GRADUATE STUDIES

This thesis, written by **MAJED SAMHAN MOHAMMED** under the direction of his Thesis Advisor, and approved by his Thesis Committee, has been presented to and accepted by the Dean of the College of Graduate Studies, in partial fulfillment of the requirements for the degree of **MASTER OF SCIENCE IN PHYSICS.**

Thesis Committee

Chairman (Professor U. K. A. KLEIN)

Member (Dr. F. F. AL-ADEL)

Member (Dr. M. A. HABIB)

Department Chairman

Dean, College of Graduate Studies

Date : 17 8 9

To My Beloved Parents

ACKNOWLEDGEMENT

Acknowledgement is due to King Fahd University of Petroleum and Minerals for support of this research.

In particular, I like to thank the Physics Department and the Laser Research Laboratory for making all their facilities available to me.

I would like to express my deep appreciation to my thesis advisor, Prof. Uwe K.A. Klein, (Laser Research Laboratory & Chemistry Department), for his patient guidance and his generous support for this research.

I would also like to express my gratefulness to other committee members, Dr. Fida F. Al-Adel, (Laser Research Laboratory & Physics Department), and Dr. Mohammed A. Habib, (Mechanical Engineering Department), for their valuable suggestions.

Special thanks are to Mr. Joe Mastermarino whose valuable assistance made the completion of this work possible, to my colleagues in Physics Department, Mr. Hassan El-Aoud, Mr. Hassane Darhmoui, Mr. Abdel-Aziz Al-Jalal, and Mr. Mohammed Redwan for their helpful remarks, and to Mr. Mohammed Daous, Mr. Yahya Garout, Mr. Adel Lafi, Nazzal Brothers and Mr. Yahya Zedan for their continuous encouragement

خلاصة الرسالة

العنوان : دراسة تطور تدفق مسبق الاضطراب في أنبوب أفقي بطريقة ليزر دوبلر لقياس السرعة

الاسم : ماجد سمحان محمد

التخصص : فيزياء

التاريخ : يوليو ١٩٩١م

لقد تم استخدام طريقة ليزر دوبلر لقياس السرعة في دراسة تطور تدفق مائي منتظم الاضطراب داخل أنبوب أفقي مستقيم بدون استعمال ناشرة عند المدخل .

أجُريت الدراسة لثلاثة ارقام رينولدز مختلفة في المدى الانسيابي والإنتقالي والمضطرب التدفق . في حالة رقم رينولدز المنخفض حدث إنتقال عكسي للتدفق من حالة الإضطراب إلى حالة التدفق الإنسيابي كامل التطور ، حيث لوحظ إقتراب منحنى تغير السرعة مع المسافة القطرية من القطع المكافئ المعروف بعد مسافة في حدود ٤٥ ضعفاً لقطر الأنبوب وبمعدل يقارب ضعف المعدل الذي تم تعيينه في دراسات سابقة تستخدم ناشرة عند المدخل . كما وجد أن شدة الأضطراب تقل أيضاً بسرعة اكبر .

لم يتم الحصول على منحنى سرعة كامل التطور للتدفق في حالة رقم رينولدز الإنتقالي بينما أمكن الحصول على منحنى سرعة يتبع القانون الأسي في حالة التدفق ذي رقم رينولدز العالي بعد مسافة في حدود ٣٠ قطراً داخل الأنبوب .

وقد أظهر تحليل توزع السرعة على طول محور الأنبوب سلوكاً غير متناظر مع تطور التدفق ، بينما لم يلاحظ أي توجه خاص لقيمة تفرطح توزع السرعة

درجة الماجستير في العلوم

جامعة الملك فهد للبترول و المعادن

الظهران – المملكة العربية السعودية

يوليو ١٩٩١

ABSTRACT

Title: **A LASER DOPPLER ANEMOMETRY STUDY OF THE DEVELOPMENT OF AN INITIALLY TURBULENT FLOW IN A HORIZONTAL TUBE**

By: **Majed Samhan Mohammed**

Major Field: **Physics**

Date: **July 1991**

Laser Doppler Anemometry was employed to study the development of an initially uniform turbulent flow of water in a horizontal straight tube without a diffuser at the inlet. The study was carried out for three different Reynolds numbers in the laminar, transitional and turbulent regimes. For low Reynolds number flow, relaminarization takes place. The velocity profile approaches the known parabolic profile within 45 tube diameters at about twice the rate reported for pipe systems with a diffuser at the inlet. Turbulence intensity is also found to decay more rapidly. No fully developed profile is observed for the transitional Reynolds number flow while, a power law profile is established for the higher Reynolds flow after an inlet length of about 30 tube diameters. Further analysis of centerline velocity distributions reveals an asymmetric behavior as the flow develops. No particular trend for the flatness is observed.

MASTER OF SCIENCE

KING FAHD UNIVERSITY OF PETROLEUM AND MINERALS
DHAHRAN, SAUDI ARABIA

July 1991

CONTENTS

LIST OF TABLES

LIST OF FIGURES

NOMENCLATURE

B	blockage factor, $1 - \frac{u_{av}}{u_c}$
D	tube diameter
g	gravitional acceleration
L	inlet length
N	reciprocal exponent in velocity power law, $\frac{u}{u_c} = (\frac{y}{R})^{1/N}$
r	radial distance from the axis
R	tube radius
Re	Reynolds number based on tube diameter, $\frac{u_{av} D}{\nu}$
u	time-mean axial velocity
u_c	centerline velocity
u_{av}	spatially averaged, time mean velocity, $\frac{2 \int u(r)\, r\, dr}{R^2}$
u'	velocity fluctuation in the axial direction
$<u'^2>$	time-mean velocity fluctuations
$<u'^2>_m$	maximum value of the time-mean velocity fluctuations
Δu_c	deviation of the experimentally determined centerline velocity from the value for fully developed flow
x	distance from the tube inlet
y	distance from the tube wall, R - r
θ	angle between the two crossing beams in LDA
λ	wave length of the laser beam

μ	dynamic vicosity
ν	kinemetic viscosity, $\nu = \frac{\mu}{\rho}$
ν_D	Doppler frequency
ρ	fluid density
σ	turbulence intensity, $\frac{\sqrt{<u'^2>}}{u}$
σ_{av}	spatially averaged turbulence intensity, $\frac{2 \int \sigma (r)\, r\, dr}{R^2}$

792c

CHAPTER I

INTRODUCTION

1.1 Objectives of This Study

The transition from laminar to turbulent flow has been investigated thoroughly in the past by many researchers, both theoretically and experimentally. In fact the term "transition" is frequently used by itself to refer to the process in which flow changes from laminar to turbulent state. However, in recent years there has been an increasing number of reported studies on "Inverse Transition", or " Relaminarization", i.e. the transition of the flow from turbulent to laminar state. These studies were largely motivated both by an interest in the basic principles behind this phenomenon and by the wide range of possible applications to real life flow systems.

The present study describes the results obtained using the Laser Doppler Anemometry technique for an initially turbulent flow undergoing relaminarization in a horizontal tube. The tube is immersed in a water channel to have a fully defined turbulent profile at the entrance. Velocity distributions and velocity profiles are obtained at different cross sections

along the tube for three distinct Reynolds numbers in the laminar, transitional and turbulent regimes, measurements are confined to Reynolds numbers up to 20,000.

Although there were some doubts put forward by other researchers concerning the possibility of achieving relaminarization of the flow in a straight tube without using a diffuser at the entrance, it was believed that at least for the case of the low Reynolds number flow a fully developed laminar profile is to be expected after some distance in the tube. Also a 1/6 turbulent profile was expected to be established after a shorter distance for the case of the higher Reynolds number. These "inlet lengths" are to be compared with those cited in literature.

Among our objectives also is the study of two additional statistical characteristics of the velocity distributions, namely the third moment -Skewness-, a measure for the asymmetry of a distribution, and the fourth moment - Kurtosis -, a measure for the flattness of a distribution, and to test wether there exists a correlation between these values and other flow parameters.

1.2 Literature Survey

1.2.1 The Navier-Stokes equations

A set of differential equations was derived from the mass and momentum conservation principles to describe the motion of a Newtonian fluid with constant properties of density and viscosity. In vector notation, the equations are given as [1] :

Continuity equation :

$$\frac{\partial \rho}{\partial t} + \nabla \cdot (\rho \bar{u}) = 0 \qquad (1)$$

Navier-Stokes equations :

$$\frac{\partial \bar{u}}{\partial t} + (\bar{u} \cdot \nabla)\bar{u} = -\frac{1}{\rho}\nabla P - \nabla g + \nu \nabla^2 \bar{u} \qquad (2)$$

where ρ is the fluid density, P is the pressure, $\bar{u}$ is the velocity vector at any point in the flow field and g is the value of the gravitational acceleration at that point. The kinematic viscocity ν is defined as the ratio of absolute viscosity μ to density ρ , and the vector operator del ∇ is defined in cartesian coordinates- for example - , as

$$\nabla(\ ) = i\frac{\partial(\ )}{\partial x} + j\frac{\partial(\ )}{\partial y} + k\frac{\partial(\ )}{\partial z} \qquad (3)$$

$$\nabla^2(\ ) = \frac{\partial^2(\ )}{\partial x^2} + \frac{\partial^2(\ )}{\partial y^2} + \frac{\partial^2(\ )}{\partial z^2} \qquad (4)$$

In principle a solution to these equations will yield a velocity profile from which all other flow parameters can be obtained. Unfortunately, these equations are extremely hard to solve for most of the practical situations encountered in fluid dynamics.

1.2.2 Laminar flow in pipes

One of the few cases in which a solution to the Navier-Stokes equation does exist is the case of a laminar steady flow in circular tubes where the fluid flows in smooth layers called laminae and a fluid particle in one layer stays in that layer. Here the effect of gravity is negligible and only the velocity component in the axial direction (u) is non-vanishing. It is further assumed that u is a function of the radial distance only, i.e, u = u(r).

The flow is subject to the following boundary conditions

1. No slip condition :

$$u(r=R) = 0 \tag{5}$$

2. Maximum velocity :

$$\frac{\partial u}{\partial r}(r=0) = 0 \tag{6}$$

The resulting velocity profile is a parabola

$$\frac{u}{u_c} = 1 - \left(\frac{r}{R}\right)^2 \tag{7}$$

where u_c is the maximum velocity (at centerline), and R is the tube's radius. This profile is also known as the Hagen-Poiseuille profile [1]. In practice, laminar flow in pipes can only exist as long as the non-dimensional Reynolds number $Re = \frac{u D}{\nu}$ is less than 2100, where D is the tube's diameter and ν is the kinematic viscosity. Beyond this value the flow is bound to be turbulent.

1.2.3 Turbulent flow in pipes

Pipe flow is usually turbulent for Reynolds numbers over 4000, where eddies and vortices mix the fluid by moving particles from one sublayer to another. For the transition region, $2100 < Re < 4000$, the flow has characteristics that are mixture between those of laminar and turbulent flows.

Turbulence is characterized by random velocity fluctuations u'(t) about the time mean velocity u. The instantaneous velocity is defined as

$$u(t) = u \pm u'(t) \tag{8}$$

and the turbulence intensity is defined as

$$\sigma = \frac{\sqrt{<u'^2>}}{u} \tag{9}$$

Although no complete solution to the Navier-Stokes equation exists so far, many empirical and semi-empirical relations were developed to describe turbulent flows in pipes. Among the best well known and most commonly

used is the "Power Law"

$$\frac{u}{u_c} = \left(1 - \frac{r}{R}\right)^{1/N} = \left(\frac{y}{R}\right)^{1/N} \qquad (10)$$

where y is the distance from the wall, y = R - r. The exponent N varies slightly with Reynolds number from N = 6 for Re = 4×10^4 to N = 10 for Re = 3.2×10^6 [1].

1.2.4 Inlet length

When a fluid is allowed to enter a circular tube from a reservoir, the velocity distribution at the entrance is uniform, further downstream the velocity profile changes due to the effect of friction until a fully developed velocity profile is attained at a certain distance behind the entrance, and remains constant downstream. This distance is known as the "inlet length".

According to the measurements performed by Schiller and Kirsten [2] in the entrance region of a 3-inch diameter smooth pipe at Reynolds numbers between 10,000 and 40,000, an inlet length greater than 50 tube diameters was needed to establish a fully developed turbulent profile. In 1932 Nikurdse [3] carried a very extensive experimental investigation into the power law and velocity profiles in smooth pipes for a wide range of Reynolds numbers $4 \times 10^3 \leq Re \leq 3.2\ 10^6$. He determined that a fully formed turbulent profile exists already after an inlet length of 25 to 40 diameters depending on the value of the Reynolds number.

Latsko [4] assumed a one-seventh power law velocity profile in the inlet region. With this assumption he predicted that the inlet length satisfies the relation

$$\frac{L}{D} = 0.625\,(\,Re\,)^{1/4} \qquad (11)$$

Actually, the one-seventh power law applies only to $2.5 \times 10^4 \leq Re \leq 1.5 \times 10^5$ in the fully developed region.

Barbin and Jones [5] conducted a series of experiments in an 8-inch diameter, 29-foot long, smooth aluminium pipe at $Re = 3.88 \times 10^5$, their measurements indicated that for $\frac{L}{D} = 40$, the velocity profile was not fully developed, and the centerline velocity did not approach the fully developed value asymptotically but rose to a value above it before settling.

A theoretical investigation of the turbulent pipe flow was carried out by Bowles and Brighton [6], the result of their calculations is summarized by the expression

$$\frac{L}{D} = 14.25\ \log_{10}(Re) - 46 \qquad (12)$$

Using pitot tubes, Wang [7] studied turbulent flow in a 12-inch diameter pipe at Reynolds numbers between 7×10^5 and 3×10^6, it was estimated that the velocity profile became fully developed at about $\frac{L}{D} = 50$.

In his 1981 review article, Klein [8] examined the variation with distance of the blockage factor B defined as the ratio of the centerline velocity u_c to the spatial mean velocity u_{av}

$$B = 1 - \left(\frac{u_{av}}{u_c}\right) \qquad (13)$$

He was able to show that, in cases where the flow has undisturbed entry conditions, the blockage factor B exhibits a maximum value in the x range of 35 to 40 tube diameters. This maximum value shortly precedes the establishment of the fully developed profile.

A more recent study was conducted by Salami [9] who made an attempt to explain the turbulent flow regimes at the the entry region of a pipe. A simple empirical formula was obtained from which it is possible to predict the length of the entry region

$$N = 5.16 + 2.18 \times 10^{-6} \left(\frac{L}{D}\right) Re \qquad (14)$$

where N is the exponent value in the power law that corresponds to the Reynolds number of the flow.

Two empirical formulas to estimate the inlet length were given by Janna [10] for laminar and turbulent flows

Laminar flow : $$\frac{L}{D} = 0.06\ Re \qquad (15)$$

Turbulent flow : $$\frac{L}{D} = 4.4\ (Re)^{\frac{1}{6}} \qquad (16)$$

The inlet length predicted by these formulas for the case of laminar flow is twice as the inlet length value predicted by the formula given by Schlichting [11].

$$\frac{L}{D} = 0.03\ Re \qquad (17)$$

1.2.5 Relaminarization

Relaminarization is a process in which an initially turbulent flow is rendered effectively laminar. In recent years relaminarization has been a major topic of interest to many researchers for two reasons. On the short run, a better knowledge of this phenomenon is very useful for the development of new models to describe turbulent and laminar flows. On the long run, relaminarization contains the seeds of the science of "turbulence control", where the ability to control turbulence helps in finding new ways to cut energy loss in pipes and other flow systems effectively.

Narasimha and Sreenivasan [12] were the first to suggest that, notwithstanding the diversity of flow situation in which relaminarization occurs, only three types of basic physical mechanisms bring about relaminarization. In the first mechanism an external body force such as

buoyancy is responsible for absorbing turbulence energy, here a critical Richardson number governs the process of relaminarization. In the second mechanism, turbulent energy is dissipated through the action of molecular parameters such as viscosity, this process is governed by a critical Reynolds number or an analogous non-dimensional parameter. In the third mechanism, relaminarization is brought about by the action of a severe stream-wise acceleration of an initially turbulent boundary layer.

Since in our experiment we are expecting viscosity to play the major role in achieving relaminarization, the following discussion will be confined only to the cases in which viscosity was responsible for relaminarizing pipe and channel flows. Experimental investigation of such reverting flows have been reported by Laufer [13], Sibulkin [14], Patel and Head [15], and Badri Narayanan [16].

In these studies, the general experimental arrangement involves the gradual enlargement of a pipe or a channel from one diameter or width to another, the angle of divergence was kept sufficiently small to ensure that no flow separation occurs. In this case, the Reynolds number goes down from say Re_1 upstream of the divergence to Re_2 downstream. If $Re_1 > Re_{cr}$ and $Re_2 < Re_{cr}$, where Re_{cr} is an appropriate critical Reynolds number, it may be expected that the approaching turbulent flow will revert to the laminar state [17].

Narasimha and Sreenivasan [12] have also shown that for pipe and channel flows undergoing reversion

$$\Delta u \sim \exp(-\alpha x/D) \qquad (18)$$

where α is a positive constant value for a given Reynolds number. According to Eq-18, the deviation of the velocity profile from the Poiseuille value, Δu, at any given y in the core of the flow decreases exponentially with distance from the inlet. Turbulence intensity at the centerline and at points that are near the wall but still close to the centerline also decay exponentially. The exponential decay does not seem to be a characteristic of fluctuations in the intermediate positions.

A chief characteristics of relaminarizing pipe or channel flows is the exponential decay of the maximum and average turbulence intensities, where the average is carried over the cross section. Badri Narayanan [16] was the first to show that for a channel flow undergoing relaminarization

$$\langle u'^2 \rangle_m \sim \exp(-k_o x/D) \qquad (18)$$

where $\langle u'^2 \rangle_m$ is the maximum value of the time mean velocity fluctuations and the constant k_o is proportional to $(Re_{cr} - Re_2)^3$. Badri Narayanan used this relation to define the critical Reynolds number as that Re_2 value at which $k_o = 0$, that is the downstream Reynolds number at which the turbulence intensity just maintain itself. Narasimha and Sreenivasan [12] showed that this relation holds for both pipe and channel flows and that all available data suggest a value of 3000 for Re_{cr}.

1.3 Laser Doppler Anemometry

1.3.1 Basic concepts

In any form of wave propagation, frequency changes can occur owing to the movement of the source, receiver, propagating medium or intervening reflector or scatterer. These shifts are generally called 'Doppler' shifts after the Austrian physicist who first considered the phenomenon in 1842. The magnitude of these shifts at normally encountered speeds are usually too small to be accurately resolved by direct spectroscopic measurements. An alternative technique that uses the principle of heterodyning of two frequencies in a device having a non-linear response is more commonly used. In this technique the Doppler shift is detected as the difference frequency between light from two sources. When the light waves from the two sources are superimposed on the photodetector surface, the mixing process in the photodetector will give the difference frequency since all other frequencies are too high to be detected [18].

Lasers provide highly intense monochromatic radiation with a narrow spectral width which, when focused on an object, gives sufficient scattered light to permit measurement of even very low velocities. The technique of using the Doppler shifts of laser light to measure flow velocities was first demonstrated in 1964 by Yeh and Cummins [19]. Their demonstration included the measurement of the velocity profile for laminar flow in a circular tube. These profiles were obtained by heterodyning light scattered from small particles added to the fluid with a reference beam derived from the same He-Ne laser used to illuminate the particles.

This new technique, which later became known as Laser Doppler Anemometry (LDA), was subject to various improvements over the years, these improvements were mainly focused on achieving better optical designs and more efficient signal processing and data handling.

1.3.2 Optical arrangements

The most commonly used arrangements for LDA employ the "Dual beam" or "reference beam" modes. A third arrangement, the "two-scattered beam", has not been used as extensively as the others.

A : The Dual Beam Mode

This is by far the most popular technique in LDA and the one that was used in our experiment. It has the following advantages:

1: With only one small particle at a time in the the measuring volume, large collection apertures can be used without violating coherence requirements.

2: It is the easiest system to align

3: With the Doppler frequency independent of the location of the collecting optics, it is a flexible system [18].

In addition to that, the "fringe model", first suggested by Rudd [20] in 1969, presents a conceptually simple alternative to the usual "Doppler model" for understanding the origin of the frequency shift.

A simple dual beam arrangement is shown in Fig. 1. The incoming laser beam is divided into two equally intense beams by a beam splitter. The two beams are then crossed to form an interference pattern in the local region of the flow where velocity measurements are required. The typical size of the crossing volume is about 10μm x 100μm x 1 mm. The interference pattern, shown in Fig. 2, is a set of fringes similar to those produced by the Young's slits experiment. Planes of equal phase separated by one wavelength (λ) are drawn for each beam. These are denoted by $A_1, A_2, \ldots, B_1, B_2, \ldots$, etc. The points where constructive interference occurs lie on planes bisecting the angle θ between the two laser beams. Consideration of the right-angled triangle XYZ shows that these bright fringes, denoted by $C_1, C_2, \ldots$ etc., are separated by a distance S given by

$$S = \frac{\lambda}{2 \sin(\frac{\theta}{2})} \qquad (20)$$

A particle moving with velocity V at an angle β normal to the fringe planes blocks off a varying amount of light. If it lies in a bright fringe it blocks off much light, in a dark fringe, only very little. Thus as the particle moves through the fringes the intensity of the scattered light will fluctuate with frequency ν_D - known as Doppler frequency - that depends on the fringe spacing and the velocity of the particle [21].

$$\nu_D = \frac{2 V \cos\beta \sin(\frac{\theta}{2})}{\lambda} \qquad (21)$$

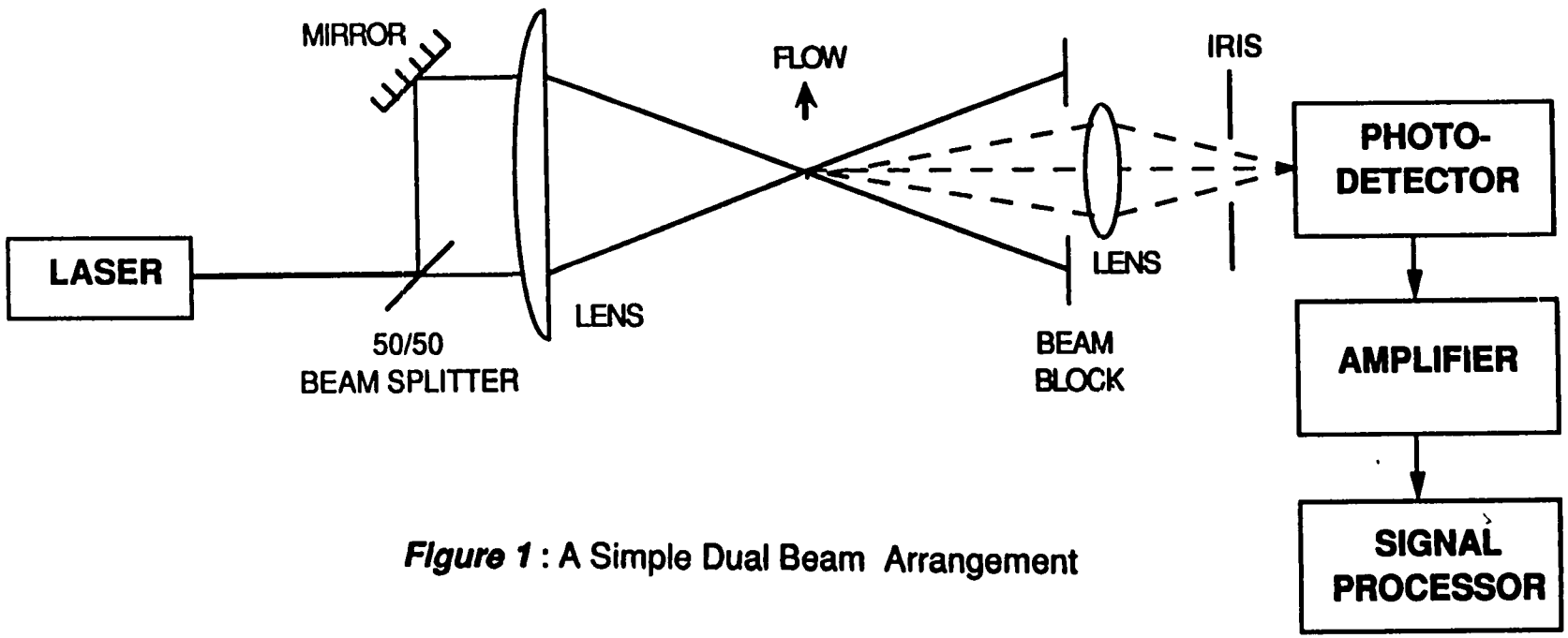

Figure 1 : A Simple Dual Beam Arrangement

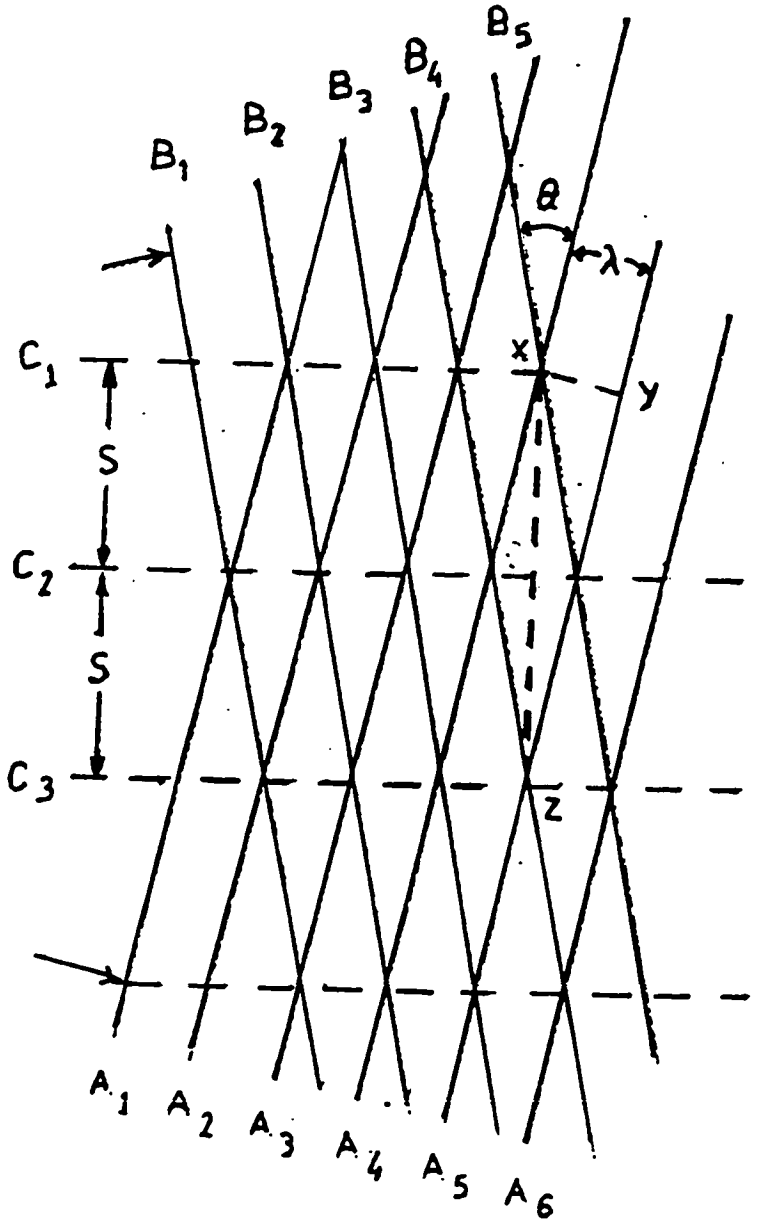

Figure 2 : Interference pattern produced by crossing laser beams

The particle's velocity component in the direction perpendicular to the fringe planes V_p is given by

$$V_p = \frac{\lambda \nu_D}{2 \sin(\frac{\theta}{2})} \qquad (22)$$

B : The Reference Beam Mode

In the reference beam mode the laser light is split into an intense scattering beam and a weak reference beam. The reference beam is directed on to a photodetector where it beats with light scattered from the strong beam by particles moving within the flow. The output of the photodetector contains a signal of the frequency difference between the two beams (Doppler shift) which is directly proportional to the particle's velocity. This arrangement was employed in the pioneering work of Yeh and Cummins and is still of use in measurements with particle dense fluids [22].

C : The Two-scatter Mode

The third optical arrangement, the two-scatter mode was first introduced by Durst and Whitelaw in 1971 [23]. A single focused laser beam is directed into the flow and the scattered beams are received in two directions simultaneously. They are then combined and directed to a photodetector by a lens system similar to the one used for beam spliting in the dual beam method. As particles move across the beam, the optical path difference to the detector via the the two scttering directions varies,

leading to alternate constructive and destructive interference in the combined beam.

The two-scattered beam has a clear advantage over the dual beam method in that two velocity components maybe measured at the same time by collecting pairs of scattered beams in mutually perpendicular planes. However, little use has been made of this technique because of alignment difficulties [22].

1.3.3 Light detection for LDA

The light intensity variations are commonly detected by either photomultipliers or photodiodes. Photomultipliers are vacuum tubes in which electrons are released by light falling on a special photoemissive surfaces. A diagram of a typical photomultiplier tube is shown in Fig. 3. The released electrons may be collected directly by a positive electrode to produce a measurable current, or as the case in many commercially available photomultiplier types, internal amplification of the photocurrent is carried out by secondary emission at intermediate dynodes at successively higher voltages with respect to the photoemissive cathode. The measured output of the photomultiplier is either the current that passes through the last anode, or more preferably an output voltage produced by this current across a resistor.

Photodiodes are semiconductor devices in which light is detected by the production of electron-hole pairs in the junction region of a p-n diode.

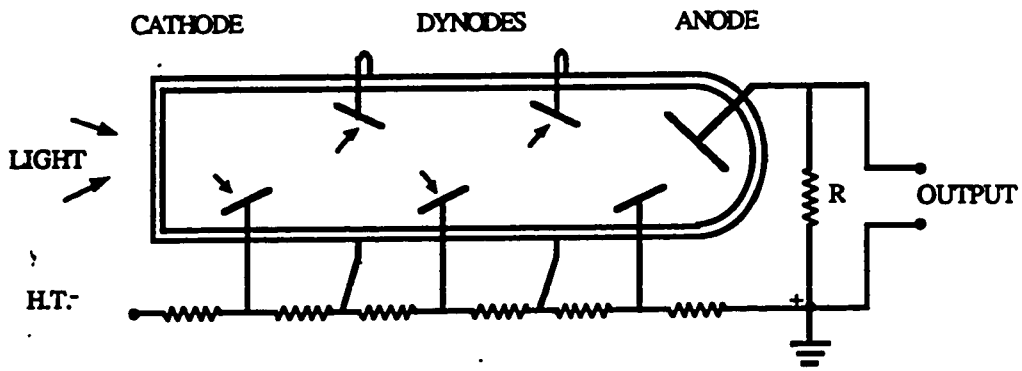

Figure 3 : Diagram of photomultiplier tube

photodiodes have the advantage of being small, relatively inexpensive and unlike photomultipliers, photodiodes do not require any high-voltage power supply. However, ordinary photodiodes do not have a built in current amplification and thus much more external amplification is required than with photomultipliers [21].

Light collection in the forward direction is preferable whenever possible. However, in cases when the optical access to the experiment is only available from one side, backward scattering configuration is unavoidable. A reduction in received scattered light of two or three orders of magnitude is to be expected.

1.3.4 Signal processing and data analysis

The signal produced at the output of the photodetector in an LDA system can take on a variety of forms depending on particle seeding density, particle size, optical design and laser power. A typical LDA signal is shown in Fig. 4. With heavy concentration of particles in the fluid, there will be more than one particle in the probe volume at any time on the average, and nearly continuous signal will result. On the other hand. with low concentration of particles, bursts of Doppler signals are observed from the passage of individual particles through the scattering region. In the cases where the particles are extremely small, the laser power is very low and the receiving aperture is severely restricted, the scattered light intensity becomes so low that photon-limited signals will be detected at the photodetector [24].

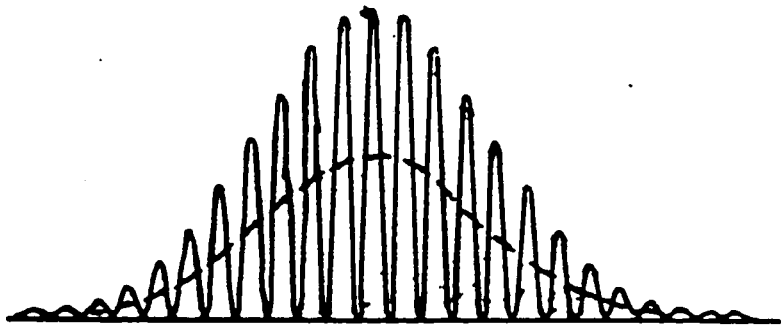

Figure 4 : A typical LDA signal

The different signal forms that are produced by the photodetectors required the use of different signal processing devices. Nearly all signal processors used in LDA systems are of either two types, frequency trackers or burst counters.

A frequency tracker uses a bandpass filter and frequency discrimination to track the frequency changes in the photodetector output. The output of most trackers is an analogue voltage proportional to the input frequency [18]. Due to the failure of the frequency trackers to follow the rapid frequency changes in highly turbulent flows as they occur, their application is usually restricted to liquid flow studies with turbulent intensities less than 20 percent [24]. On the other hand, burst counters are capable of measuring the frequency of a single Doppler burst. They are particularly useful in low particle density flow systems such as gas flows where heavy seeding is impractical. The fundamental output of burst counters is digital and there is no restriction on the turbulence intensity of the flow since large frequency changes between the bursts have no effect on operation. Available burst counters are capable of handling Doppler frequencies up to 200 MHz [24].

Once the signal processor converted the signal from frequency to voltage (frequency trackers) or to numbers (burst counters) proportional to velocity, the next step is to extract the required information from the available data. This is usually done by interfacing the signal processor with a computer. Computers can help in analyzing the data quickly and very efficiently.

1.3.5 Application survey

The LDA technique of fluid velocity measurements is capable of operating in a velocity range of 10^{-3} cm/s to $2x10^{6}$ m/s. The spatial resolution, typically 20-100 μm exceeds that obtainable by any other method. Precision of measurements by LDA can be as small as 3%. LDA has two advantages over the hot wire anemometry in connection with measurements in turbulent flow. Unlike the hot wire anemometry LDA has a linear relation between the output and the velocity of the flow tracing particles (Eq-16). The other advantage of LDA is that there is no need to insert a probe in the fluid, since such probes may disturb the flow and thus affect the accuracy of measurements [24].

In principle the velocity measurements by LDA are not much affected by the number or optical properties of the scattering particles, but as mentioned earlier, insufficient number of particles present in the fluid may result in poor signal to noise ratios from the photomultiplier and long measurement times. Fortunately, enough suitable particles are usually present in fluids being studied by LDA. This is often true in liquids, but in the study of flow in gases there is always the need to add more particles to the flow.

A source of error usually observed when dealing with turbulent gas flow is the uncertainity concerning weighting the results from individual passage of particles. More high velocity than low velocity particles per unit time would pass through the measuring volume, Therefore to give all

measurements an equal weight will cause the velocity distribution to have a mean value higher than the actual value. For high turbulence intensities the error introduced in the velocity distribution can be significant and a correction is needed.

One other limitation of the LDA technique is the need to have an optical access to the flow area. This access is usually provided by a transparent tube or window which is not necessarily of a high quality. A summary of the advantages and disadvantages of the laser Doppler technique are given in table-1 [21].

Table 1

Velocity measurement by LDA

Advantages	Disadvantages
Does not disturb the flow	Medium must be transparent
High spatial resolution	Needs scattering particles
Response linear and fast	Optical access is required
Possible directional discrimination	Expensive signal processing equipment needed
Operation not seriously affected by temperature, as long the temperature gradiant is not high	Not suited for measurements of total flow. Integration over the cross section is required

CHAPTER II

EXPERIMENTAL SET-UP

2.1 The Water Channel

The experiments described in this study were conducted in the Molecular Dynamics Laboratory of Laser Research Laboratory, the laboratory is part of Division II of the Research Institute located at King Fahd University of Petroleum and Minerals. A general layout of the experimental set-up used for this study is shown in Fig. 5.

The water channel was provided by the British firm Plint and Partners Ltd. The major features of the water channel will be described by proceeding in the direction of the flow. Water from a large tank was pumped through a pipe of 13 cm inner diameter into a stilling tank, which in turn runs into a 20cmx30cmx8m water channel with transparent walls.

The pump used for this purpose is a low speed centrifugal pump developing a moderate head. The maximum flow rate obtained in the pipe with the flow control valve wide open was 38.3 L/s. However, for the conditions employed in the experimental runs, volumetric flow rates were kept below this value, this was achieved by throttling the flow control valve.

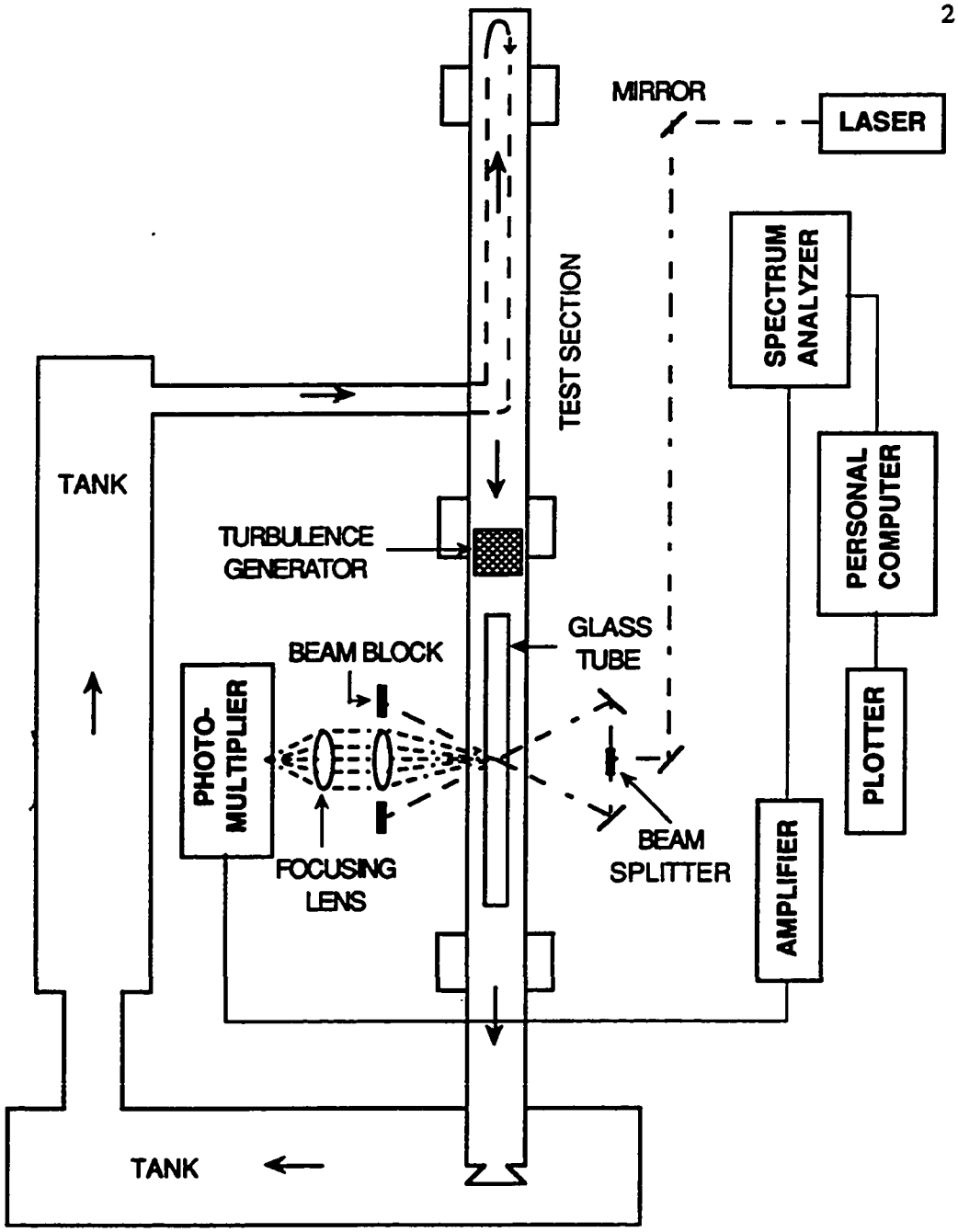

Figure 5 : General layout of the experimental set-up

The stilling tank was not part of the original water channel as delivered by the manufacturers. It was designed and manufactured at the KFUPM workshops. The main function of the stilling tank is to suppress turbulence in the flow and create a laminar viscous flow in the test section of the water channel.

A glass tube of 32 mm inner diameter and length of 160 cm (L/D = 50) was installed in the test section of the water channel with the axis at a height of 18 cm from the channel floor. A 20cmx20cmx30cm cage filled with metallic fragments randomly distributed inside was placed 30 cm in front of the tube opening. Since the tube was going to be immersed in water for long periods of time, both the cage and the holders that carry the tube were painted with an anti-rust paint.

The cage works as a turbulence generator, it creates a "top hat" turbulent flow profile at the entrance to the tube. Figure 6 show the velocity distribution and the velocity vs. time distributions at a point located on the tube's axis and 1 cm before the opening respectively. Similar distributions were obtained at distances 5 and 10 mm away from the axis. The turbulence intensities at these points were nearly the same and around 16 % for the low and intermediate Reynolds number flows and around 12 % for the high Reynolds number flow.

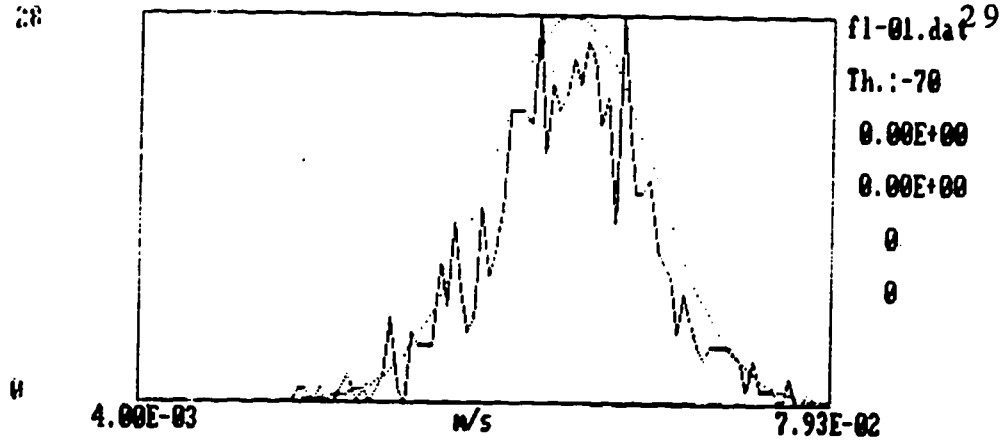

Velocity Distribution

Mean	: 5.095E-02 m/s	Dist. From Inlet	: -1.000E+00 cm
Stand. deviat.	: 8.791E-03 m/s	Radial Distance	: 0.000E+00 mm

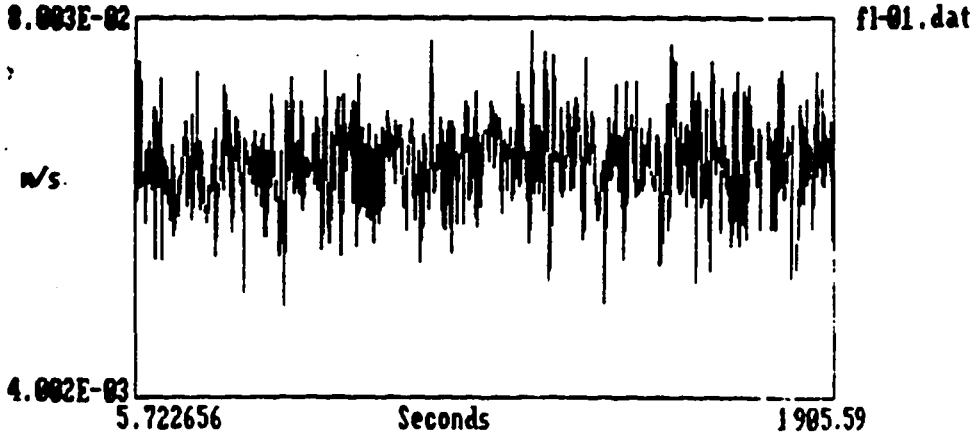

Velocity versus Time

Dist. From Inlet	:	-1.000E+00 cm
Radial Distance	:	0.000E+00 mm

Figure 6 : Velocity distribution and velocity vs. time distribution, Re = 1670, (r = 0 mm, x = -1 cm).

2.2 Velocity Measuring System

2.2.1 Velocity measurement set-up

An Argon-Ion laser - Spectra Physics model 171 - was used in this experiment. The Argon-Ion laser was chosen over the He-Ne laser which is also common in LDA measurements for the following reasons :

1: It has more powerful output. The Argon-Ion laser has a typical light output power up to a few watts, while the He-Ne laser can only produce light with an output power of few milliwatts.

2: It is always polarized.

3: Principal Wavelength in the green region at 514.5 nm. Most available photomultipliers have their highest sensitivity in the blue and green regions of the spectrum, sensitivity to red light being poor unless special cathode emitting materials are used [21].

The laser Doppler anemometer is operated in the forward scatter mode (Fig. 5). The incoming laser beam, with a wavelength of 514.5 nm and a power approximately 40 mw is divided equally by the cubic beam splitter. One beam is directed straight towards the channel and focused via a lens in the middle of the channel. The other beam leaves the cubic beam splitter at a 90 degree angle with respect to the original beam direction and is directed with a mirror towards the channel and focused via a second lens in the middle of the channel. The two beams cross inside the tube with an angle $\alpha = 37.5°$ between the two beams. The two outgoing beams are then blocked on the other side of the channel by two beam blocks .

The scattered light induced by particles crossing the fringe pattern is then collected via a lens system. This lens system is designed to allow only the scattered light coming from the crossing of the two laser beams to reach the photomultiplier. It was necessary to run the whole experiment in complete darkness, not only to obtain a high signal to noise ratio, but also to avoid damaging the photomultiplier. The photomultiplier - NRC model 270 - was maintained at a voltage difference of 600 V, which made it highly sensitive to even very low light intensities and direct light most probably would have damage it.

The photomultiplier signal was then amplified - Hewlett Packard model 8447D - and fed to a spectrum analyzer - Hewlett Packard model 8568B -. The spectrum analyzer is a frequency tracker type processor. An IBM compatible PC -DigiSystems Jetta AD - was interfaced with the spectrum analyzer through an IEEE-488 adapter card that allowed the transfer of data between the computer and the spectrum analyzer. The data acquisition (ACQUI) and the display (DISP) programs were used for the purpose of data analysis. The original DISP program was modified in a way that in addition to the mean velocity and standard deviation, higher moments of the distribution are calculated and displayed. A plotter - EPSON model LQ 1050 - was connected to the computer for hard copies.

The calculated velocity u as a function of the detected frequency of the signal is

$$u = \frac{\lambda \nu_D}{2 \sin(\frac{\alpha}{2})} = 8.003 \times 10^{-7} . \nu_D \quad [\frac{m}{s}] \qquad (23)$$

where u is the flow velocity component in the axial direction, λ is the wavelength of the laser light, and ν is the measured Doppler frequency in Hz.

2.2.2 *The scanning devices*

Two separate scanning devices were used in this study to allow the variation of the crossing point of the two laser beams inside the tube in the x-direction (x = distance behind the opening) and in the r-direction (r = distance in the radial direction from the axis). The glass tube was mounted on two holders at distance 1 m apart. These two holders were designed and made in the LRL workshop specially for this experiment. The upper part of each holder is resting on a dove tail base that has the ability to move inward and outward in the r-direction without having the need to change the incoming laser beam. The movement of the holders is controlled with a precision of about 0.5 mm.

A carriage movable on rails on top of the channel was used to do the necessary scanning in the x-direction [26]. The dimensions of this carriage are capable of carrying all optical elements needed on both sides of the channel. The laser beam is directed from the laser head via a mirror system towards a mirror M_1 which sends the beam 5 cm above the water channel towards mirror M_2 fixed on the carriage. As the alignment of the laser

beam going from M_1 to M_2 is absolutely parallel to the channel, any movement of mirror M_2 will not change the position of the laser beam on it. And thus it is possible to scan in the x-direction without having to change the incoming laser beam on M_1. The movement of the carriage in the x-direction is also controlled with a precision of 0.5 mm.

Mirror M_3 which finally sends the laser beam focused by subsequent lens into the water channel is fixed on a plate on the carriage absolutely perpendicular to mirror M_2. The plate can be moved vertically upward and downward. This movement of the plate is controlled by four micrometers with a precision of about 25 microns which, gives the carriage an additional ability to do scanning in the z-direction. The photomultiplier unit is also fixed on a movable stand to enable the detection at any point x, z inside the channel [26].

2.2.3 Measurement procedure

Velocity distributions were obtained at different cross sections along the tube for three different flow rates, the average bulk velocities in front of the tube were $u_{av} \approx 5.20$ cm/s, 11.8 cm/s and 51.6 cm/s. The corresponding Reynolds numbers for the flow of water ($\nu = 10^{-2}\,cm^2/sec$) in a 3.2 cm diameter tube at these velocities were Re = 1670 (Laminar regime), Re = 3680 (Transitional regime) and Re = 16700 (Turbulent regime) respectively.

To obtain the required distributions the following steps were usually taken for each Reynolds number. Firstly, the carriage is moved to a position

that allows the two laser beams to cross at the designated x-position behind the entrance. Before applying the voltage to the photomultiplier, the optical alignment is carefully rechecked to make sure that the two beams are indeed crossing at that point and that enough scattered light from the crossing region is reaching the photomultiplier. When a set of velocity measurements is completed for a sufficient number of r values, which as mentioned earlier is done by moving the tube instead of moving the laser beam, the carriage is moved to another x-position to start a new set of measurements.

The first velocity profile measurement was always taken at a distance 1 cm in front of the tube to check on the the value of the bulk velocity and more importantly to make sure that a uniform turbulent profile exists at the entrance. The rest of the measurements were taken at x-distances of x= 2, 6, 12, 30, 60, 100 and 150 (all in centimeters). and at r-distances of r=0, 5, 10, 12, 14 and when possible at r=15 (all in millimeters). the complete set of the velocity distributions is in Appendix-B.

CHAPTER III

RESULTS AND ANALYSIS

3.1 VELOCITY PROFILES

The mean velocities for the three studied Reynolds numbers as a function of r and x are shown in tables A.1,A.2 and A.3 (Appendix A). The following is a detailed discussion of the velocity profile development in the tube for each Reynolds number.

3.1.1 Re = 1670

A: Velocity Profile Development

Figure 7 shows the development of the velocity profile for this Reynolds number from a highly turbulent uniform "top hat" profile at the entrance to a much lesser turbulent parabolic profile near the end. The profile is not completely uniform at the entrance since it can be clearly seen that the mean velocities are slightly lower in the middle region of the flow. We think this is caused by the way the metallic fragments responsible for creating turbulence are distributed inside the cage. However, we believe that this has no major effect on the development of the velocity profiles as it disappears completely at x = 12 cm (x/D = 3.8).

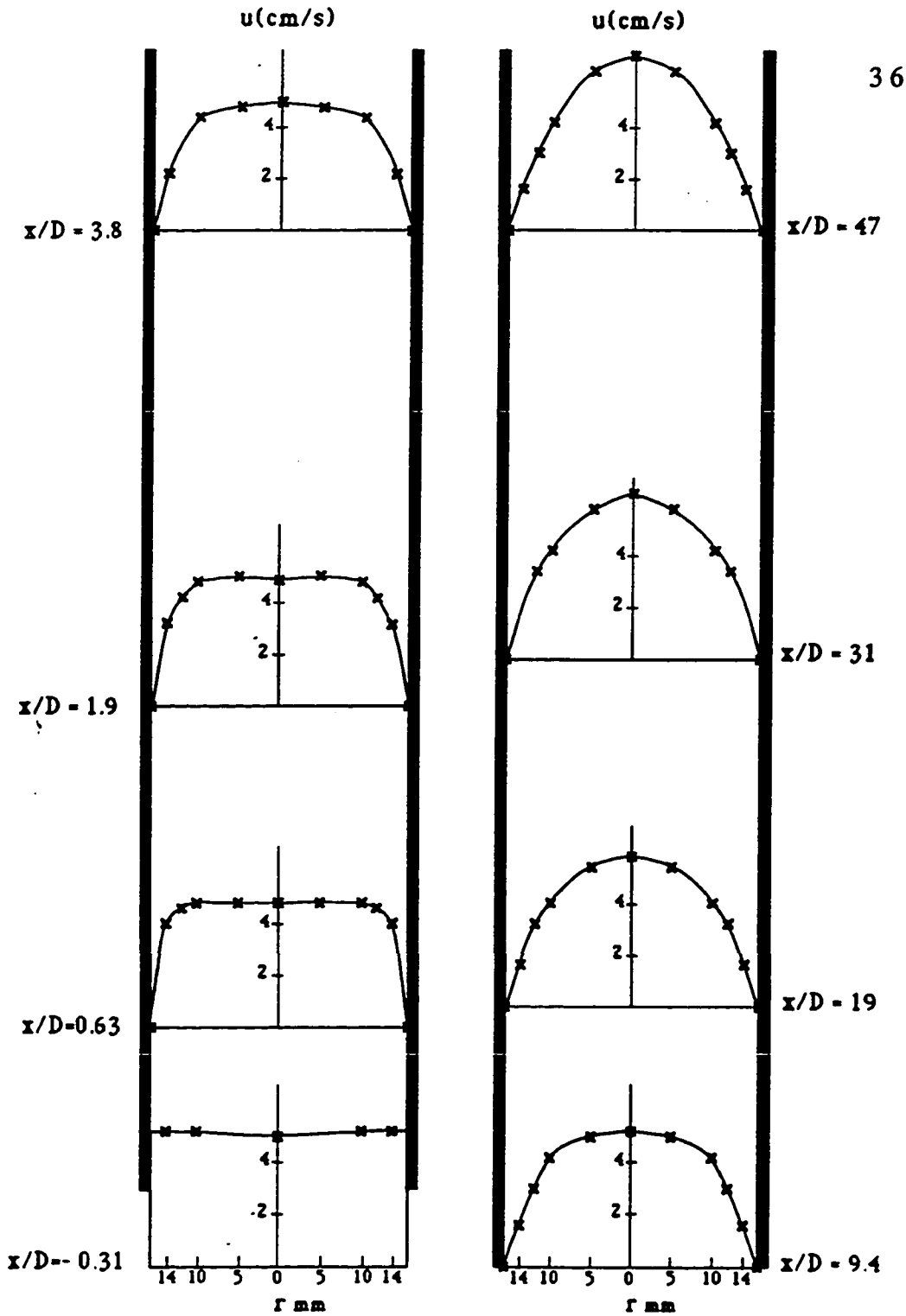

Figure 7 : Velocity profile development, Re = 1670

As the flow enters the tube, because of the non-slip condition, $u_{r=R} = 0$, particles adjacent to the wall will immediately have a zero velocity, further downstream the effect of the wall presence travels inward causing particles in the regions near the wall to slow down. At the same time, this is accompanied by an increase in the velocity at the centerline and in regions close to it. This will continue till the establishment of the fully developed profile. The velocity profile development is illustrated in Fig. 8 which shows three sample velocity distributions obtained at the centerline at distances x = -1 and 150 cm behind the entrance. The dashed lines represent the corresponding Gaussian distribution. Figure 9 shows the velocity profiles as a function of the normalized velocity ($\frac{u}{u_c}$) versus the normalized distance from the wall ($\frac{y}{R}$).

The points given in Table A.2 and plotted in Fig. 7 can be easily fitted to a simple polynomial function and thus an expression of the velocity profile at each inlet distance x as a function of the radial distance r, i.e. u(r) can be easily obtained. The average velocity u_{av} is found by carrying out an integration of u(r) over the cross section and then dividing by the area of the cross section A,

$$u_{av} = \frac{\int u(r)\, dA}{A} \qquad (24)$$

Since there is no angular dependence in u, dA can be simply written as $dA = 2\pi r\, dr$, substituting dA and $A = \pi R^2$, the above expression

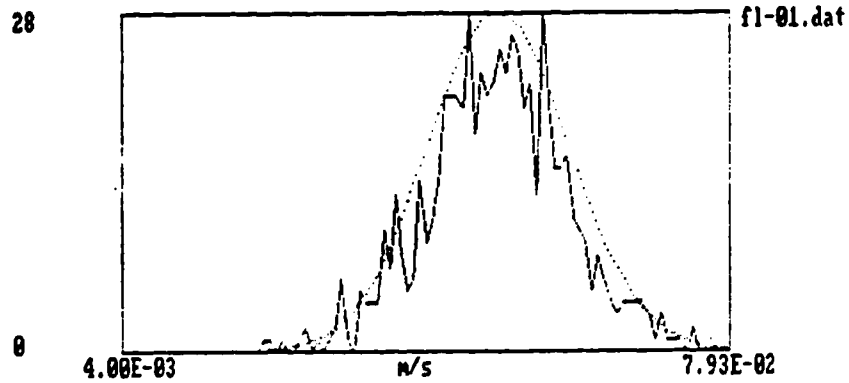

Velocity Distribution

Mean	: 5.095E-02 m/s	Dist. From Inlet	: -1.000E+00 cm
Stand. deviat.	: 8.791E-03 m/s	Radial Distance	: 0.000E+00 mm

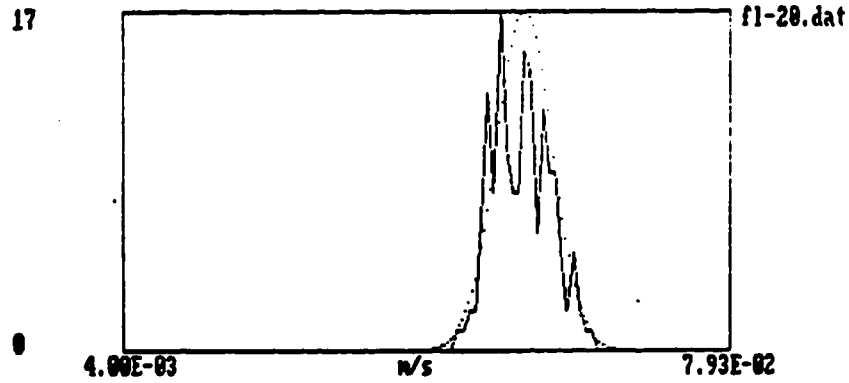

Velocity Distribution

Mean	: 5.415E-02 m/s	Dist. From Inlet	: 3.000E+01 cm
Stand. deviat.	: 3.495E-03 m/s	Radial Distance	: 0.000E+00 mm

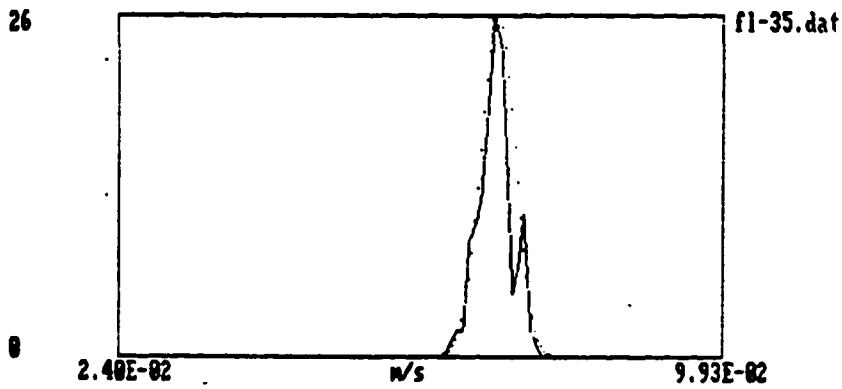

Velocity Distribution

Mean	: 7.163E-02 m/s	Dist. From Inlet	: 1.500E+02 cm
Stand. deviat.	: 2.092E-03 m/s	Radial Distance	: 0.000E+00 mm

Figure 8 : Velocity Distributions, Re = 1670
(r = 0 mm, x = -1, 30, 150 cm)

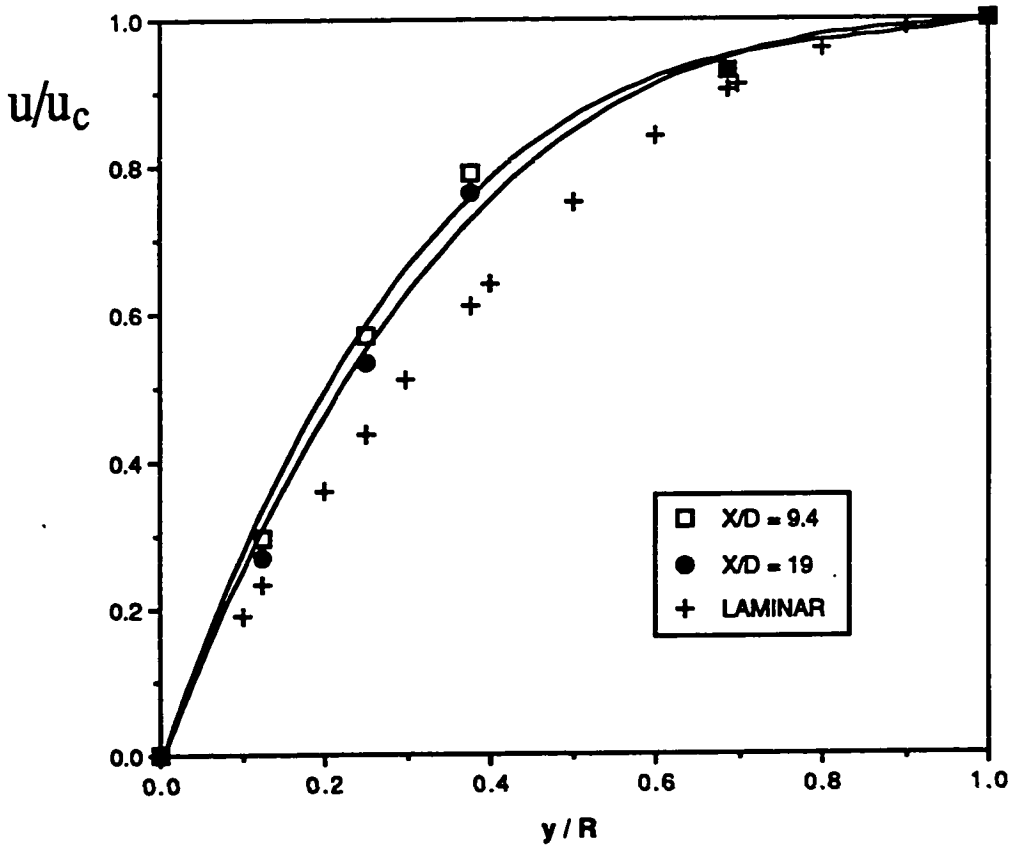

Figure 9(a) : Normalized mean velocity (u/u_c) versus normalized distance from the wall (y/R), Re = 1670, (x/D = 9.4, 19, Laminar).

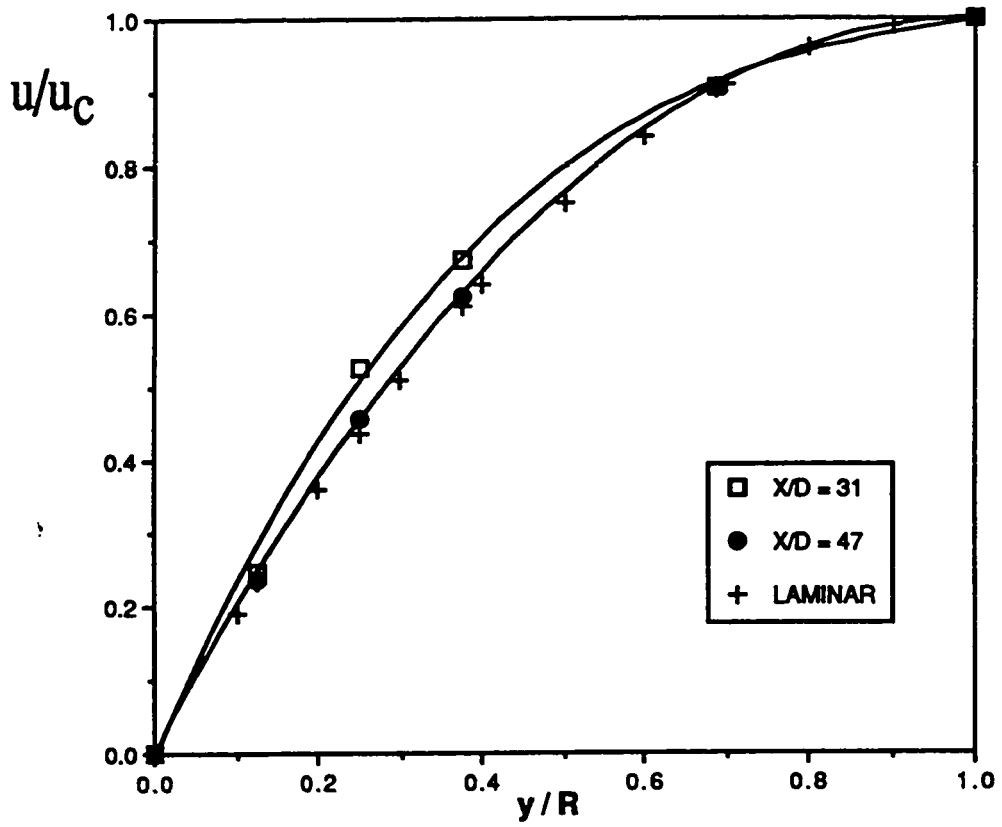

Figure 9(b) : Normalized mean velocity (u/u_c) versus normalized distance from the wall (y/R), Re = 1670, (x/D = 31, 47, Laminar).

reduces to

$$u_{av} = \frac{2\int u(r)\, r\, dr}{R^2} \qquad (25)$$

As mentioned previously, a fully developed laminar flow is represented by a parabolic profile (Hagen-Poiseulle profile) given as

$$u(r) = u_c\left[1 - \left(\frac{r}{R}\right)^2\right] \qquad (7)$$

by substituting u(r) in eq-25, and with little calculations the ratio of the average velocity to the centerline velocity ($\frac{u_{av}}{u_c}$) is found to be 0.5. In other words, for a fully developed laminar profile the centerline velocity is twice the average velocity. The same procedure is used to obtain the average velocities for Re = 3680 and Re = 16700 flows at each inlet distance. These average velocities are recorded in Table A.4(a).

B: The Deviation From The Laminar Profile

In the following we will examine the deviation Δu_c of the experimentally determined mean velocity at the centerline $(u_c)_{exp}$, from the value for a fully developed laminar flow, $(u_c)_{lam} = 2\, u_{av}$, where u_{av} is the average velocity given in Table A.4(a). For normalization, Δu_c can be written as

$$\Delta u_c = \left[\frac{(u_c)_{lam} - (u_c)_{exp}}{u_{av}}\right] x\, 100 \qquad (26)$$

Table 6 shows the Δu_c values obtained in the experiment for Re = 1670

Table 2*

Deviation of the centerline velocity from laminar value

x/D	0	0.63	1.9	3.8	9.4	19	31	47
Δu_c	101	91.3	80.2	41.3	30.5	20.5	14.8	3.52

Narasimha and Sreenivasan [12] have shown that one of the important characteristics of relaminarizing channel or pipe flows is the exponential decay of the deviation of the centerline velocity from the Poiseulle value,

$$\Delta u_c \sim \exp(-\alpha\, x/D) \qquad (18)$$

The plot of Δu_c versus x/D (Fig. 10) shows that beyond a downstream distance of $x/D > 3$ there is a clear exponential decay of Δu_c with a decay rate α equal to 0.053, and the best fit equation is

$$\Delta u_c = 54.2 \exp(-0.053\, x/D) \qquad (27)$$

---

* For optical reasons the Δu_c value at x/D = 0 was actually obtained at x/D = -0.31 but it is assumed that the flow will not change at all between x/D = -0.31 and x/D = 0.

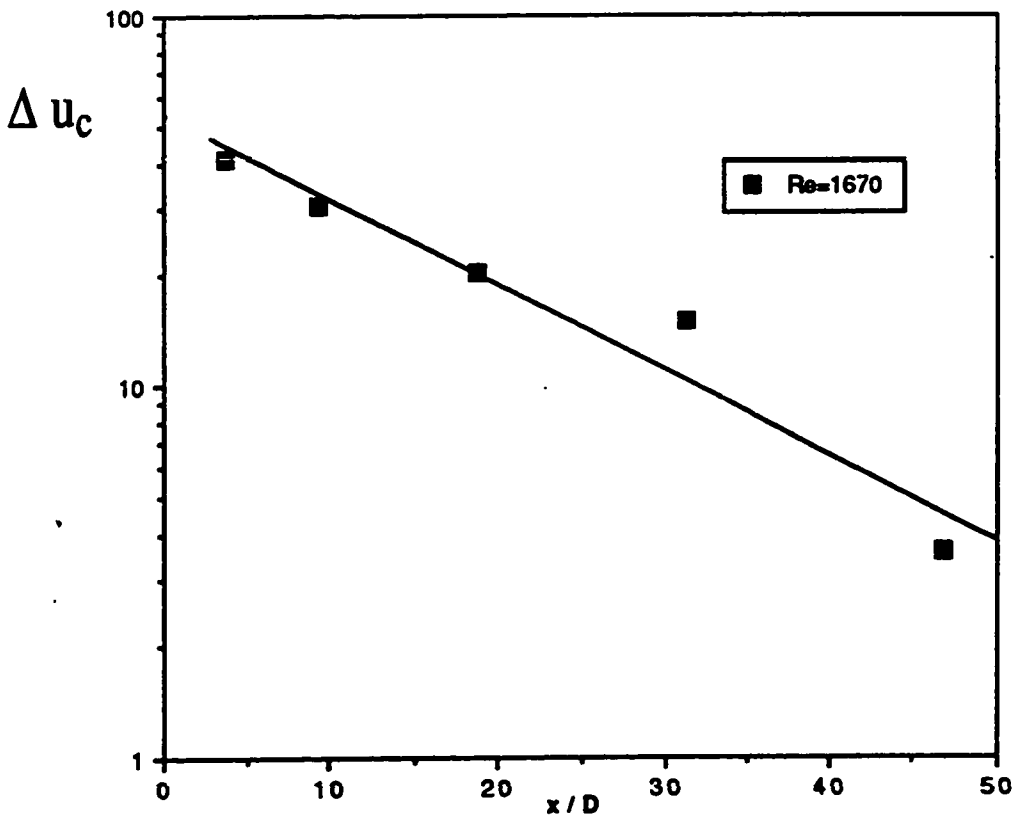

Figure 10 : The deviation of the experimentally determined mean velocity at the centerline from the value for fully developed laminar flow, Re = 1670.

the decay rate values obtained by previous reaserchers can be approximately estimated to be :

Sibulkin [11] :

$$Re = 600, \qquad \alpha \approx 0.077$$

$$Re = 1200, \qquad \alpha \approx 0.042$$

$$Re = 2400, \qquad \alpha \approx 0.022$$

Laufer [10] :

$$Re = 1400, \qquad \alpha \approx 0.035$$

Figure 11 shows the dependence of these decay rates on the Reynolds number of the flow. It is interesting to note that the decay rate obtained in this experiment is at least twice as that expected for the same Reynolds number using an enlargement in front of the tube opening. In effect this means that the inlet length needed to laminarize a highly turbulent low Reynolds number flow in a simple tube like the one used in our experiment is shorter than the inlet length needed in a tube with a diffuser in front as used in previous studies.

The decay of the deviation from the Poiseulle value is not restricted to the centerline only. Figure 12 which is based on the data given in Table A.5 shows this exponential decay (Δu_r) for different radial distances (r) from the axis.

$$\Delta u_r = \left[\frac{(u)_{exp} - (u)_{lam}}{u_c} \right] x\ 100 \qquad (28)$$

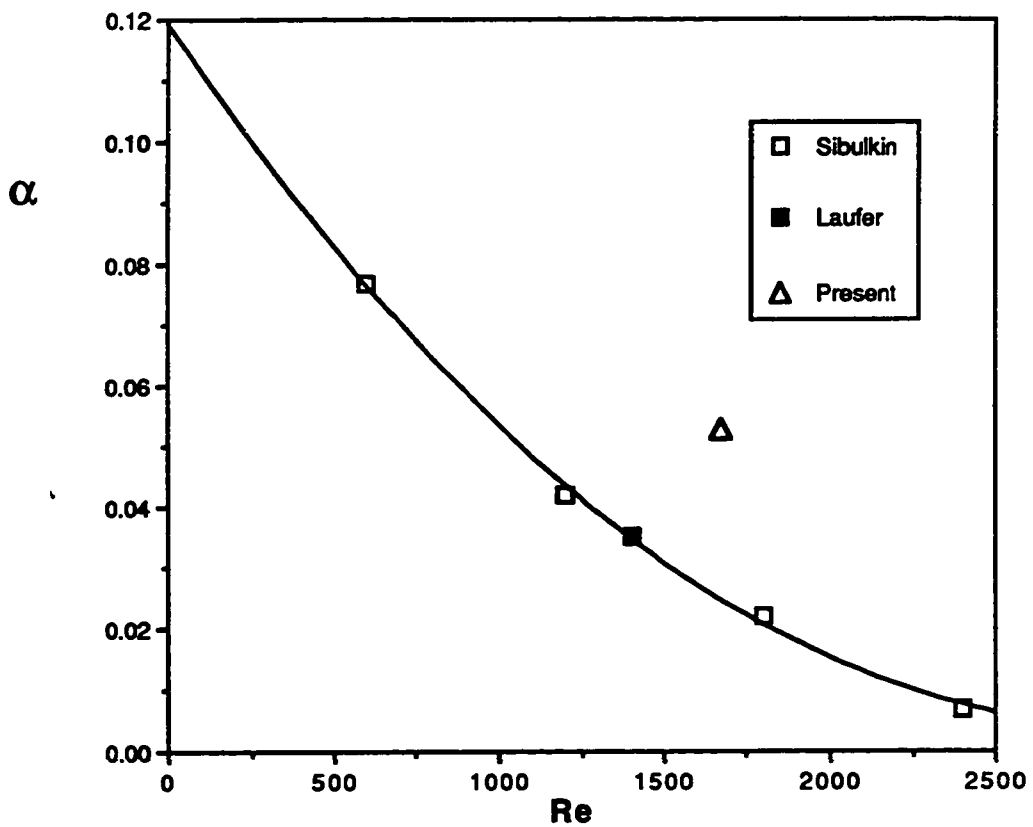

Figure 11 : Dependence on Reynolds number of rate of approach of the experimentally determined centerline mean velocity to the fully developed laminar value

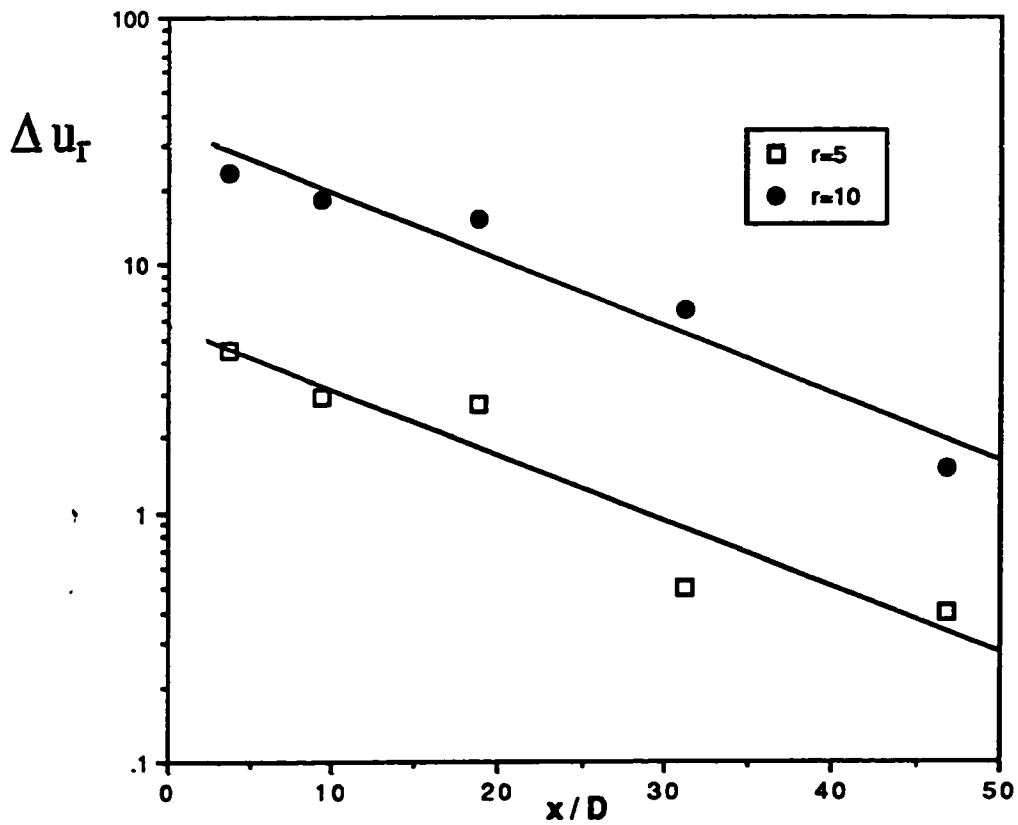

Figure 12(a) : The deviation of the experimentally determined mean velocity at radial distance r from the value for fully developed laminar flow, Re = 1670, (r = 5, 10 mm).

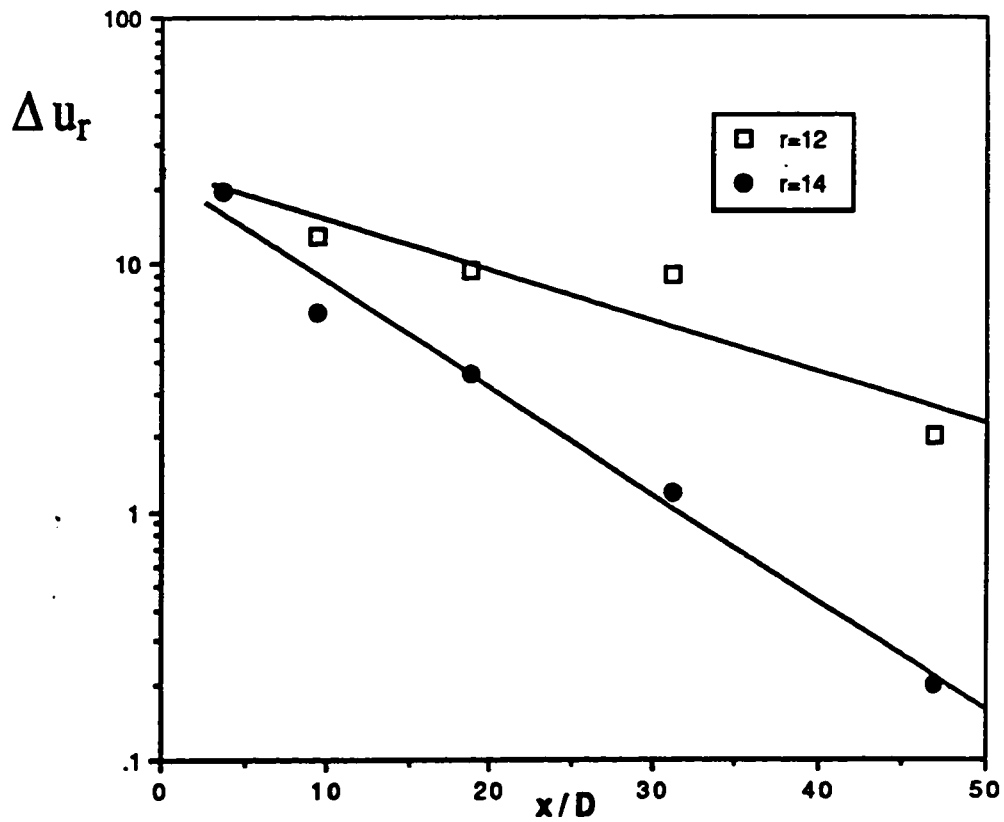

Figure 12(b) : The deviation of the experimentally determined mean velocity at radial distance r from the value for fully developed laminar flow, Re = 1670,.(r = 12, 14 mm).

where $(u)_{exp}$ is the experimentally determined value, $(u)_{lam}$ is the value for fully developed laminar profile as given in eq-7 and u_c is the centerline velocity. The obtained decay rates are given below :

$$\alpha(r=5) = 0.061$$

$$\alpha(r=10) = 0.063$$

$$\alpha(r=12) = 0.047$$

$$\alpha(r=14) = 0.099$$

This brings us to the question of how to determine when the flow is said to be fully laminarized. We propose using Δu_c as a criteria for determining the inlet length needed to establish a laminar profile. By assuming that whenever Δu_c is less than a certain value, say 5 %* , then we can say that the flow was fully laminarized at the corresponding x/D value. In our experiment Δu_c = 5 % corresponds to an inlet length of 45 tube diameters. This value is about the same like the inlet length of 50 diameters predicted by Schlichting [11], L = 0.03 D Re, and about half of the inlet length of 100 diameters predicted by Janna [10], L = 0.06 D Re.

As mentioned in section 1.2.5 (Relaminarization) , Narasimha and Sreenivasan [12] have reached the conclusion that only a critical Reynolds number governs the processes in which relaminarization is thought to be brought about by the effect of viscosity. In our opinion, the experimental

---

* The choice of this value depends on the experimental uncertainties. In our study a 5 % value seems very reasonable for Δu_c.

results obtained in this study clearly show that this the case regardless of how much turbulent the flow was at the entrance. Furthermore, our success in achieving relaminarization in a normal tube with only rounded edges indicates that the use of an enlargement or a diffuser at the entrance is not a necessity.

3.1.2 Re = 3680

A: Velocity Profile Development

The development of the velocity profile for this Reynolds number is shown in Fig. 13. The effect of the non-uniformity of the flow at the inlet is evident at x/D = 0.63 and to a lesser degree at x/D = 1.9 and it disappears completely at x/D = 3.8 behind the inlet. The velocity distributions at the centerline are to some degree similar to those obtained for Re = 1670, velocity distributions at x = -1 and 150 cm are shown in Fig. 14 as an example.

The plot of the normalized velocity (u/u_c) versus the normalized distance from the wall (y/R) clearly shows that the flow was still developing even after a distance of 50 diameters inside the tube (Fig. 15).

B: The Deviation From The Transitional Profile

The same criteria used previously to estimate the length needed to establish a laminar profile for Re = 1670 can be used here to verify the

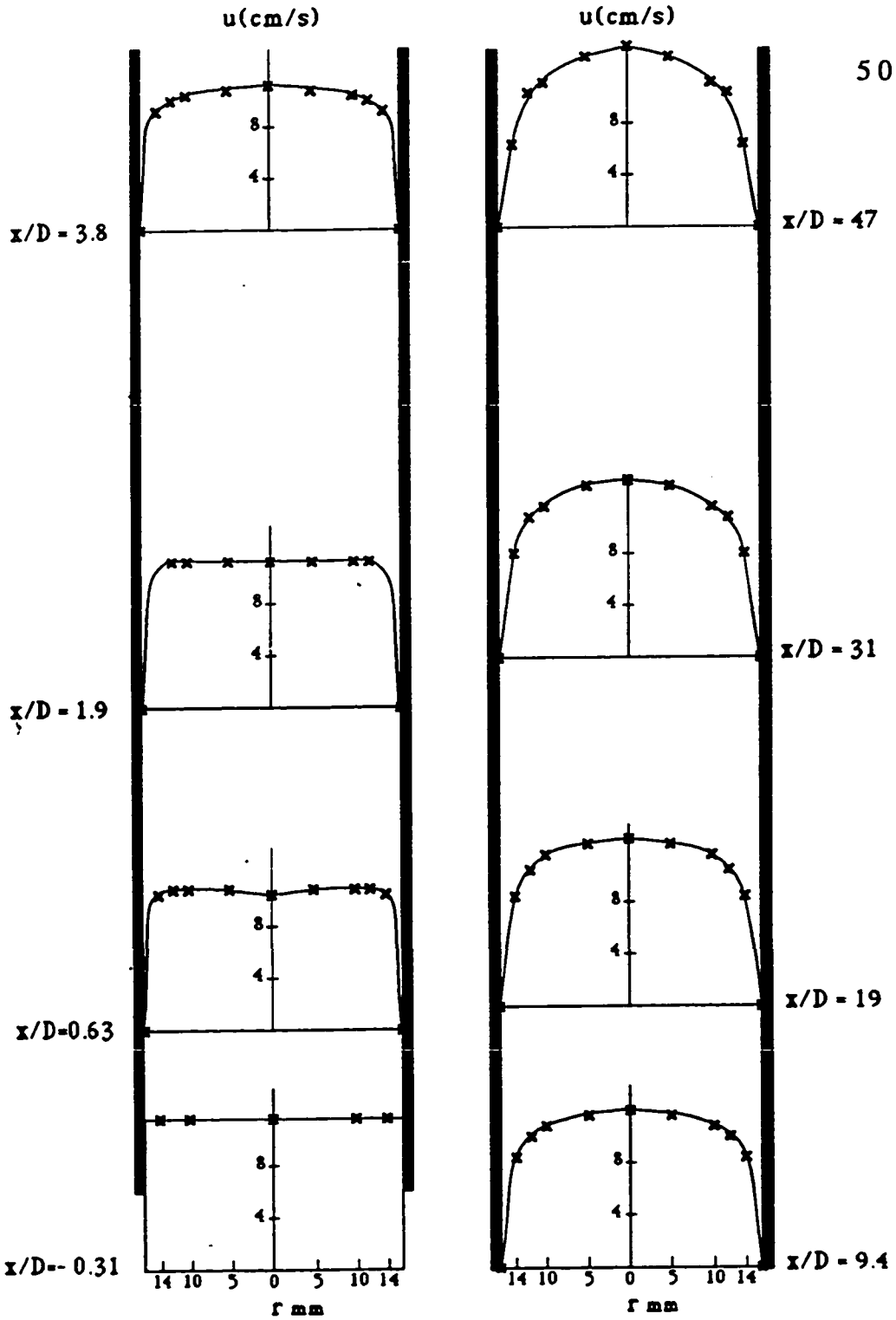

Figure 13 : Velocity profile development, Re = 3680

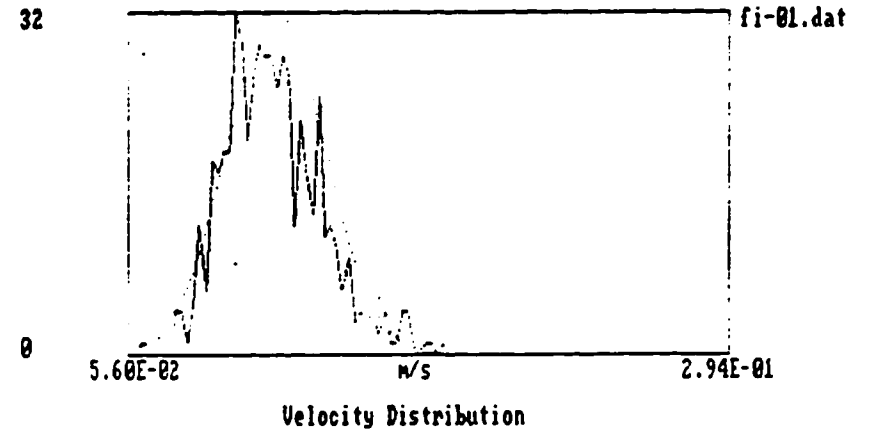

Mean	: 1.155E-01 m/s	Dist. From Inlet	: -1.000E+00 cm
Stand. deviat.	: 1.983E-02 m/s	Radial Distance	: 0.000E+00 mm

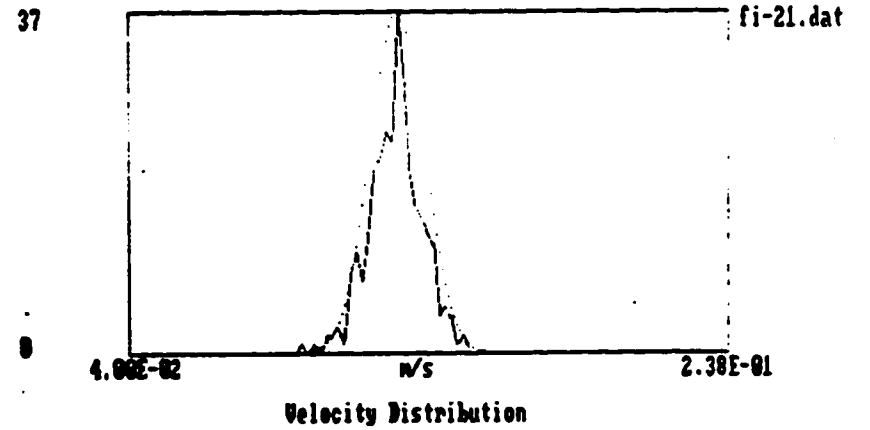

Mean	: 1.299E-01 m/s	Dist. From Inlet	: 3.000E+01 cm
Stand. deviat.	: 9.013E-03 m/s	Radial Distance	: 0.000E+00 mm

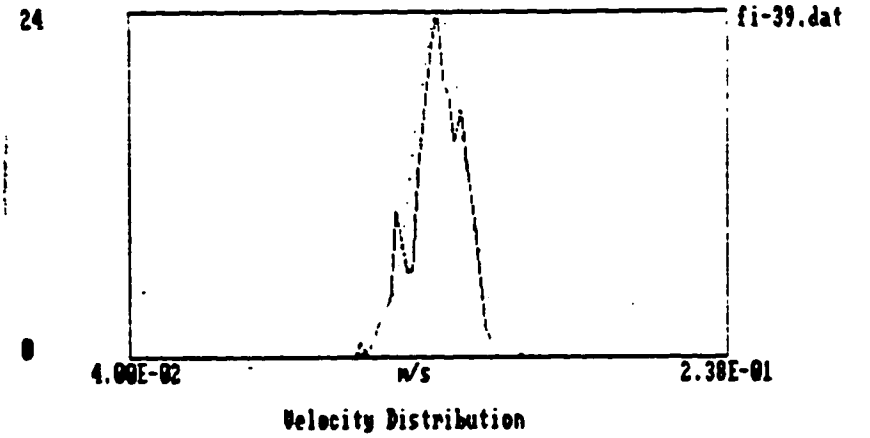

Mean	: 1.449E-01 m/s	Dist. From Inlet	: 1.500E+02 cm
Stand. deviat.	: 8.448E-03 m/s	Radial Distance	: 0.000E+00 mm

Figure 14 : Velocity Distributions, Re = 3680
(r = 0 mm, x = -1, 30, 150 cm)

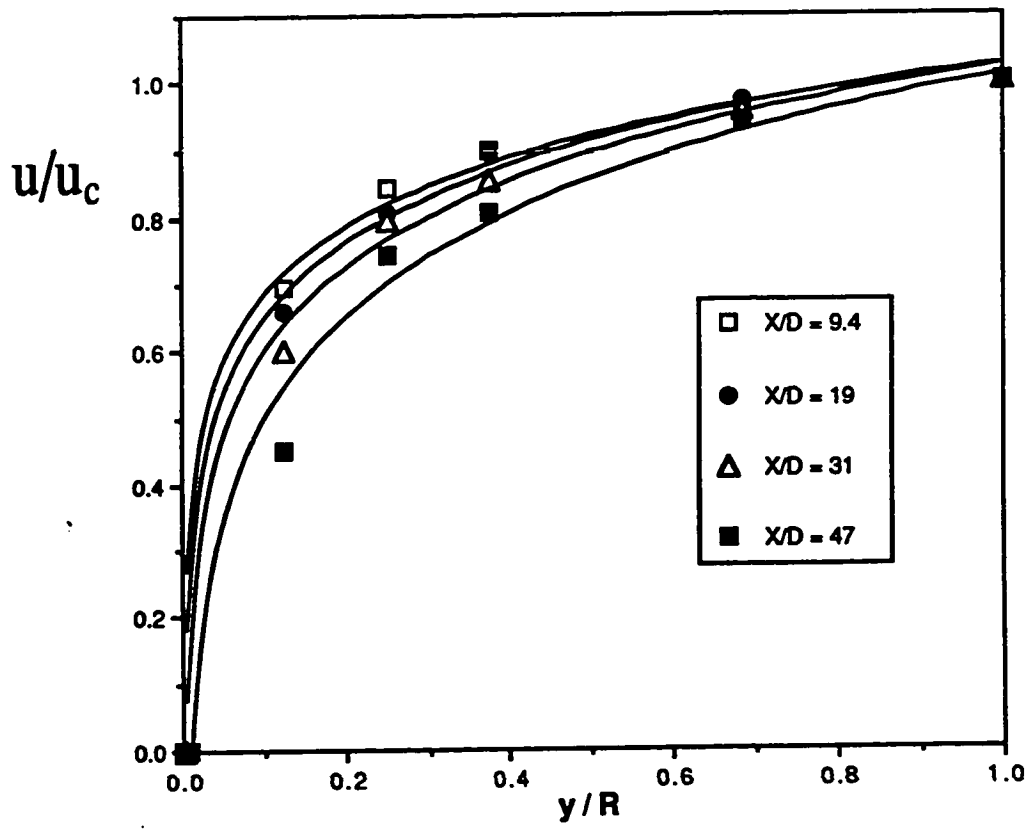

Figure 15 : Normalized mean velocity (u/u_c) versus normalized distance from the wall (y/R), Re = 3680, (x/D = 9.4, 19, 31, 47).

above conclusion. However since there is no known theoretical or empirical relations from which it is possible to obtain the $(\frac{u_{av}}{u_c})$ ratio for this particular Reynolds number, we have to derive this ratio from the experimental data reported by earlier researchers.

A plot of $(\frac{u_{av}}{u_c})$ for supposedly fully developed flows in the transitional region versus Reynolds number is given in [29]. From the best line that passes through the points shown in that graph, the $(\frac{u_{av}}{u_c})$ ratio that corresponds to Re = 3680 is equal to 0.742. For this case Δu_c can be written as

$$\Delta u_c = \left[\frac{(u_c)_{tran} - (u_c)_{exp}}{u_{av}}\right] x\ 100 \qquad (29)$$

Here $(u_c)_{exp}$ is the experimentally determined velocity at the centerline for Re = 3680 and $(u_c)_{tran}$ is the value for a "fully developed transitional profile", $(u_c)_{tran} = 1.348\ u_{av}$, where u_{av} is the average velocity values given in Table A.4(a)

The Δu_c obtained at different cross sections for Re = 3680 are shown in the following table

Table 3

Deviation of the centerline velocity from the transional value

x/D	0	0.63	1.9	3.8	9.4	19	31	47
Δu_c	34.8	34.6	31.3	19.3	11.3	7.89	2.17	-14.2

The negative value at x/D = 47 is due to the fact that the centerline velocity there is higher than the expected value, which is another indication that the flow is still developing.

The plot of the blockage factor B defined as

$$B = 1 - \left(\frac{u_{av}}{u_c}\right) \qquad (13)$$

against x/D (Fig. 16, Table A.4(b)) shows a remarkable similarity between the two curves obtained for Re = 1670 and Re = 3680. The B value increases rapidly from $B \approx 0$ at the entrance to B = 0.370 (Re = 1670) and B = 0.134 (Re = 3680) after a distance of only 10 diameters. The rate of increase slows down after that, but while in the case of Re = 1670 the blockage factor approaches it's fully developed value of B = 0.5, the blockage factor for Re = 3680 exceeds the expected value of B = 1 − 0.742 = 0.258 without attaining a fully developed profile.

From the above discussion one can conclude that not only the flow was not fully developed after an inlet length of 50 tube diameters but also

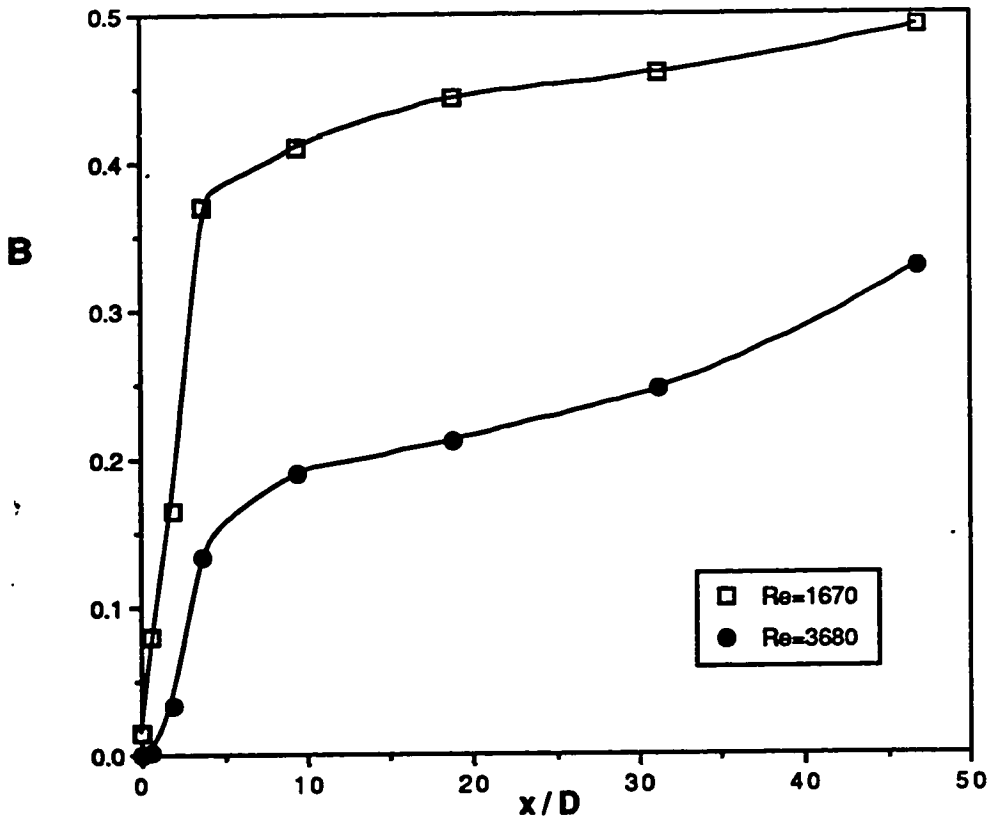

Figure 16 : Variation of the blockage factor with distance from inlet, Re = 1670, 3680.

that there is a probability that the value of $(\frac{u_{av}}{u_c})$ obtained from [29] actually does not represent a fully developed flow. It is of course questionable wether there is a fully developed flow for the transitional region.

3.1.3 Re ≐ 16700

A: Velocity Profile Development

A flow with this Reynolds number is considered in literature to be in the turbulent regime, where a power law profile is expected to be established after an inlet length of 20 to 50 tube diameters. The velocity profile development for this Reynolds number is shown in Fig. 17. The velocity profile at x/D = 0.63 behind the entrance shows no trace at all of the non-uniformity of the initial flow at x/D = -0.31 caused by the non-evenness distributio of the metallic fragments in the cage. It seems that the efficiency of the turbulence generator increases with the Reynolds number of the flow, or more specifically with the flow's bulk velocity. The average velocity profiles obtained for Re = 3680 and Re = 16700 are very much similar up to x/D = 3.8 behind the inlet. Starting from x/D = 9.4, the flow at Re = 16700 exhibits a slightly different velocity profile from the one obtained for the flow with Re = 3680. In the latter case particles close to the wall have relatively lower velocities. At x/D = 47 the two profiles are completely different. The obtained centerline velocity distributions for Re = 16700 at x = -1, 30 and 150 cm are shown in Fig. 18.

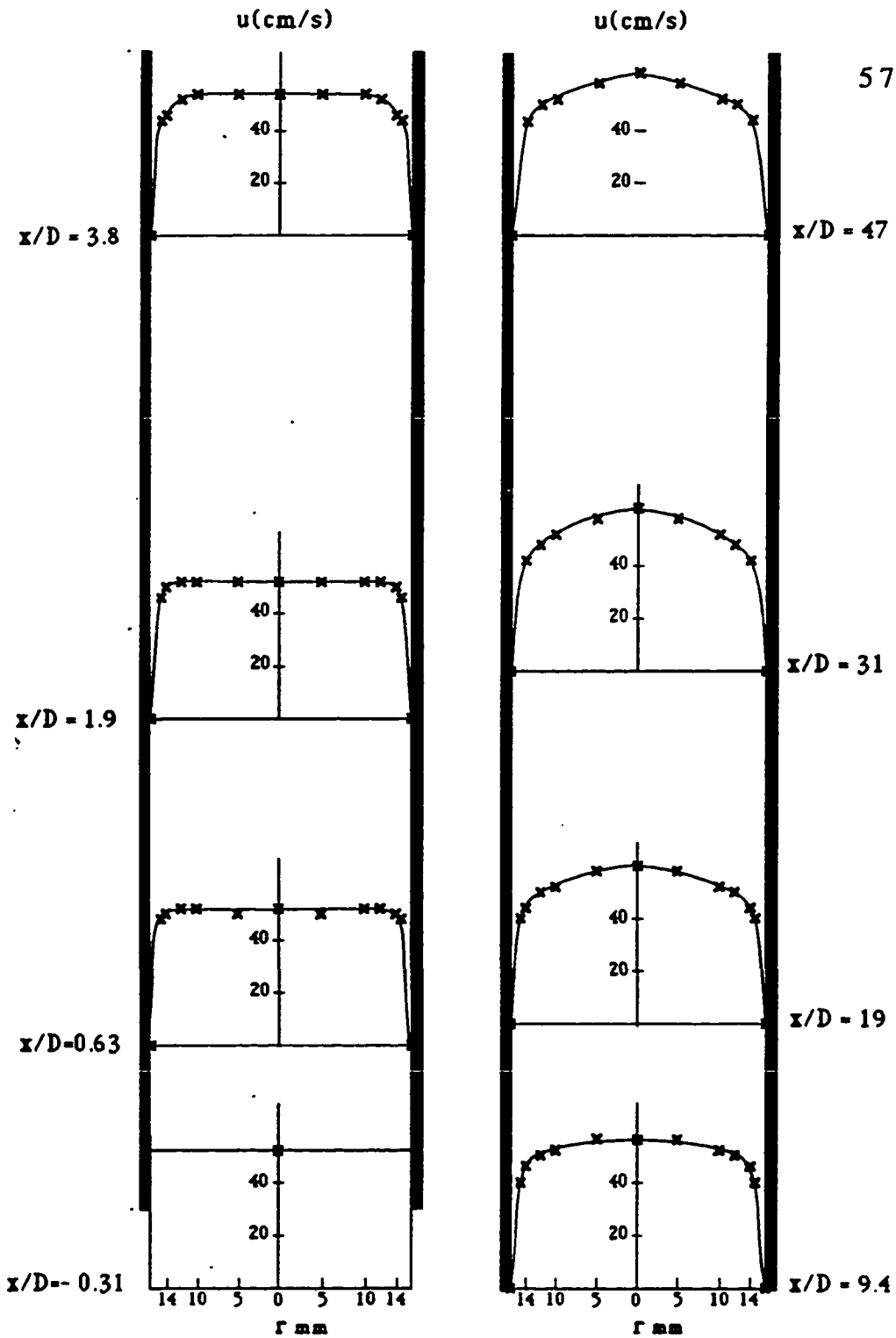

Figure 17 : Velocity profile development, Re = 16700

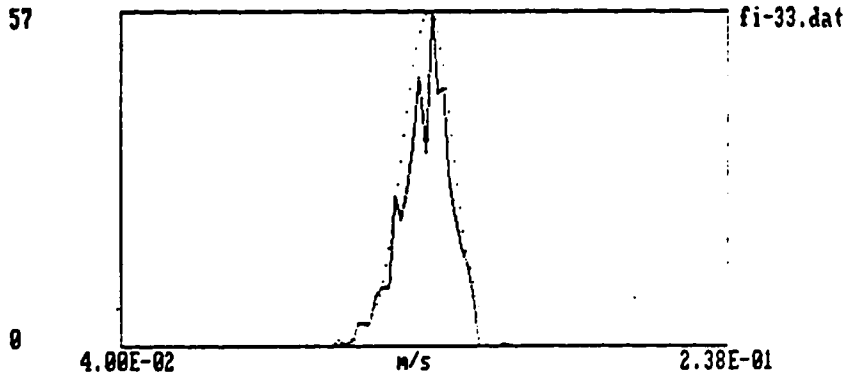

Mean	: 1.410E-01 m/s	Dist. From Inlet	: 1.000E+02 cm
Stand. deviat.	: 8.245E-03 m/s	Radial Distance	: 0.000E+00 mm

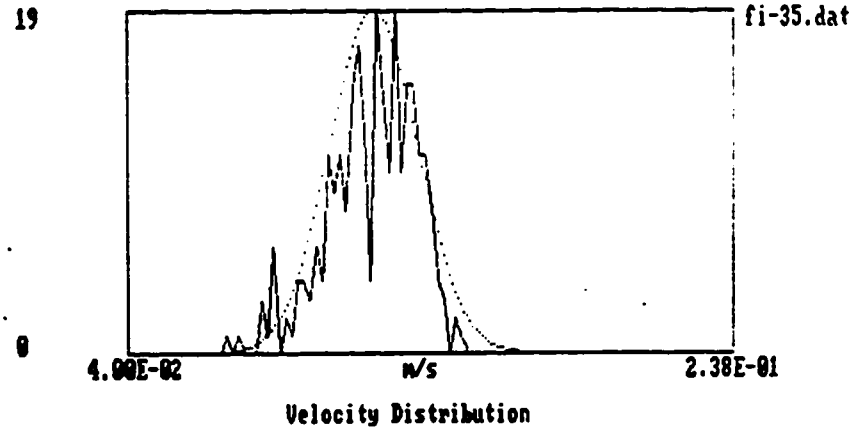

Mean	: 1.211E-01 m/s	Dist. From Inlet	: 1.000E+02 cm
Stand. deviat.	: 1.458E-02 m/s	Radial Distance	: 1.000E+01 mm

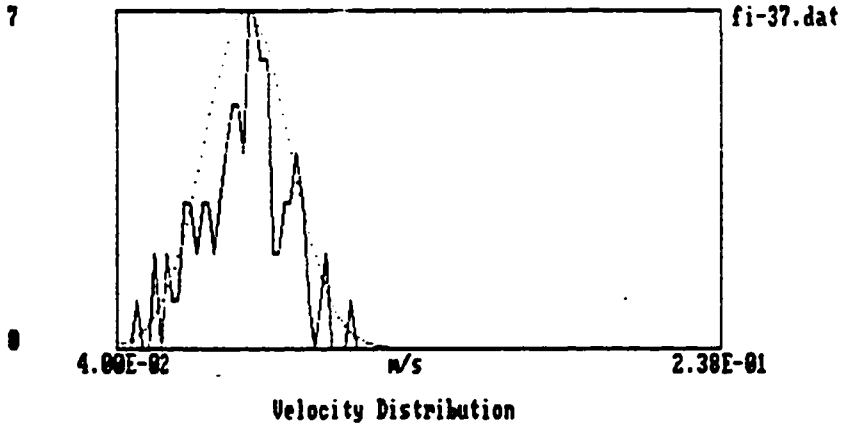

Mean	: 8.317E-02 m/s	Dist. From Inlet	: 1.000E+02 cm
Stand. deviat.	: 1.442E-02 m/s	Radial Distance	: 1.409E+01 mm

Figure 18 : Velocity Distributions, Re = 16700
(r = 0 mm, x = -1, 30, 150 cm)

The difference between the profiles obtained for the above two Reynolds numbers is also evident from the comparison of Fig. 15 and Fig. 19 which are plots of the normalized velocity (u/u_c) versus the normalized distance from the wall (y/R). Figure 19(b) is specially interesting since it shows that at $x/D = 31$ and $x/D = 47$ the two profiles are nearly identical, which may suggest that the flow had reached it's fully developed profile around $x/D = 31$ behind the inlet.

Figure 20 suggests that it is possible to describe not only the fully developed profile but also the developing profiles by a power law of the type

$$\frac{u}{u_c} = \left(\frac{y}{R}\right)^{1/N} \qquad (10)$$

This is specially true for $x/D > 10$. Since there is no known formula to us that relates the N value to the corresponding Reynolds number, we have to estimate the exponent N value that corresponds to Re = 16700 by other means. The power law representation by Schlichting [11] of the data obtained by Nikurdse [3] shows that the exponent N varies with Reynolds number as shown in the following table

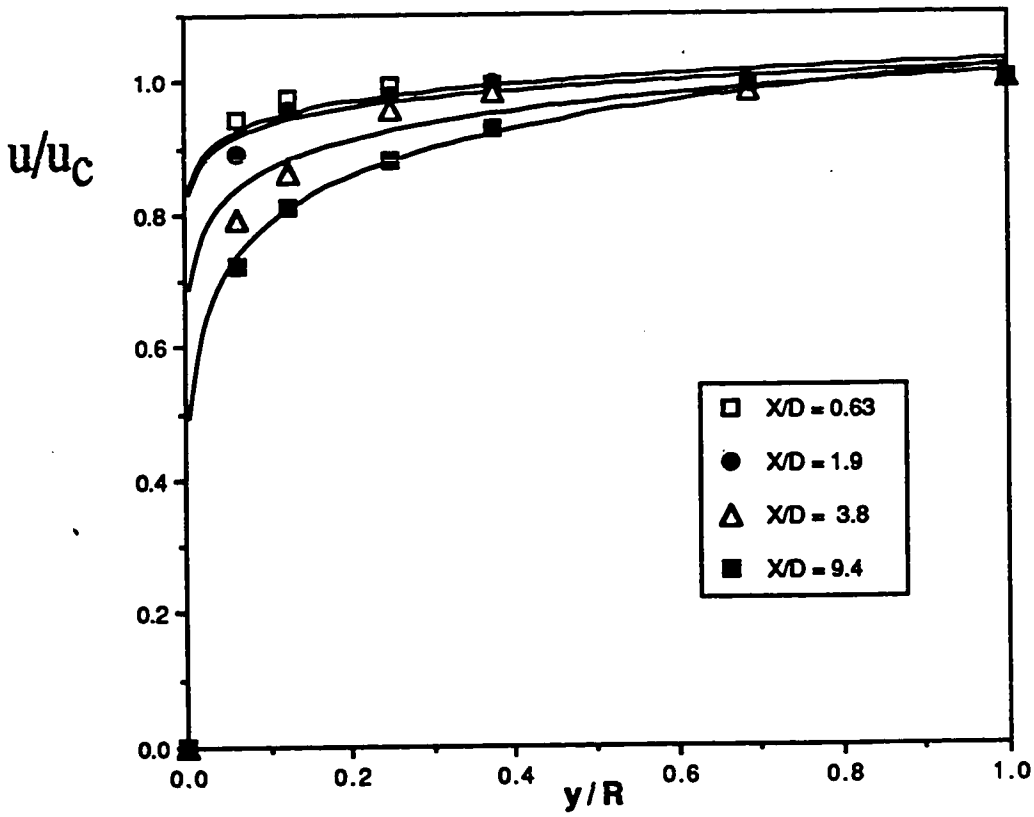

Figure 19(a) : Normalized mean velocity (u/u_c) versus normalized distance from the wall (y/R), Re = 16700,(x/D = 0.63, 1.9, 3.8, 9.4).

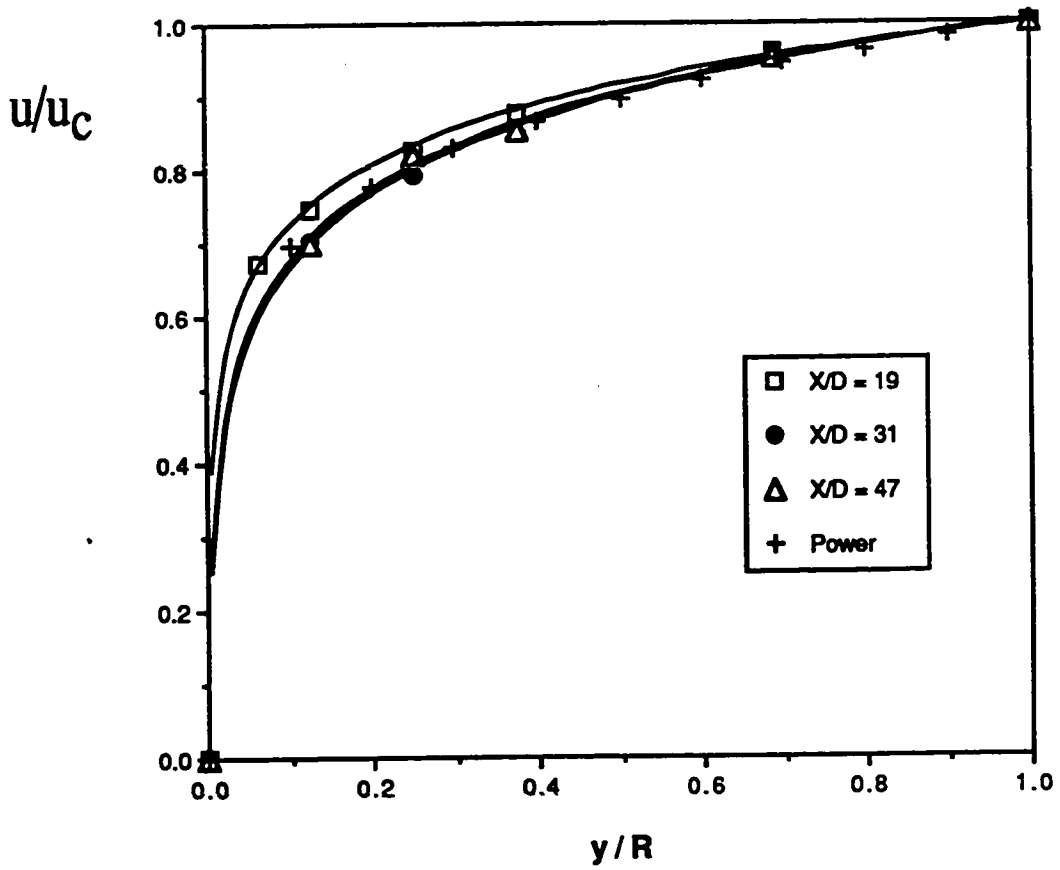

Figure 19(b) : Normalized mean velocity (u/u_c) versus normalized distance from the wall (y/R), Re = 16700, (x/D = 19, 31, 47, Power).

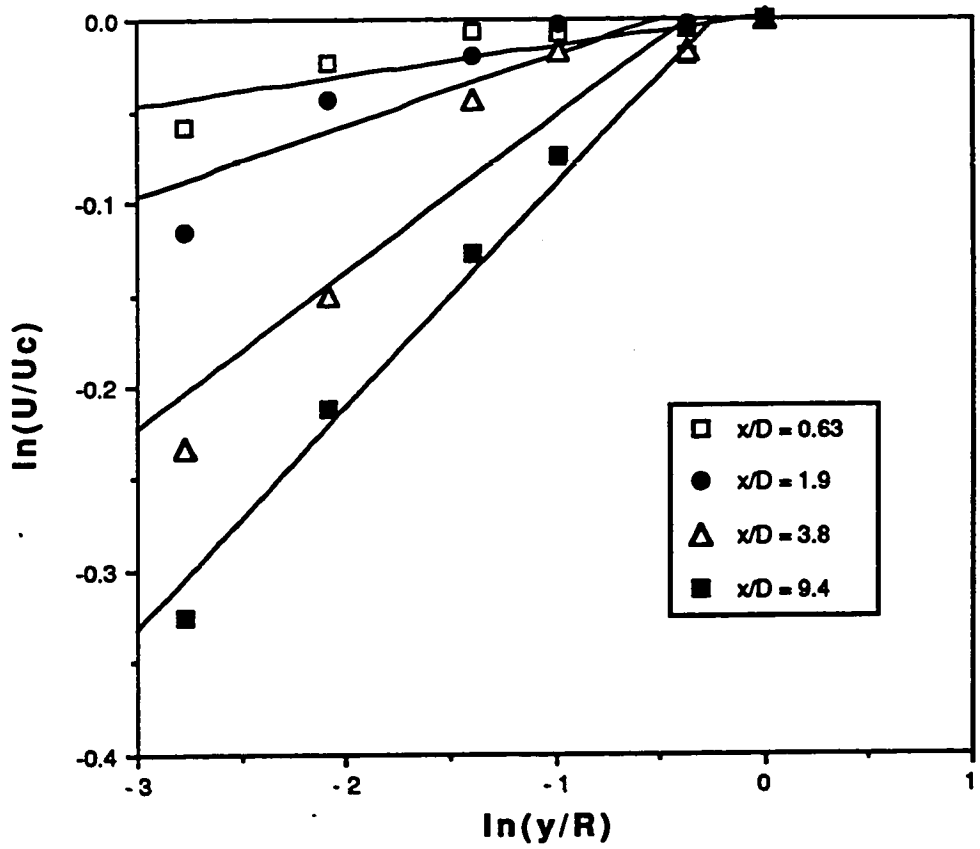

Figure 20(a) : Natural logarithim of the normalized mean velocity $\ln(u/u_c)$ versus natural logarithim of the normalized distance from the wall ln(y/R), Re = 16700, (x/D = 0.63, 1.9, 3.8, 9.4)

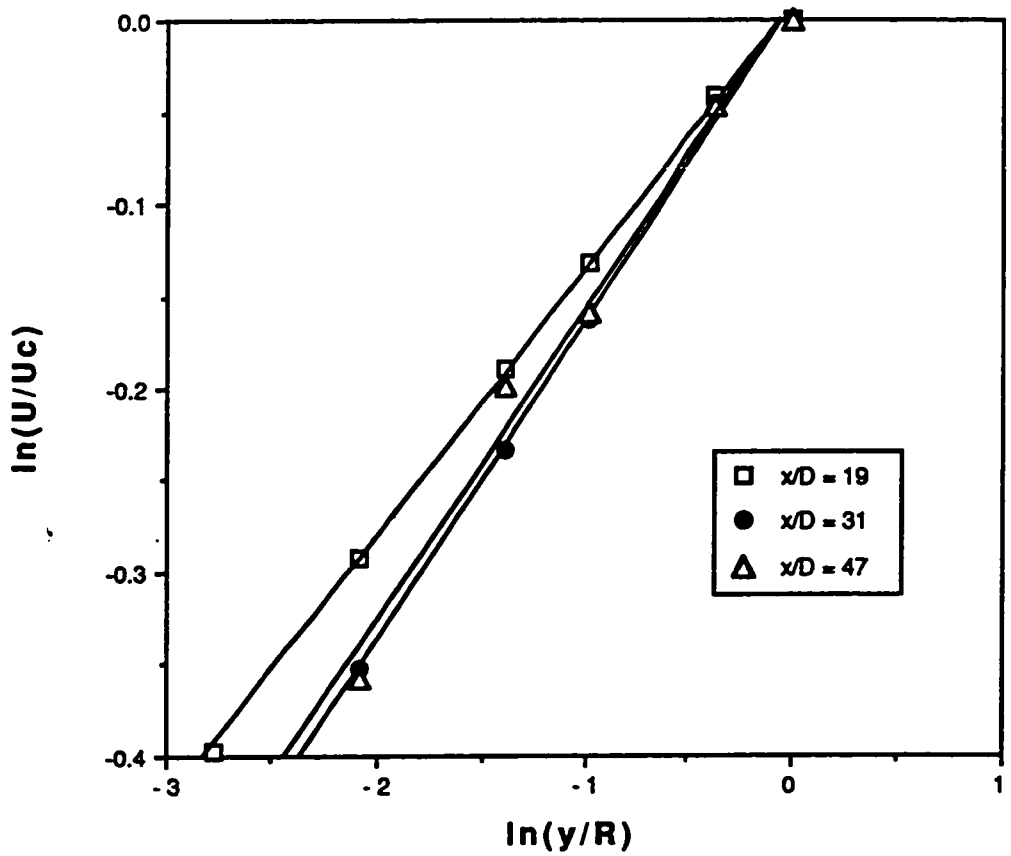

Figure 20(b) : Natural logarithim of the normalized mean velocity $\ln(u/u_c)$ versus natural logarithim of the normalized distance from the wall ln(y/R), Re = 16700, (x/D = 19, 31, 47)

Table 4

The exponent N value for different Reynolds numbers

Re	4.0×10^3	2.3×10^4	1.1×10^5	1.1×10^6	2.0×10^6	3.2×10^6
N	6.0	6.6	7.0	8.8	10	10

Assuming that between Re = 4000 and Re = 23000 the following linear relation is valid

$$N = a + b\,(Re) \qquad (30)$$

substituting Re = 4000 and Re = 23000 and the corresponding N values from table 8 the constants a and b are found to be

$$a = 5.874$$

$$b = 3.158 \times 10^{-5}$$

substituting Re = 16700 and the above values of a and b in eq-25, the resultant N value is N = 6.4.

The ratio of the average velocity u_{av} to the centerline velocity can be found in a similar way to the one used previously for laminar profile. Eq-10 can be written as

$$u(r) = u_c \left(1 - \frac{r}{R}\right)^{1/N} \qquad (31)$$

substituting u(r) in eq-24

$$u_{av} = \frac{2\int u(r)\, r\, dr}{R^2} \qquad (24)$$

will give the desired ratio as a function of N, the general solution to the above integral is

$$\frac{u_{av}}{u_c} = \frac{2N^2}{(N+1)(2N+1)} \qquad (32)$$

substituting N = 6.4 in the above equation yields the following value for $(\frac{u_{av}}{u_c}) = 0.802$.

B: The Deviation From The Turbulent Profile

The same criteria used before for Re = 1670 and Re = 3680 to estimate when the flow is fully developed will be applied here too. The following table shows the Δu_c values obtained for this Reynolds number at each cross section. Δu_c is defined here as

$$\Delta u_c = \left[\frac{(u_c)_{turb} - (u_c)_{exp}}{(u_{av})} \right] x\ 100 \qquad (33)$$

where $(u_c)_{exp}$ is the experimentally determined centerline velocity and $(u_c)_{turb}$ is the value for the fully developed turbulent flow, $(u_c)_{turb} = 1.247\ u_{av}$, where u_{av} is the average velocity obtained at each distance from the inlet and recorded in table A.4(a).

Table 5

Deviation of the centerline velocity from the turbulent value

x/D	0	0.63	1.9	3.8	9.4	19	31	47
Δu_c	24.7	21.7	20.8	15.5	9.10	2.61	-3.19	-2.04

The negative values of Δu_c at x/D = 31 and x/D = 47 can be easily explained by considering the plot of of the blockage factor B versus the normalized distance x/D for Re = 16700 (Fig. 21). Klein [8] has shown that B increases gradually until at about 40 diameters it reaches a value that exceeds the expected value of B for a fully developed profile. Beyond this maximum value, B decreases again to the expected value for such flow.

Recalling the definition of the blockage factor

$$B = 1 - \left(\frac{u_{av}}{u_c}\right) \qquad (10)$$

For B to have a value higher than the value expected for fully developed profile, u_c must be higher than the expected value $(u_c)_{turb}$. In turn this means that Δu_c will have negative values. The expected B value for Re = 16700 is B = 1 - 0.802 = 0.198. Using the information given in both Table A.4(b) and Table 5, at x/D = 19 cm B has a value of 0.181 which is lower than expected value, (Δu_c = 2.6), at x/D = 31, B = 0.218 which is higher than the expected value, (Δu_c = -3.2), at x/D = 47, B = 0.211.

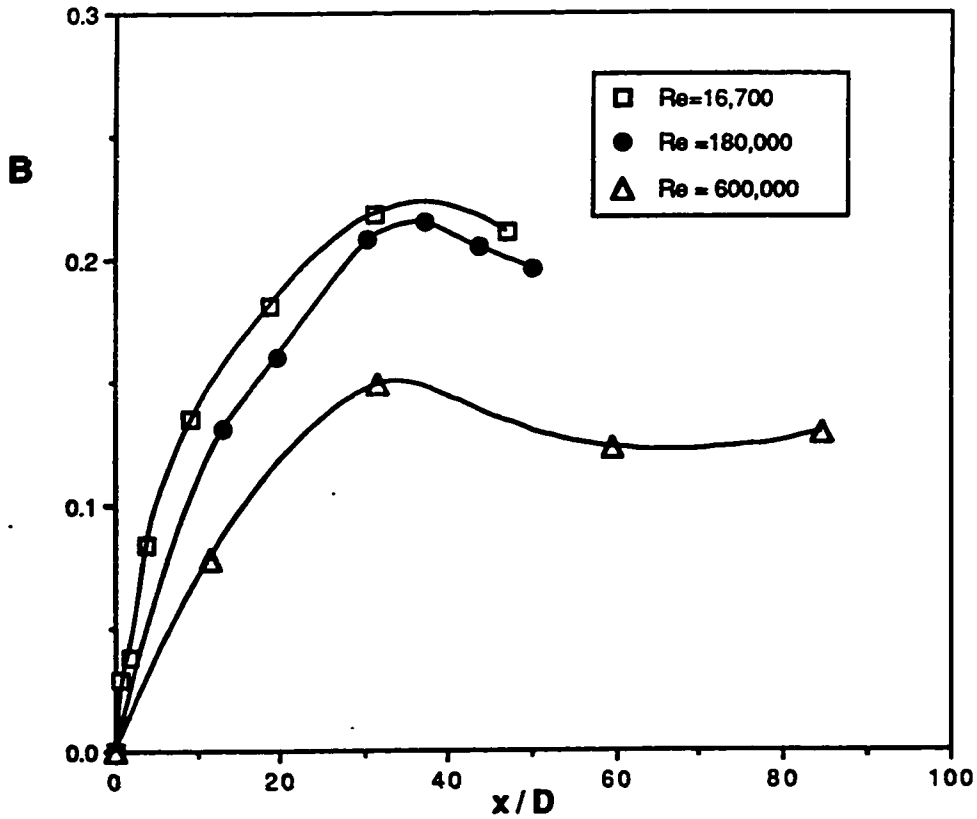

Figure 21 : Variation of the blockage factor with distance from inlet (□: present,....•, Δ: Ref.8).

This value is still higher than the expected value but since it is lower than the maximum B value we should expect Δu_c to be less negative, which is the case indeed since Δu_c at x = 150 cm is equal to -2.0 .

C: The Inlet Length

The question of when the flow develops fully arises again. It is clear from Table 5 that Δu_c crosses the 5 % limit value after a distance of 30 to 60 cm inside the tube which corresponds to an inlet length in the range of $L \approx 10\,D$ to 19 D. However, the blockage factor has a maximum value around $x/D \approx 31$. which as shown by Klein this maximum shortly precedes the actuall establishment of the fully developed profile. Therefore we believe that the true inlet length is in the range of L = 31 to 47 tube diameters.

We can easily compare this inlet length with the inlet length values predicted by the empirical and semi-empirical formulas given by previous researchers for the same Reynolds number.

1. Latsko (1950) :

$$\frac{L}{D} = 0.625\,(Re)^{1/4} \qquad (11)$$

Sub. Re = 16700 in the above equation yields L = 7 D. This inlet length is far shorter than the one obtained in our experiment and that could be attributed to the fact that Latsko assumed a 1/7 velocity profile in the inlet region, where actually the 1/7 power can be used

to describe fully developed profile in the range $2.5 \times 10^4 \leq Re \leq 1.5 \times 10^5$.

2. Bowlus and Brighton (1962) :

$$\frac{L}{D} = 14.25 \log_{10} Re - 46 \qquad (12)$$

Sub. Re = 16700 in this equation gives an inlet length value of 14 tube diameters. It is clear that although the inlet length value predicted by Bowlus and Brighton compare favourably with Barbin and Jones experimental data for Re = 3.88×10^5, their predicted value for a much lower Reynolds number is smaller than the actual inlet length.

3. Salami (1986) :

$$N = 5.16 + 2.18 \times 10^{-6} \left(\frac{L}{D}\right) Re \qquad (14)$$

Sub. N = 6.4 and Re = 16700, the inlet length predicted by the above equation is L = 34 D. This value lies in the range of inlet lengths obtained in our experiment.

4. Janna (1989) :

$$\frac{L}{D} = 4.4 (Re)^{1/6} \qquad (15)$$

Sub. Re = 16700 in this equation yields L = 22.2 D.

We believe that the difference between our measured value for the inlet length and the values given by the above relations is due to the fact that most studies on turbulent developing pipe flow were carried out on Reynolds numbers exceeding 100,000, where the empirical formulas given above give results close to the actual experimental findings.

It can be also seen from Fig. 21 that the maximum B value in our experiment, $B_{max} = 0.233$ is clearly higher than the maximum blockage factor values reported by Klein [8], i.e. $B_{max}=0.155$ for Re = 13×10^5 (Miller [27]) and $B_{max}=0.215$ for Re = 1.8×10^5 (Cockrell and Markland [28]), which also confirms the conclusion reached by Klein, namely that larger Reynolds numbers produce lower peak values, and smaller Reynolds numbers higher peak values.

3.2 Turbulence Intensity

Figures 22-24 show, for the three studied Reynolds, numbers the variation of the turbulence intensity with distance from the inlet. The turbulence intensity σ is defined as

$$\sigma = \frac{\sqrt{<u'^2>}}{u} \qquad (9)$$

where u' is the random velocity fluctuation about the time mean velocity value u at any instance of time. The above figures are based on the turbulence intensity data given in Tables A.6, A.7 and A.8.

A common observation in all three figures is that unlike the velocity profiles, where the velocity increases in the middle region of the tube and decreases at points close to the wall, turbulence intensity profiles show the complete opposite behavior, turbulence decreases in the central region and increases near the wall. Figure 25 give an example of the change in the velocity distributions along the cross section (Re = 3680, x = 100 cm, r = 0, 5, 14 mm). The following is a comparisons among the turbulence profiles obtained in this study.

3.2.1 Re = 1670

A: Turbulence Intensity Development

We propose a definition of the average turbulence intensity as

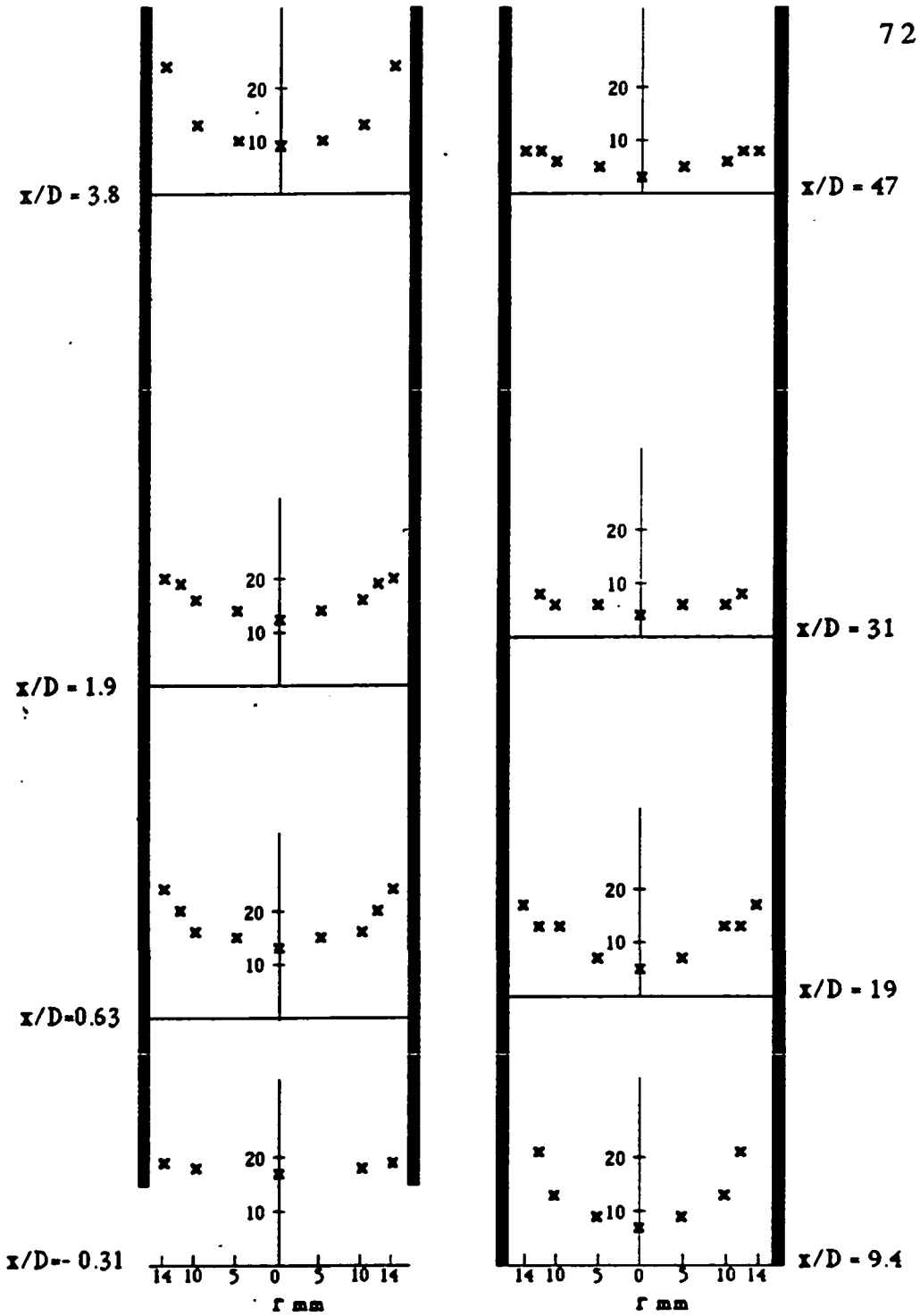

Figure 22 : Turbulence Intensity, Re = 1670

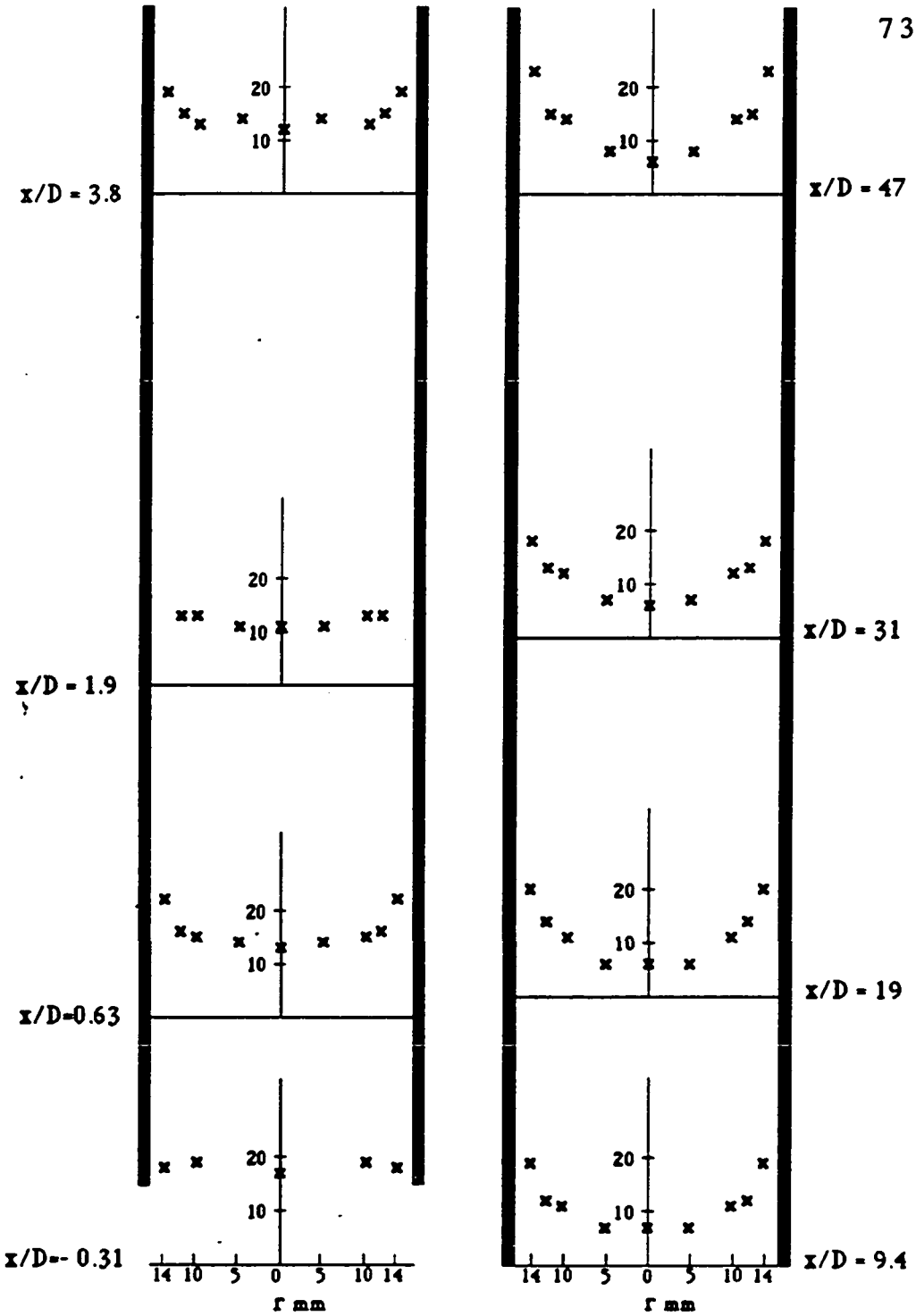

Figure 23 : Turbulence Intensity, Re = 3680

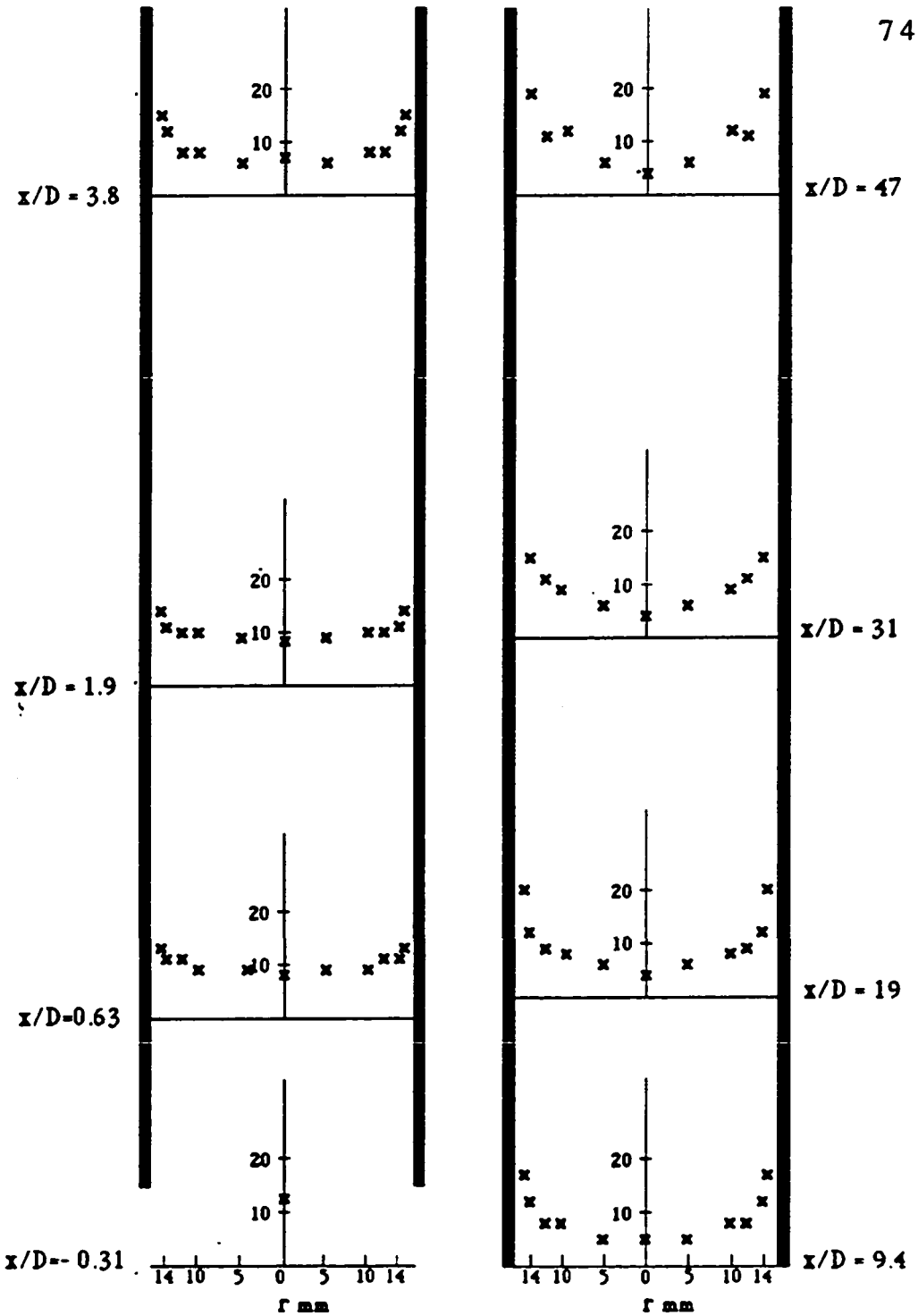

Figure 24 : Turbulence Intensity, Re = 16700

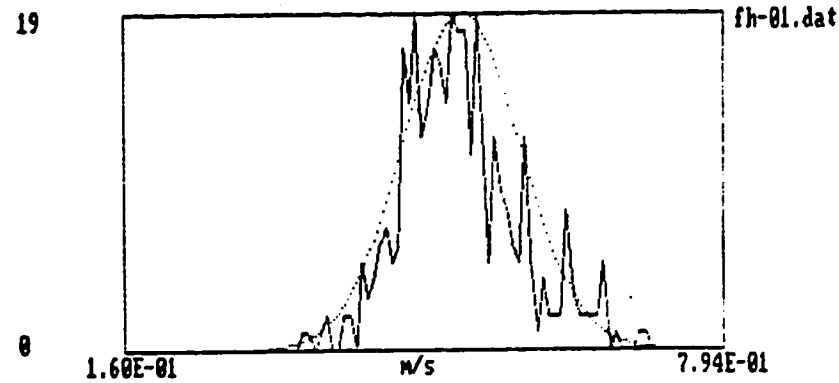

Velocity Distribution

Mean	: 5.157E-01 m/s	Dist. From Inlet	: -1.000E+00 cm
Stand. deviat.	: 6.270E-02 m/s	Radial Distance	: 0.000E+00 mm

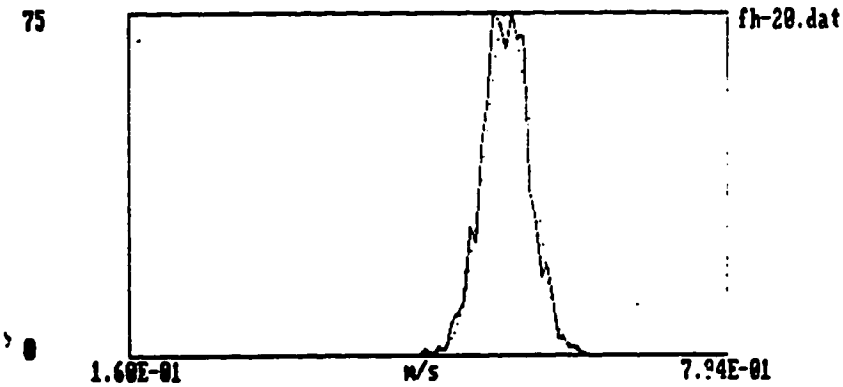

Velocity Distribution

Mean	: 5.600E-01 m/s	Dist. From Inlet	: 3.000E+01 cm
Stand. deviat.	: 2.507E-02 m/s	Radial Distance	: 0.000E+00 mm

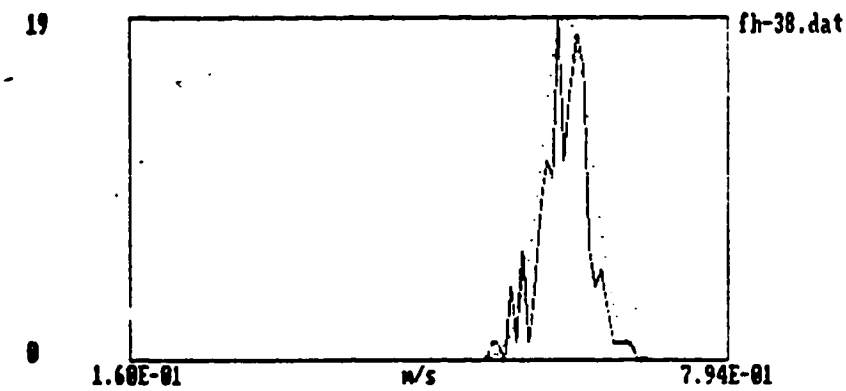

Velocity Distribution

Mean	: 6.230E-01 m/s	Dist. From Inlet	: 1.500E+02 cm
Stand. deviat.	: 2.630E-02 m/s	Radial Distance	: 0.000E+00 mm

Figure 25 : Velocity Distributions, Re = 3680
(x = 100 cm, r = 0, 5, 14 mm)

$$\sigma_{av} = \frac{2\int \sigma(r)\, r\, dr}{R^2} \qquad (34)$$

Table A.9 gives at each distance behind the inlet the corresponding average turbulence intensity σ_{av}. In our experiment it was not possible to get more than 1 mm close to the wall (because our r-scanning device has a precision of only 0.5 mm), Therefore, σ_{av} in fact represents the average turbulence of the bulk of the flow, the integral limits are taken from r = 0 to r = 14, and R^2 = 196. The average turbulence intensity for Re = 1670 decays exponentially - as can be seen from Table A.9 and Fig. 26 - from it's initial high value of 18 % to a value around 3 % near the exit, which means that the establishment of the laminar profile was accompanied by an overall reduction of more than 80 % in the turbulence intensity. Figure 27 shows for Re = 1670 the velocity fluctuations at the centerline as a function of time at x = -1, 30 and 150 cm.

A plot of the turbulence intensity decay at each r-distance from the centerline (Fig. 28) shows that for x/D > 5 the decay has a better exponential fitting at r = 0, 5 and 14 mm than at r = 10, 12. The decay rates k together with the CI values are given below : (CI or the "Correlation Index" is a measure of how good the regression curve fits the data, $0 \le CI \le 1$, CI = 1 for perfect fitting.)

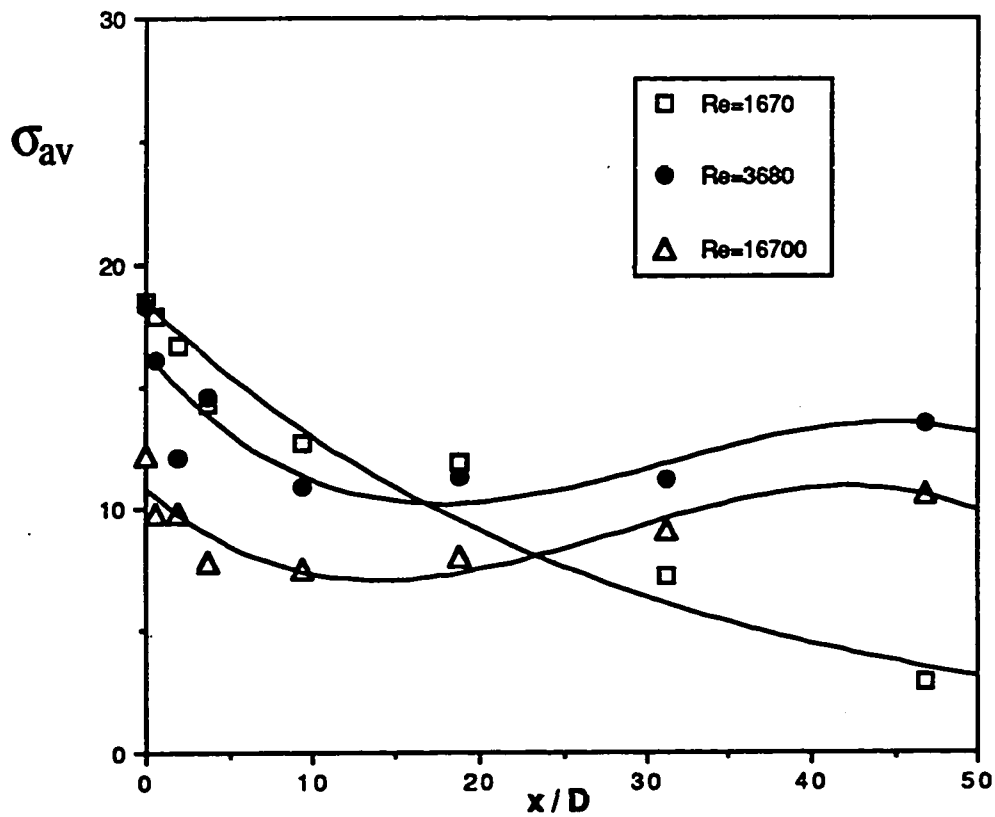

Figure 26 : Variation of the average turbulence intensity σ_{av} with distance from inlet.

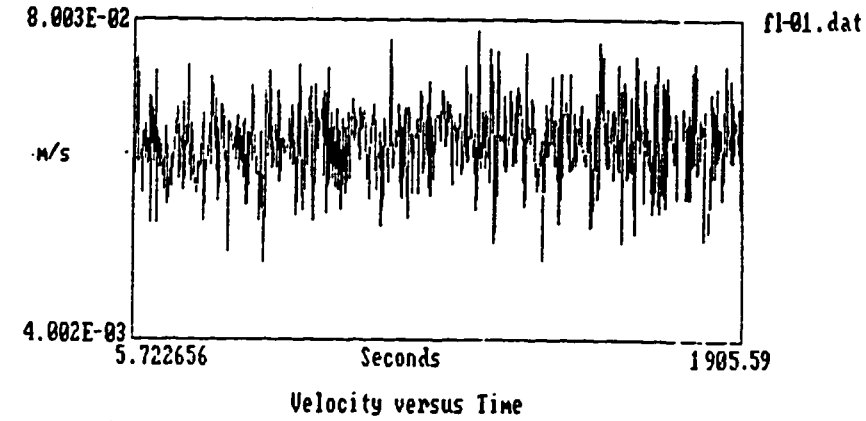

Dist. From Inlet : -1.000E+00 cm
Radial Distance : 0.000E+00 mm

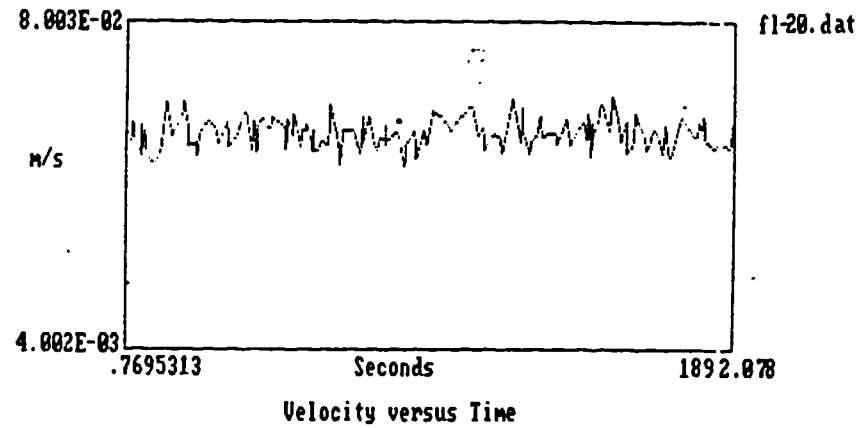

Dist. From Inlet : 3.000E+01 cm
Radial Distance : 0.000E+00 mm

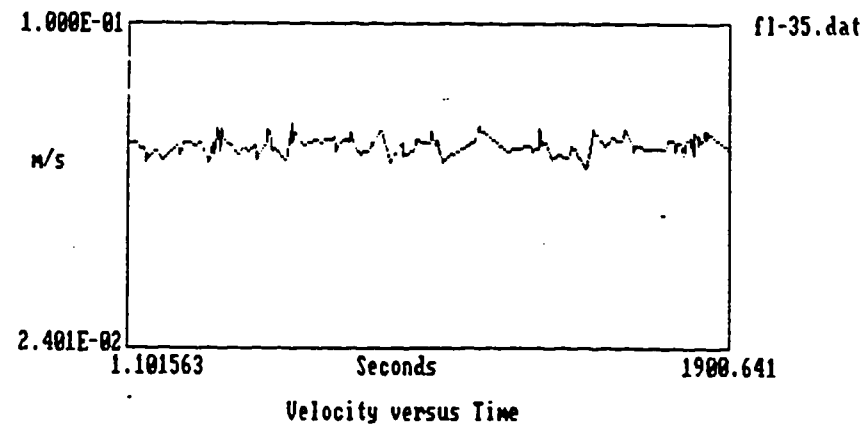

Dist. From Inlet : 1.500E+02 cm
Radial Distance : 0.000E+00 mm

Figure 27 : Velocity versus time distributions, Re = 1670
(r = 0 mm, x = -1, 30, 150 cm)

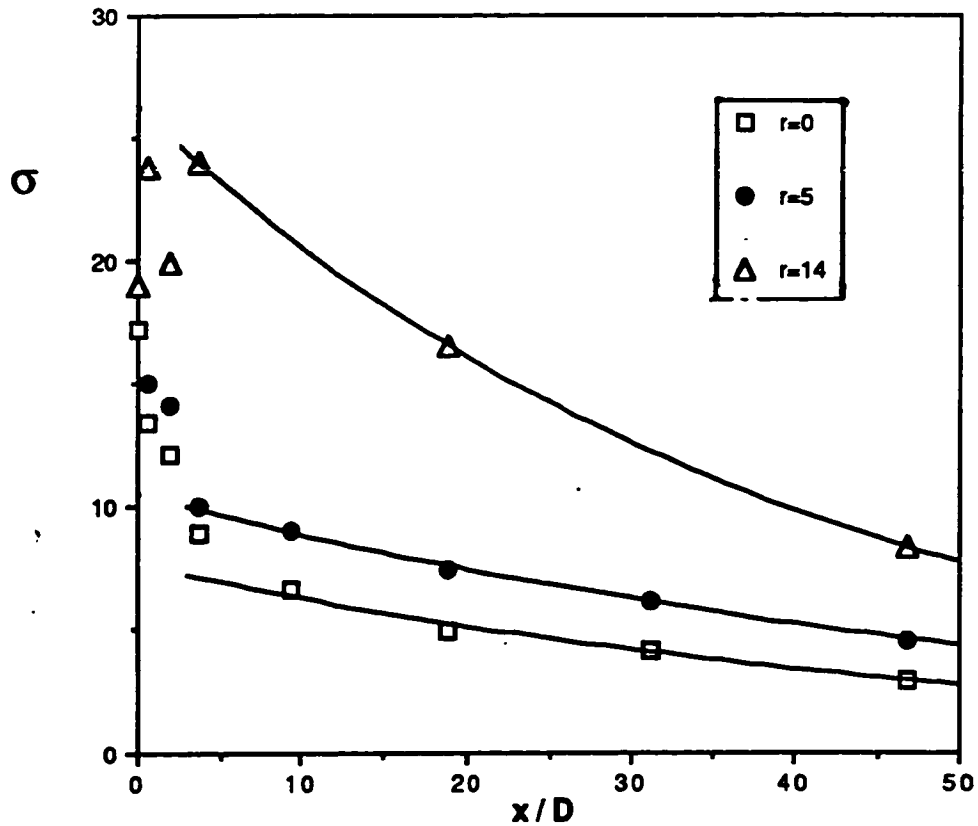

Figure 28(a) : Decay of turbulence intensity σ with distance from inlet, Re = 1670, (r = 0, 5, 14 mm).
(A good exponential fit for x/D > 5)

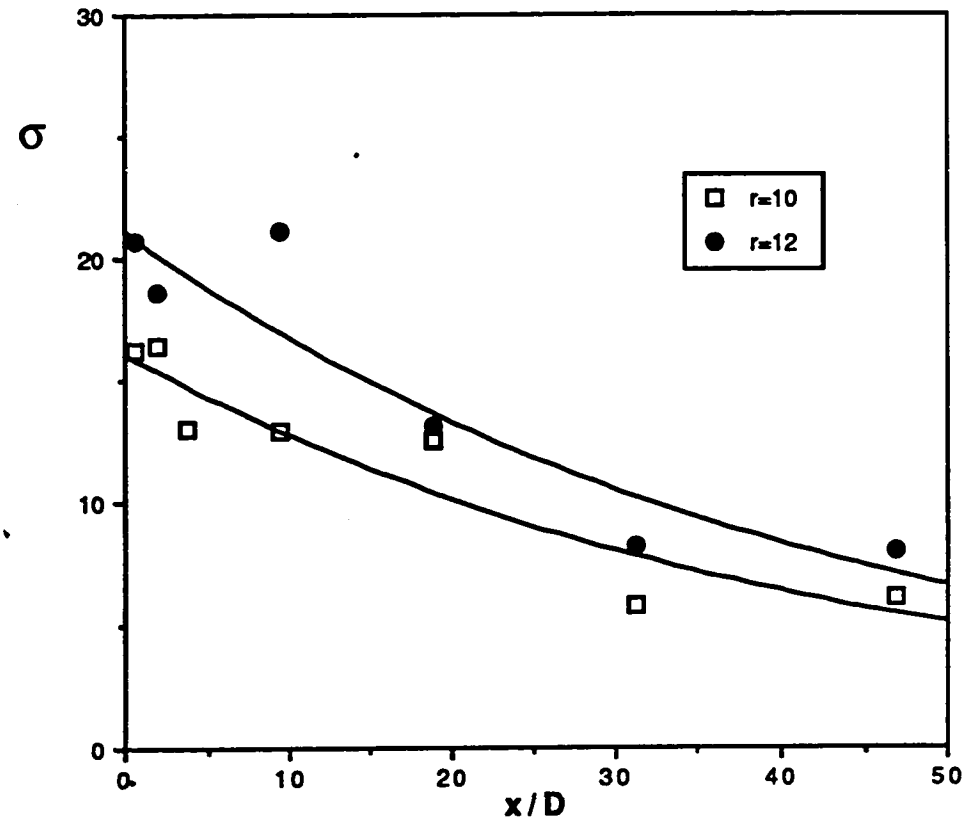

Figure 28(b) : Decay of turbulence intensity σ with distance from inlet, Re = 1670, (r = 10, 12 mm).
(A poor exponential fit for all values of x/D)

k(r=0) = 0.021,	CI = 0.984
k(r=5) = 0.018,	CI = 0.998
k(r=10) = 0.024,	CI = 0.768
k(r=12) = 0.026,	CI = 0.833
k(r=14) = 0.025,	CI = 1.000

This should come as no surprise to us since as mentioned in 1.2.5 one of the characteristics of relaminarizing flows is the exponential decay of the turbulence intensity at points near the centerline and at points near the wall but still close to the centerline.

B: The Decay of The Mean Velocity Fluctuations

One other characteristic of relaminarizing flows also discussed in section 1.2.5 is the exponential decay of the maximum value of the mean velocity fluctuations $<u'^2>_m$ as

$$<u'^2>_m \sim \exp(-k_o x/D) \qquad (19)$$

where k_o is a constant that depends on Reynolds number. Table A.10 gives the standard deviation values obtained at each distance from the inlet. The maximum $<u'^2>_m$ values obtained from Table A.10 are given in the following table

Table 6

The maximum value of the mean velocity fluctuations

x/D	0	0.63	1.9	3.8	9.4	19	31	47
$<u'^2>_m$	0.96	0.85	0.66	--	0.40	0.27	0.12	0.08

Figure 29 shows a plot of $<u'^2>_m$ versus x/D. For x/D > 5, $<u'^2>_m$ decays exponentially according to

$$<u'^2>_m = 0.65 \exp(-0.048x/D) \qquad (35)$$

It's interesting to note that both the turbulence decay rate (k_o) and the decay rate of Δu_c are nearly equal. The decay of the turbulence intensity of the flow goes hand in hand with the establishment of the laminar profile.

We can easily compare the decay rate value $k_o = 0.048$ obtained here with those obtained by other researchers for pipe and channel flows. From [12] it is possible to estimate the decay rates obtained previously for different Reynolds numbers as follows :

Sibulkin [14]: (pipe flow)

$$Re = 1200, \qquad k_o = 0.064$$

Laufer [13]: (pipe flow)

$$Re = 1400, \qquad k_o = 0.038$$

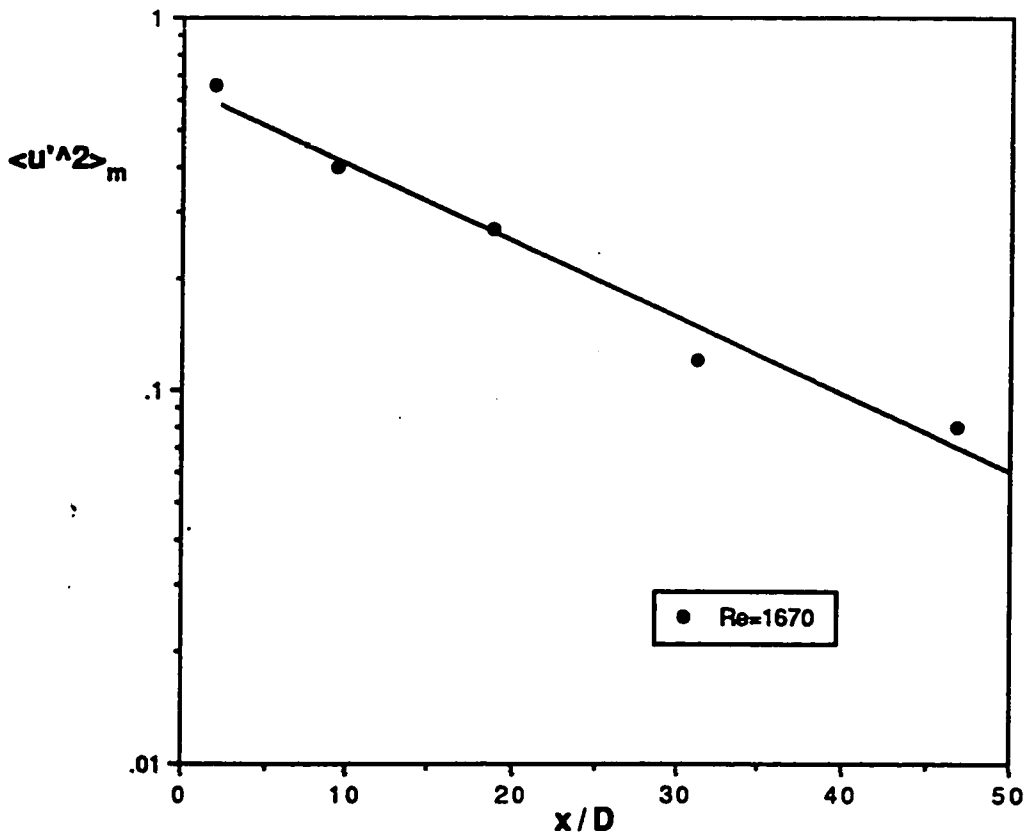

Figure 29 : Decay of the maximum value of the mean velocity fluctuations $\langle u'^2 \rangle_m$ with distance, Re = 1670.

Badri-Narayanan [16]: (channel flow)

Re = 1250,	k_o = 0.039
Re = 1730,	k_o = 0.023
Re = 1960,	k_o = 0.008
Re = 2500,	k_o = 0.002

Figure 30 shows these decay rates together with the one obtained here. It is clear that the decay rate k_o obtained in our study is again nearly twice the expected value for the same Reynolds number if we were using similar set up to the one employed in the studies shown above.

It should be mentioned here that in drawing Fig. 22 (and also Fig. 23 and Fig. 24) it was assumed that the velocity fluctuations u'(t) about the time mean value u is symmetric. There are as many particles with speeds lower than the mean as there are with speeds higher than the mean. However, a study on the symmetry of the velocity distributions along the centerline (Section 3.3) shows that most of the time the flow exhibits a small but nevertheless clear asymmetry in the velocity fluctuations about the mean value. This unfortunately means that these figures give only an approximate picture to the real turbulence intensity profiles.

3.2.2 Re = 3680 and Re = 16700

Although the flows with these Reynolds numbers had different velocity profiles specially near the end of the tube (Re = 16700 had a fully

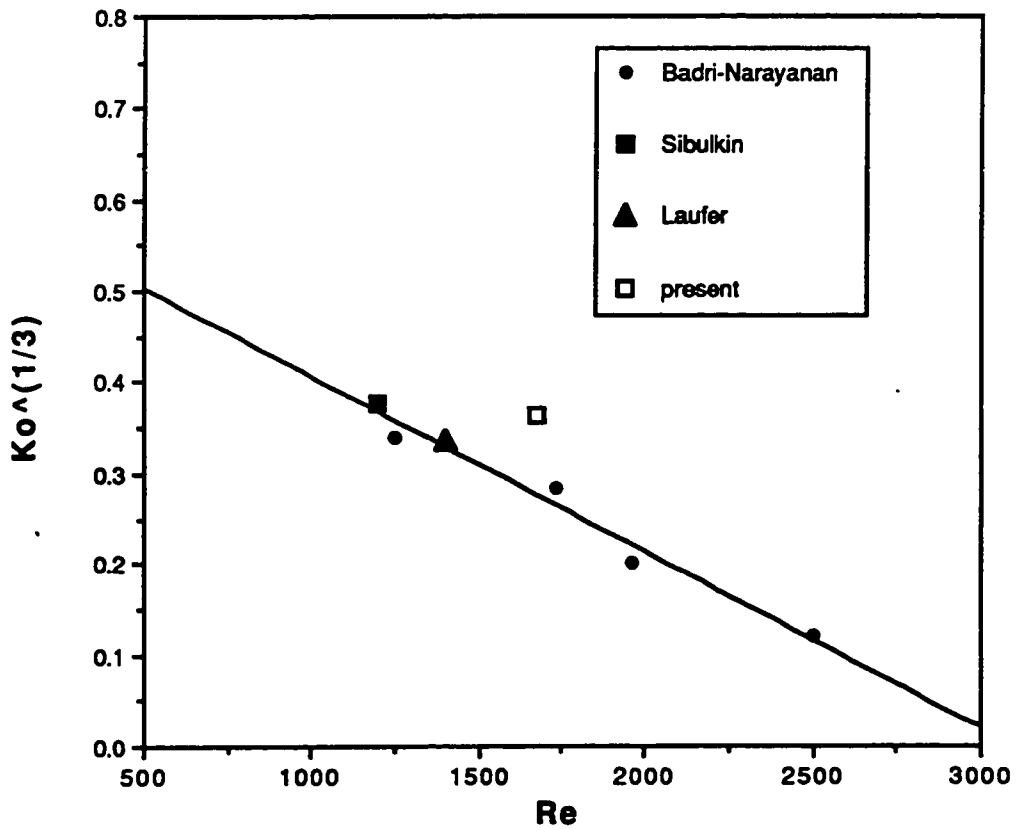

Figure 30 : Dependence on Reynolds number of the turbulence decay rate K_o.

developed profile at x/D = 47, Re = 3680 had not), nevertheless thier turbulence profiles as can be seen from Fig. 23 and Fig. 24 show a great deal of resemblance which may justify putting them both under one subtitle.

Figure 31 shows that for Re = 3680 the turbulence intensity at the centerline decreases rapidly from it's initial value of 17 % to a lower value of 7 % after an inlet length of only 10 diameters. Up to this point the decay follows the one obtained for Re = 1670, beyond that the turbulence intensity of the lower Reynolds number flow keeps decreasing while the turbulence intensity of the transitional flow stays more or less the same. Similarly the centerline turbulence intensity of the Re = 16700 decays from σ = 12 % at the entrance to σ = 5 % after the same distance of 10 diameters and stays nearly constant downstream.

Regarding the average turbulence intensity σ_{av} both flows again show very similar behavior. σ_{av} decreases from it's initial value to a minimum value at x/D $\approx$ 10 and then start increasing again. This can be clearly seen in Fig. 26 which is a plot of σ_{av} values given in Table A.9(a) versus x/D. The ratio of the σ_{av} value at x = 10 D and the σ_{av} value at the entrance is around 0.6 for both Re = 3680 and Re = 16700 (Table A.9(b)). The fact that after a distance of only 10 diameters the flow is 40 % less turbulent in our opinion is very important. It suggests that in certain situations where it is essential to keep turbulence under control, for example in the case of flow in curved pipes where turbulence increases after going through the

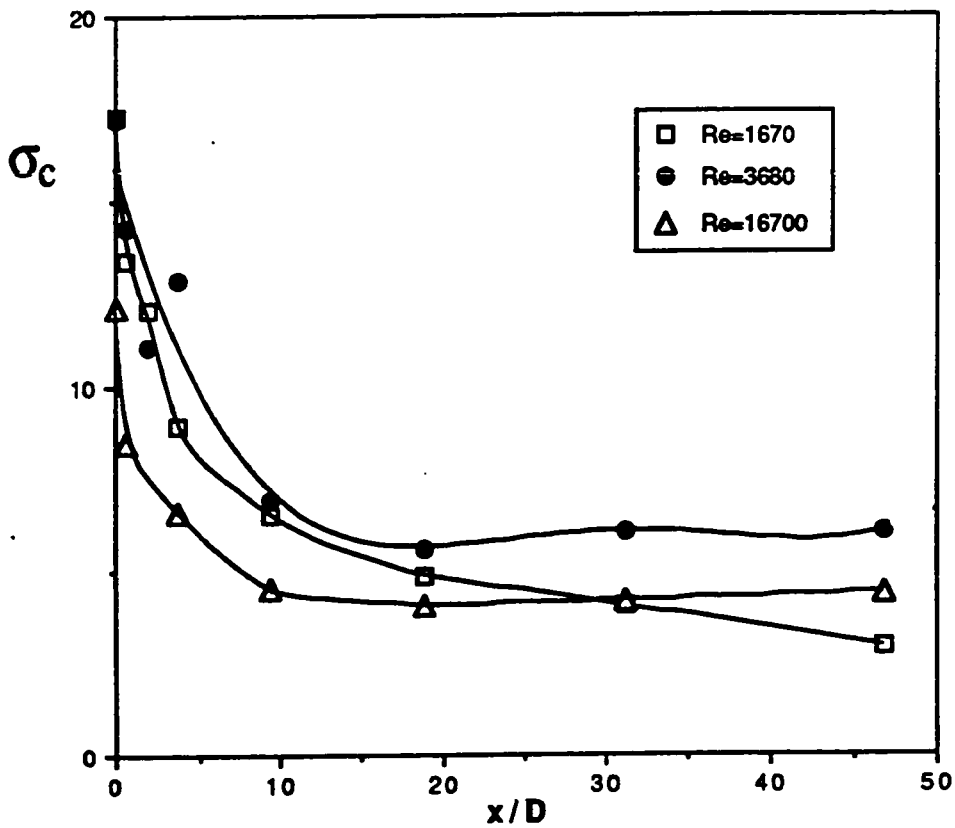

Figure 31: Variation of the centerline turbulence intensity σ_c with distance from inlet.

curve, it is possible to eliminate much of the created turbulence by inserting a short tube (or a bundle of short tubes) in the flow stream on the condition that the tube's length does not exceed 10 diameters. This is just an idea originated by the results obtained here and it has to be tested in an actual set up before it is approved effective.

3.3 Skewness and Kurtosis

To our knowledge, no one attempted before to study the higher statistical moments of the velocity profiles of a relaminarizing flow. The third moment (Skewness) and the fourth moment (Kurtosis) are defined as [30] :

$$\text{Skew} = \frac{1}{N}\sum_{i=0}^{N}\left[\frac{x_i - \bar{x}}{\sigma}\right]^3 \qquad (38)$$

$$\text{Kurt} = \frac{1}{N}\sum_{i=0}^{N}\left[\frac{x_i - \bar{x}}{\sigma}\right]^4 \qquad (39)$$

In order for these higher moments to be meaningful, it is a must to have a large number of measured values (x_i's). In our experiment, this is true only in the measurements taken at points along the centerline. Therefore, the following discussion will be confined to the variation of these moments along the tube's axis. The data of Fig. 32 and Fig. 33 are given in Table A.11 and Table A.12.

Skewness is a nondimensional quantity that characterizes the degree of asymmetry of a distribution around the mean value. The skewness value of a normal (Gaussian) distribution is zero. A positive skewness value signifies a distribution with an asymmetry tail extending out towards higher values around the average value, while a negative skewness value indicates that the asymmetry tail extends out towards lower values around the average value.

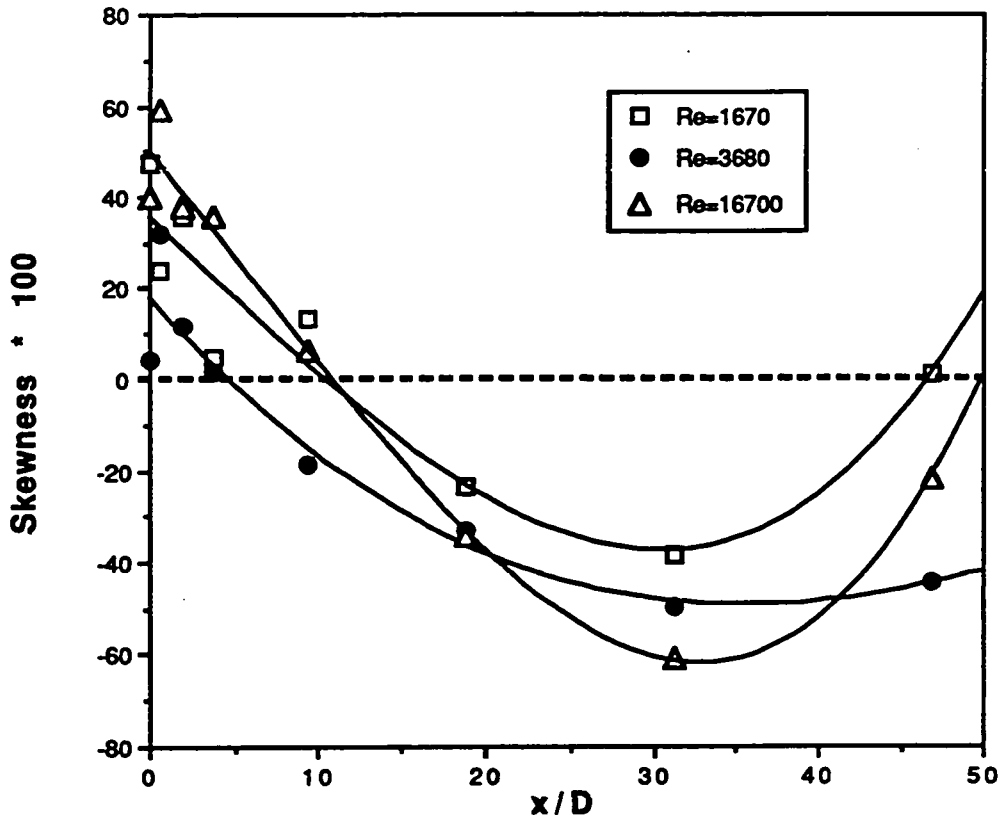

Figure 32 : Variation of the skewness value at the centeline with distance form inlet

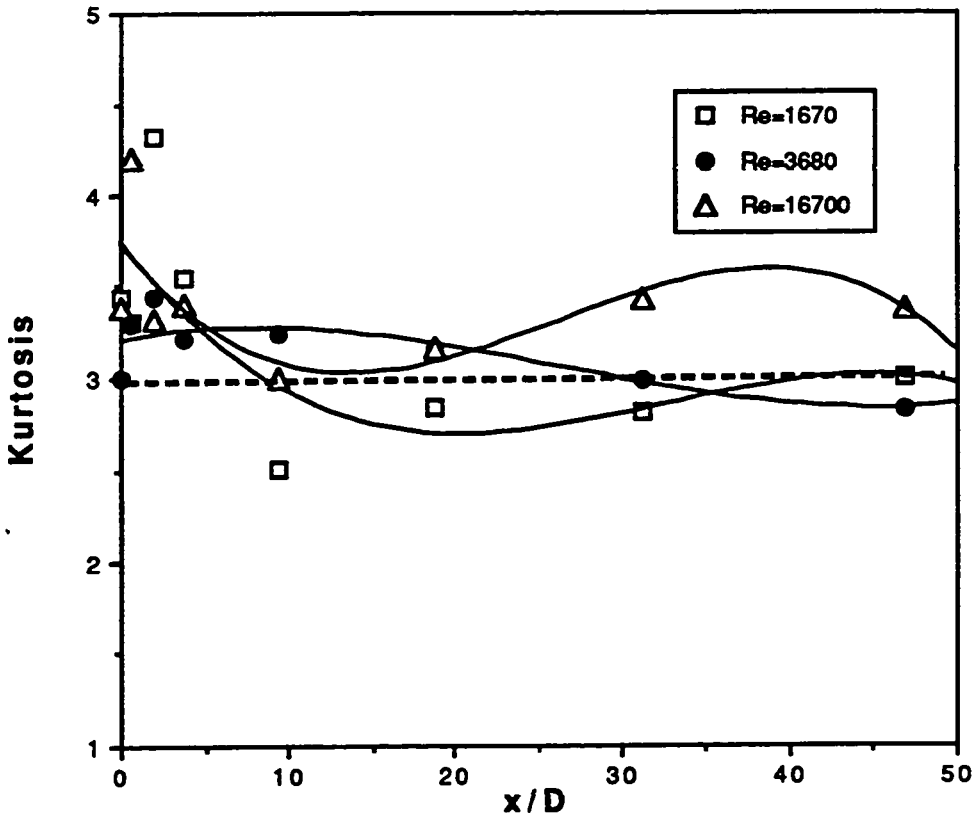

Figure 33 : Variation of the Kurtosis value at the centerline with distance from inlet.

The skewness values obtained in our experiment were between 0.6 and -0.6. Figure 32 describes the variation of the skewness value at the centerline with distance from the inlet. It can be immediately seen that there exists a clear trend for the skewness to start with a positive value at the entrance, probably induced by our turbulence generating cage and, as the flow approaches it's fully developed profile, the skewness value changes from positive to negative inside the tube and close to zero (the Gaussian value) near the end.

The asymmetry of the velocity distribution is mostly affected by both the upstream history of the flow and by the sign of the radial velocity v and, therefore, on the direction of the turbulent transport.

A velocity distribution with a negative skewness means that the most probable value of the velocity is higher than the mean velocity, which in turn indicates that the flow was at a higher speed upstream. Similarly, if the the flow had a lower speed upstream then the velocity distribution will have its most probable value lower than the mean value and hence the distribution will be positively skewed.

The effect of the direction of the turbulent transport on the asymmetry of the distribution was studied by Ribeiro and Whitelaw [31]. Velocity distributions were obtained in the self-preserving region of a round free jet at 57 diameters. Their results showed that velocity distributions on the centerline is nearly symmetric and no dependence on the sign of v exists. Away from the centerline a positive v (outward transport) is associated

with a Gaussian u distribution, and a negative v (inward transport) is associated with a positive skewed distribution of the axial velocity.

For the case in hand, close to the exit, true for Re = 1670 and Re = 16700, the velocity profiles are supposedly fully developed and hence there should be no change in the velocity profiles. Therefore, the centerline velocity distribution is expected to be Gaussian. Figure 32 shows that this the case indeed.

In the developing region of the flow, although the velocity distributions along the centerline are expected to be positively skewed (since the flow is at a higher speed upstream all the time), The obtained distributions infact show the opposite skewness sign. A satisfactory explanation of this disagreement should include a study of the effect of the other flow parameters, especially the effect of the radial velocity on the axial velocity distribution in the developing region.

Kurtosis is also a nondimensional quantity that measures the relative peakedness or flatness of a distribution relative to a normal distribution. A normal distribution has a Kurtosis value of 3. As far as we can tell from Fig. 33 which is a plot of the Kurtosis value of the centerline velocity distribution against the normalized distance, there exists no physical correlation between the Kurtosis value and other flow characteristics.

CHAPTER IV

CONCLUSIONS AND RECOMMENDATIONS

4.1 Summary of Results

Following are the conclusions that can be drawn from the the results of the present investigation :

1. Experimental Set Up :

- The present design of the LDA optical components utilized in this experiment enabled us to successfully obtain the needed information with great ease.

- It was essential to come up with a way to produce a uniform highly turbulent profile at the entrance to the tube. Although simple in design, the cage used to generate turbulence was capable of generating nearly homogeneously distributed turbulence intensities that exceed 10% even for bulk velocities as high as 50 cm/sec.

2. Relaminarization :

- For relaminarization in tubes it is not necessary to have a diffuser at the inlet. Our tube immersed in the flow clearly showed that a laminar profile was established at $x \approx 45$ D for the initially highly

turbulent, low Reynolds number flow Re = 1670. This inlet length was determined from eq-27 which expresses the deviation Δu_c of the experimentally determined centerline velocity from the value for a fully developed laminar flow as a function of the distance inside the tube.

$$\Delta u_c = 54.2 \exp(-0.053x/D) \qquad (27)$$

The exponential decay of Δu_c clearly described by eq-27 is a major characteristic of relaminarized flows. If we choose Δu_c = 5 % as the limit after which the flow is assumed to be fully relaminarized, then substituting this value in eq-27 will immediately yields the above inlet length value. This value agrees well with one calculated from Schlichting's formula L ≈ 0.03 D Re. Our results confirm the previous conclusion by Narasimha and Sreenivasan that only a critical Reynolds number governs the processes in which viscosity is responsible for achieving relaminarization.

- Both the rate at which the velocity profiles approach the fully developed laminar profile and the decay rate of velocity fluctuations were found to be higher than those reported by previous researchers who achieved relaminarization in pipes by allowing the flow to go from one section of the pipe where the flow has a Reynolds number higher than a certain critical Reynolds number (Re_{cr}) via a diffuser to another section where the flow has a Reynolds number lower than the critical Reynolds number.

3. Inlet Length :

- No fully developed profile was obtained for Re = 3680. It is clear that the distance required for full flow development exceeds 50 tube diameters which is the length of the tube used in this experiment. In fact the existence of a fully developed flow in the transitional region is questionable.

- The inlet length value for the Re = 16700 flow was estimated to be in the range of 31 to 47 tube diameters. This result is in disagreement with what is predicted by some of the empirical and semi-empirical formulas given by previous researchers.This could be due to the fact that these formulas were originally written to fit the inlet length values obtained for flows with much higher Reynolds numbers.

4. Skewness and Kurtosis :

- The deviation of the velocity distributions along the centerline from the Gaussian profile was not large. However, the clear trend of the skewness value to start with a positive value at the entrance and changes to a negative value near the end indicates that there may exist some correlation between the skewness value and other flow parameters such as turbulence intensity and blockage factor. No such correlation is expected however between the kurtosis value and other flow parameters.

- If the results concerning the variation of the skewness value with distance along the tube were later verified by a more detailed study at points not only on the axis but also along the whole cross section, in our opinion we may have reasons to doubt that the basic representation of the instantaneous velocity in case of a turbulent flow as symmetric velocity fluctuations about a mean value

$$u(t) = u \pm u'(t)$$

is not completely true.

4.2 Recommendations

As a continuation of this line of investigation, we propose the following,

- For a better representation of the velocity profiles and a more accurate estimate of the average values, it is necessarily that measurements should be taken at more radial distances, preferably at points much closer to the wall. However, this requires the fabrication of a scanning device with a very high precision.

- If it happens that later study was conducted on a flow with turbulence intensities that exceeds 20%, it is recommended that a frequency shifter be used to have a distinction between positive and negative velocities of equal magnitude. A burst counter type processor may also be useful for better signal processing.

- In this study it was found that the average turbulence intensity of the transitional and turbulent flows with Re = 3680 and Re = 16700 dropped nearly 40 % after only a distance of 10 diameters. It was concluded that by placing a bundle of small tubes near locations where turbulence is expected to be created (e.g. curved pipes) then it is possible to keep turbulence under control and possibly reduce the overall resistance of bends etc to a flow. Of course this concept has to be tested more thoroughly in a future study.

Appendix A

For representation of the values in Appendix A . various discrimination levels are taken into account

Table A.1(a)
Mean velocity u (cm/s), Re = 1670

Radial dis. (mm)	Distance from inlet (cm)							
	x=-1	x=2	x=6	x=12	x=30	x=60	x=100	x=150
r=0	5.095	4.712	4.844	5.087	5.294	5.887	6.362	6.757
r=5	---	4.758	4.987	4.817	4.930	5.467	5.773	6.122
r=10	5.242	4.830	4.766	4.296	4.188	4.132	4.288	4.214
r=12	---	4.633	4.355	---	3.011	3.139	3.360	3.094
r=14	5.160	3.973	3.291	2.192	1.575	1.592	1.564	1.592

Table A.1(b)
Normalized mean velocity (u/u_c), Re = 1670

N. radial dis. r/R	Norm. distance from inlet x/D							
	-0.31	0.63	1.9	3.8	9.4	19	31	47
0	1	1	1	1	1	1	1	1
0.313	---	1.01	1.03	0.947	0.931	0.929	0.907	0.906
0.625	1.03	1.03	0.984	0.845	0.791	0.762	0.674	0.624
0.750	---	0.983	0.899	---	0.569	0.533	0.528	0.458
0.875	1.01	0.843	0.679	0.431	0.298	0.270	0.246	0.236
1	---	0	0	0	0	0	0	0

Table A.2(a)
Mean velocity u (cm/s), Re = 3680

Radial dis. (mm)	Distance from inlet (cm)							
	x=-1	x=2	x=6	x=12	x=30	x=60	x=100	x=150
r=0	11.55	10.44	11.22	11.41	12.21	12.90	13.58	13.83
r=5	---	10.63	11.27	10.97	11.70	12.52	13.00	13.04
r=10	11.70	10.84	11.08	10.41	10.96	11.52	11.63	11.14
r=12	---	10.74	11.15	10.21	10.29	10.42	10.81	10.28
r=14	11.96	10.59	---	9.185	8.510	8.514	8.175	6.237

Table A.2(b)
Normalized mean velocity (u/u_c), Re = 3680

N. radial dis. r/R	Norm. distance from inlet x/D							
	-0.31	0.63	1.9	3.8	9.4	19	31	47
0	1	1	1	1	1	1	1	1
0.313	---	1.02	1.00	0.961	0.958	0.971	0.957	0.943
0.625	1.01	1.04	0.988	0.921	0.898	0.893	0.856	0.805
0.750	---	1.03	0.993	0.895	0.843	0.808	0.795	0.743
0.875	1.04	1.01	---	0.805	0.697	0.660	0.602	0.451
1	---	0	0	0	0	0	0	0

Table A.3(a)
Mean velocity u (cm/s), Re = 16700

Radial dis. (mm)	Distance from inlet (cm)							
	x=-1	x=2	x=6	x=12	x=30	x=60	x=100	x=150
r=0	51.57	51.67	52.19	54.30	55.94	59.80	60.95	61.50
r=5	---	50.62	52.08	53.39	55.64	57.40	58.27	58.67
r=10	---	51.26	52.07	53.35	51.94	52.38	51.79	52.48
r=12	---	51.33	51.16	51.99	49.24	49.54	48.26	50.40
r=14	---	50.41	49.95	46.96	45.25	44.67	42.87	43.04
r=15	---	48.72	46.49	43.03	40.39	40.19	---	---

Table A.3(b)
Normalized mean velocity (u/u_c), Re = 16700

N. radial dis. r/R	Norm. distance from inlet x/D							
	-0.31	0.63	1.9	3.8	9.4	19	31	47
0	1	1	1	1	1	1	1	1
0.313	---	0.980	0.998	0.983	0.995	0.960	0.956	0.954
0.625	---	0.992	0.997	0.983	0.928	0.876	0.850	0.853
0.750	---	0.993	0.980	0.957	0.880	0.828	0.792	0.819
0.875	---	0.976	0.957	0.860	0.809	0.747	0.703	0.700
0.938	---	0.943	0.891	0.792	0.722	0.672	---	---
1	---	0	0	0	0	0	0	0

Table A.4(a)
Spatially averged mean velocity u_{av} (cm/s)

Reynolds Number	Norm. distance from inlet (x/D)							
	-0.31	0.63	1.9	3.8	9.4	19	31	47
1670	5.170	4.335	4.045	3.205	3.123	3.279	3.435	3.439
3680	11.55	10.42	10.84	9.881	9.890	10.17	10.24	9.280
16700	51.57	50.17	50.21	49.74	48.39	48.98	47.66	48.52

Table A.4(b)
Blockage factor

Reynolds Number	Norm. distance from inlet (x/D)							
	-0.31	0.63	1.9	3.8	9.4	19	31	47
1670	0.015	0.080	0.165	0.370	0.410	0.443	0.460	0.491
3680	0.0	0.002	0.034	0.134	0.190	0.212	0.246	0.329
16700	0.0	0.029	0.039	0.084	0.135	0.181	0.218	0.211

Table A.5
Δu_r, Re = 1670

Radial dis. (mm)	Norm. distance from inlet (x/D)							
	-0.31	0.63	1.9	3.8	9.4	19	31	47
r=5	---	10.8	12.8	4.50	2.90	2.70	0.500	0.400
r=10	68.9	42.1	37.5	23.6	18.2	15.3	6.50	1.50
r=12	---	54.5	46.1	---	13.1	9.50	9.00	2.00
r=14	77.6	60.9	44.5	19.7	6.40	3.60	1.20	0.200

Table A.6
Turbulence. intensity σ (%), Re = 1670

Radial dis. (mm)	Distance from inlet (cm)							
	x=-1	x=2	x=6	x=12	x=30	x=60	x=100	x=150
r=0	17.25	13.39	12.07	8.910	6.561	4.891	4.051	2.927
r=5	---	15.05	14.06	9.981	8.959	7.425	6.142	4.543
r=10	18.42	16.21	16.43	13.04	12.94	12.52	5.830	6.130
r=12	---	20.66	18.65	---	21.09	13.14	8.155	7.990
r=14	19.01	23.82	19.91	24.01	---	16.51	---	8.279

Table A.7
Turbulence intensity σ (%), Re = 3680

Radial dis. (mm)	Distance from inlet (cm)							
	x=-1	x=2	x=6	x=12	x=30	x=60	x=100	x=150
r=0	17.17	14.27	11.04	12.85	6.953	5.626	6.086	6.050
r=5	---	14.45	11.16	13.76	7.174	6.318	6.515	8.221
r=10	18.57	15.47	12.72	13.31	10.57	10.68	11.95	14.21
r=12	---	16.36	12.59	15.31	12.49	14.48	12.93	15.19
r=14	18.11	22.49	---	19.49	18.60	19.81	18.20	23.29

Table A.8
Turbulence intensity σ (%), Re= 16700

Radial dis. (mm)	Distance from inlet (cm)							
	x=-1	x=2	x=6	x=12	x=30	x=60	x=100	x=150
r=0	12.16	8.455	8.471	6.631	4.525	4.078	4.188	4.402
r=5	---	9.494	8.715	6.175	4.881	6.028	5.831	6.387
r=10	---	9.190	10.41	7.679	7.753	7.929	8.907	11.76
r=12	---	10.80	9.750	8.180	8.385	9.267	10.86	11.19
r=14	---	10.82	10.66	11.90	11.97	11.78	14.99	18.89
r=15	---	13.18	13.60	15.11	16.57	20.06	---	---

Table A.9(a)
Spatially averaged turbulence intensity σ_{av} (%)

Reynolds Number	Norm. distance from inlet (x/D)							
	-0.31	0.63	1.9	3.8	9.4	19	31	47
1670	18.50	17.86	16.72	14.30	12.66	11.91	7.236	2.867
3680	18.29	16.09	12.09	14.57	10.87	11.25	11.19	13.54
16700	12.16	9.841	9.803	7.779	7.461	8.019	9.071	10.62

Table A.9(b)
Relative average turbulence intensity

Reynolds Number	Norm. distance from inlet (x/D)							
	-0.31	0.63	1.9	3.8	9.4	19	31	47
1670	1.000	0.965	0.904	0.773	0.684	0.644	0.391	0.155
3680	1.000	0.880	0.661	0.797	0.594	0.615	0.612	0.740
16700	1.000	0.809	0.806	0.640	0.614	0.660	0.746	0.873

Table A.10
Standard deviation x 100, Re = 1670

Radial dis. (mm)	Norm. distance from inlet (x/D)							
	-0.31	0.63	1.9	3.8	9.4	19	31	47
r=0	87.89	63.09	58.45	45.32	34.73	28.79	25.77	19.78
r=5	---	71.61	70.10	48.07	44.17	40.59	35.46	27.81
r=10	96.56	78.28	78.30	56.00	54.17	51.71	24.99	25.83
r=12	---	95.70	81.23	---	63.49	41.75	27.40	24.72
r=14	98.04	94.64	65.51	52.62	---	26.28	---	13.50

Table A.11
Skewness x 100

Reynolds Number	Norm. distance from inlet (x/D)							
	-0.31	0.63	1.9	3.8	9.4	19	31	47
1670	47.65	24.12	35.70	4.576	13.22	-23.59	-38.53	1.315
3680	4.148	31.87	11.49	1.465	-18.75	-32.94	-49.63	-44.41
16700	40.25	59.20	37.63	35.54	6.158	-34.01	-60.64	-21.71

Table A.12
Kurtosis

Reynolds Number	Norm. distance from inlet (x/D)							
	-0.31	0.63	1.9	3.8	9.4	19	31	47
1670	3.438	3.309	4.319	3.546	2.502	2.840	2.813	3.002
3680	3.003	3.294	3.444	3.211	3.235	3.164	2.991	2.827
16700	3.388	4.205	3.326	3.396	3.001	3.163	3.428	3.373

Appendix B

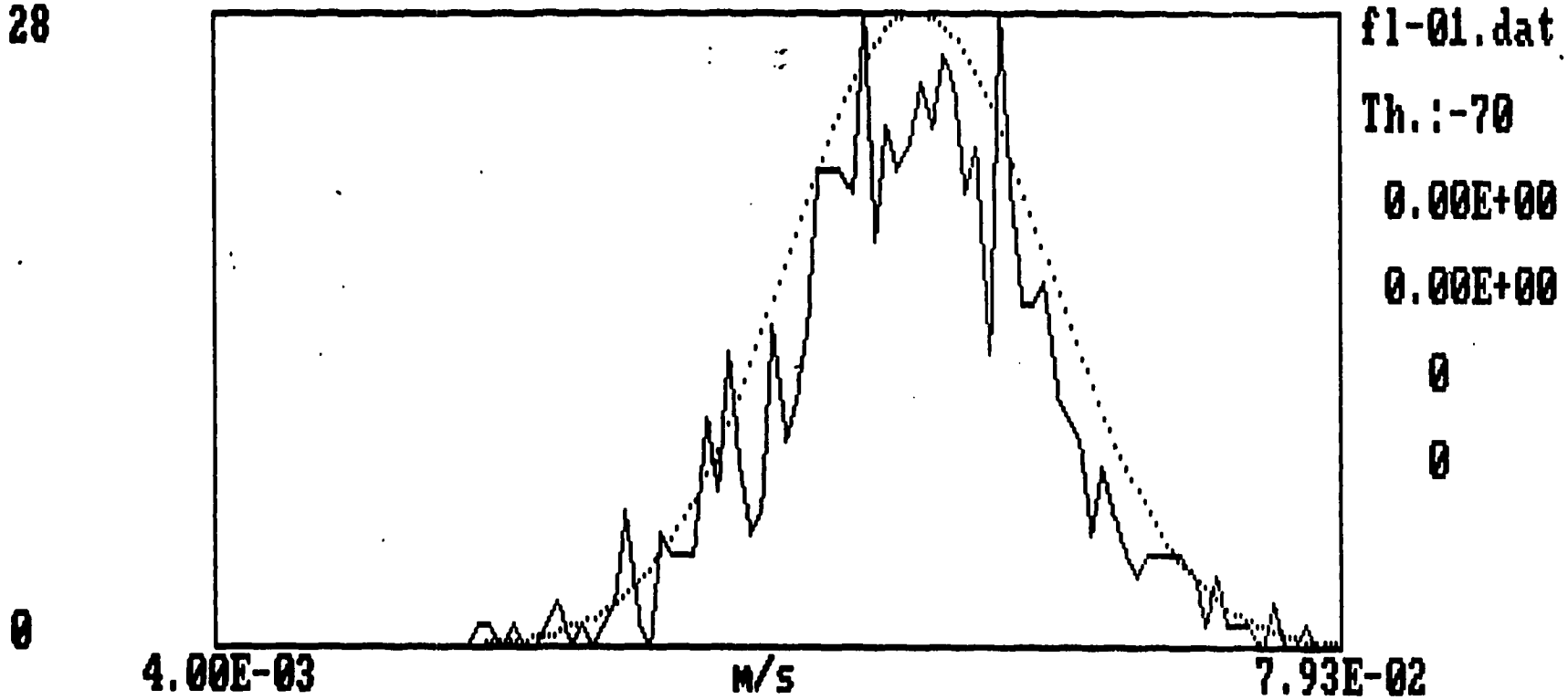

Velocity Distribution

Mean	: 5.095E-02 m/s	Dist. From Inlet		:	-1.000E+00 cm
Stand. deviat.	: 8.791E-03 m/s	Radial Distance		:	0.000E+00 mm
Veloc. for max.	: 4.734E-02 m/s	Bulk velocity		:	5.200E-02 m/s
Skewness :	-1.080E-01	Kurtosis : 3.268E+00	Re.	:	1.670E+03

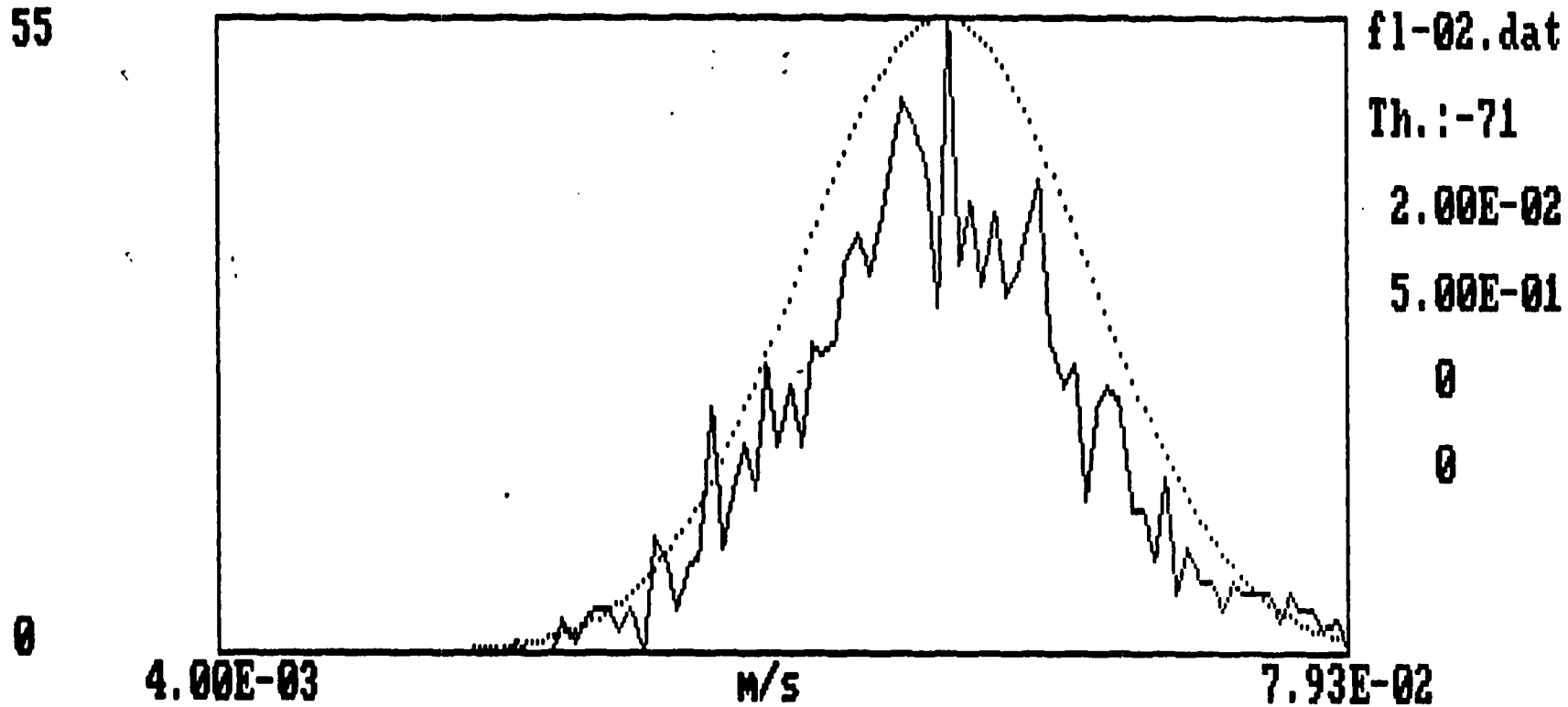

Velocity Distribution

Mean	: 5.240E-02 m/s	Dist. From Inlet	:	-1.000E+00	cm
Stand. deviat.	: 9.636E-03 m/s	Radial Distance	:	1.000E+01	mm
Veloc. for max.	: 5.266E-02 m/s	Bulk velocity	:	5.200E-02	m/s
Skewness : 9.823E-02	Kurtosis : 2.970E+00	Re.	:	1.670E+03	

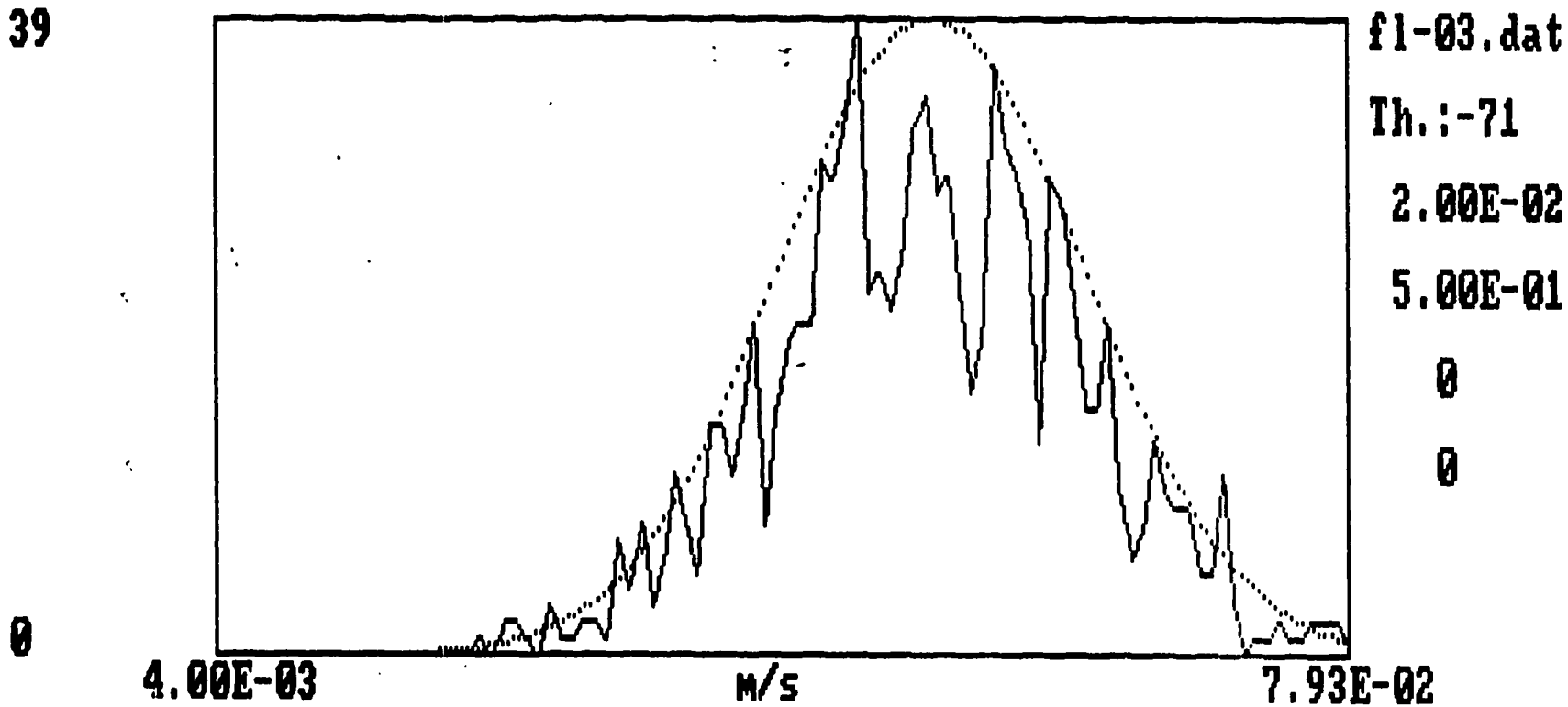

Velocity Distribution

Mean	: 5.157E-02 m/s	Dist. From Inlet		:	-1.000E+00 cm
Stand. deviat.	: 1.012E-02 m/s	Radial Distance		:	1.500E+01 mm
Veloc. for max.	: 4.658E-02 m/s	Bulk velocity		:	5.200E-02 m/s
Skewness :	-3.586E-02	Kurtosis :	2.806E+00	Re. :	1.670E+03

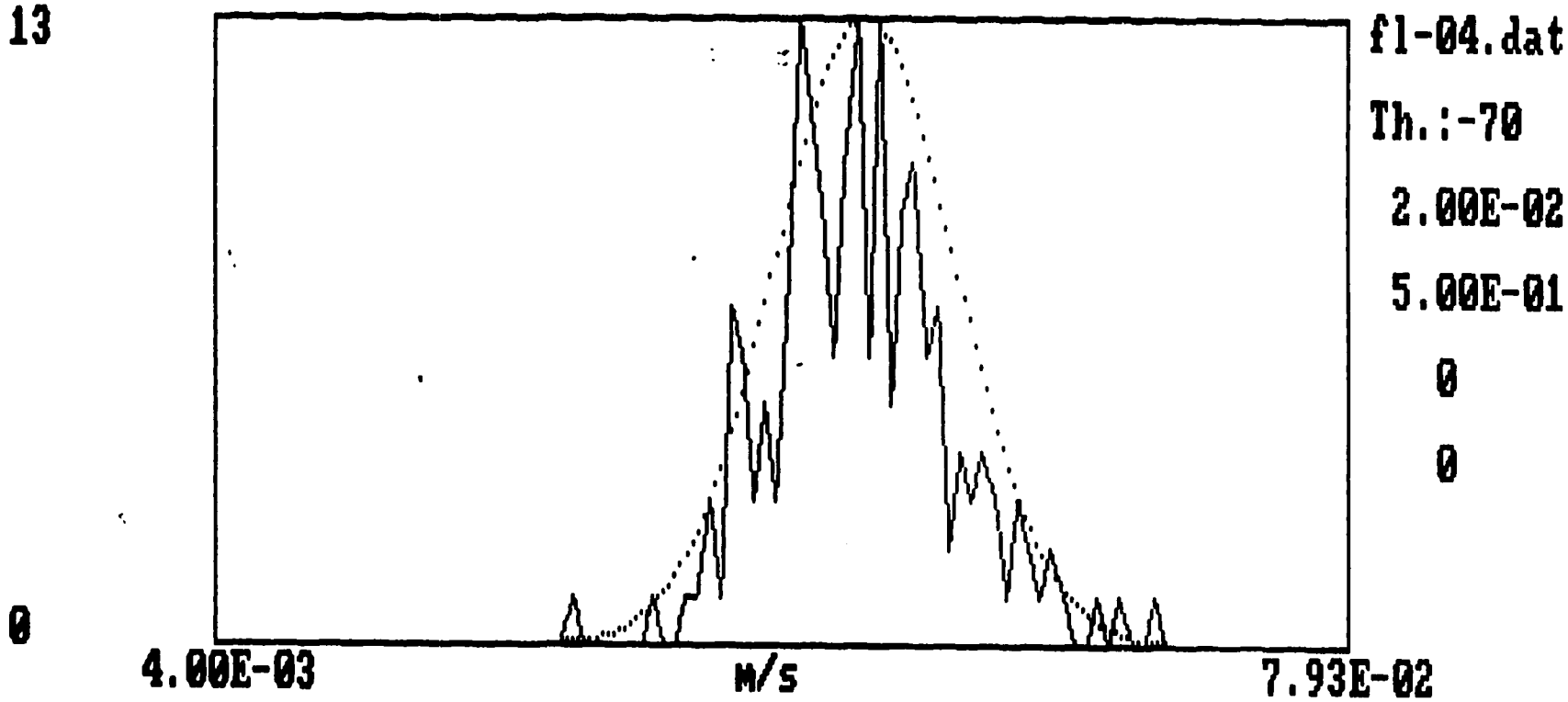

Velocity Distribution

Mean	: 4.712E-02 m/s	Dist. From Inlet	:	2.000E+00	cm
Stand. deviat.	: 6.040E-03 m/s	Radial Distance	:	0.000E+00	mm
Veloc. for max.	: 4.278E-02 m/s	Bulk velocity	:	5.200E-02	m/s
Skewness : 2.932E-01	Kurtosis : 3.463E+00	Re.	:	1.670E+03	

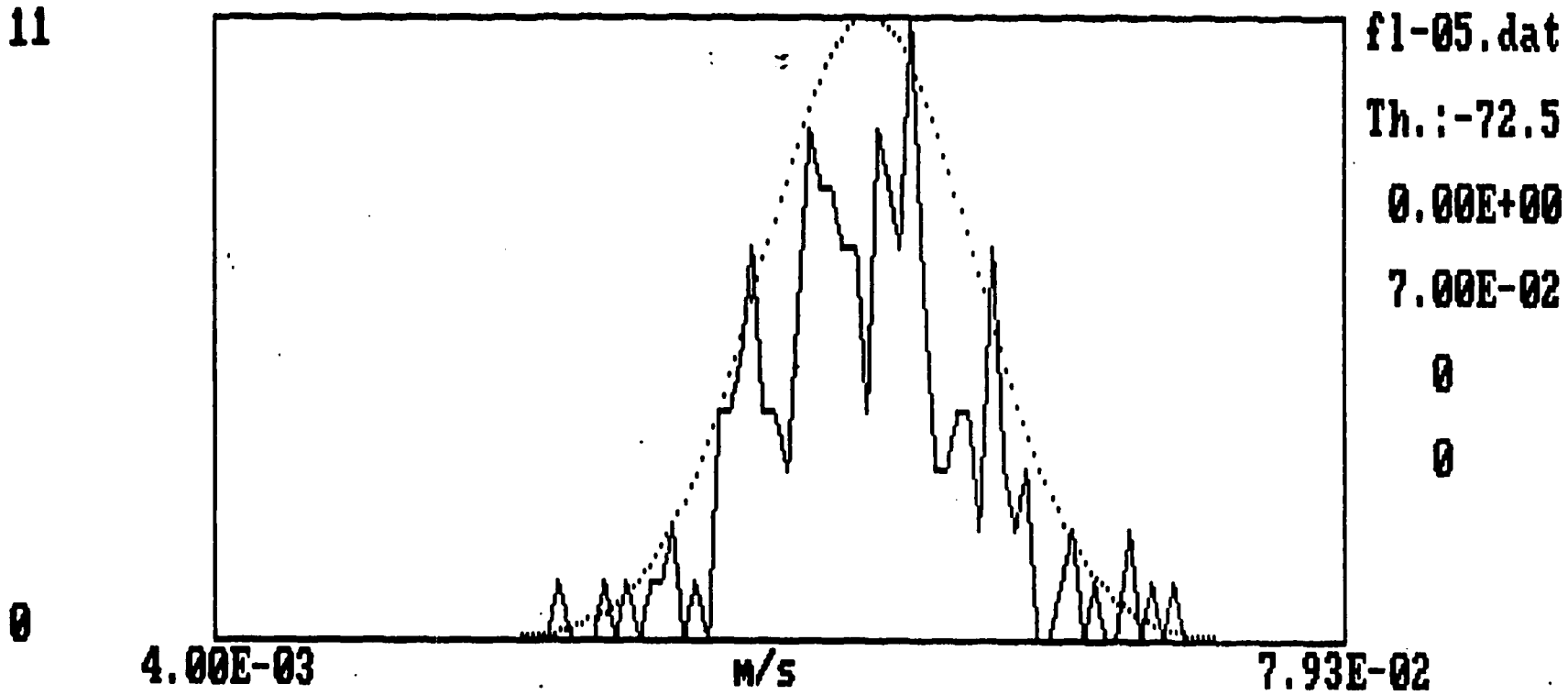

Velocity Distribution

Mean	: 4.755E-02 m/s	Dist. From Inlet	:	2.000E+00 cm	
Stand. deviat.	: 7.107E-03 m/s	Radial Distance	:	5.000E+00 mm	
Veloc. for max.	: 5.038E-02 m/s	Bulk velocity	:	5.200E-02 m/s	
Skewness : 1.667E-01	Kurtosis : 3.263E+00	Re.	:	1.670E+03	

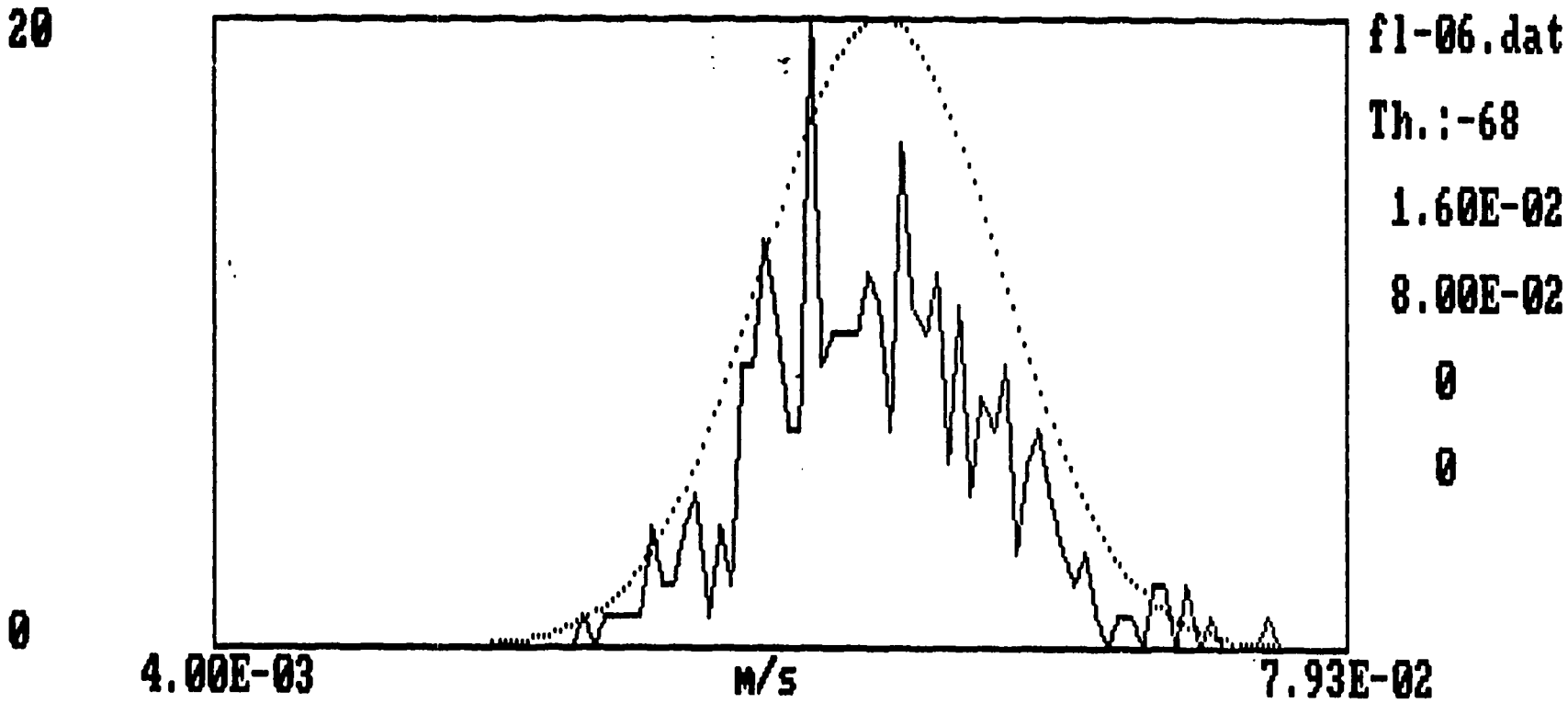

Velocity Distribution

Mean	: 4.829E-02 m/s	Dist. From Inlet	:	2.000E+00 cm	
Stand. deviat.	: 7.945E-03 m/s	Radial Distance	:	1.000E+01 mm	
Veloc. for max.	: 4.354E-02 m/s	Bulk velocity	:	5.200E-02 m/s	
Skewness : 2.684E-01	Kurtosis : 3.001E+00	Re.	:	1.670E+03	

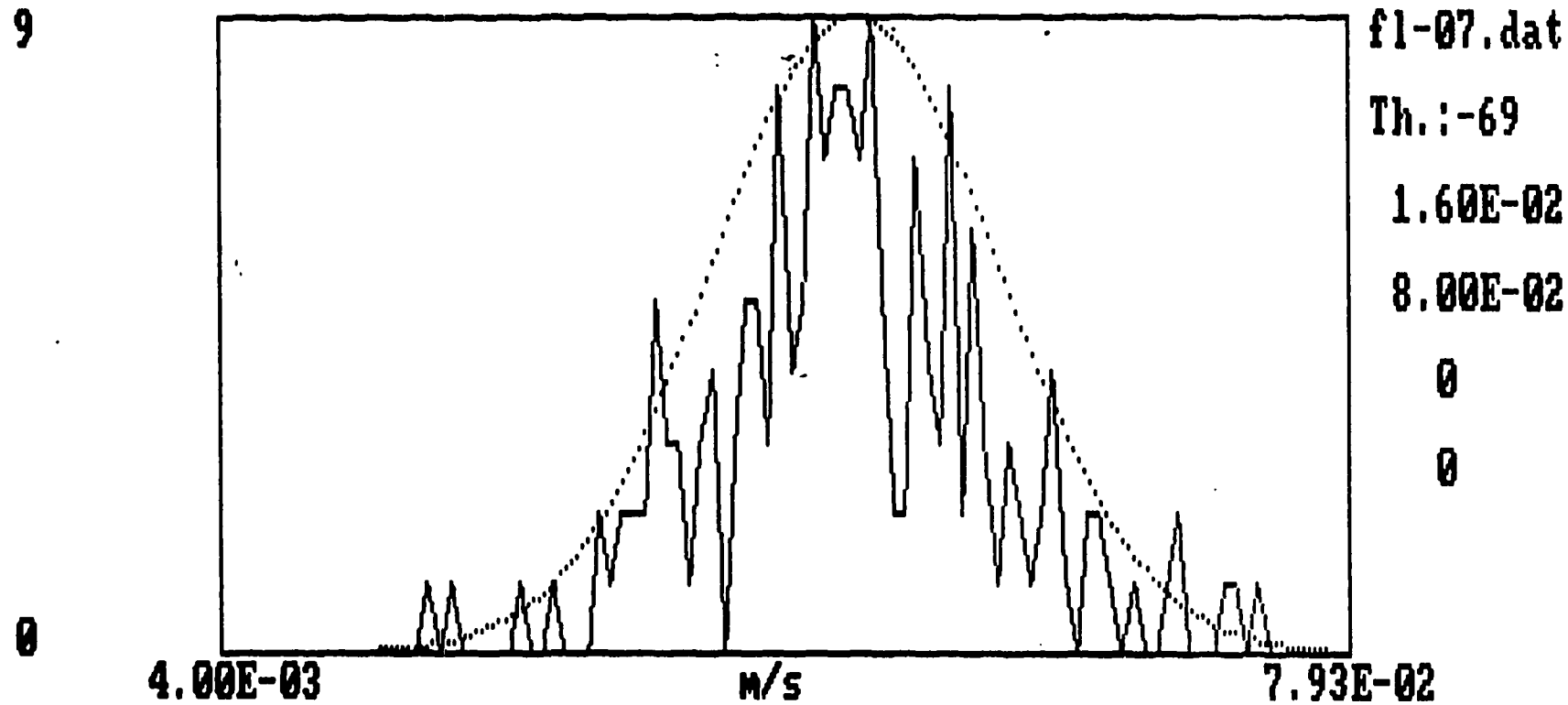

Velocity Distribution

Mean	: 4.631E-02 m/s	Dist. From Inlet	:	2.000E+00	cm
Stand. deviat.	: 9.673E-03 m/s	Radial Distance	:	1.200E+01	mm
Veloc. for max.	: 4.354E-02 m/s	Bulk velocity	:	5.200E-02	m/s
Skewness : 1.215E-01	Kurtosis : 3.400E+00	Re.	:	1.670E+03	

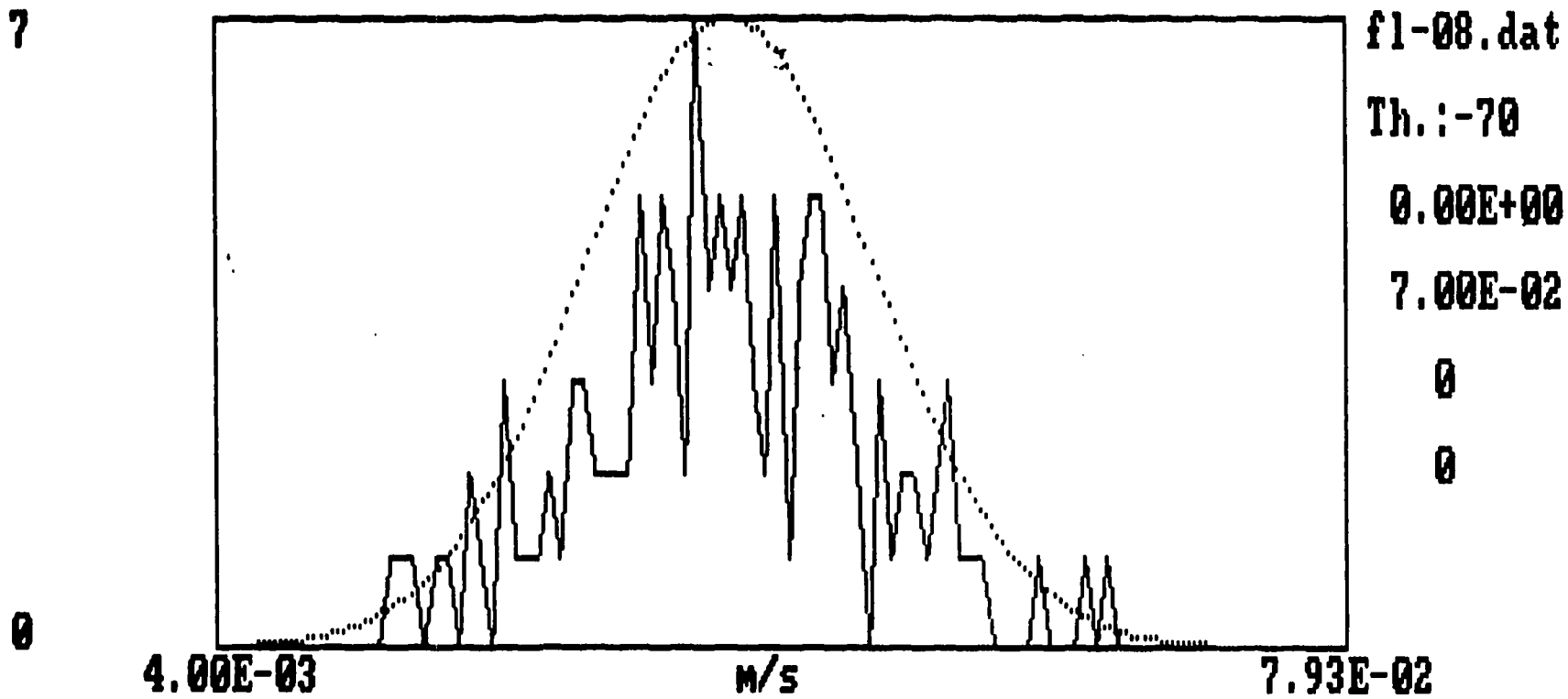

Velocity Distribution

Mean	: 3.813E-02 m/s	Dist. From Inlet		:	2.000E+00 cm
Stand. deviat.	: 9.668E-03 m/s	Radial Distance		:	1.400E+01 mm
Veloc. for max.	: 3.593E-02 m/s	Bulk velocity		:	5.200E-02 m/s
Skewness :	-2.534E-03	Kurtosis :	2.828E+00	Re. :	1.670E+03

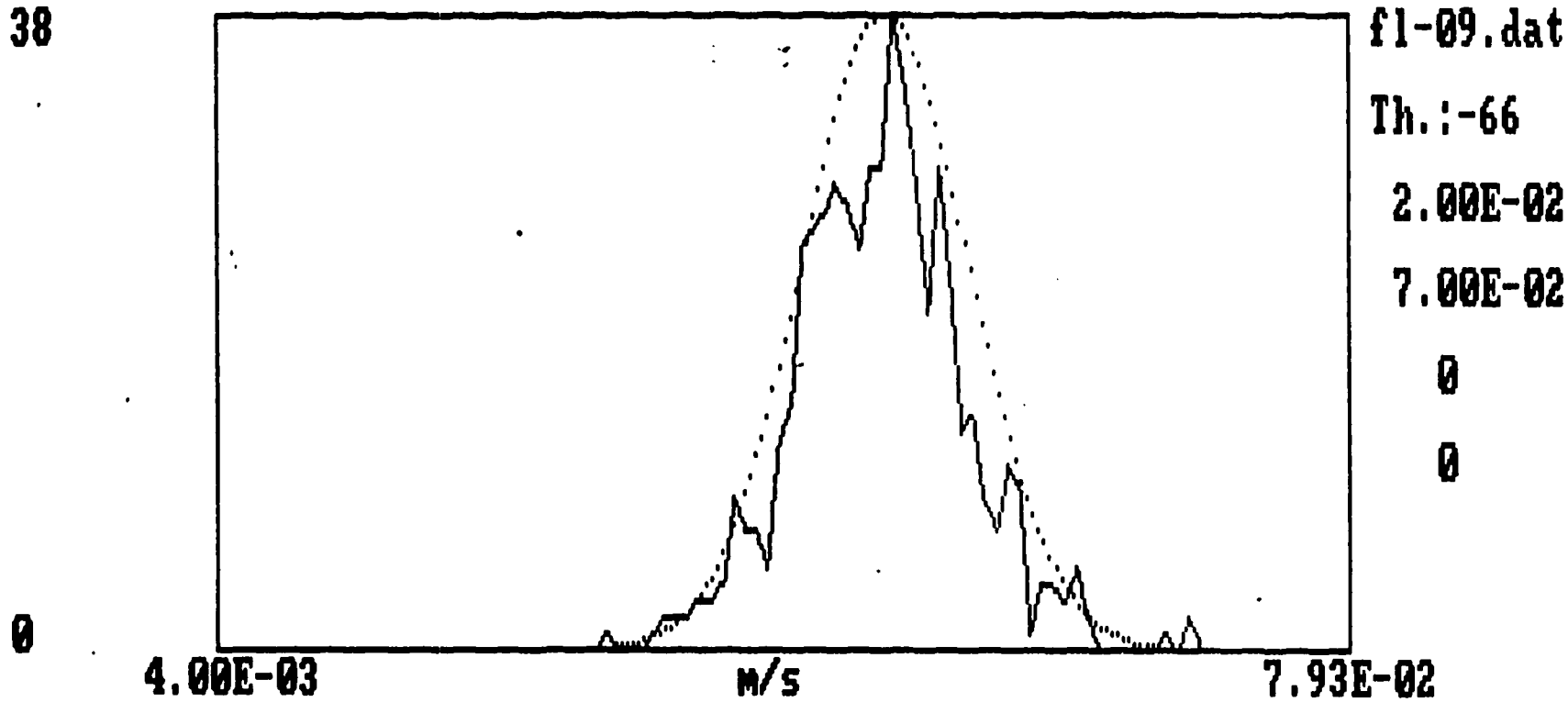

Velocity Distribution

Mean	: 4.837E-02 m/s	Dist. From Inlet	:	6.000E+00 cm	
Stand. deviat.	: 5.589E-03 m/s	Radial Distance	:	0.000E+00 mm	
Veloc. for max.	: 4.886E-02 m/s	Bulk velocity	:	5.200E-02 m/s	
Skewness : 1.581E-01	Kurtosis : 3.629E+00	Re.	:	1.670E+03	

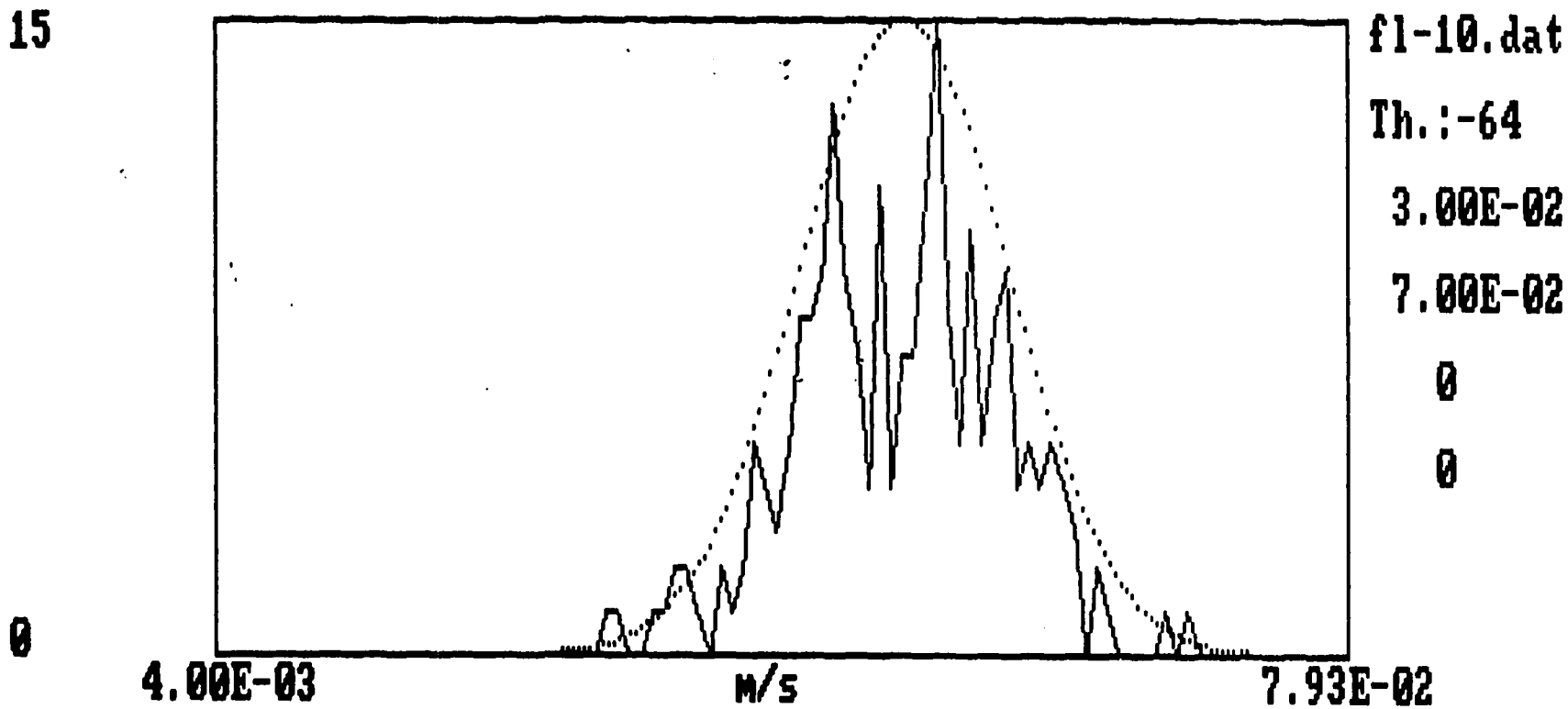

Velocity Distribution

Mean	: 4.974E-02 m/s	Dist. From Inlet	:	6.000E+00 cm	
Stand. deviat.	: 6.954E-03 m/s	Radial Distance	:	5.000E+00 mm	
Veloc. for max.	: 5.190E-02 m/s	Bulk velocity	:	5.200E-02 m/s	
Skewness : -1.526E-01	Kurtosis : 2.833E+00	Re.	:	1.670E+03	

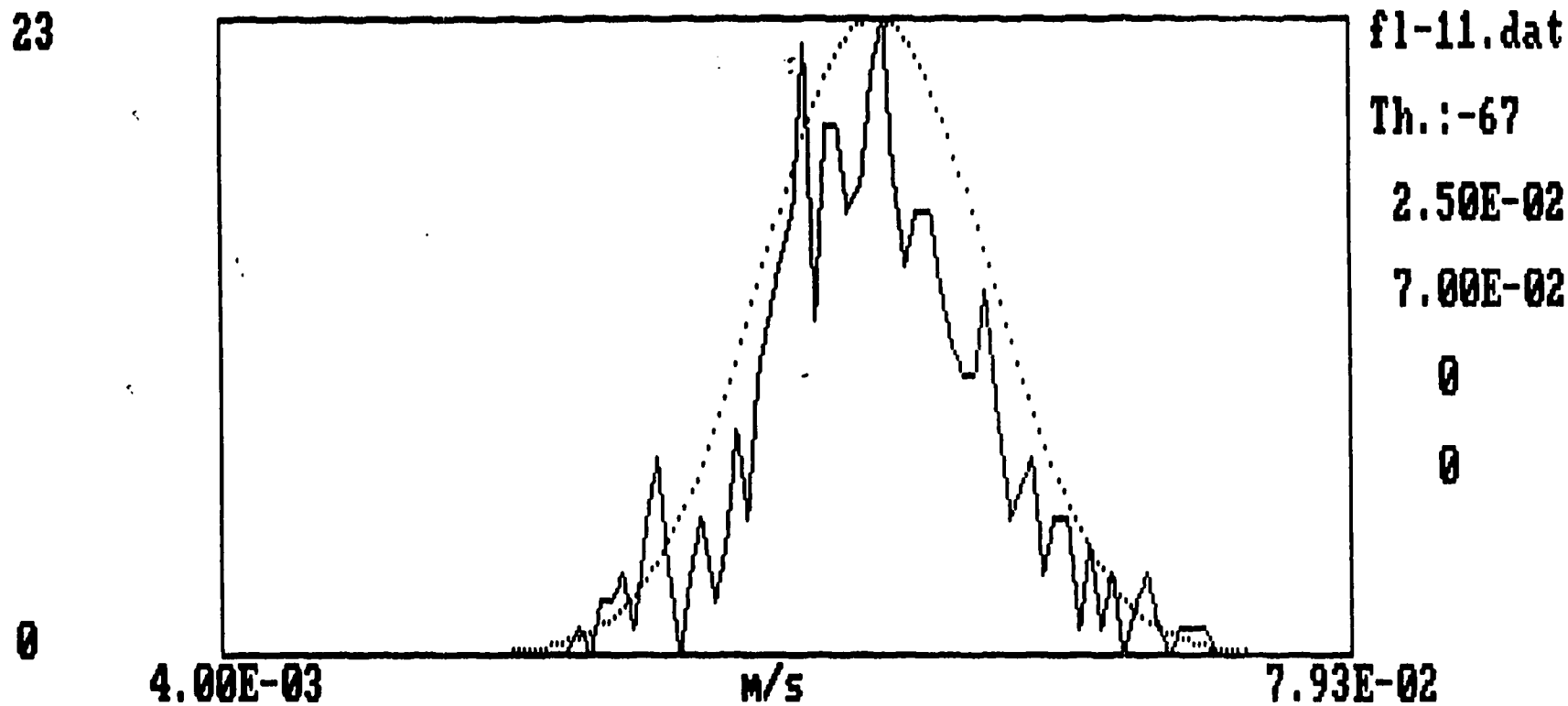

Velocity Distribution

Mean	: 4.765E-02 m/s	Dist. From Inlet	:	6.000E+00	cm
Stand. deviat.	: 7.501E-03 m/s	Radial Distance	:	1.000E+01	mm
Veloc. for max.	: 4.810E-02 m/s	Bulk velocity	:	5.200E-02	m/s
Skewness : 1.029E-01	Kurtosis : 3.155E+00	Re.	:	1.670E+03	

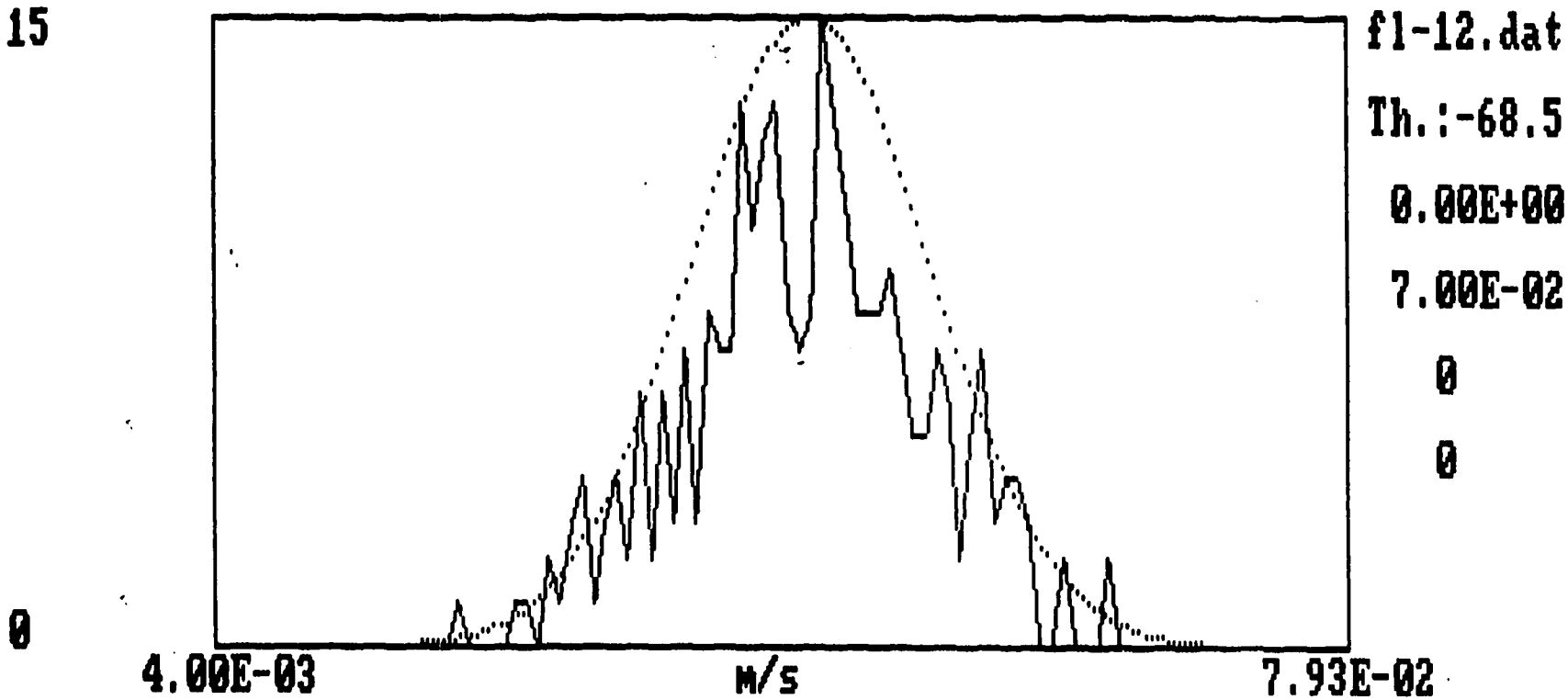

Velocity Distribution

Mean	: 4.355E-02 m/s	Dist. From Inlet	:	6.000E+00	cm
Stand. deviat.	: 7.978E-03 m/s	Radial Distance	:	1.200E+01	mm
Veloc. for max.	: 4.430E-02 m/s	Bulk velocity	:	5.200E-02	m/s
Skewness : -9.837E-02	Kurtosis : 2.747E+00	Re.	:	1.670E+03	

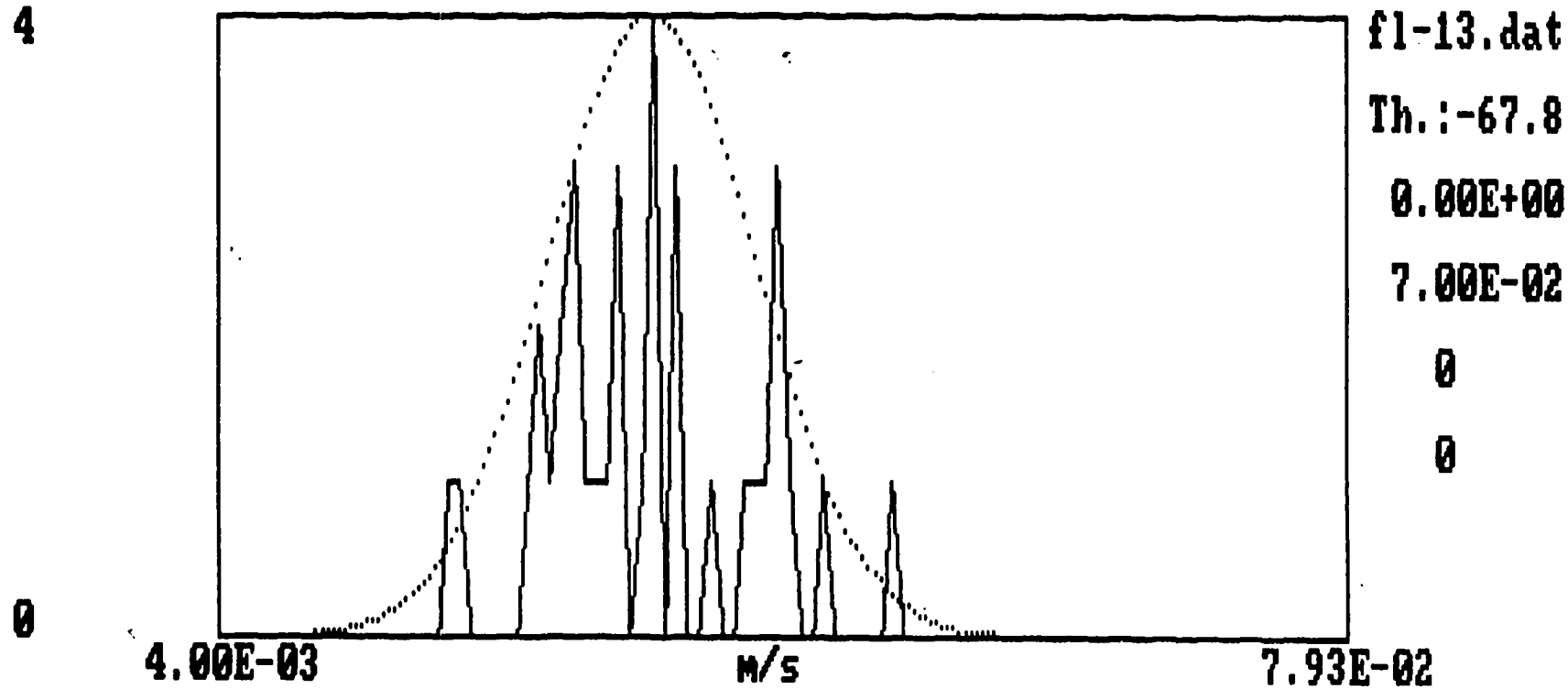

Velocity Distribution

Mean	: 3.286E-02 m/s	Dist. From Inlet	:	6.000E+00	cm
Stand. deviat.	: 6.919E-03 m/s	Radial Distance	:	1.400E+01	mm
Veloc. for max.	: 3.289E-02 m/s	Bulk velocity	:	5.200E-02	m/s
Skewness : 2.827E-01	Kurtosis : 2.413E+00	Re.	:	1.670E+03	

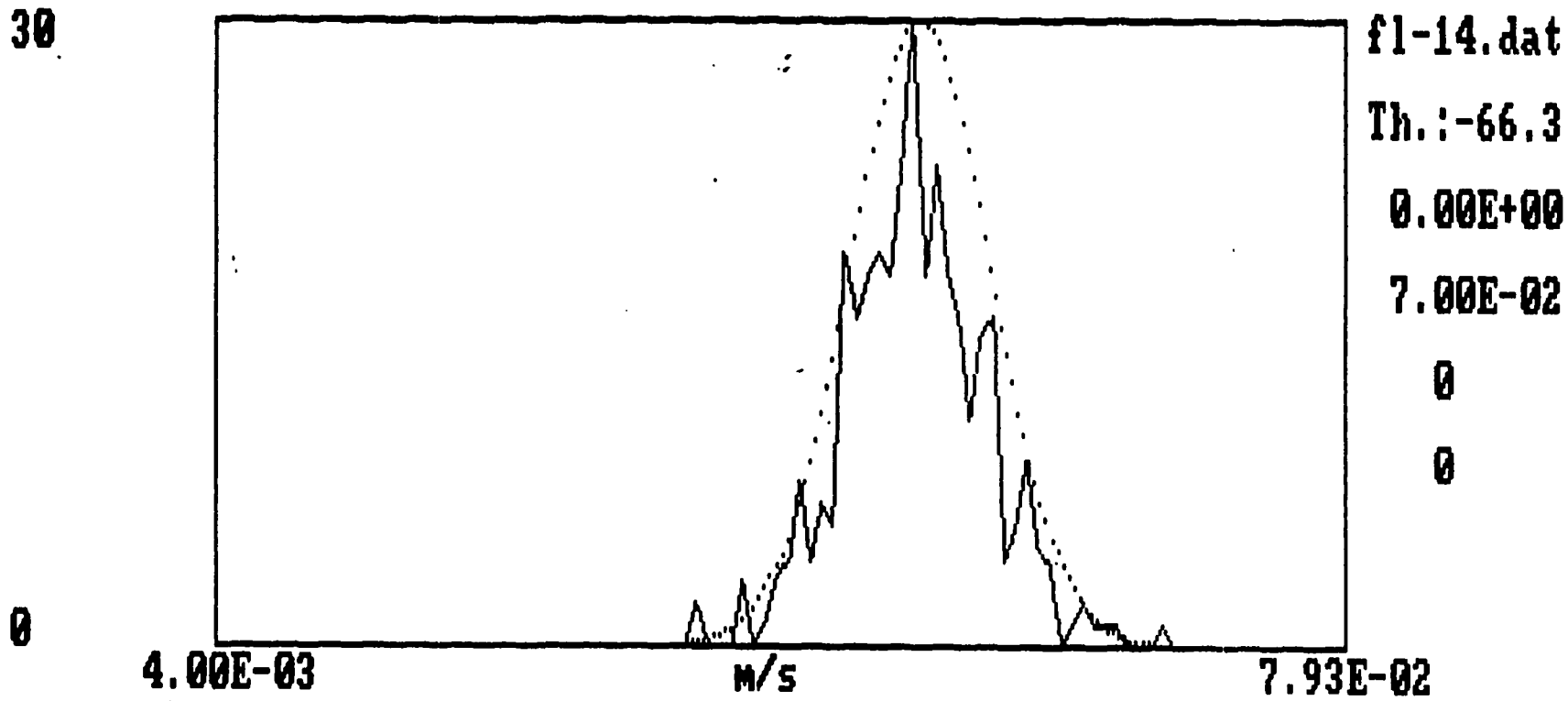

Velocity Distribution

Mean	: 5.087E-02 m/s	Dist. From Inlet	:	1.200E+01 cm	
Stand. deviat.	: 4.726E-03 m/s	Radial Distance	:	0.000E+00 mm	
Veloc. for max.	: 5.038E-02 m/s	Bulk velocity	:	5.200E-02 m/s	
Skewness : 8.187E-02	Kurtosis : 3.432E+00	Re.	:	1.670E+03 5	

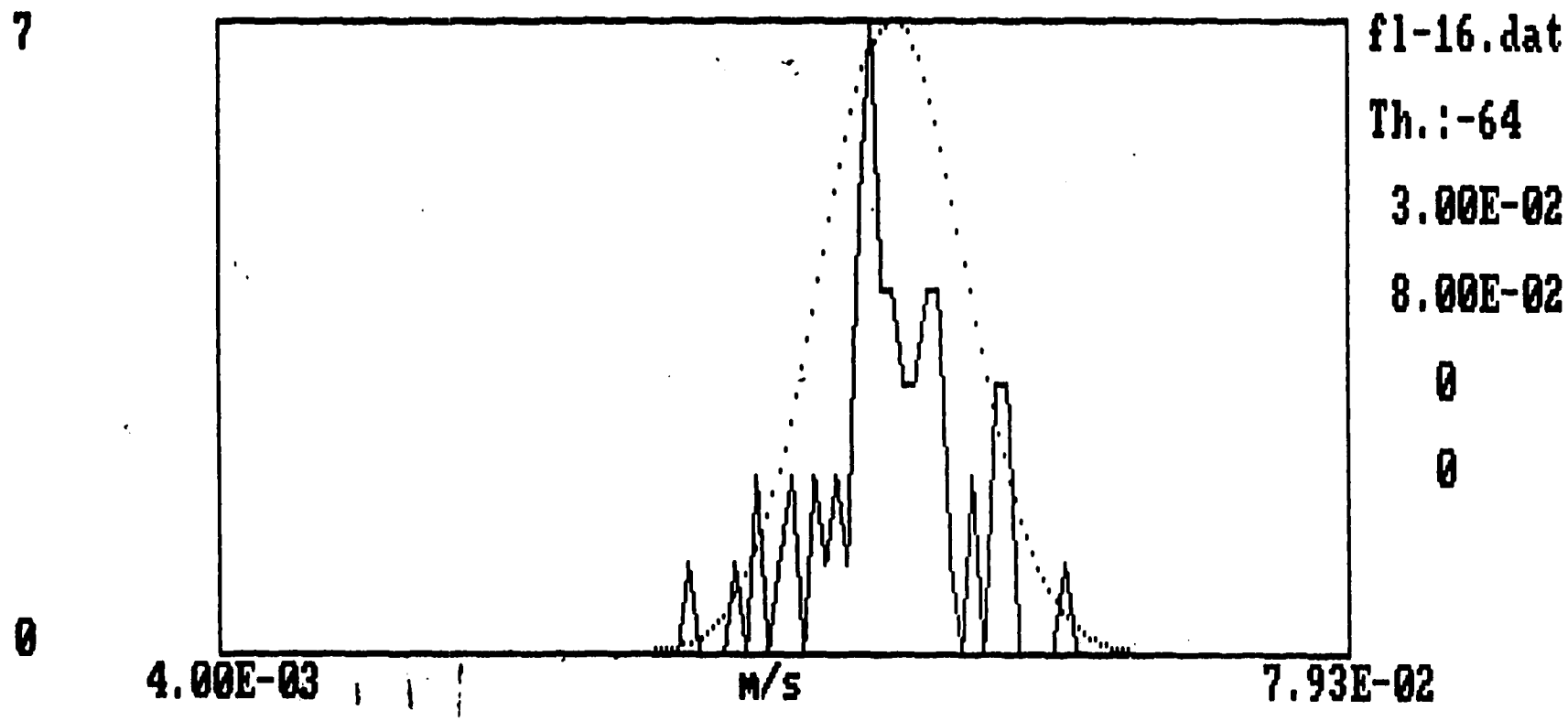

Velocity Distribution

Mean	: 4.891E-02 m/s	Dist. From Inlet	:	1.200E+01 cm	
Stand. deviat.	: 4.860E-03 m/s	Radial Distance	:	5.000E+00 mm	
Veloc. for max.	: 4.734E-02 m/s	Bulk velocity	:	5.200E-02 m/s	
Skewness : -2.327E-01	Kurtosis : 3.175E+00	Re.	:	1.670E+03	

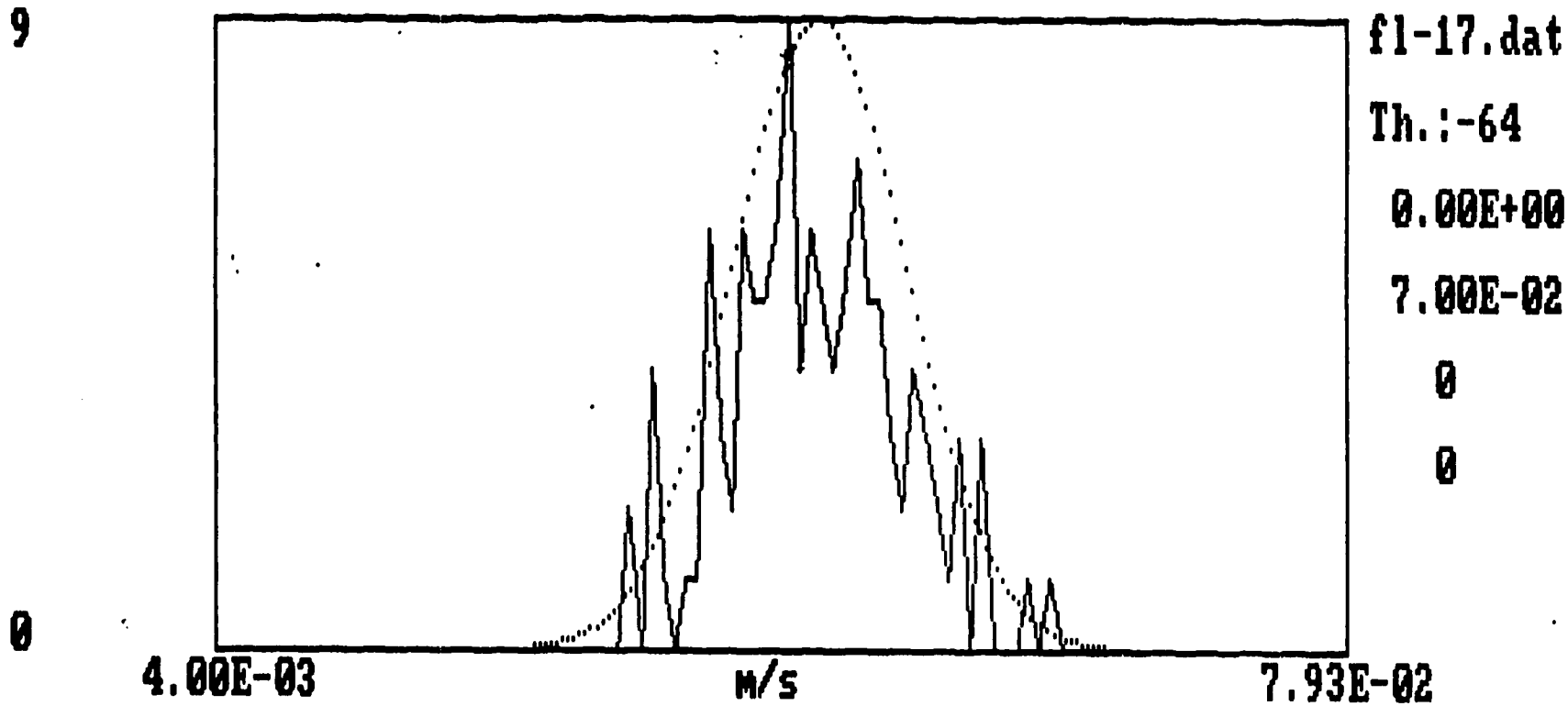

Velocity Distribution

Mean	: 4.411E-02 m/s	Dist. From Inlet	:	1.200E+01 cm	
Stand. deviat.	: 5.834E-03 m/s	Radial Distance	:	1.000E+01 mm	
Veloc. for max.	: 4.202E-02 m/s	Bulk velocity	:	5.200E-02 m/s	
Skewness : 1.680E-01	Kurtosis : 2.753E+00	Re.	:	1.670E+03	

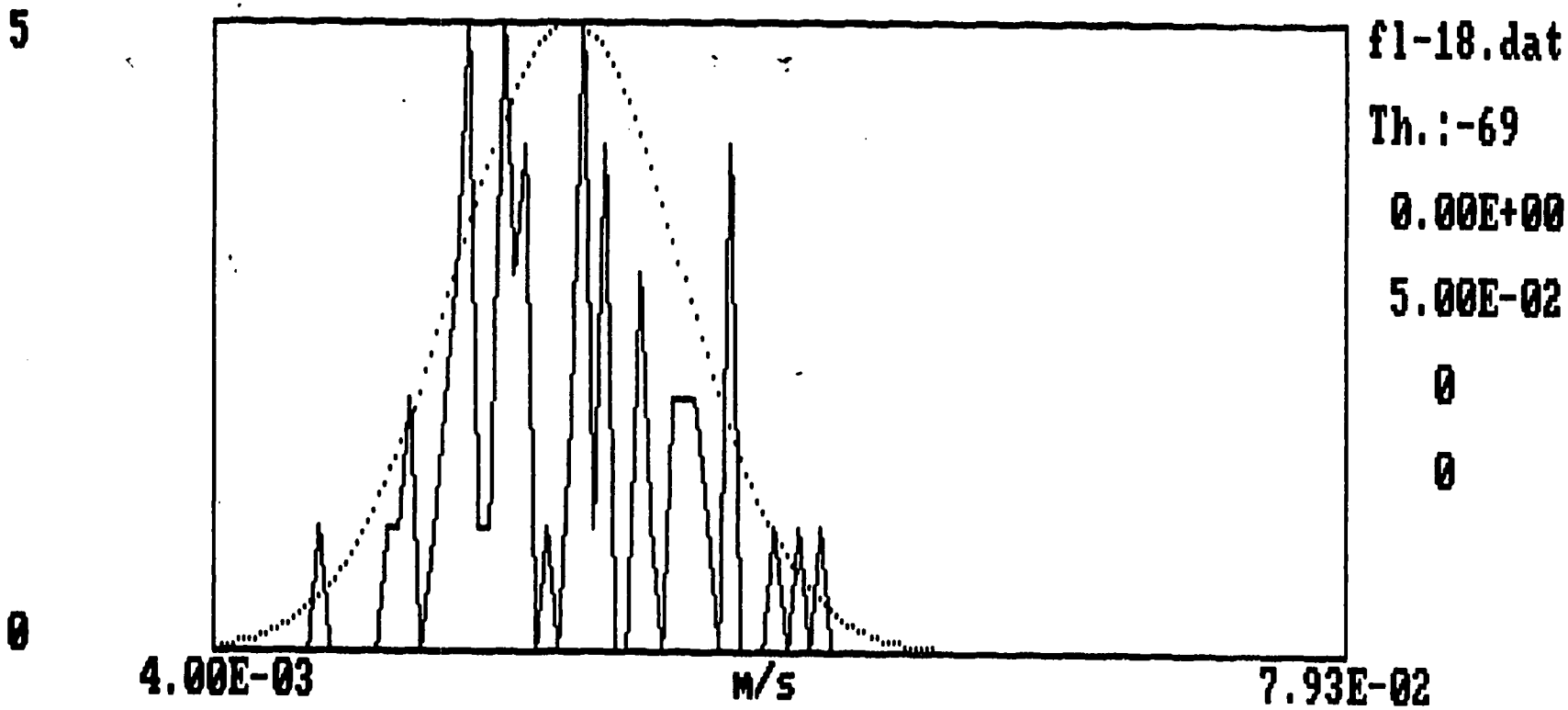

Velocity Distribution

Mean	: 2.750E-02 m/s	Dist. From Inlet		:	1.200E+01 cm
Stand. deviat.	: 7.495E-03 m/s	Radial Distance		:	1.200E+01 mm
Veloc. for max.	: 2.073E-02 m/s	Bulk velocity		:	5.200E-02 m/s
Skewness :	2.923E-01	Kurtosis :	2.308E+00	Re. :	1.670E+03

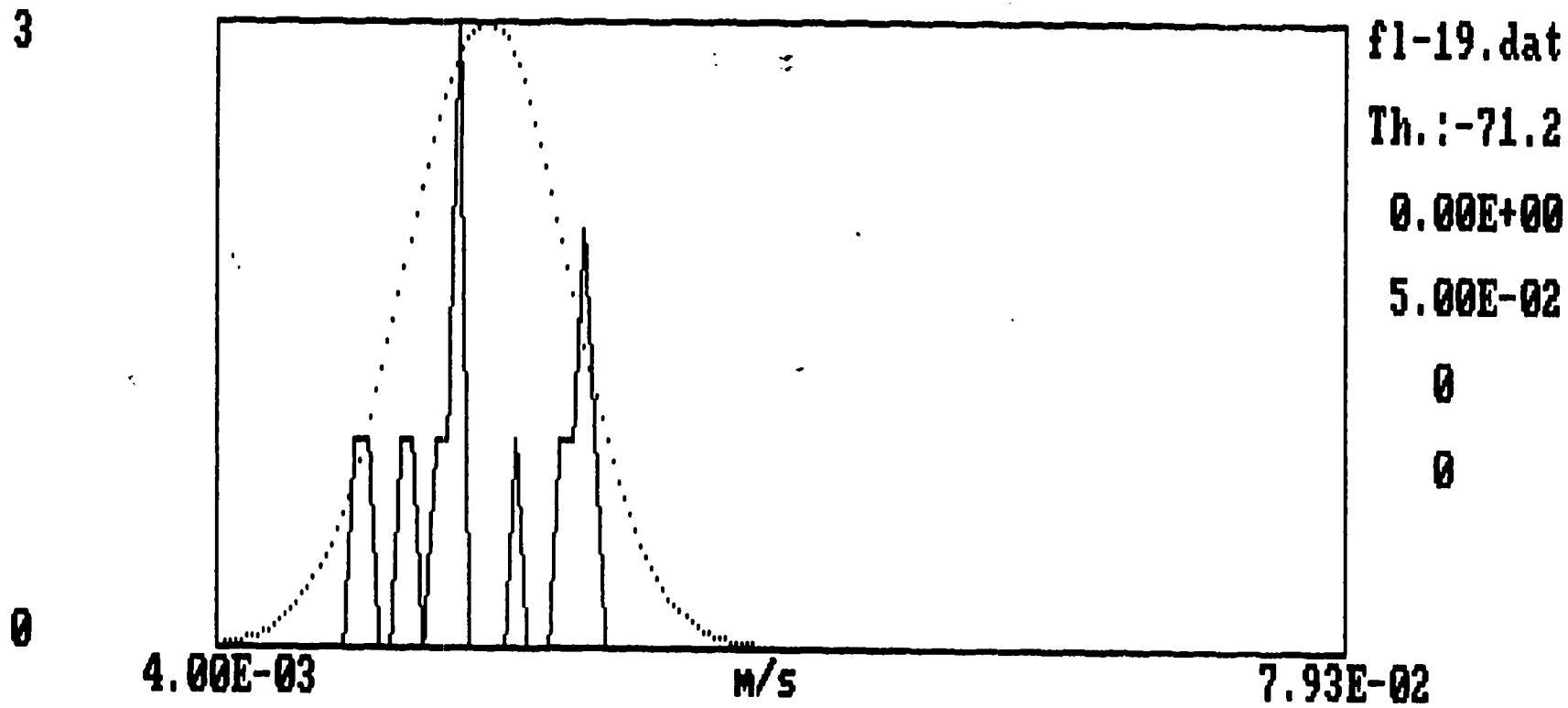

Velocity Distribution

Mean	: 2.186E-02 m/s	Dist. From Inlet		:	1.200E+01 cm
Stand. deviat.	: 5.458E-03 m/s	Radial Distance		:	1.400E+01 mm
Veloc. for max.	: 1.997E-02 m/s	Bulk velocity		:	5.200E-02 m/s
Skewness :	1.277E-01	Kurtosis : 1.449E+00	Re.	:	1.670E+03

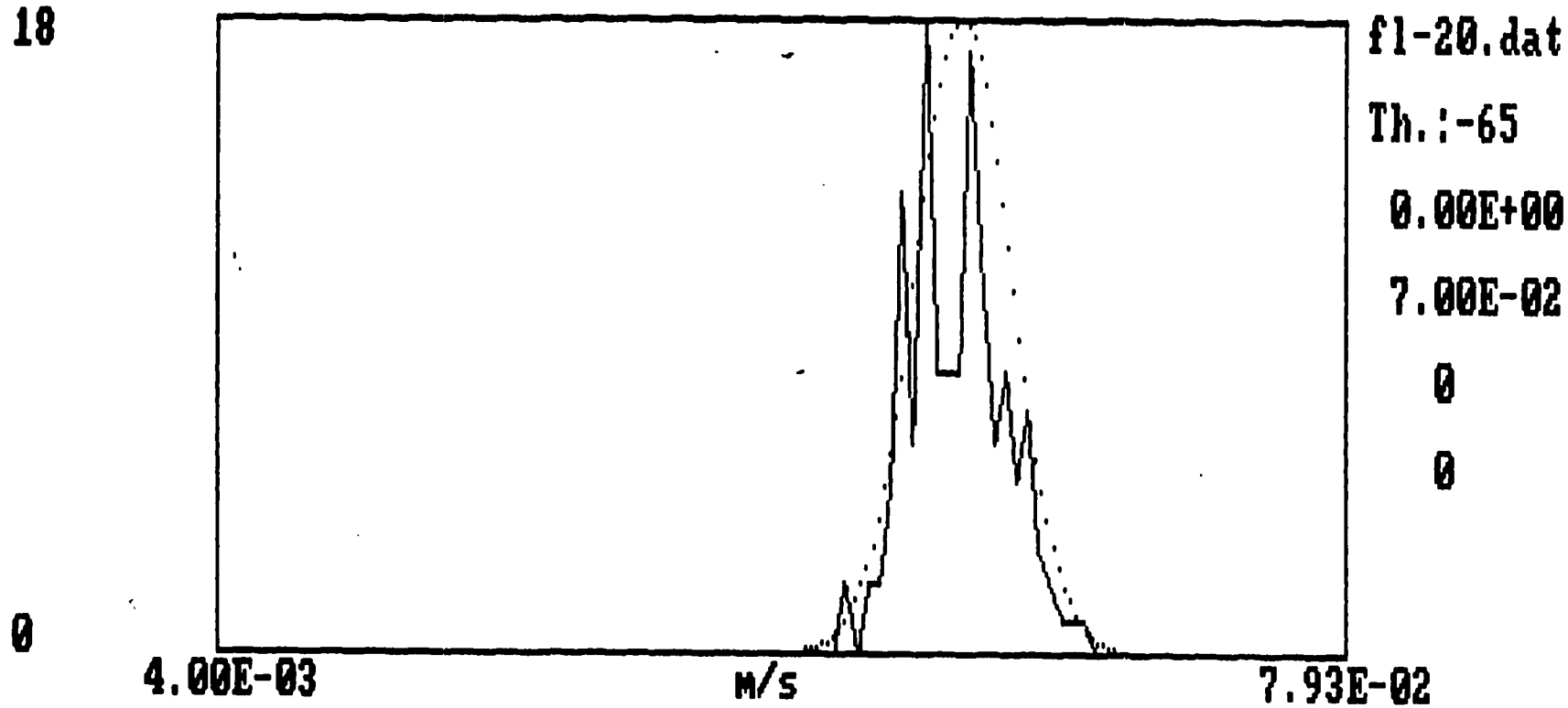

Velocity Distribution

Mean	: 5.366E-02 m/s	Dist. From Inlet	:	3.000E+01	cm
Stand. deviat.	: 3.211E-03 m/s	Radial Distance	:	0.000E+00	mm
Veloc. for max.	: 5.114E-02 m/s	Bulk velocity	:	5.200E-02	m/s
Skewness : 1.810E-01	Kurtosis : 2.580E+00	Re.	:	1.670E+03	

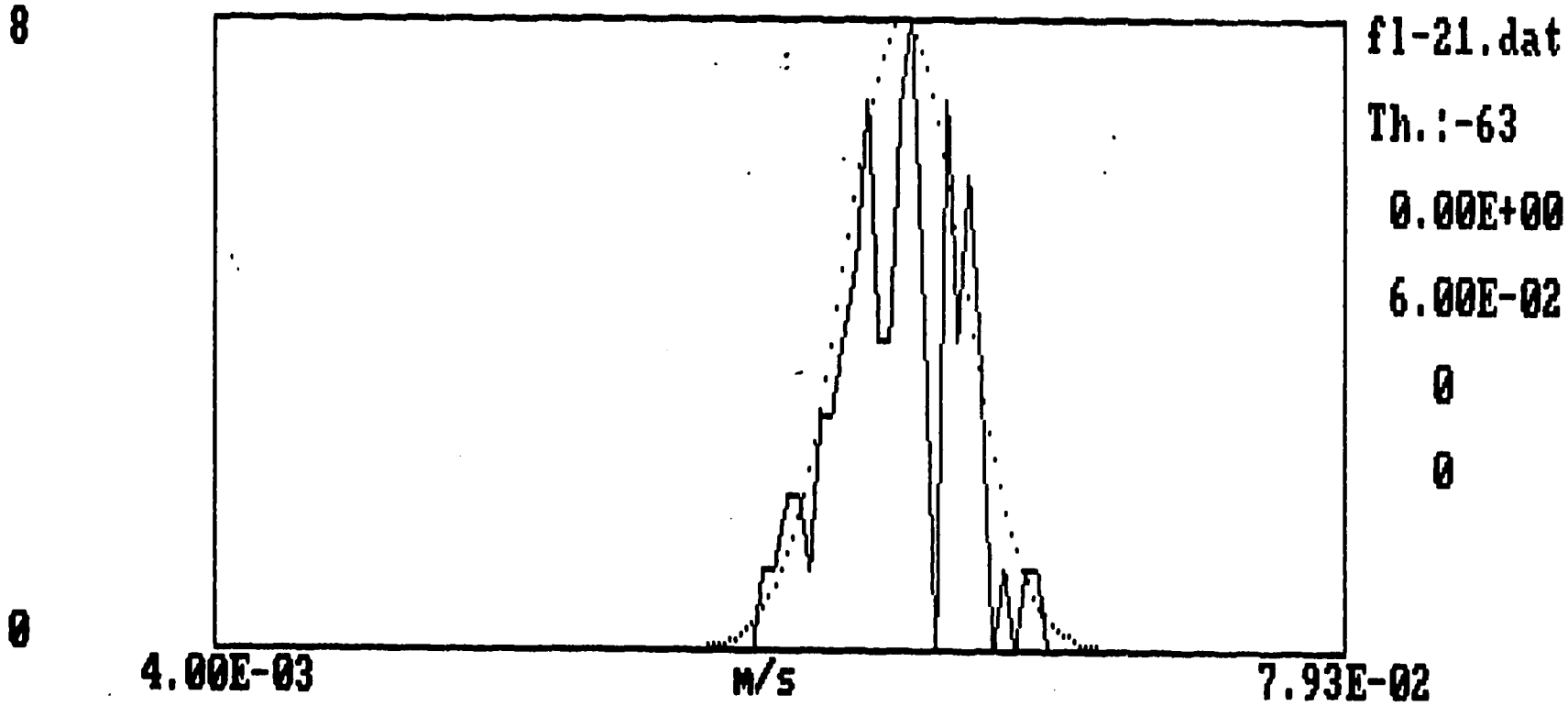

Velocity Distribution

Mean	: 4.978E-02 m/s	Dist. From Inlet	:	3.000E+01 cm
Stand. deviat.	: 3.991E-03 m/s	Radial Distance	:	5.000E+00 mm
Veloc. for max.	: 5.038E-02 m/s	Bulk velocity	:	5.200E-02 m/s
Skewness : -2.640E-02	Kurtosis : 2.525E+00	Re.	:	1.670E+03

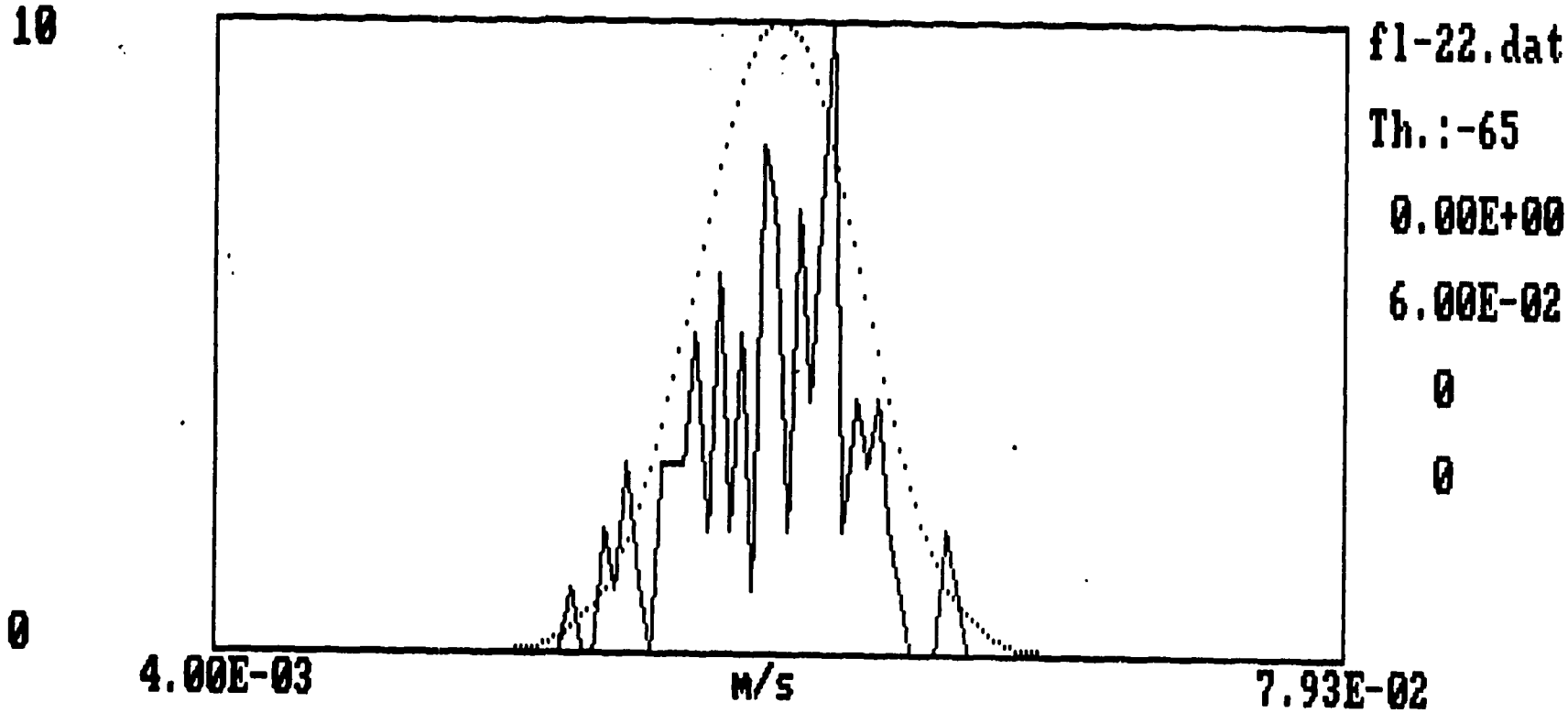

Velocity Distribution

Mean	: 4.146E-02 m/s	Dist. From Inlet		:	3.000E+01 cm
Stand. deviat.	: 5.421E-03 m/s	Radial Distance		:	1.000E+01 mm
Veloc. for max.	: 4.506E-02 m/s	Bulk velocity		:	5.200E-02 m/s
Skewness :	-2.175E-01	Kurtosis :	2.567E+00	Re. :	1.670E+03

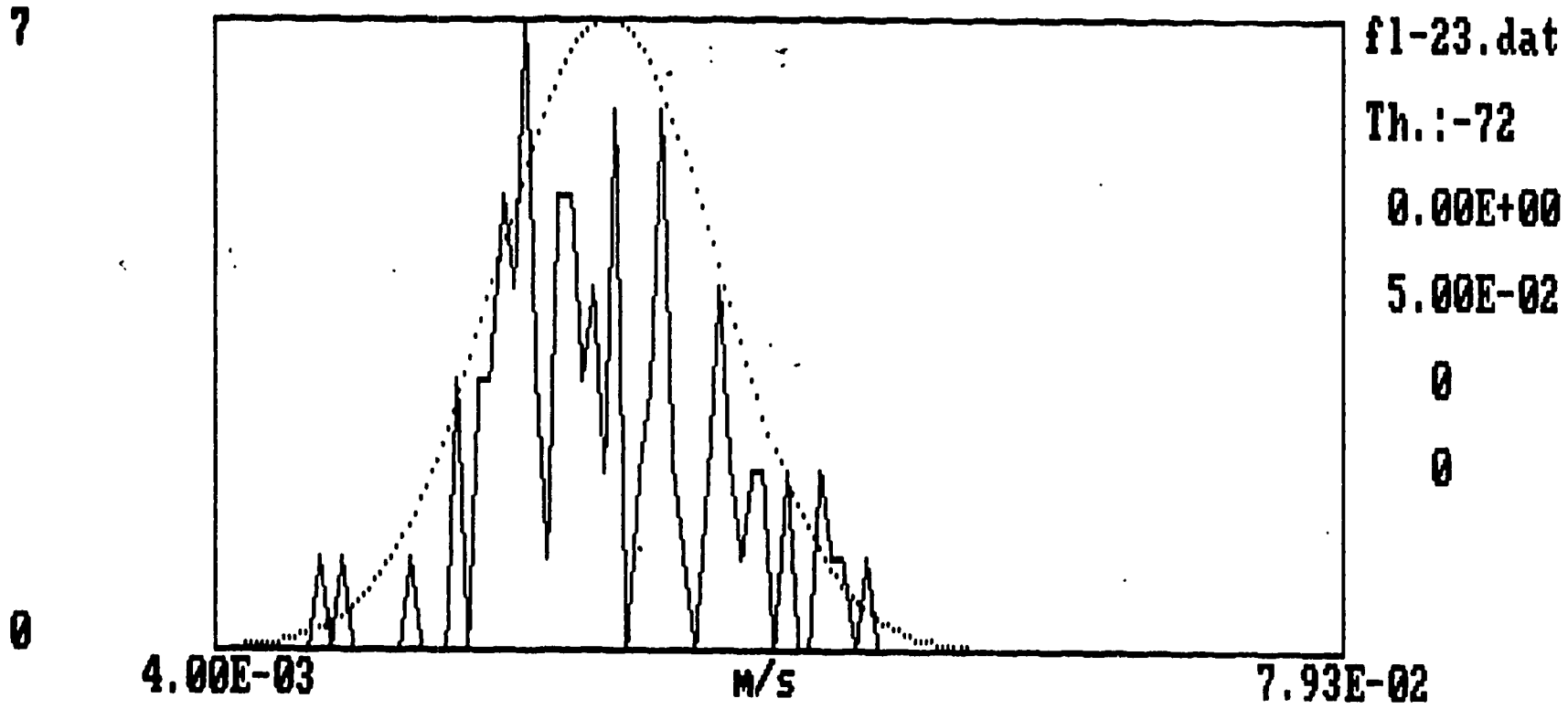

Velocity Distribution

Mean	: 3.011E-02 m/s	Dist. From Inlet	:	3.000E+01	cm
Stand. deviat.	: 7.393E-03 m/s	Radial Distance	:	1.200E+01	mm
Veloc. for max.	: 2.453E-02 m/s	Bulk velocity	:	5.200E-02	m/s
Skewness : 2.394E-01	Kurtosis : 2.794E+00	Re.	:	1.670E+03	

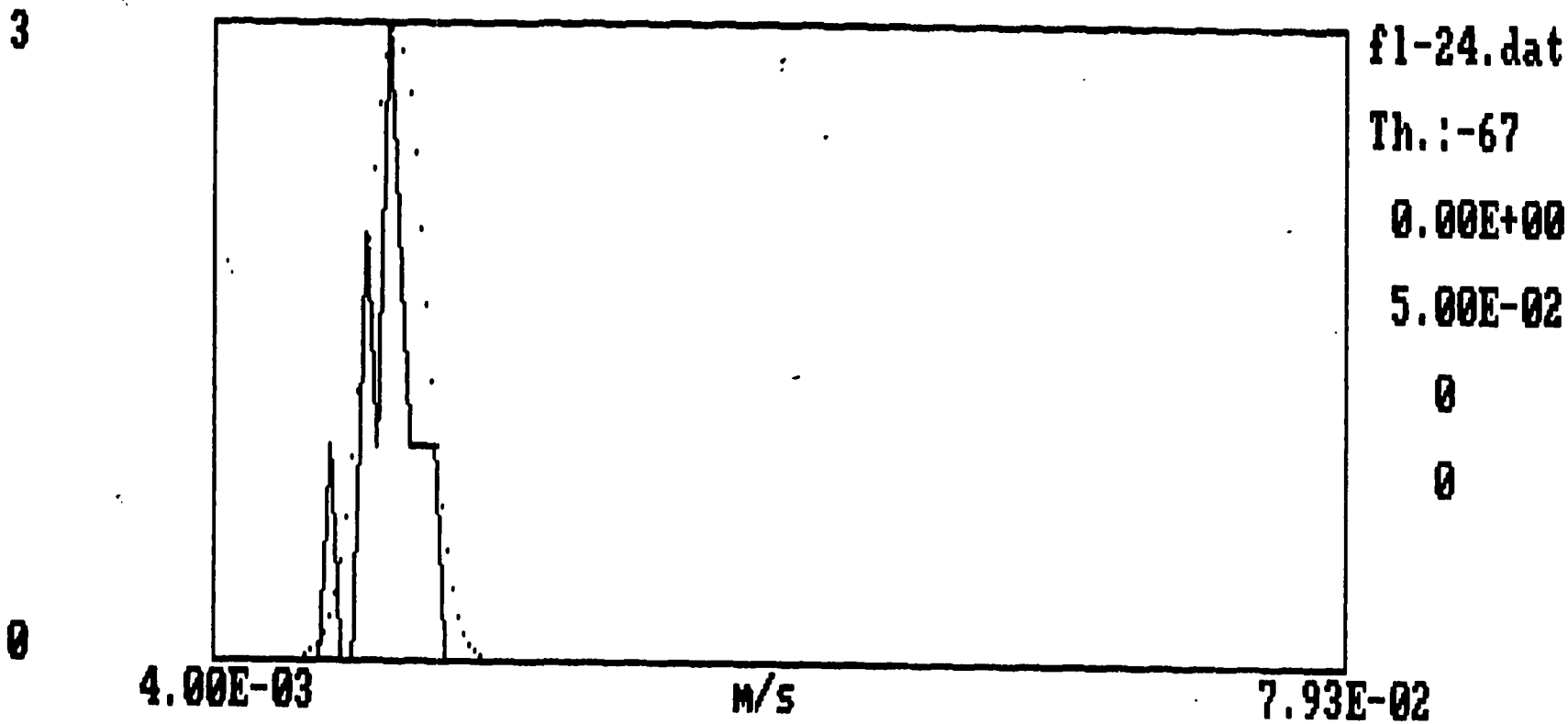

Velocity Distribution

Mean	: 1.589E-02 m/s	Dist. From Inlet		:	3.000E+01 cm
Stand. deviat.	: 1.876E-03 m/s	Radial Distance		:	1.400E+01 mm
Veloc. for max.	: 1.541E-02 m/s	Bulk velocity		:	5.200E-02 m/s
Skewness :	-6.018E-01	Kurtosis : 2.934E+00	Re.	:	1.670E+03

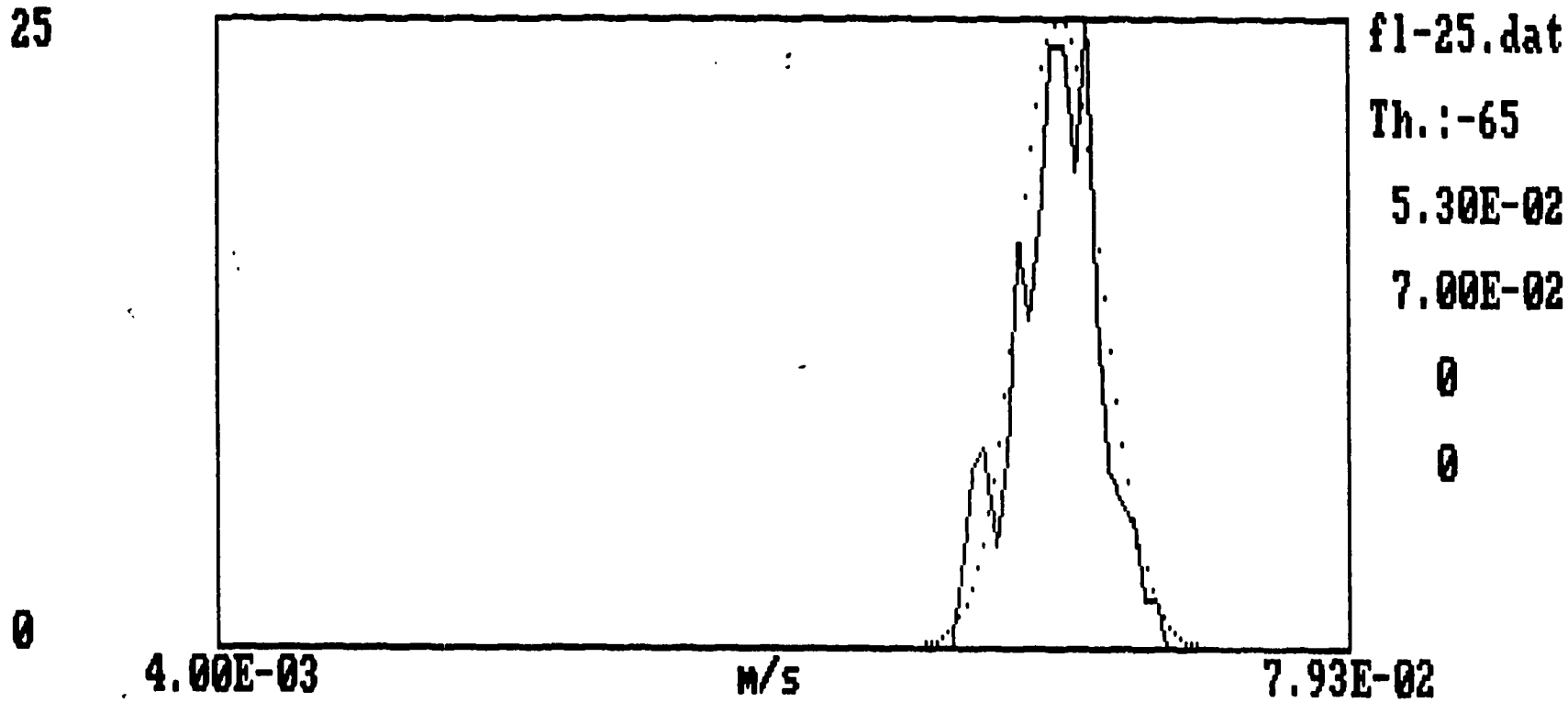

Velocity Distribution

Mean	: 6.007E-02 m/s	Dist. From Inlet	:	6.000E+01	cm
Stand. deviat.	: 2.767E-03 m/s	Radial Distance	:	0.000E+00	mm
Veloc. for max.	: 6.178E-02 m/s	Bulk velocity	:	5.200E-02	m/s
Skewness : -1.859E-01	Kurtosis : 2.677E+00	Re.	:	1.670E+03	

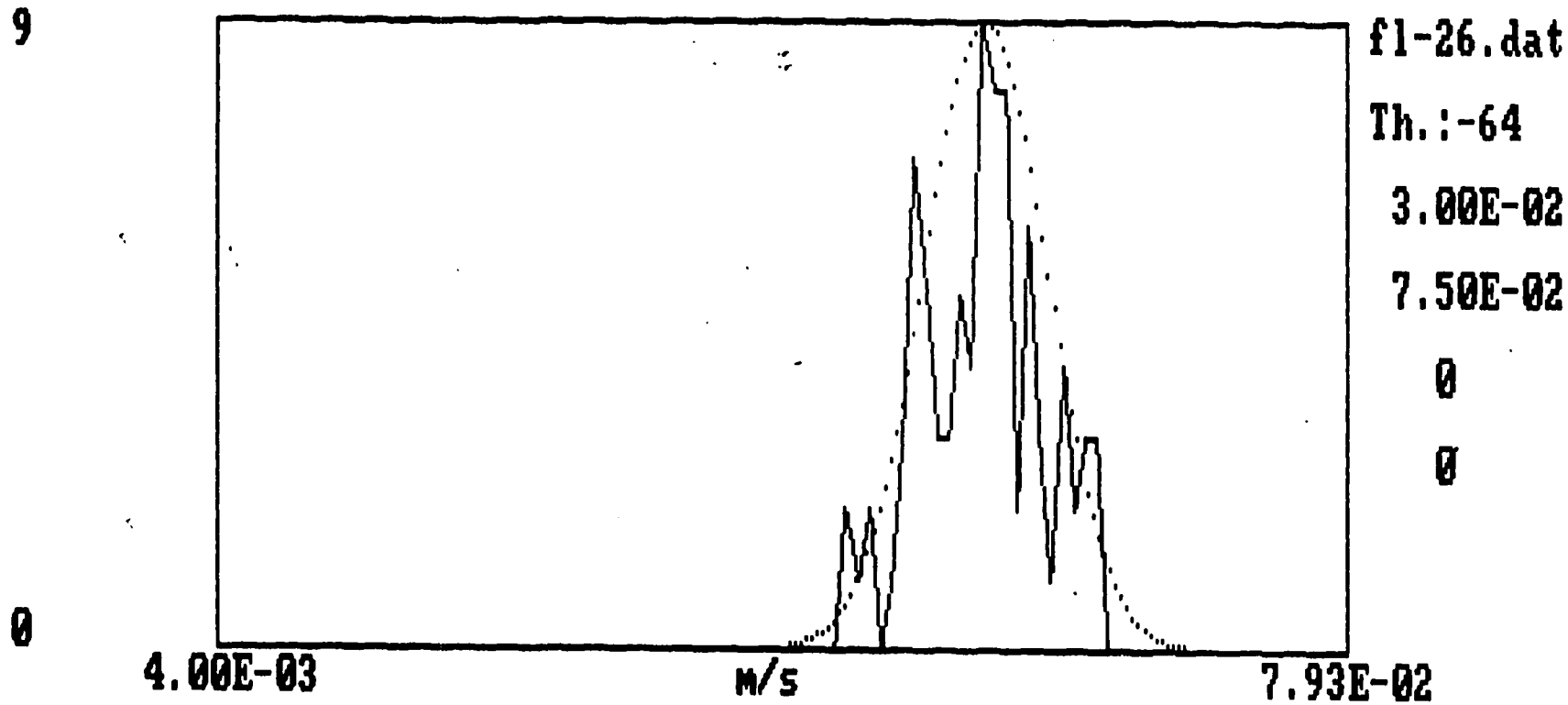

Velocity Distribution

Mean	: 5.515E-02 m/s	Dist. From Inlet	:	6.000E+01	cm
Stand. deviat.	: 4.082E-03 m/s	Radial Distance	:	5.000E+00	mm
Veloc. for max.	: 5.494E-02 m/s	Bulk velocity	:	5.200E-02	m/s
Skewness : -1.515E-01	Kurtosis : 2.483E+00	Re.	:	1.670E+03	

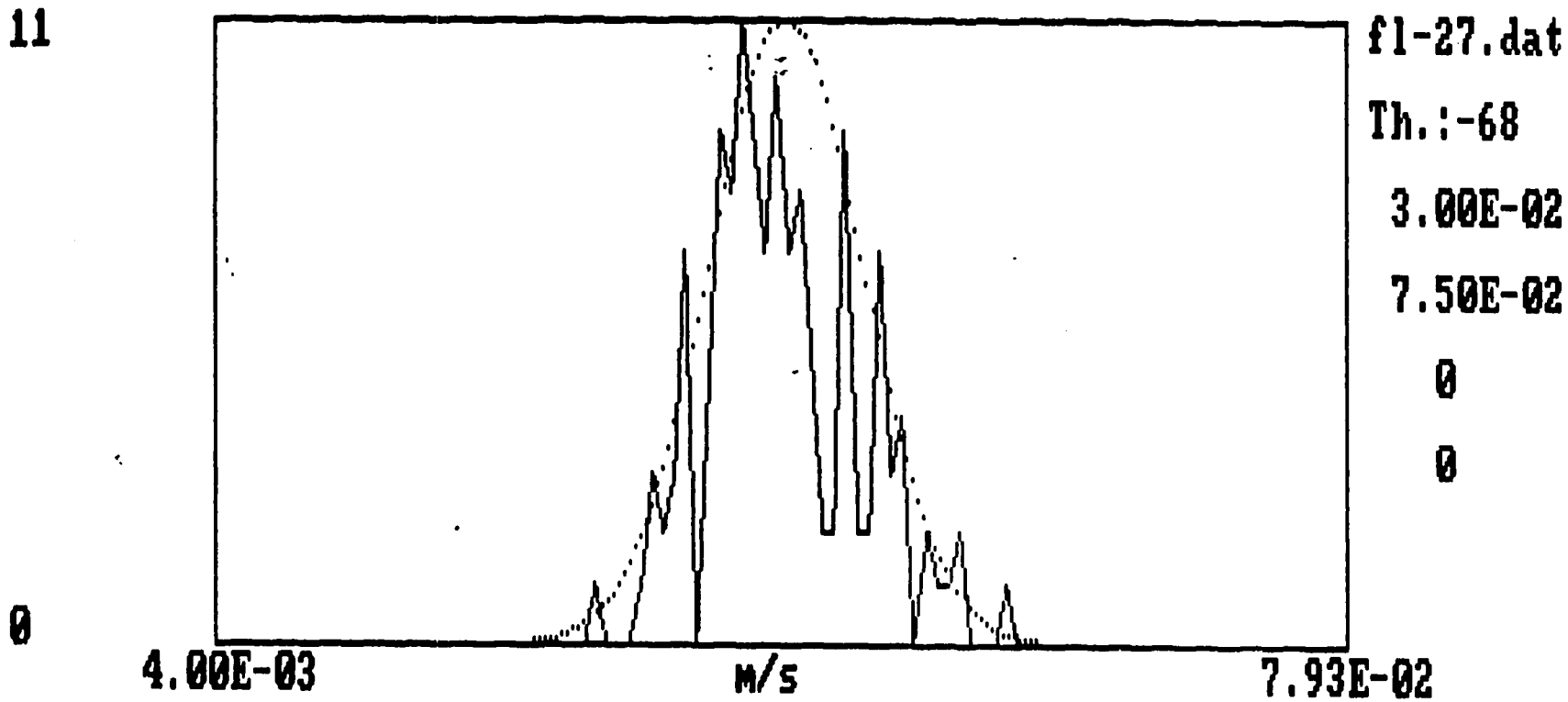

Velocity Distribution

Mean	: 4.190E-02 m/s	Dist. From Inlet	:	6.000E+01 cm	
Stand. deviat.	: 5.155E-03 m/s	Radial Distance	:	1.000E+01 mm	
Veloc. for max.	: 3.897E-02 m/s	Bulk velocity	:	5.200E-02 m/s	
Skewness : 3.953E-01	Kurtosis : 2.812E+00	Re.	:	1.670E+03	

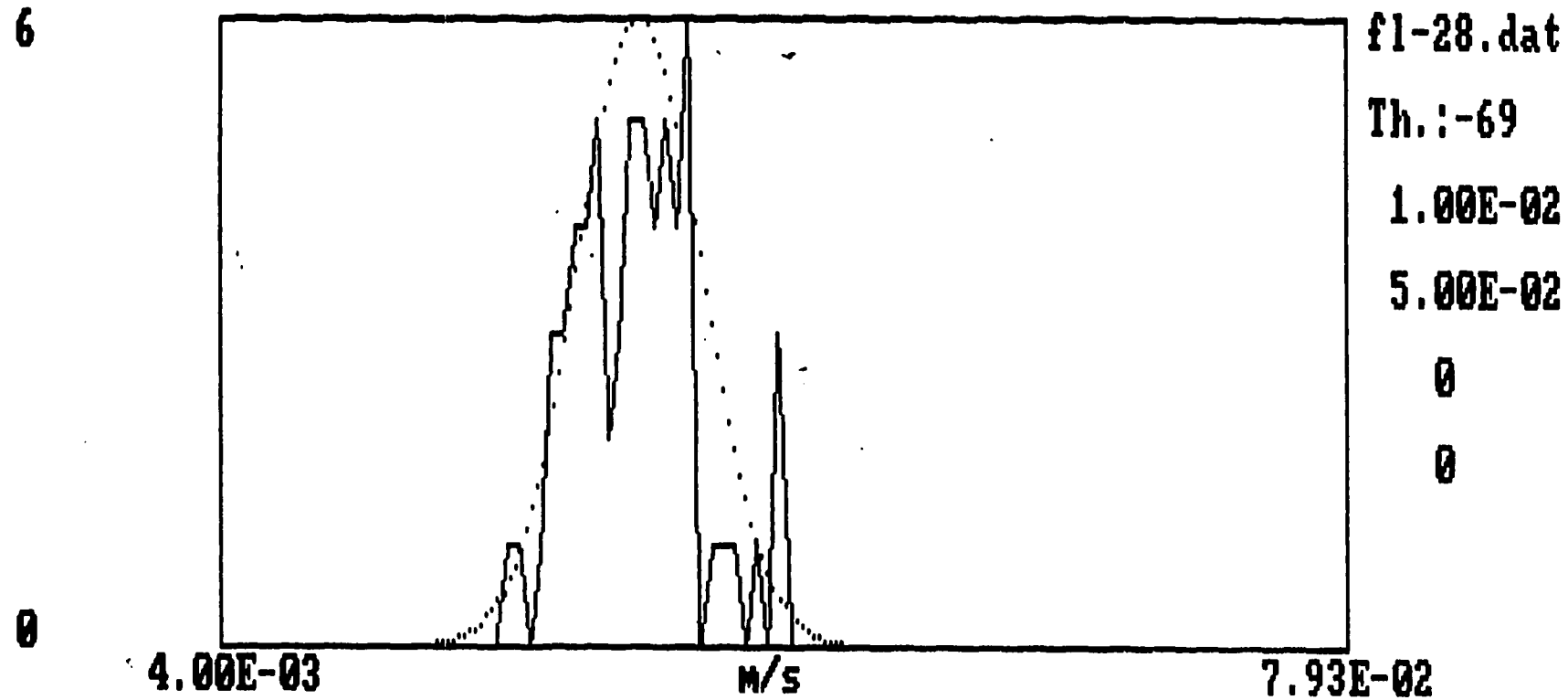

Velocity Distribution

Mean	: 3.194E-02 m/s	Dist. From Inlet	:	6.000E+01	cm
Stand. deviat.	: 4.151E-03 m/s	Radial Distance	:	1.200E+01	mm
Veloc. for max.	: 3.517E-02 m/s	Bulk velocity	:	5.200E-02	m/s
Skewness : 3.318E-01	Kurtosis : 2.722E+00	Re.	:	1.670E+03	

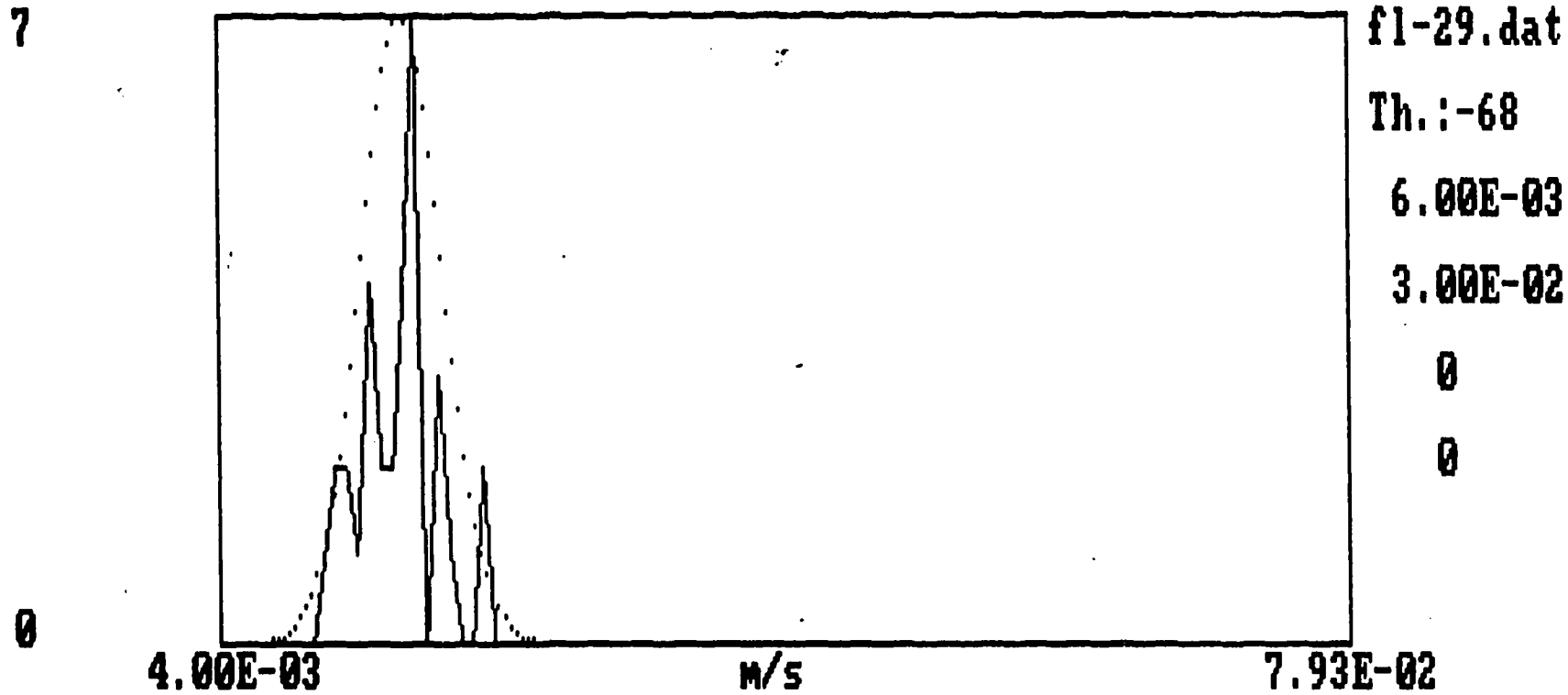

Velocity Distribution

Mean	: 1.605E-02 m/s	Dist. From Inlet	: 6.000E+01 cm
Stand. deviat.	: 2.676E-03 m/s	Radial Distance	: 1.400E+01 mm
Veloc. for max.	: 1.693E-02 m/s	Bulk velocity	: 5.200E-02 m/s
Skewness : 6.435E-02	Kurtosis : 2.394E+00	Re.	: 1.670E+03

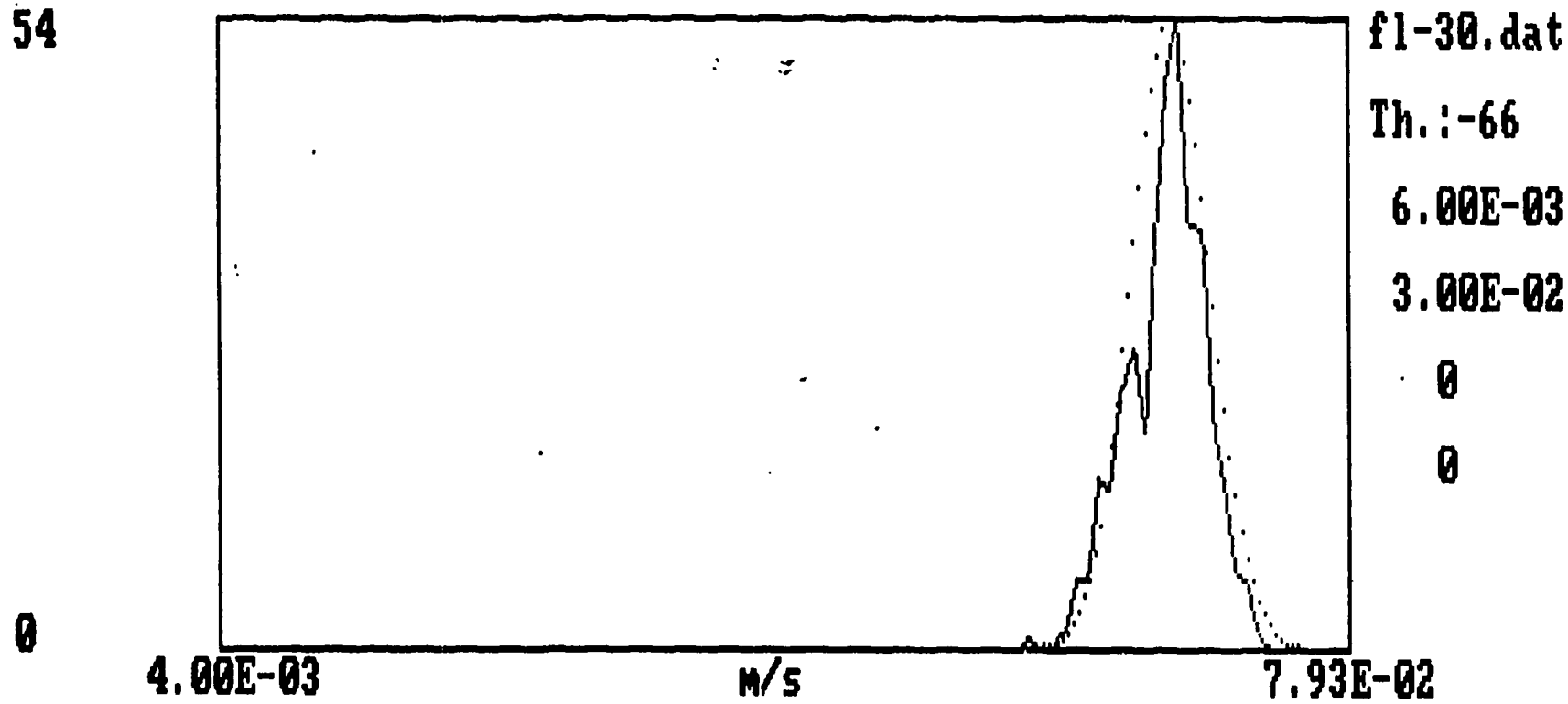

Velocity Distribution

Mean	: 6.738E-02 m/s	Dist. From Inlet		:	1.000E+02 cm
Stand. deviat.	: 2.602E-03 m/s	Radial Distance		:	0.000E+00 mm
Veloc. for max.	: 6.787E-02 m/s	Bulk velocity		:	5.200E-02 m/s
Skewness :	-3.579E-01	Kurtosis :	2.882E+00	Re. :	1.670E+03

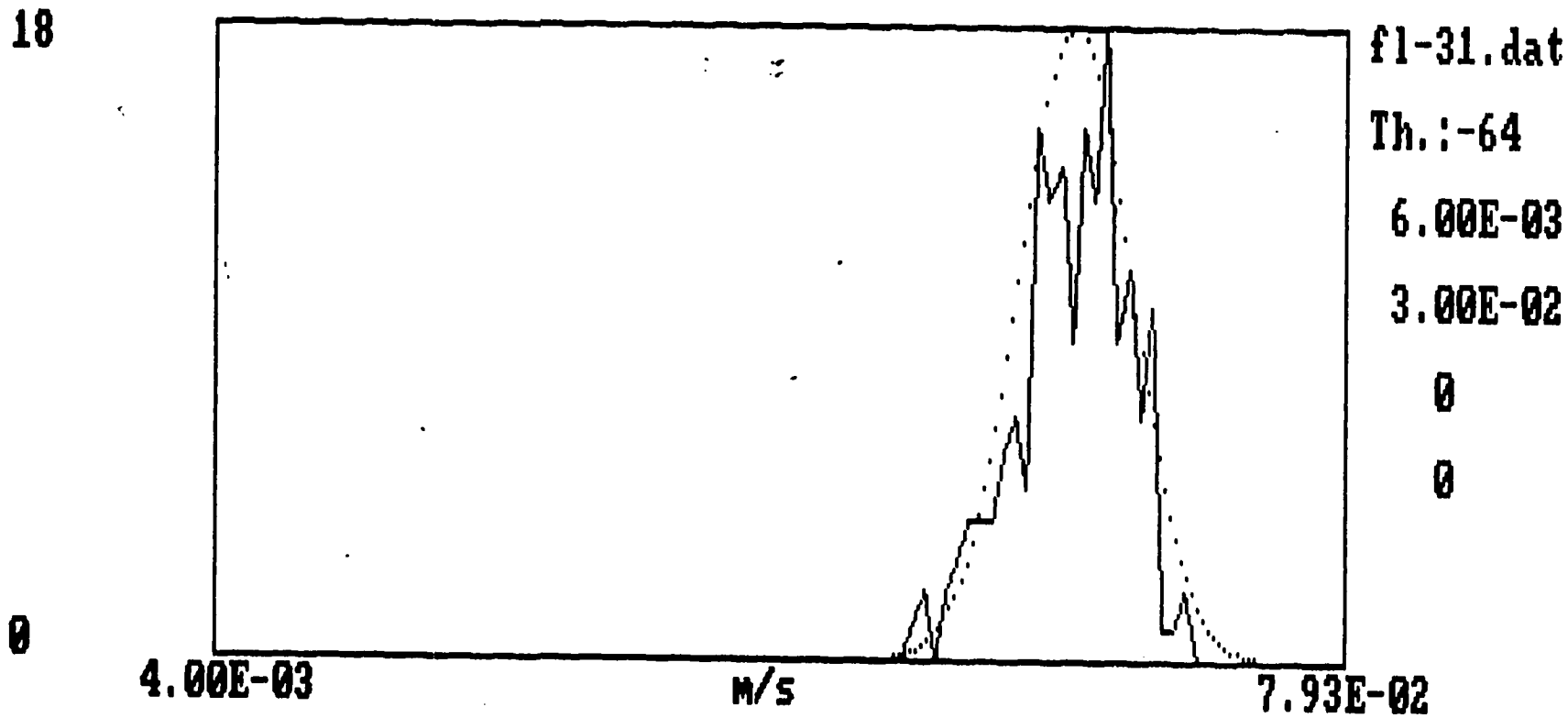

Velocity Distribution

Mean	: 6.123E-02 m/s	Dist. From Inlet		:	1.000E+02 cm
Stand. deviat.	: 3.736E-03 m/s	Radial Distance		:	5.000E+00 mm
Veloc. for max.	: 6.330E-02 m/s	Bulk velocity		:	5.200E-02 m/s
Skewness :	-4.391E-01	Kurtosis : 2.746E+00	Re.	:	1.670E+03

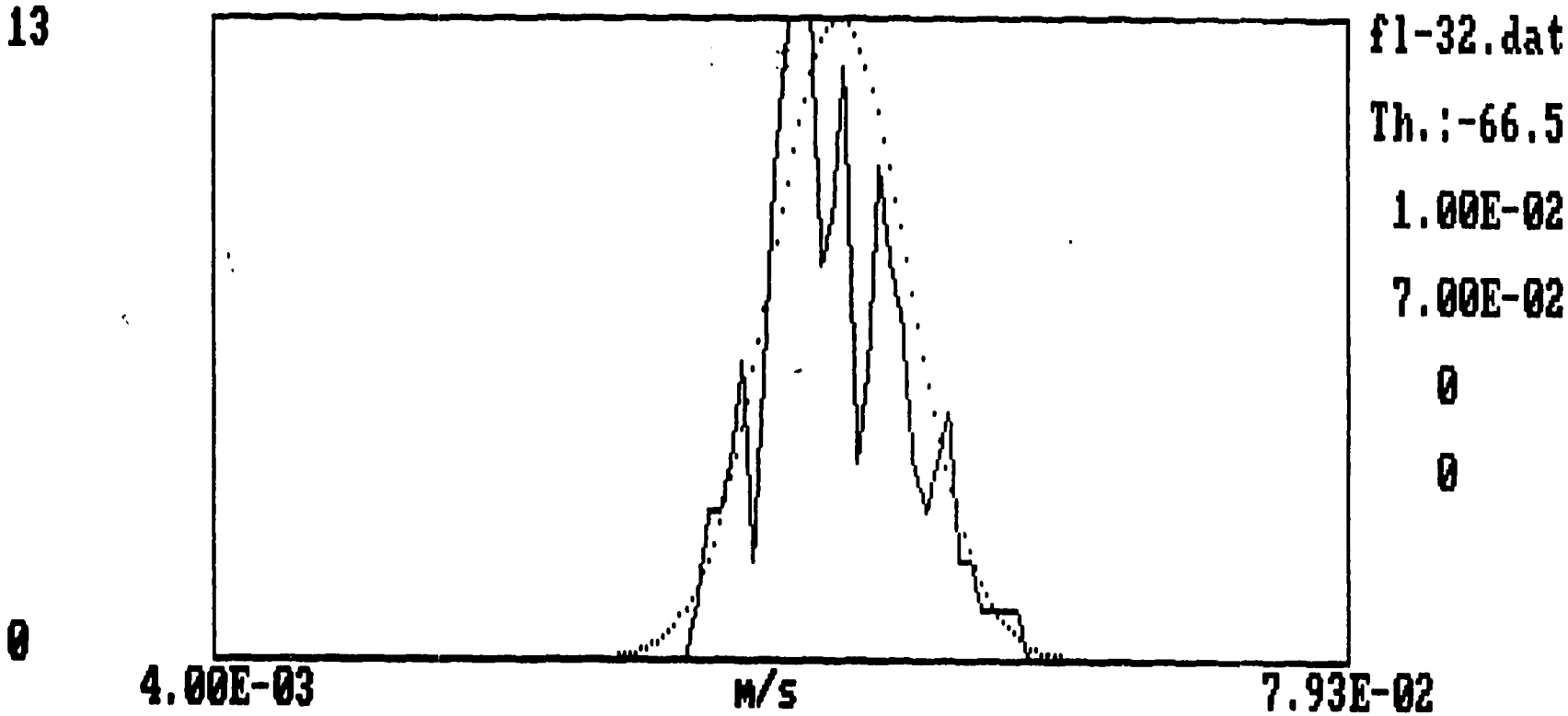

Velocity Distribution

Mean	: 4.548E-02 m/s	Dist. From Inlet	:	1.000E+02 cm	
Stand. deviat.	: 4.544E-03 m/s	Radial Distance	:	1.000E+01 mm	
Veloc. for max.	: 4.202E-02 m/s	Bulk velocity	:	5.200E-02 m/s	
Skewness : 3.433E-01	Kurtosis : 2.599E+00	Re.	:	1.670E+03	

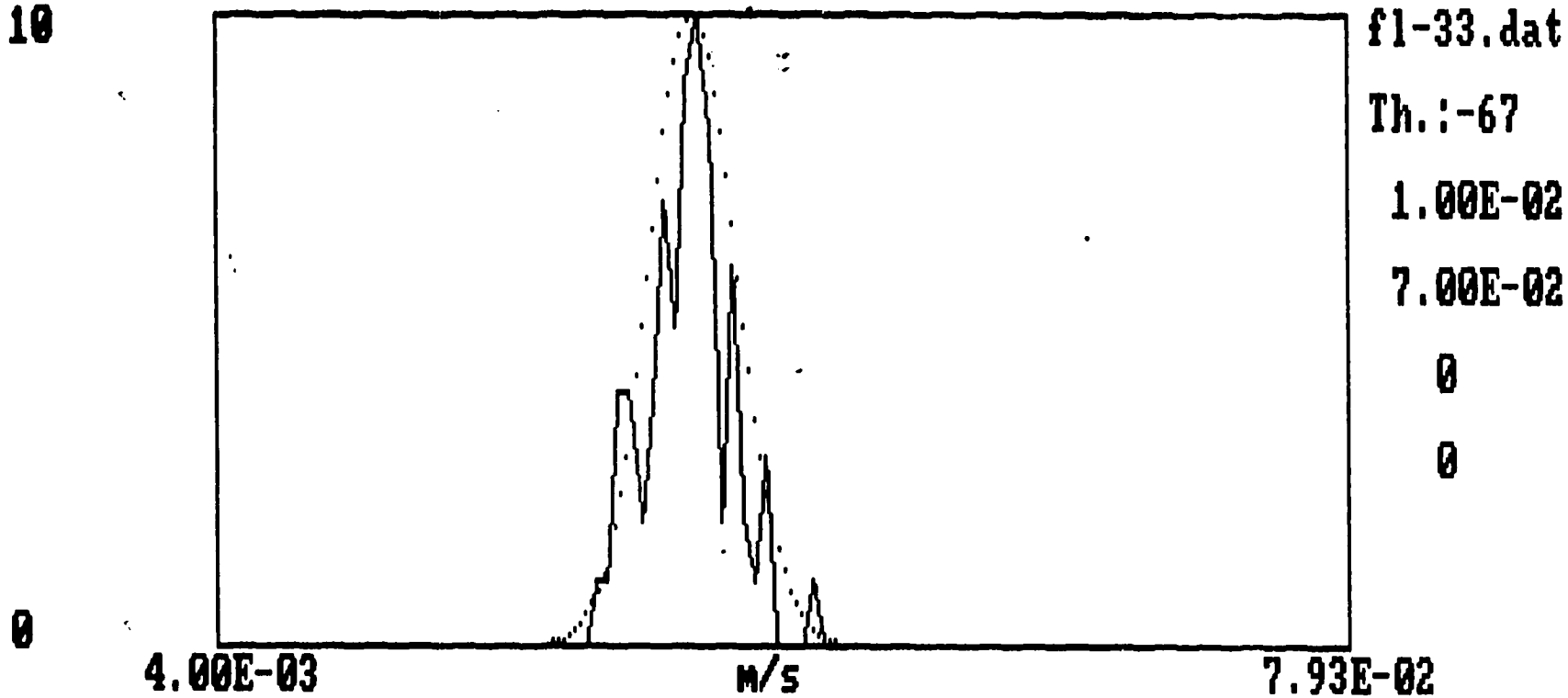

Velocity Distribution

Mean	: 3.562E-02 m/s	Dist. From Inlet	:	1.000E+02	cm
Stand. deviat.	: 2.900E-03 m/s	Radial Distance	:	1.200E+01	mm
Veloc. for max.	: 3.593E-02 m/s	Bulk velocity	:	5.200E-02	m/s
Skewness : 1.684E-01	Kurtosis : 2.876E+00	Re.	:	1.670E+03	

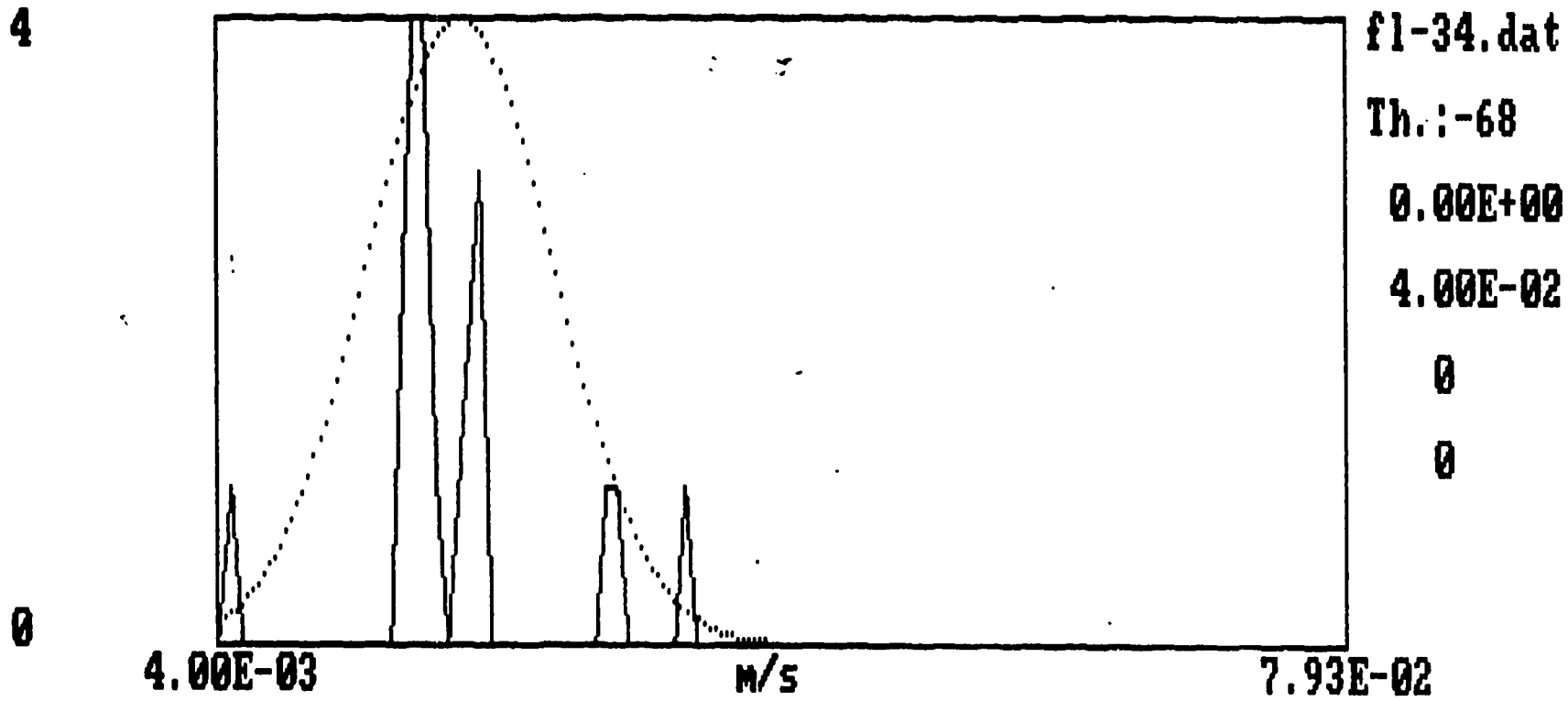

Velocity Distribution

Mean	: 2.015E-02 m/s	Dist. From Inlet		:	1.000E+02 cm
Stand. deviat.	: 6.249E-03 m/s	Radial Distance		:	1.400E+01 mm
Veloc. for max.	: 1.693E-02 m/s	Bulk velocity		:	5.200E-02 m/s
Skewness : 4.854E-01	Kurtosis : 4.298E+00		Re.	:	1.670E+03

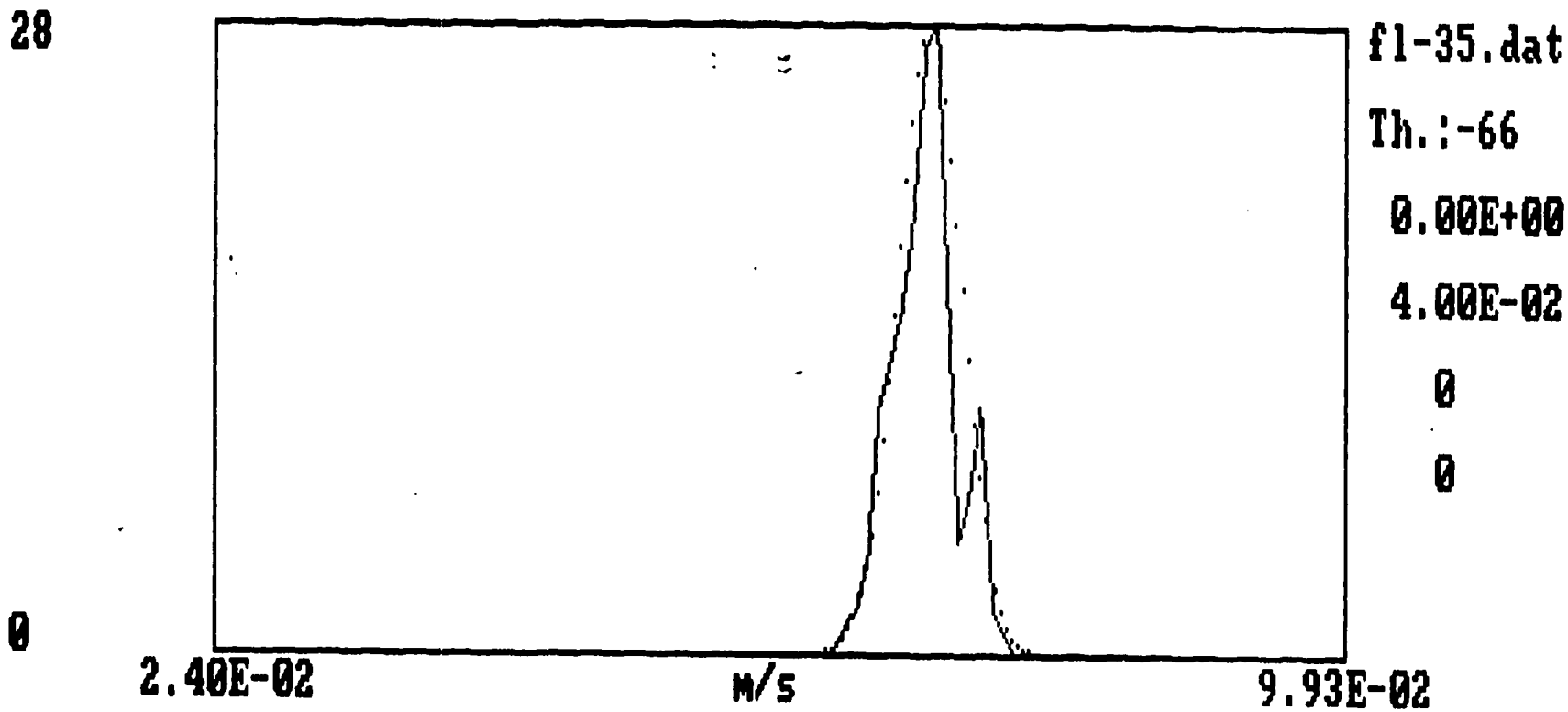

Velocity Distribution

Mean	: 7.149E-02 m/s	Dist. From Inlet	:	1.500E+02	cm
Stand. deviat.	: 2.092E-03 m/s	Radial Distance	:	0.000E+00	mm
Veloc. for max.	: 7.191E-02 m/s	Bulk velocity	:	5.200E-02	m/s
Skewness : 7.167E-02	Kurtosis : 2.731E+00	Re.	:	1.670E+03	

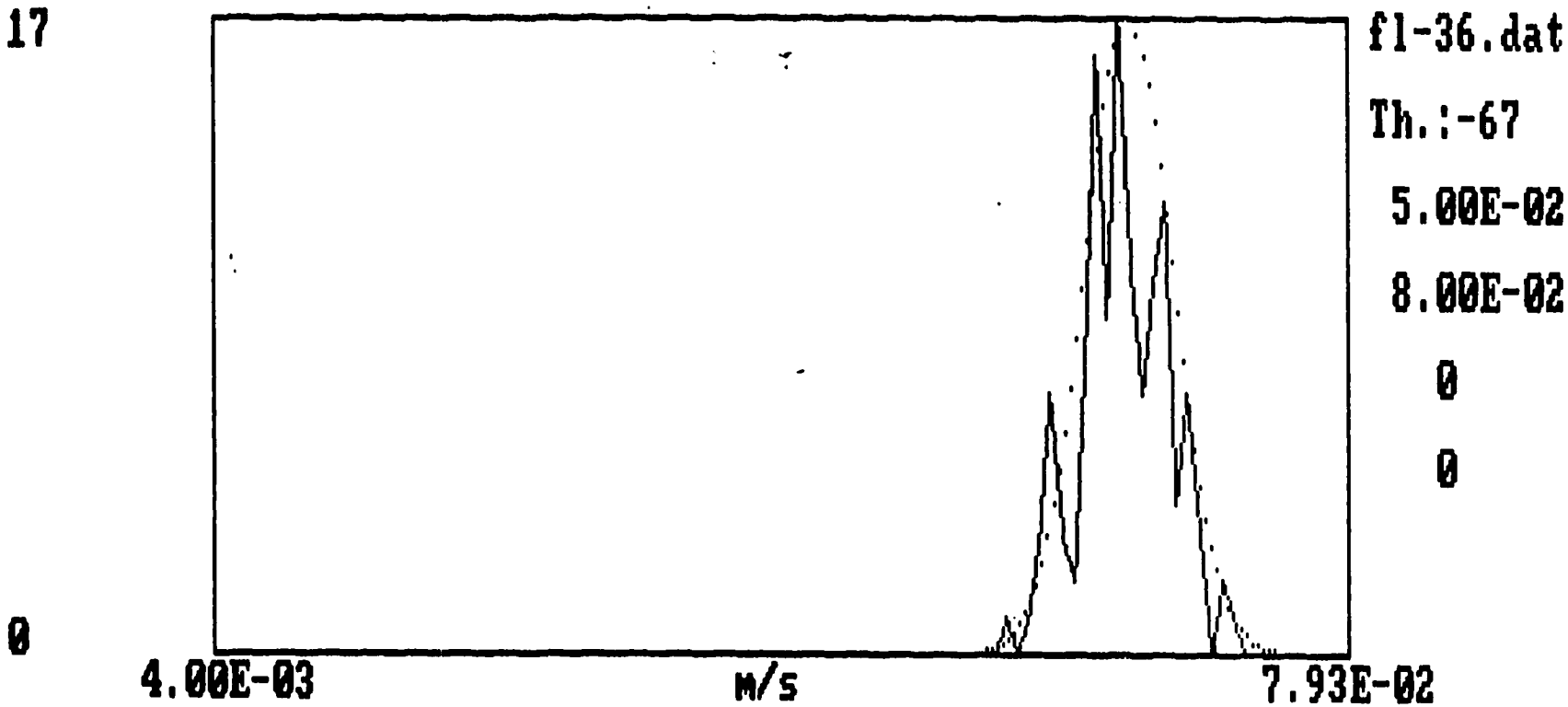

Velocity Distribution

Mean	: 6.470E-02 m/s	Dist. From Inlet	:	1.500E+02	cm
Stand. deviat.	: 2.949E-03 m/s	Radial Distance	:	5.000E+00	mm
Veloc. for max.	: 6.406E-02 m/s	Bulk velocity	:	5.200E-02	m/s
Skewness : -3.777E-02	Kurtosis : 2.630E+00	Re.	:	1.670E+03	

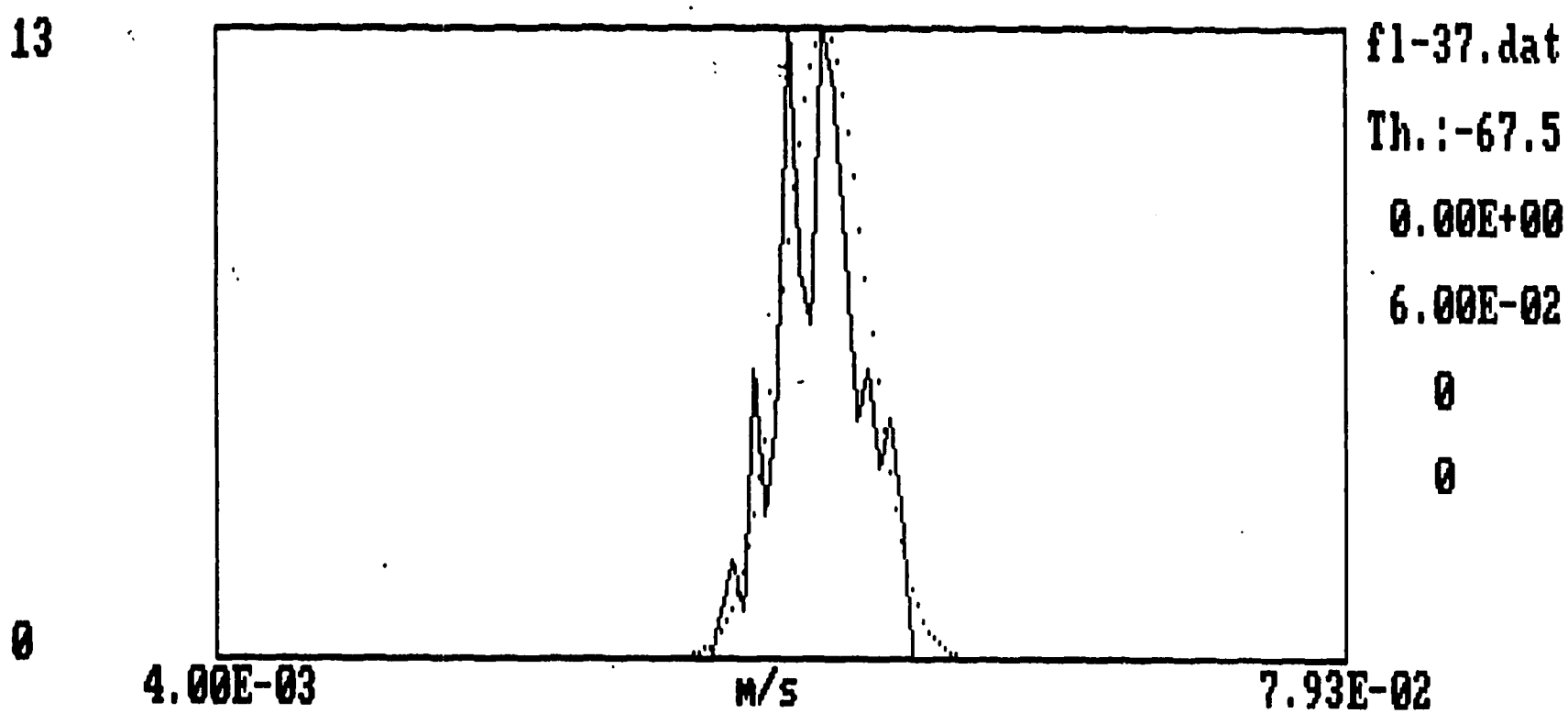

Velocity Distribution

Mean	: 4.450E-02 m/s	Dist. From Inlet	:	1.500E+02	cm
Stand. deviat.	: 2.773E-03 m/s	Radial Distance	:	1.000E+01	mm
Veloc. for max.	: 4.202E-02 m/s	Bulk velocity	:	5.200E-02	m/s
Skewness : -6.582E-02	Kurtosis : 2.475E+00	Re.	:	1.670E+03	

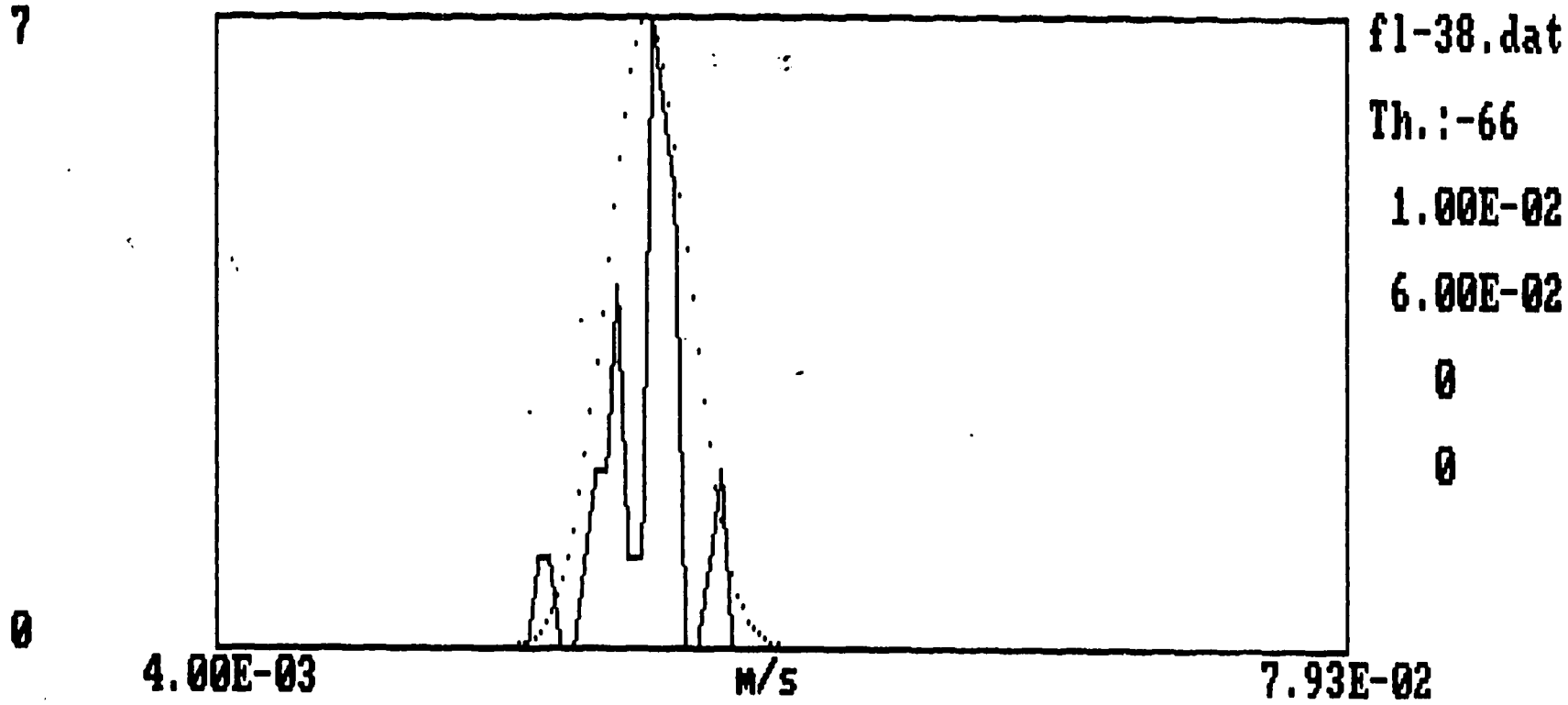

Velocity Distribution

Mean	: 3.265E-02 m/s	Dist. From Inlet		:	1.500E+02 cm
Stand. deviat.	: 2.716E-03 m/s	Radial Distance		:	1.200E+01 mm
Veloc. for max.	: 3.289E-02 m/s	Bulk velocity		:	5.200E-02 m/s
Skewness :	-5.018E-01	Kurtosis :	3.089E+00	Re. :	1.670E+03

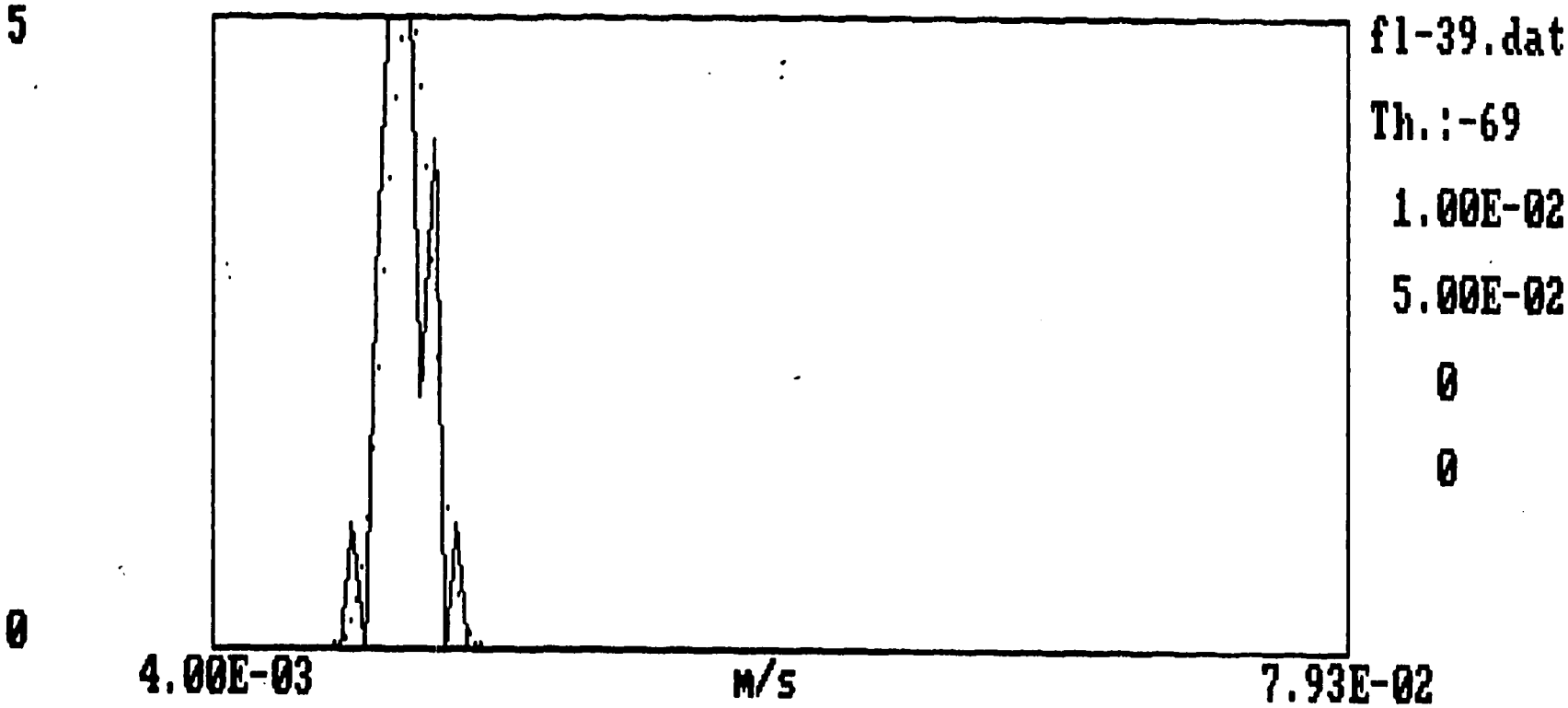

Velocity Distribution

Mean	: 1.682E-02 m/s	Dist. From Inlet		:	1.500E+02 cm
Stand. deviat.	: 1.503E-03 m/s	Radial Distance		:	1.400E+01 mm
Veloc. for max.	: 1.541E-02 m/s	Bulk velocity		:	5.200E-02 m/s
Skewness :	1.410E-01	Kurtosis : 2.699E+00	Re.	:	1.670E+03

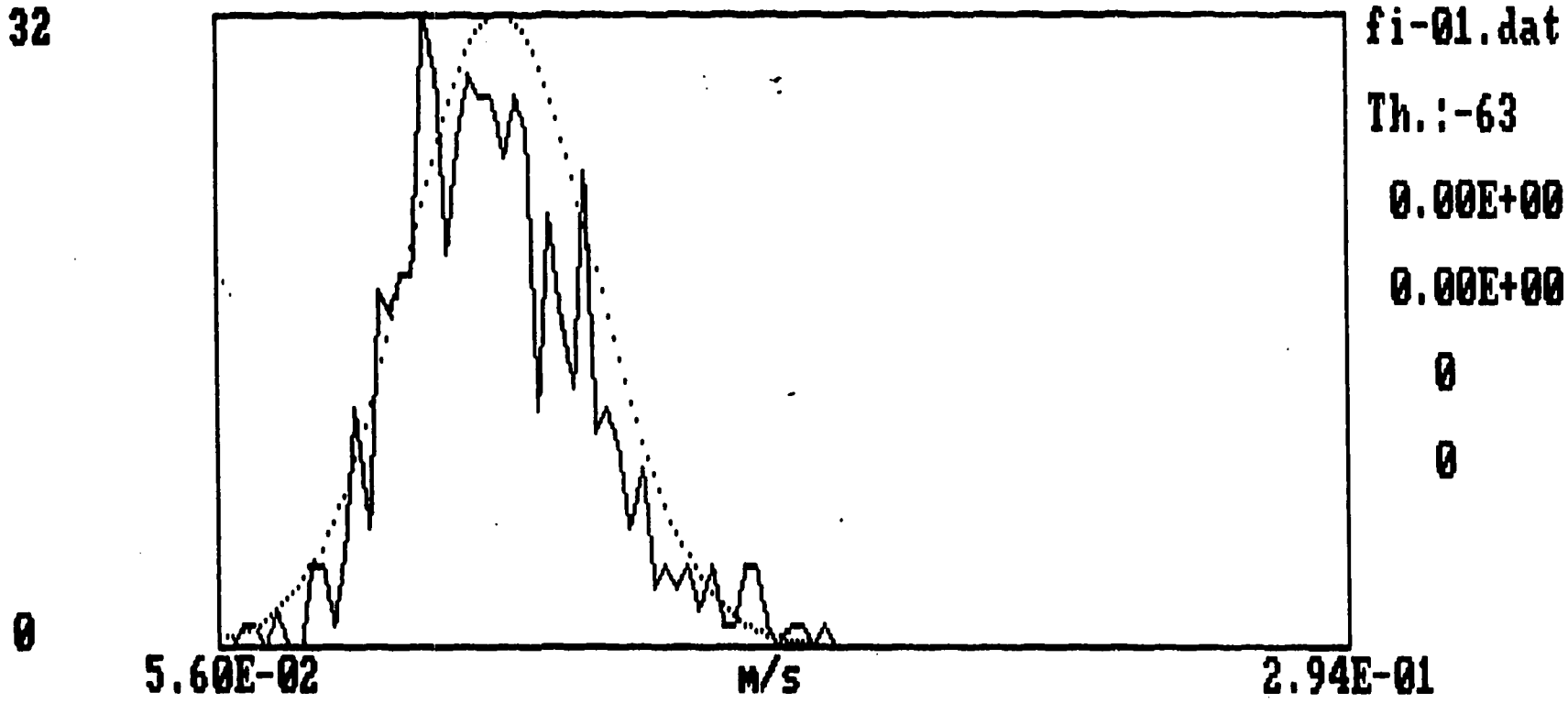

Velocity Distribution

Mean	: 1.155E-01 m/s	Dist. From Inlet	:	-1.000E+00	cm
Stand. deviat.	: 1.983E-02 m/s	Radial Distance	:	0.000E+00	mm
Veloc. for max.	: 9.924E-02 m/s	Bulk velocity	:	1.180E-01	m/s
Skewness : 5.223E-01	Kurtosis : 3.405E+00	Re.	:	3.680E+03	

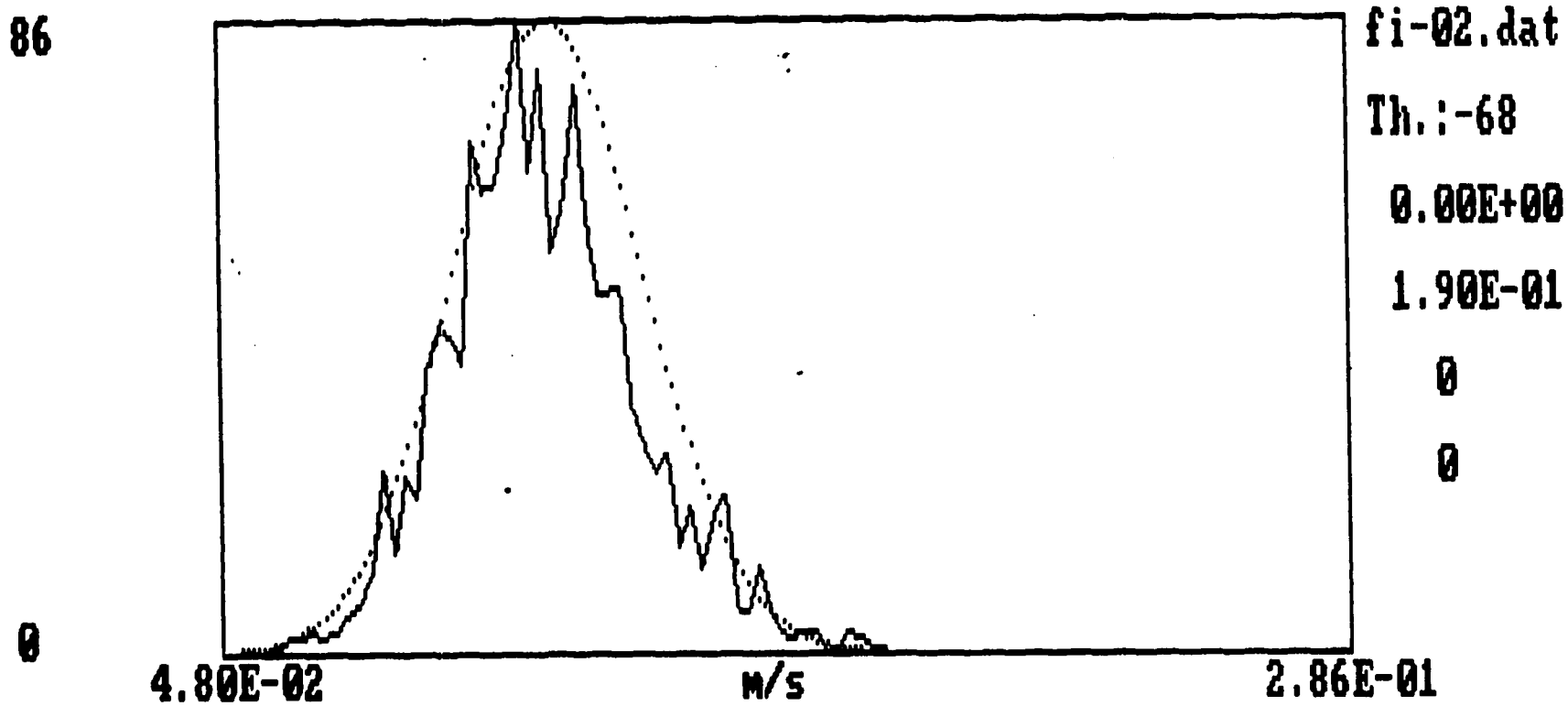

Velocity Distribution

Mean	: 1.169E-01 m/s	Dist. From Inlet	:	-1.000E+00	cm
Stand. deviat.	: 2.002E-02 m/s	Radial Distance	:	1.000E+01	mm
Veloc. for max.	: 1.104E-01 m/s	Bulk velocity	:	1.180E-01	m/s
Skewness : 3.776E-01	Kurtosis : 3.266E+00	Re.	:	3.680E+03	

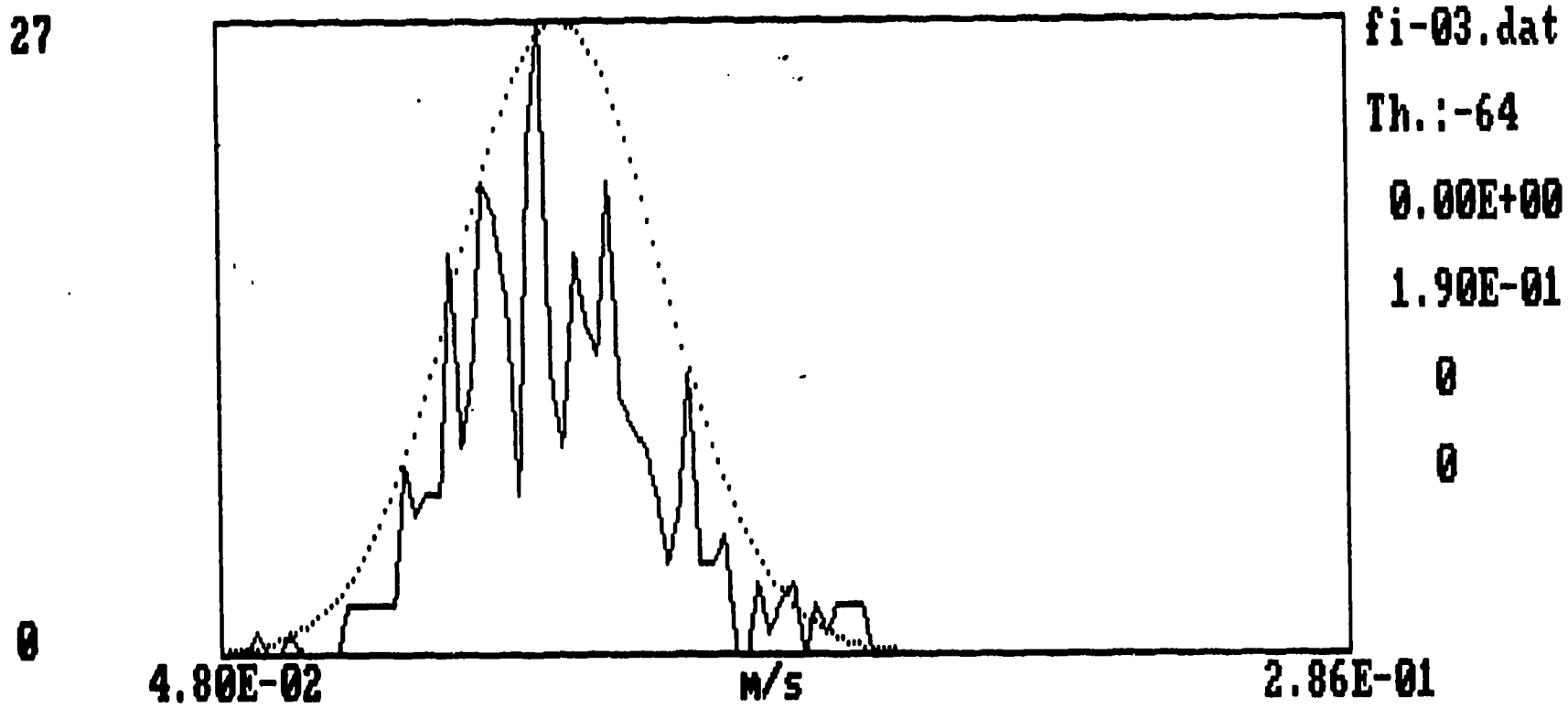

Velocity Distribution

Mean	: 1.196E-01 m/s	Dist. From Inlet		:	-1.000E+00 cm
Stand. deviat.	: 2.159E-02 m/s	Radial Distance		:	1.500E+01 mm
Veloc. for max.	: 1.152E-01 m/s	Bulk velocity		:	1.180E-01 m/s
Skewness :	4.751E-01	Kurtosis : 3.413E+00	Re.	:	3.680E+03

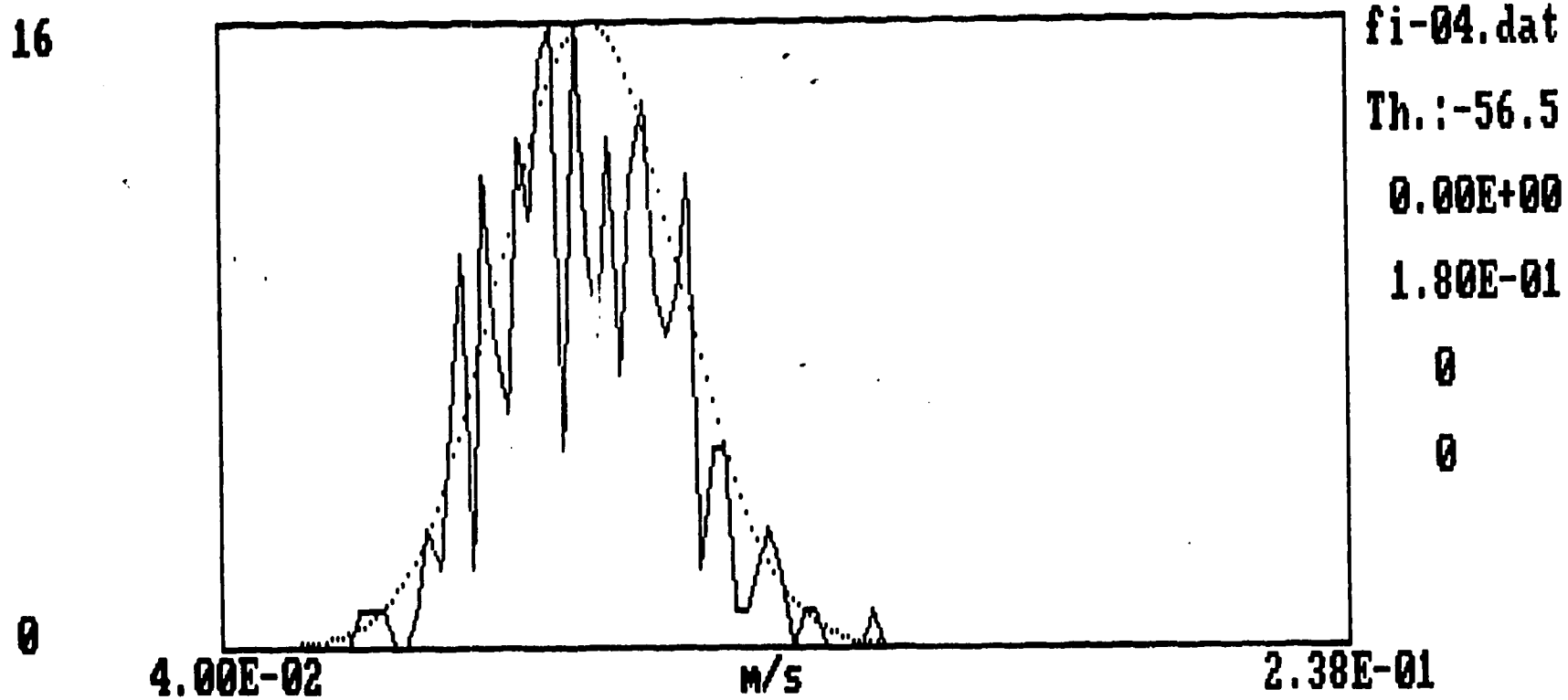

Velocity Distribution

Mean	: 1.047E-01 m/s	Dist. From Inlet	:	2.000E+00 cm	
Stand. deviat.	: 1.562E-02 m/s	Radial Distance	:	0.000E+00 mm	
Veloc. for max.	: 9.804E-02 m/s	Bulk velocity	:	1.180E-01 m/s	
Skewness : 1.839E-01	Kurtosis : 2.775E+00	Re.	:	3.680E+03	

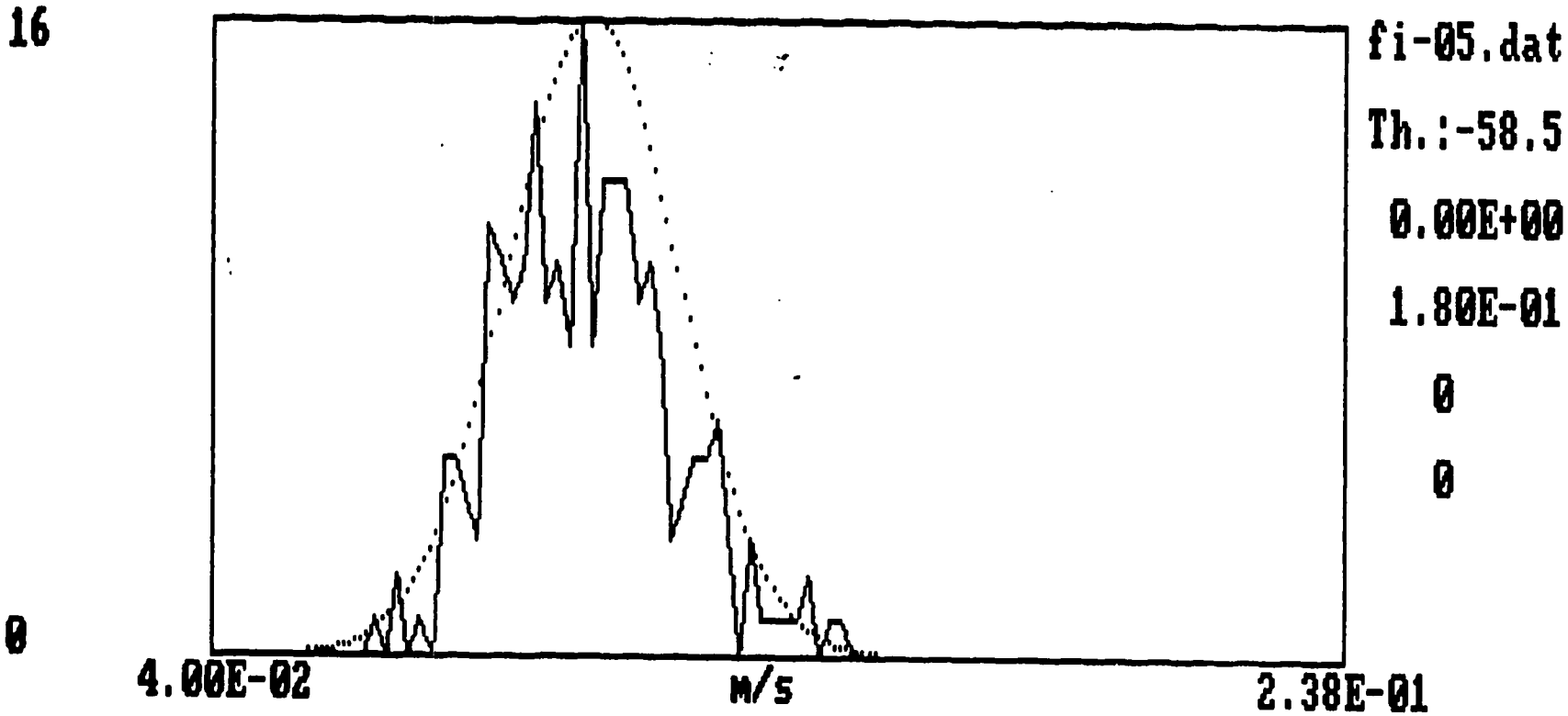

Velocity Distribution

Mean	: 1.062E-01 m/s	Dist. From Inlet	:	2.000E+00	cm
Stand. deviat.	: 1.523E-02 m/s	Radial Distance	:	5.000E+00	mm
Veloc. for max.	: 1.040E-01 m/s	Bulk velocity	:	1.180E-01	m/s
Skewness :	3.522E-01	Kurtosis : 2.977E+00	Re. :	3.680E+03	

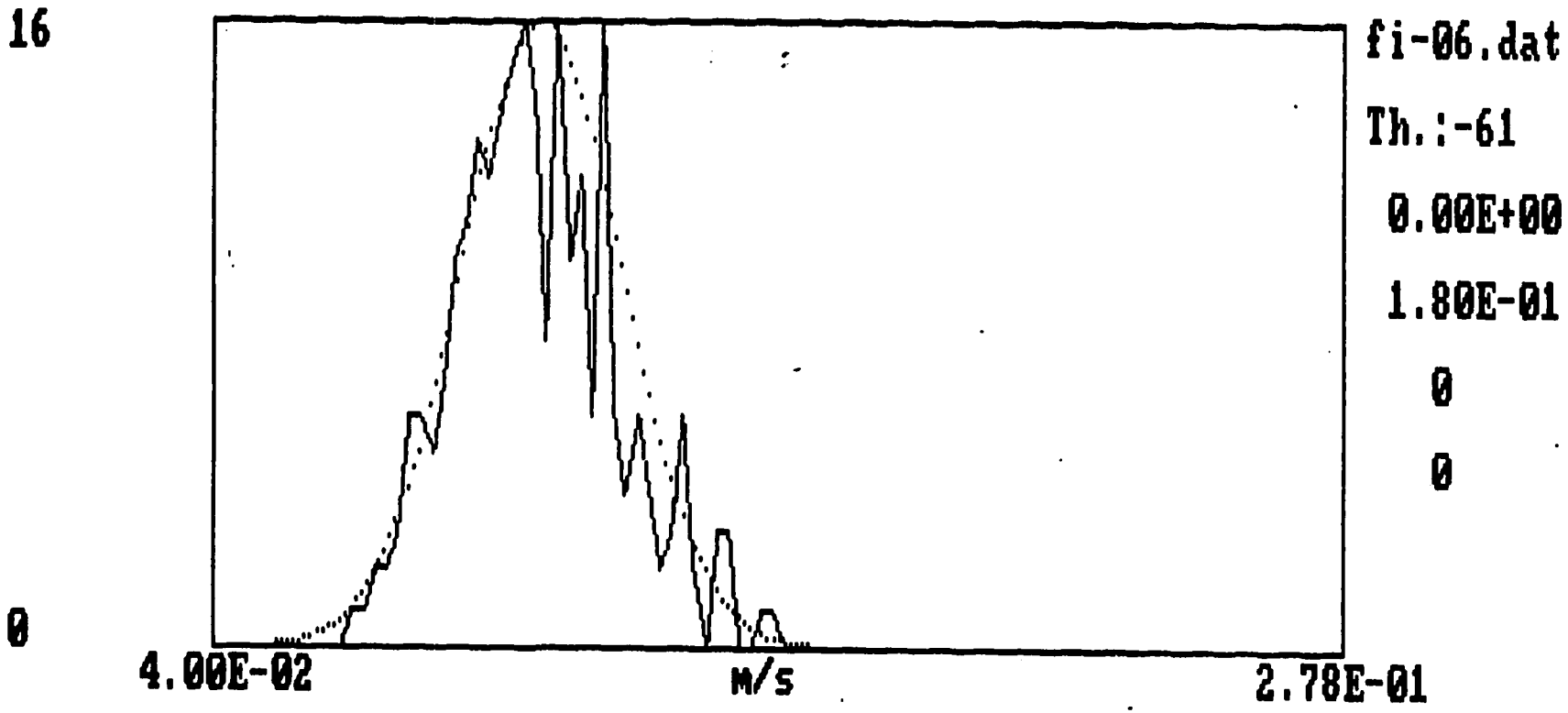

Velocity Distribution

Mean	: 1.087E-01 m/s	Dist. From Inlet	:	2.000E+00	cm
Stand. deviat.	: 1.710E-02 m/s	Radial Distance	:	1.000E+01	mm
Veloc. for max.	: 1.048E-01 m/s	Bulk velocity	:	1.180E-01	m/s
Skewness : 3.509E-01	Kurtosis : 2.871E+00	Re.	:	3.680E+03	

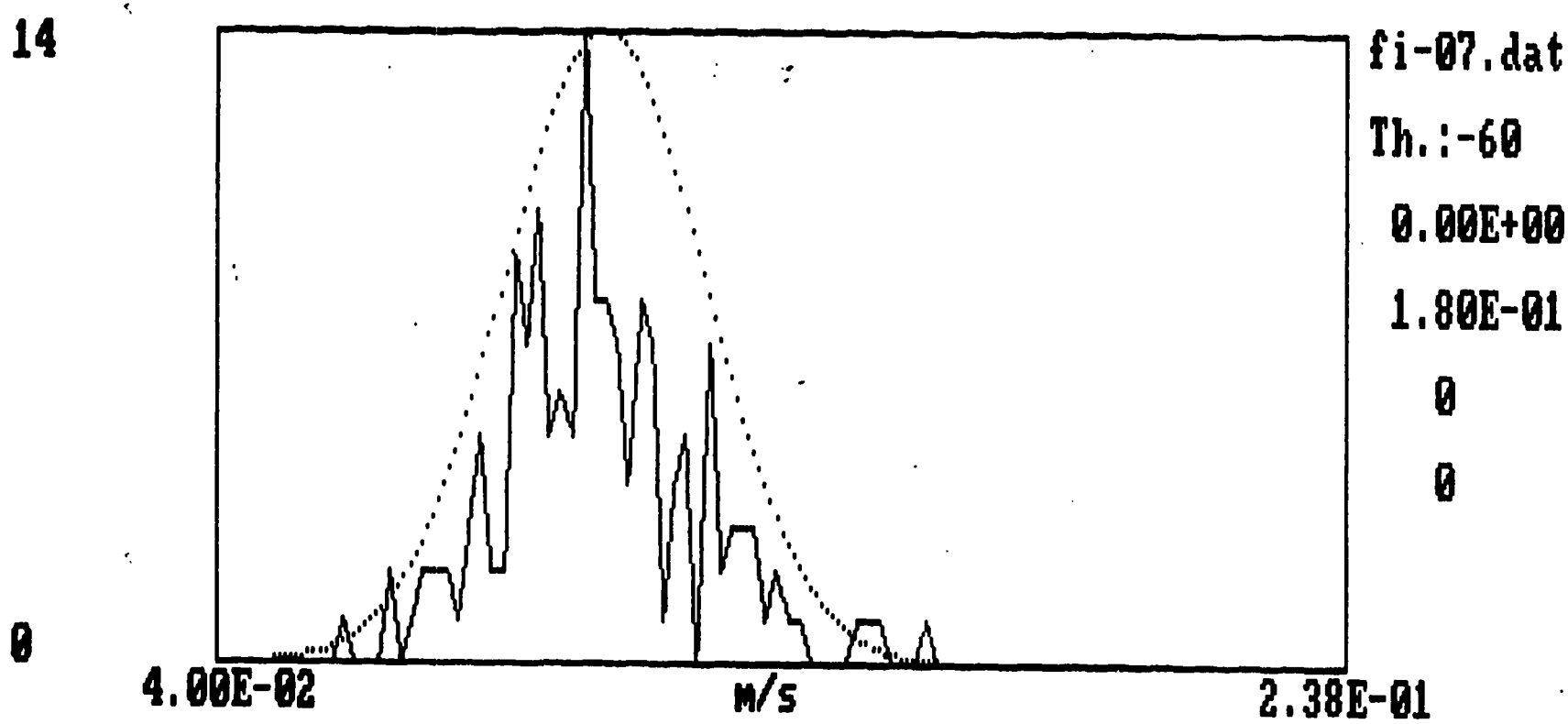

Velocity Distribution

Mean	: 1.078E-01 m/s	Dist. From Inlet	:	2.000E+00	cm
Stand. deviat.	: 1.766E-02 m/s	Radial Distance	:	1.200E+01	mm
Veloc. for max.	: 1.040E-01 m/s	Bulk velocity	:	1.180E-01	m/s
Skewness : 4.272E-01	Kurtosis : 3.455E+00	Re.	:	3.680E+03	

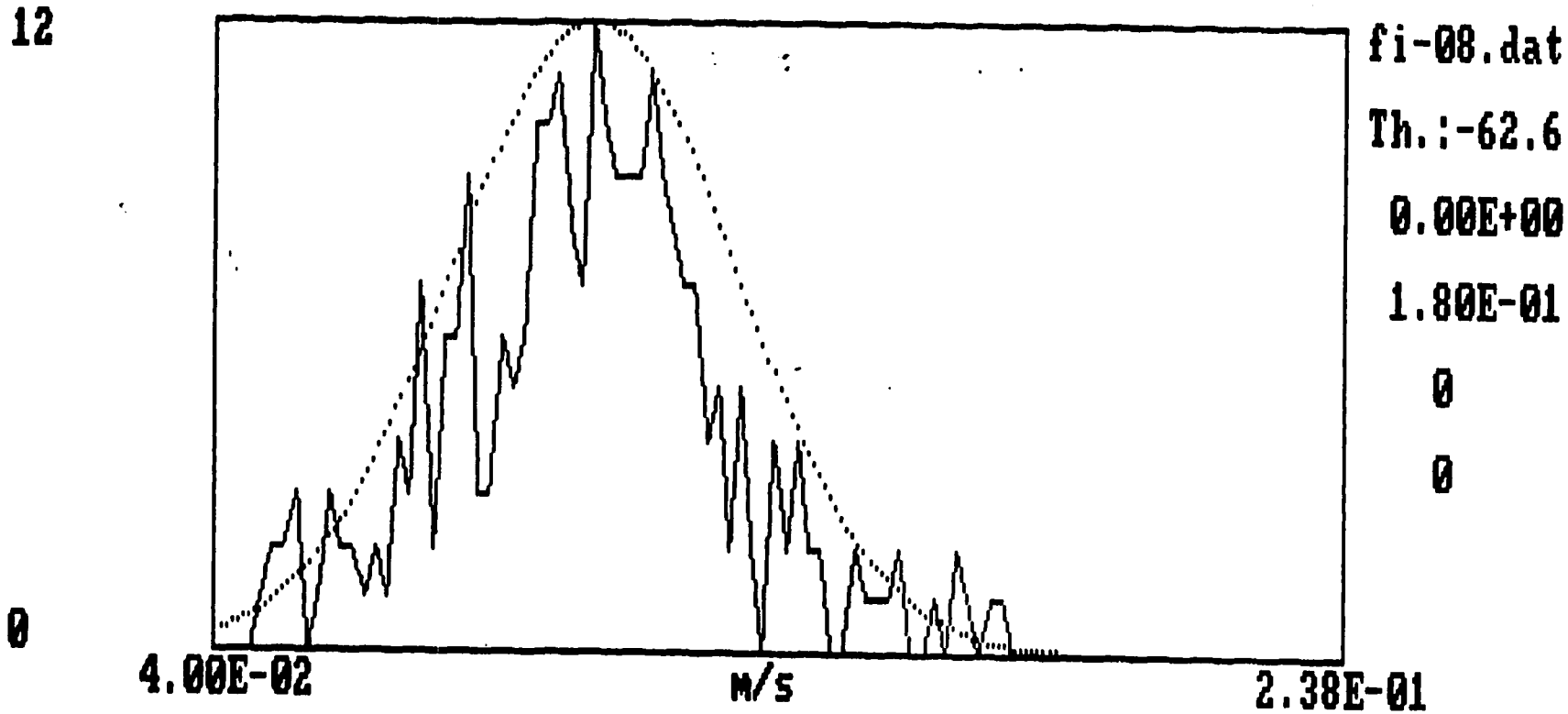

Velocity Distribution

Mean	: 1.063E-01 m/s	Dist. From Inlet	:	2.000E+00 cm	
Stand. deviat.	: 2.489E-02 m/s	Radial Distance	:	1.400E+01 mm	
Veloc. for max.	: 1.060E-01 m/s	Bulk velocity	:	1.180E-01 m/s	
Skewness : 2.080E-01	Kurtosis : 3.283E+00	Re.	:	3.680E+03	

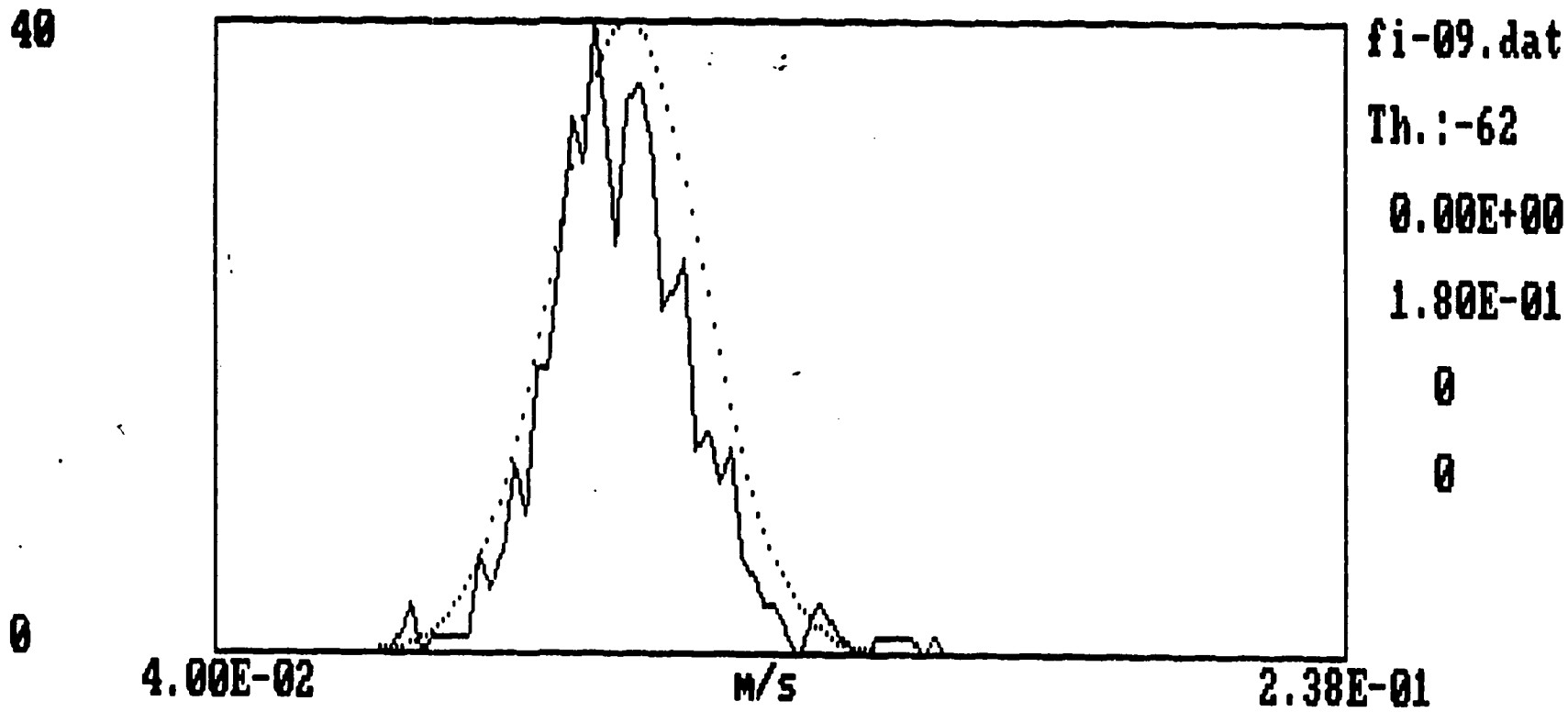

Velocity Distribution

Mean	: 1.121E-01 m/s	Dist. From Inlet	:	6.000E+00 cm
Stand. deviat.	: 1.331E-02 m/s	Radial Distance	:	0.000E+00 mm
Veloc. for max.	: 1.060E-01 m/s	Bulk velocity	:	1.180E-01 m/s
Skewness : 5.106E-01	Kurtosis : 4.424E+00	Re.	:	3.680E+03

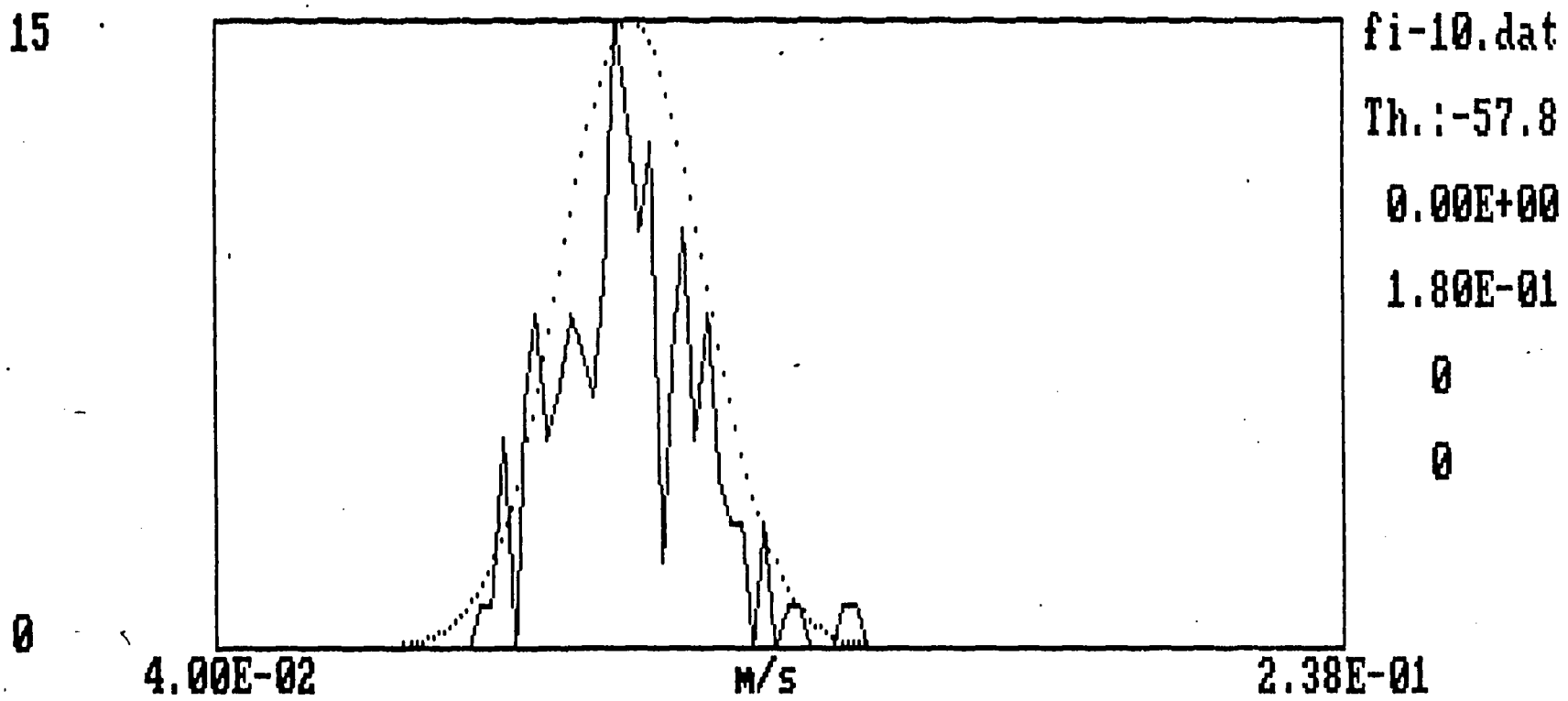

Velocity Distribution

Mean	: 1.130E-01 m/s	Dist. From Inlet	:	6.000E+00 cm	
Stand. deviat.	: 1.247E-02 m/s	Radial Distance	:	5.000E+00 mm	
Veloc. for max.	: 1.100E-01 m/s	Bulk velocity	:	1.180E-01 m/s	
Skewness : 3.618E-01	Kurtosis : 3.129E+00	Re.	:	3.680E+03	

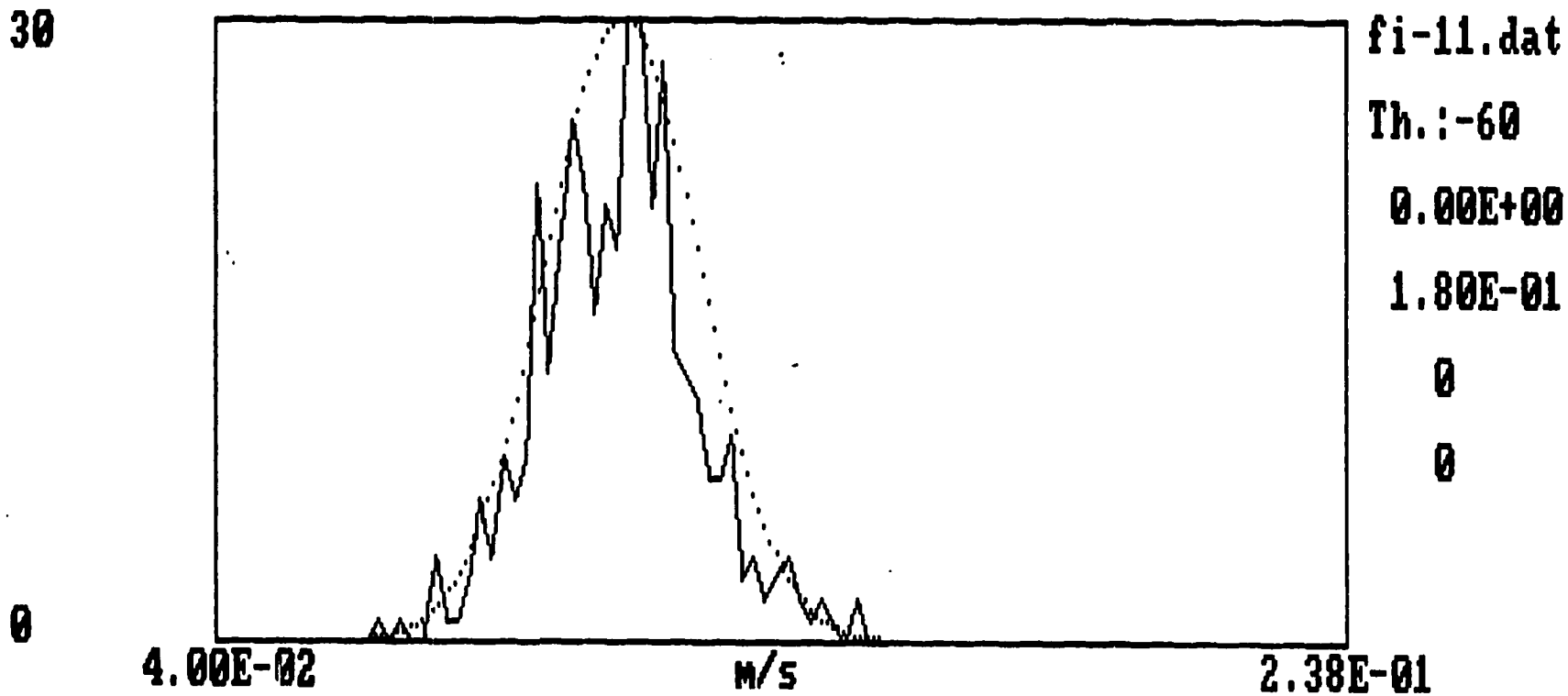

Velocity Distribution

Mean	: 1.111E-01 m/s	Dist. From Inlet	:	6.000E+00	cm
Stand. deviat.	: 1.367E-02 m/s	Radial Distance	:	1.000E+01	mm
Veloc. for max.	: 1.120E-01 m/s	Bulk velocity	:	1.180E-01	m/s
Skewness : 1.485E-01	Kurtosis : 3.320E+00	Re.	:	3.680E+03	

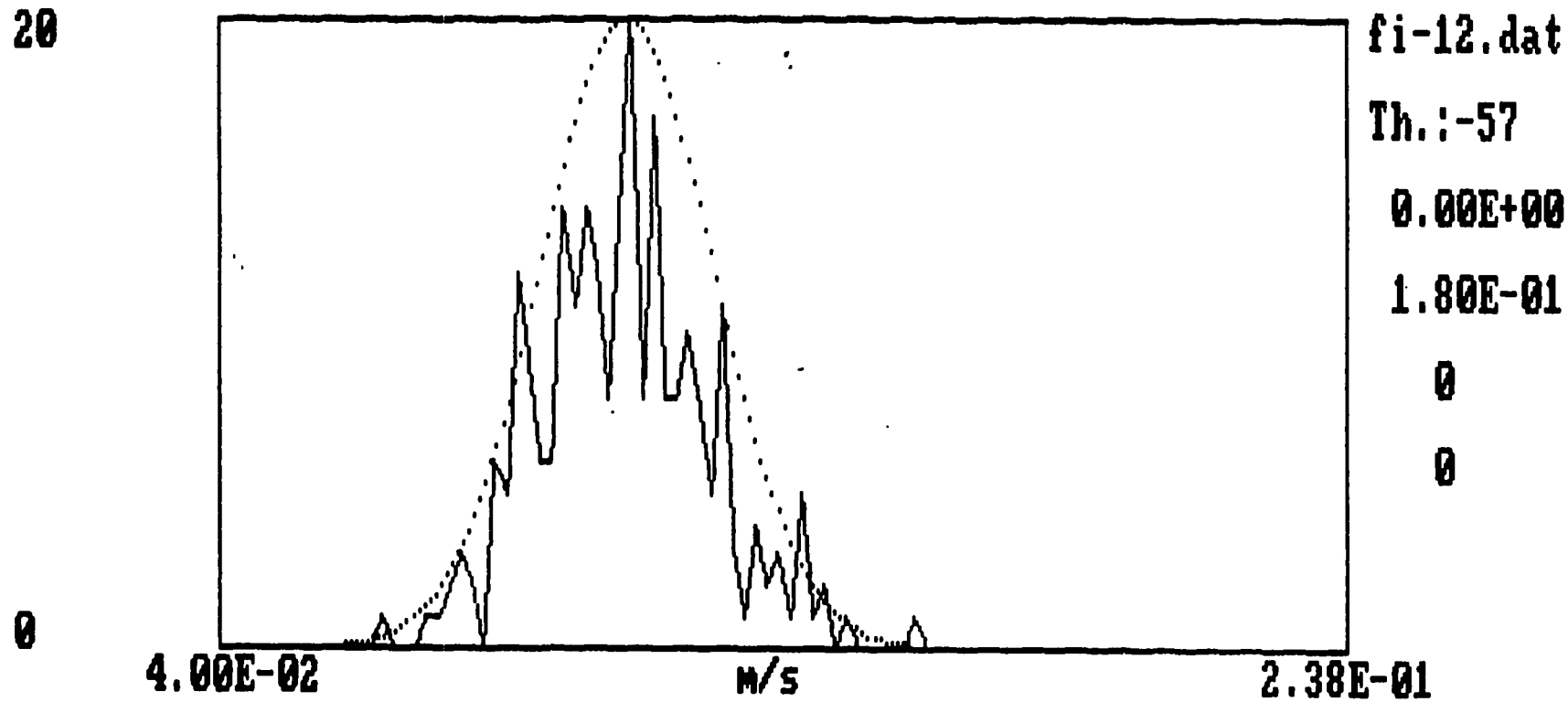

Velocity Distribution

Mean	: 1.114E-01 m/s	Dist. From Inlet	:	6.000E+00 cm	
Stand. deviat.	: 1.532E-02 m/s	Radial Distance	:	1.200E+01 mm	
Veloc. for max.	: 1.120E-01 m/s	Bulk velocity	:	1.180E-01 m/s	
Skewness : 2.616E-01	Kurtosis : 3.127E+00	Re.	:	3.680E+03	

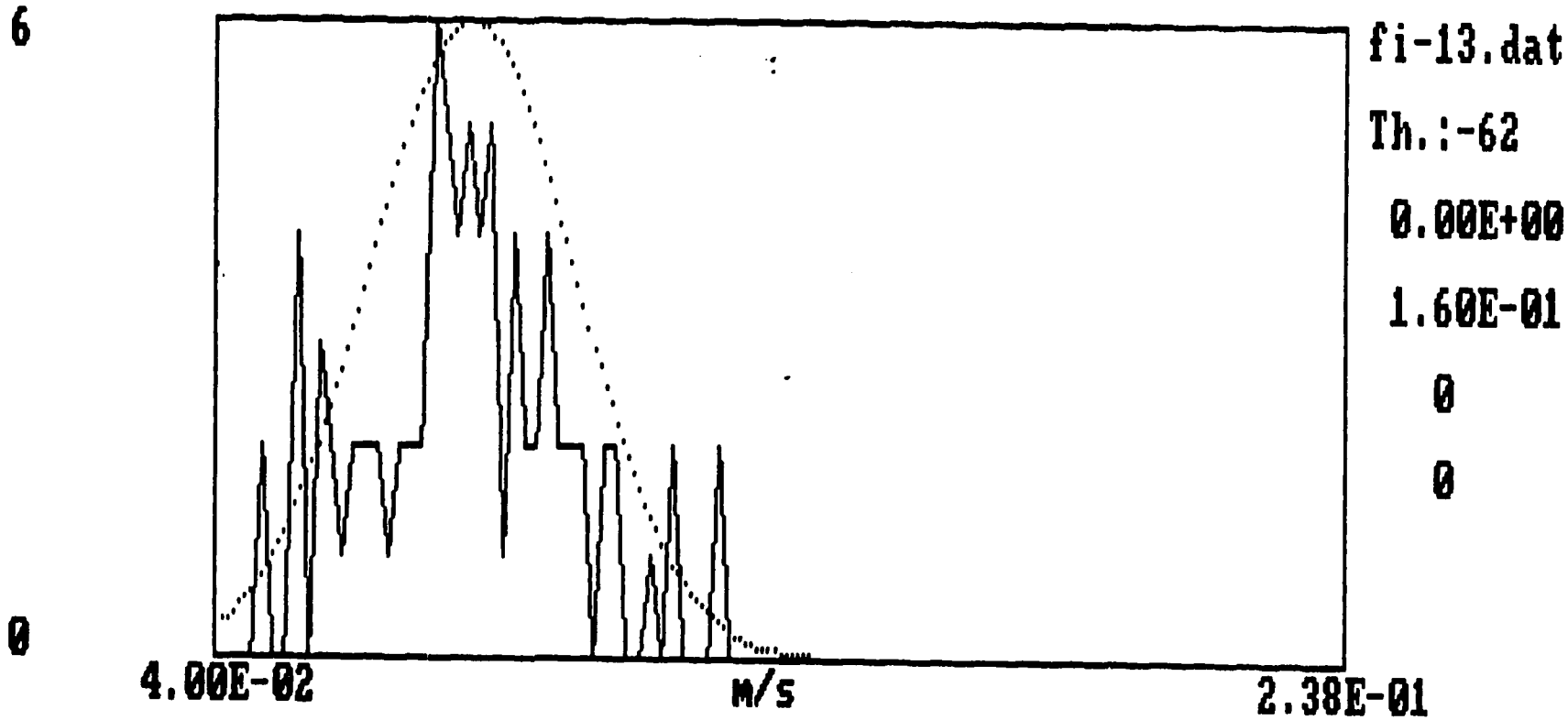

Velocity Distribution

Mean	: 8.468E-02 m/s	Dist. From Inlet	:	6.000E+00	cm
Stand. deviat.	: 1.820E-02 m/s	Radial Distance	:	1.400E+01	mm
Veloc. for max.	: 7.803E-02 m/s	Bulk velocity	:	1.180E-01	m/s
Skewness : 2.032E-01	Kurtosis : 2.779E+00	Re.	:	3.680E+03	

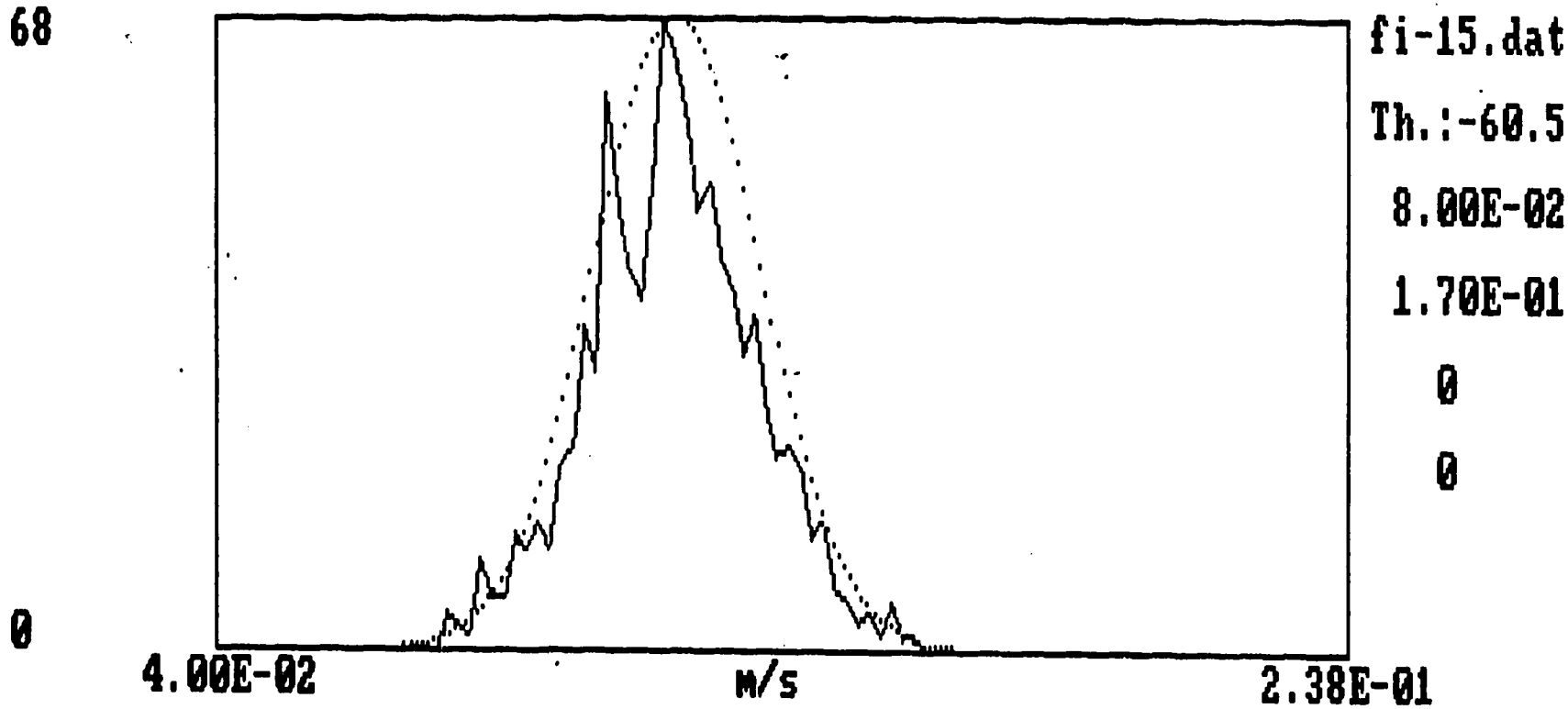

Velocity Distribution

Mean	: 1.204E-01 m/s	Dist. From Inlet	:	1.200E+01	cm
Stand. deviat.	: 1.473E-02 m/s	Radial Distance	:	0.000E+00	mm
Veloc. for max.	: 1.180E-01 m/s	Bulk velocity	:	1.180E-01	m/s
Skewness : 1.433E-02	Kurtosis : 2.970E+00	Re.	:	3.680E+03	

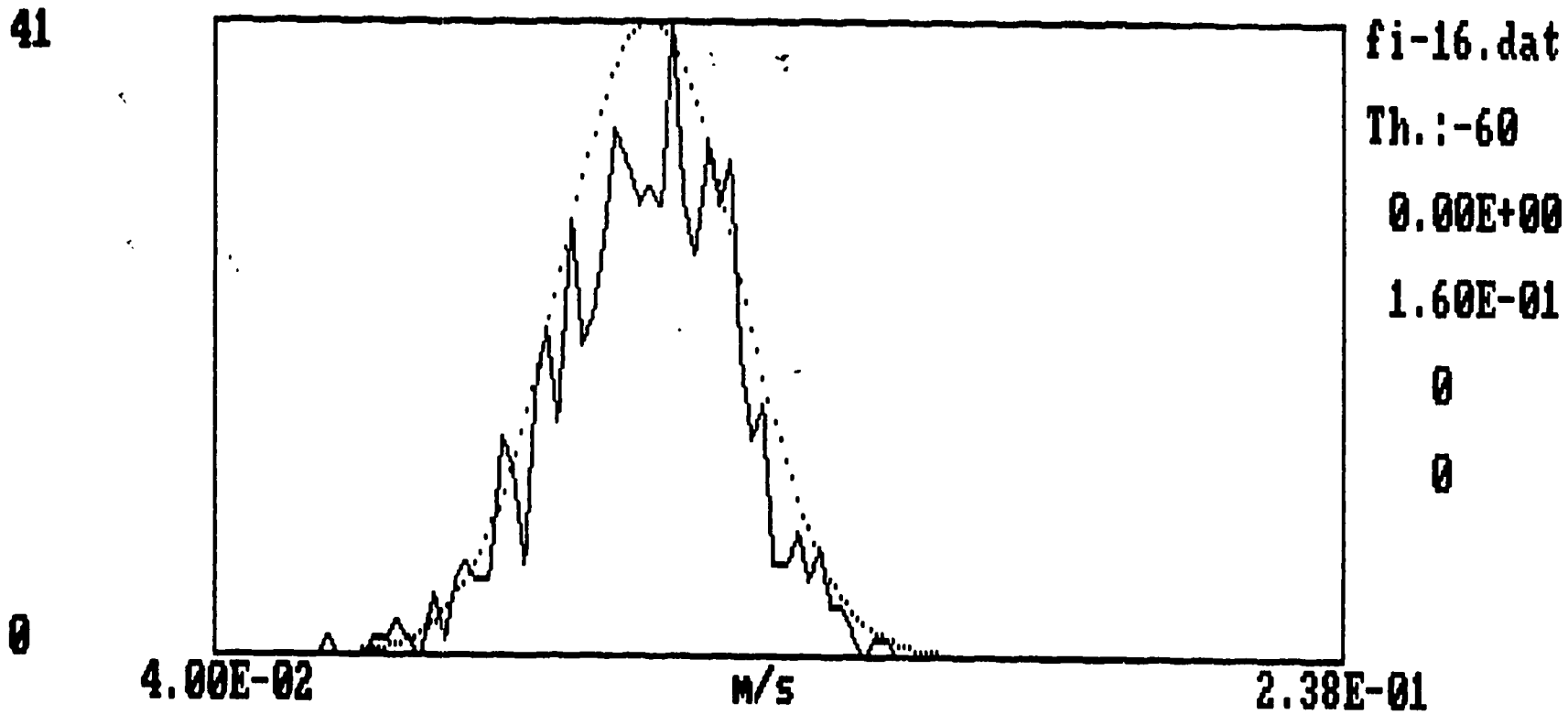

Velocity Distribution

Mean	: 1.161E-01 m/s	Dist. From Inlet		:	1.200E+01 cm
Stand. deviat.	: 1.559E-02 m/s	Radial Distance		:	5.000E+00 mm
Veloc. for max.	: 1.200E-01 m/s	Bulk velocity		:	1.180E-01 m/s
Skewness : -2.389E-01	Kurtosis	: 3.003E+00	Re.	:	3.680E+03

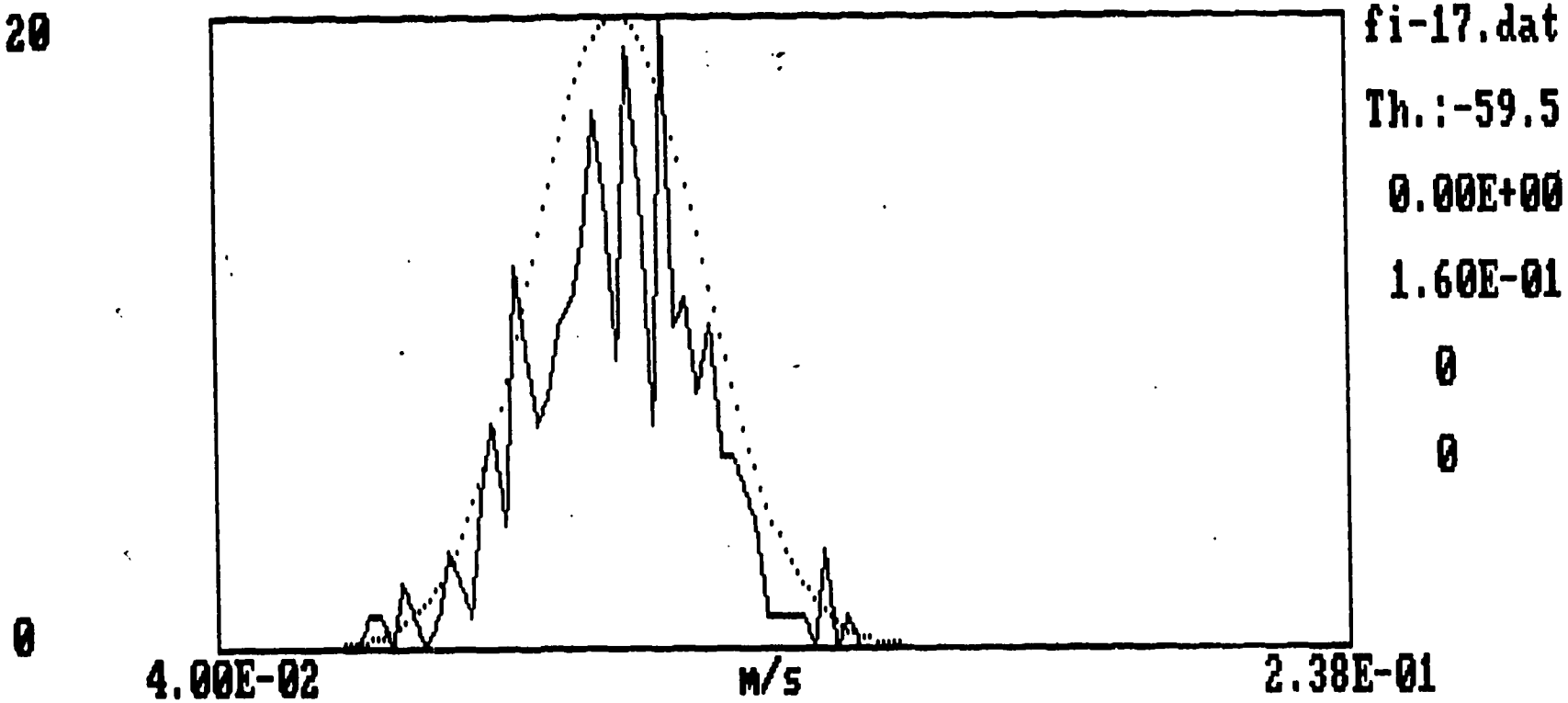

Velocity Distribution

Mean	: 1.103E-01 m/s	Dist. From Inlet	:	1.200E+01 cm	
Stand. deviat.	: 1.493E-02 m/s	Radial Distance	:	1.000E+01 mm	
Veloc. for max.	: 1.180E-01 m/s	Bulk velocity	:	1.180E-01 m/s	
Skewness : -1.260E-01	Kurtosis : 3.020E+00	Re.	:	3.680E+03	

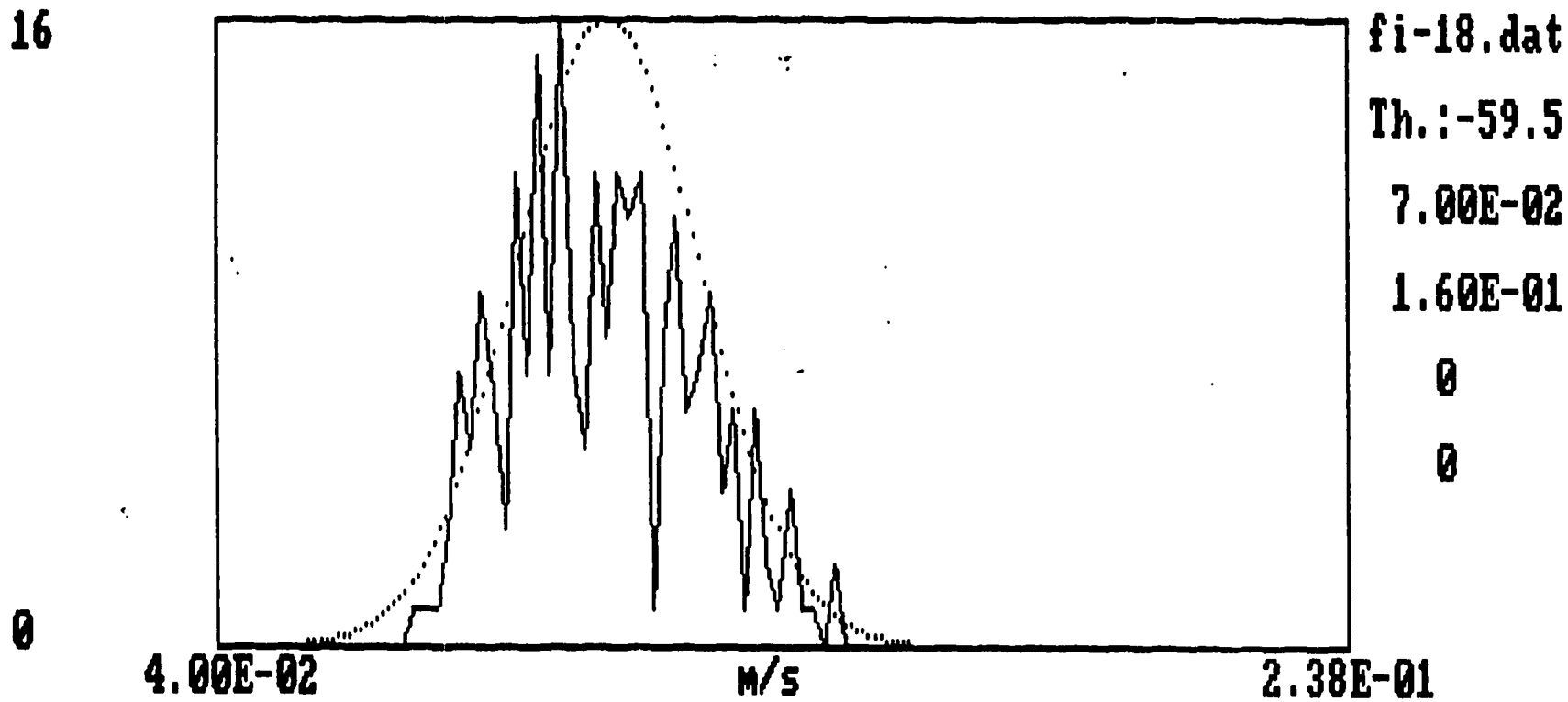

Velocity Distribution

Mean	: 1.083E-01 m/s	Dist. From Inlet	:	1.200E+01 cm	
Stand. deviat.	: 1.620E-02 m/s	Radial Distance	:	1.200E+01 mm	
Veloc. for max.	: 1.000E-01 m/s	Bulk velocity	:	1.180E-01 m/s	
Skewness :	2.481E-01	Kurtosis : 2.325E+00	Re. :	3.680E+03	

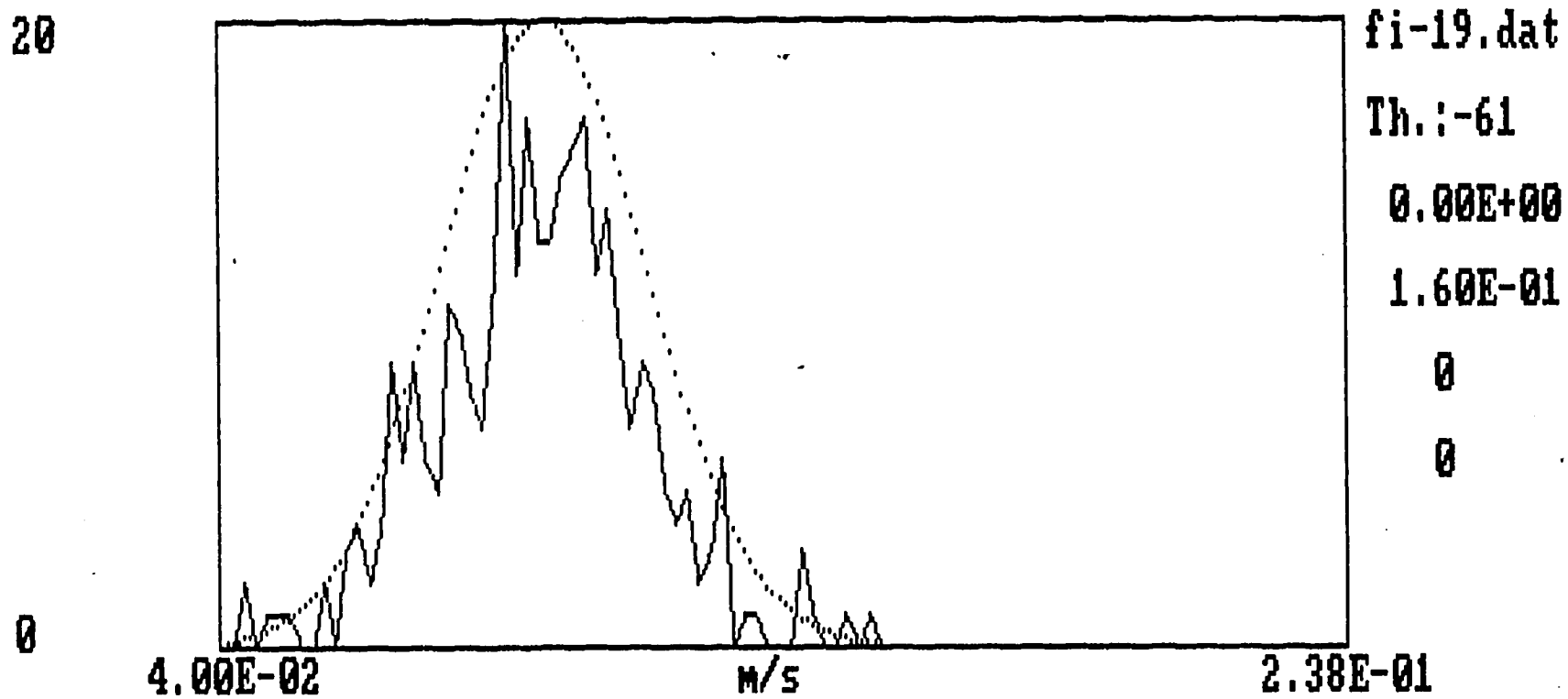

Velocity Distribution

Mean	: 9.683E-02 m/s	Dist. From Inlet	:	1.200E+01 cm	
Stand. deviat.	: 1.817E-02 m/s	Radial Distance	:	1.400E+01 mm	
Veloc. for max.	: 9.003E-02 m/s	Bulk velocity	:	1.180E-01 m/s	
Skewness : 3.948E-02	Kurtosis : 3.375E+00	Re.	:	3.680E+03	

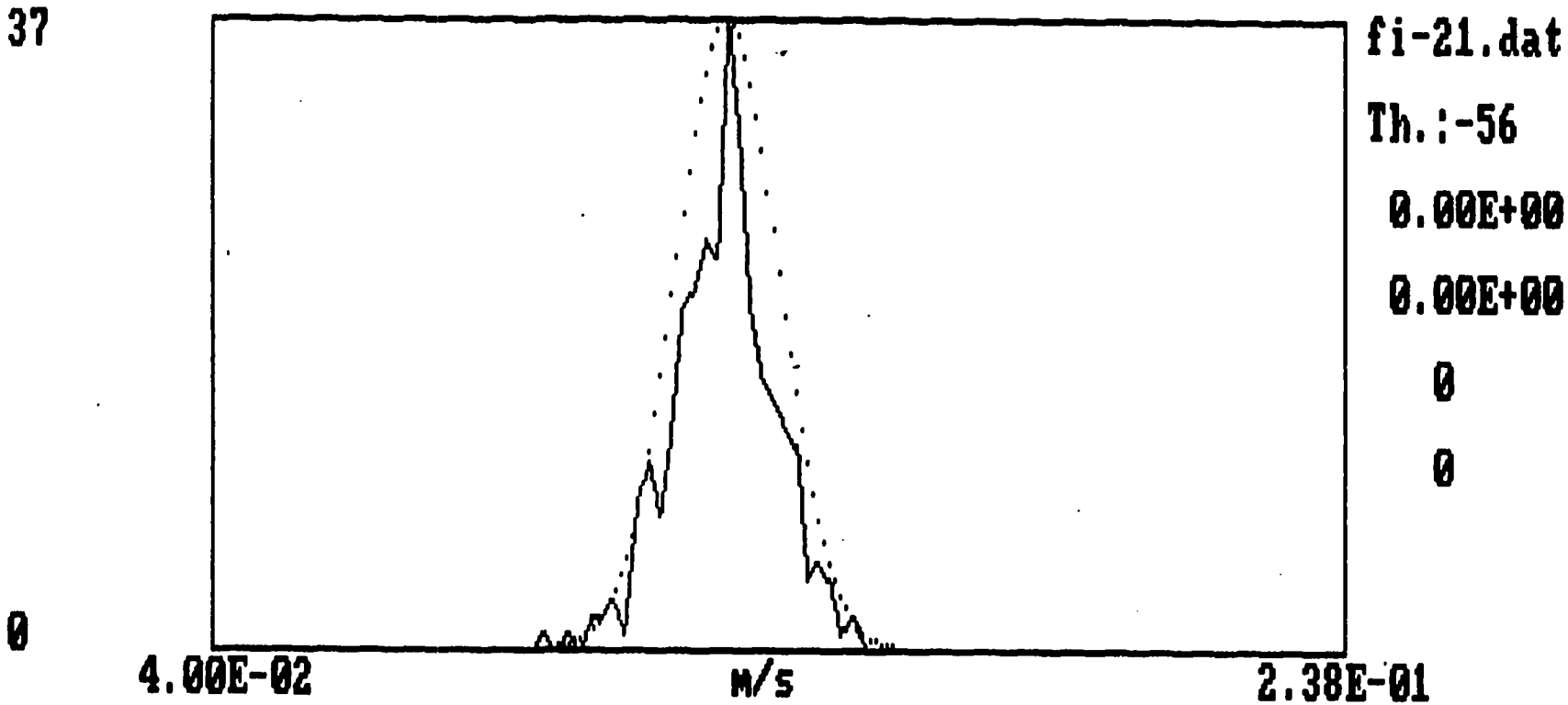

Velocity Distribution

Mean	: 1.299E-01 m/s	Dist. From Inlet	:	3.000E+01	cm
Stand. deviat.	: 9.013E-03 m/s	Radial Distance	:	0.000E+00	mm
Veloc. for max.	: 1.300E-01 m/s	Bulk velocity	:	1.180E-01	m/s
Skewness : -1.765E-01	Kurtosis : 3.224E+00	Re.	:	3.680E+03	

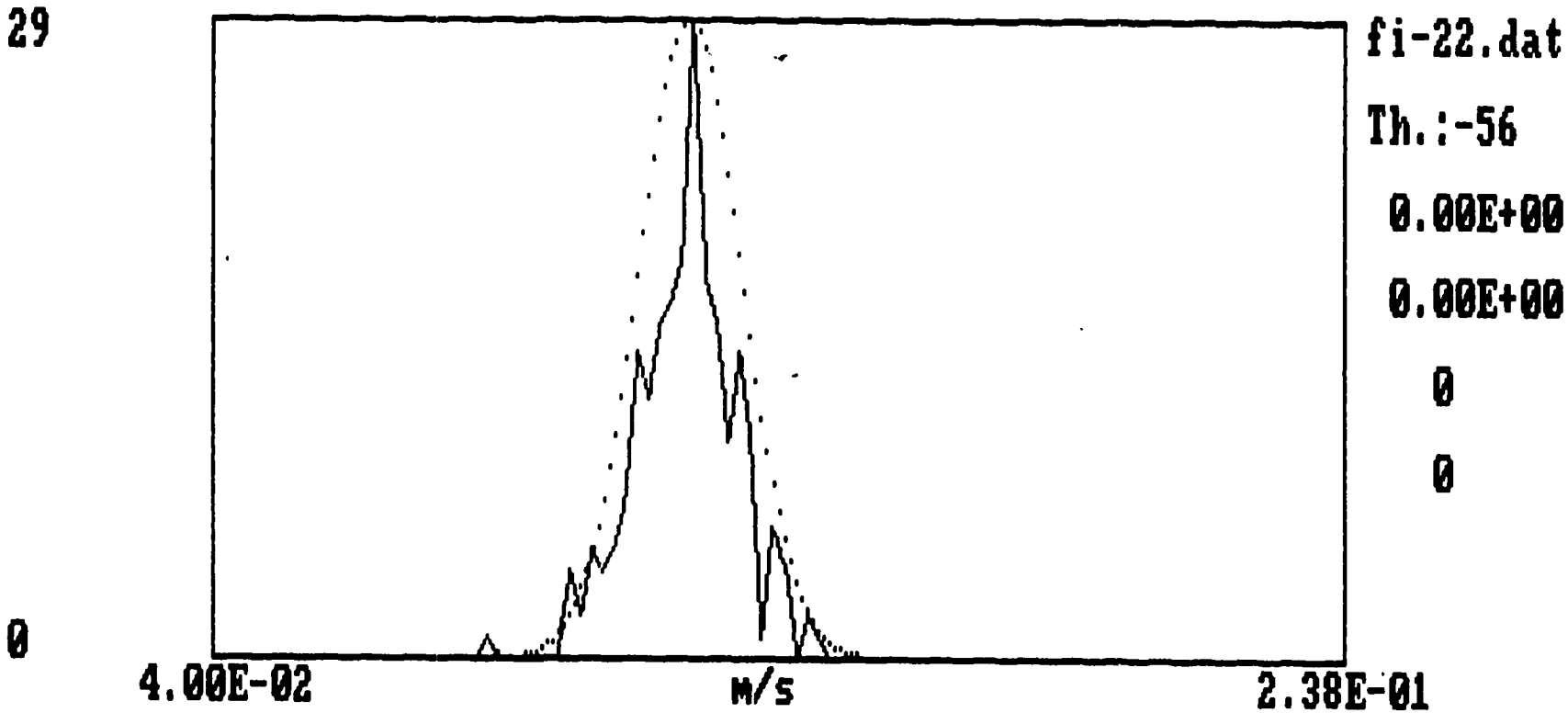

Velocity Distribution

Mean	: 1.235E-01 m/s	Dist. From Inlet	:	3.000E+01 cm	
Stand. deviat.	: 9.059E-03 m/s	Radial Distance	:	5.000E+00 mm	
Veloc. for max.	: 1.240E-01 m/s	Bulk velocity	:	1.180E-01 m/s	
Skewness : -2.962E-01	Kurtosis : 3.417E+00	Re.	:	3.680E+03	

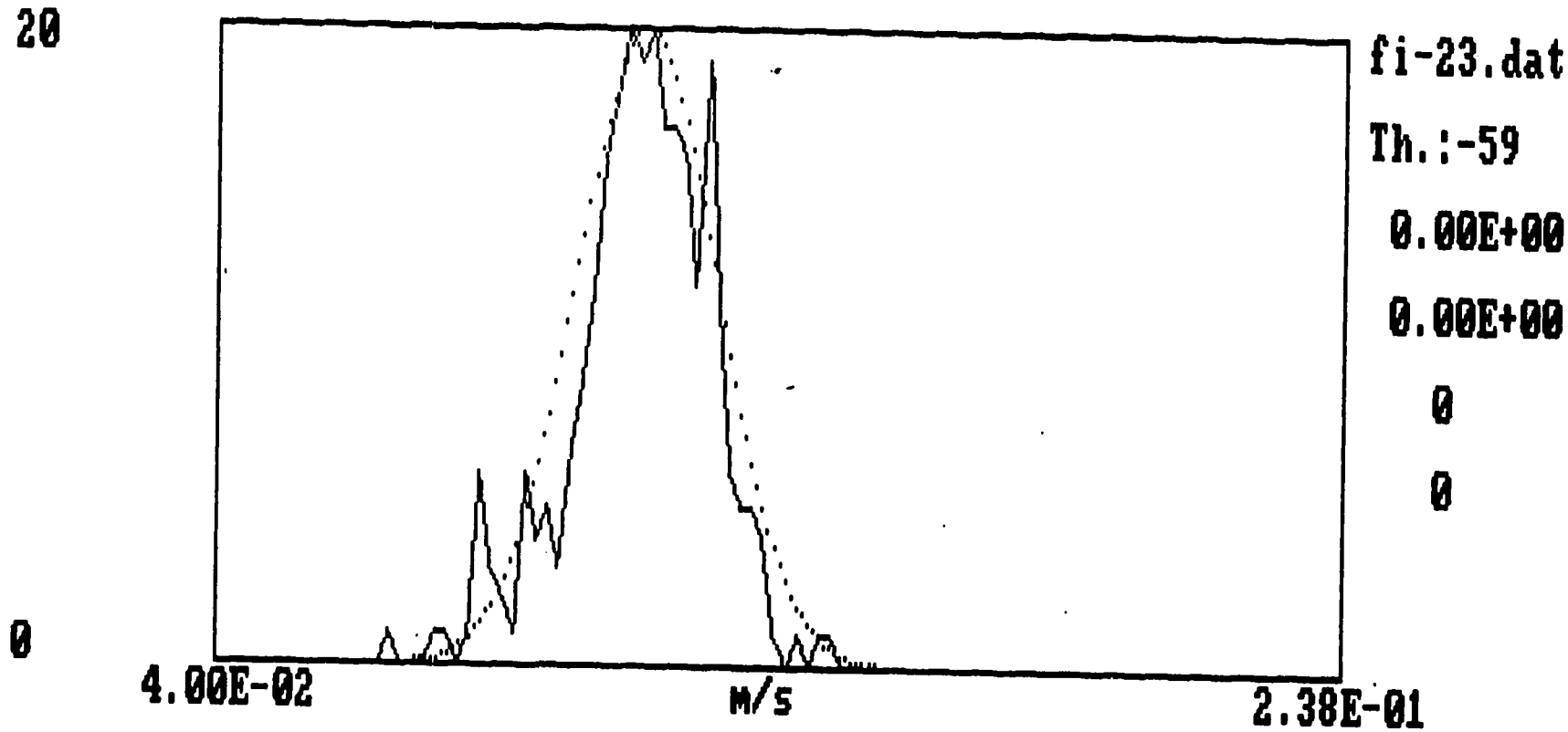

Velocity Distribution

Mean	: 1.153E-01 M/S	Dist. From Inlet		:	3.000E+01 CM
Stand. deviat.	: 1.239E-02 M/S	Radial Distance		:	1.000E+01 MM
Veloc. for max.	: 1.120E-01 M/S	Bulk velocity		:	1.180E-01 M/S
Skewness :	-4.884E-01	Kurtosis : 3.610E+00	Re.	:	3.680E+03

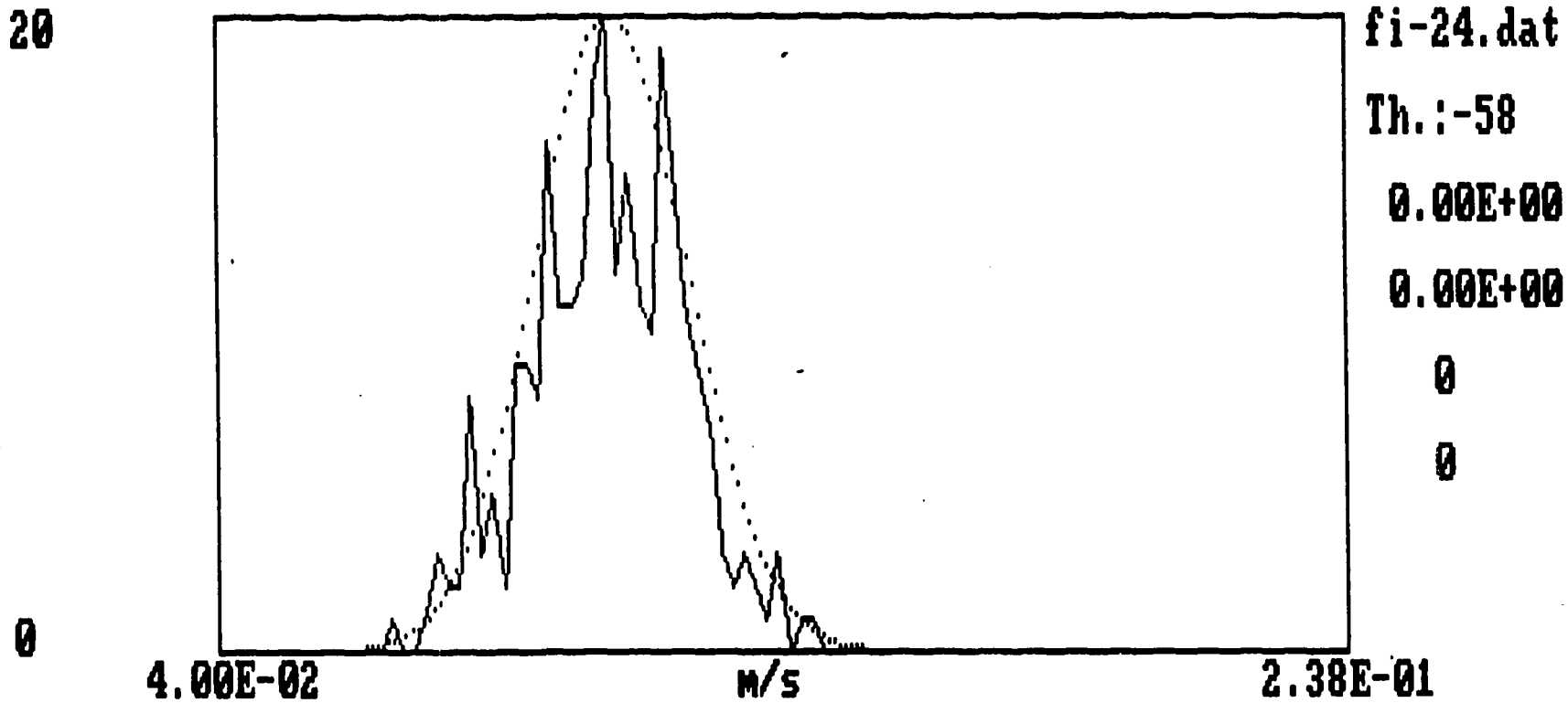

Velocity Distribution

Mean	: 1.091E-01 m/s	Dist. From Inlet	:	3.000E+01	cm
Stand. deviat.	: 1.347E-02 m/s	Radial Distance	:	1.200E+01	mm
Veloc. for max.	: 1.080E-01 m/s	Bulk velocity	:	1.180E-01	m/s
Skewness : -1.153E-01	Kurtosis : 2.789E+00	Re.	:	3.680E+03	

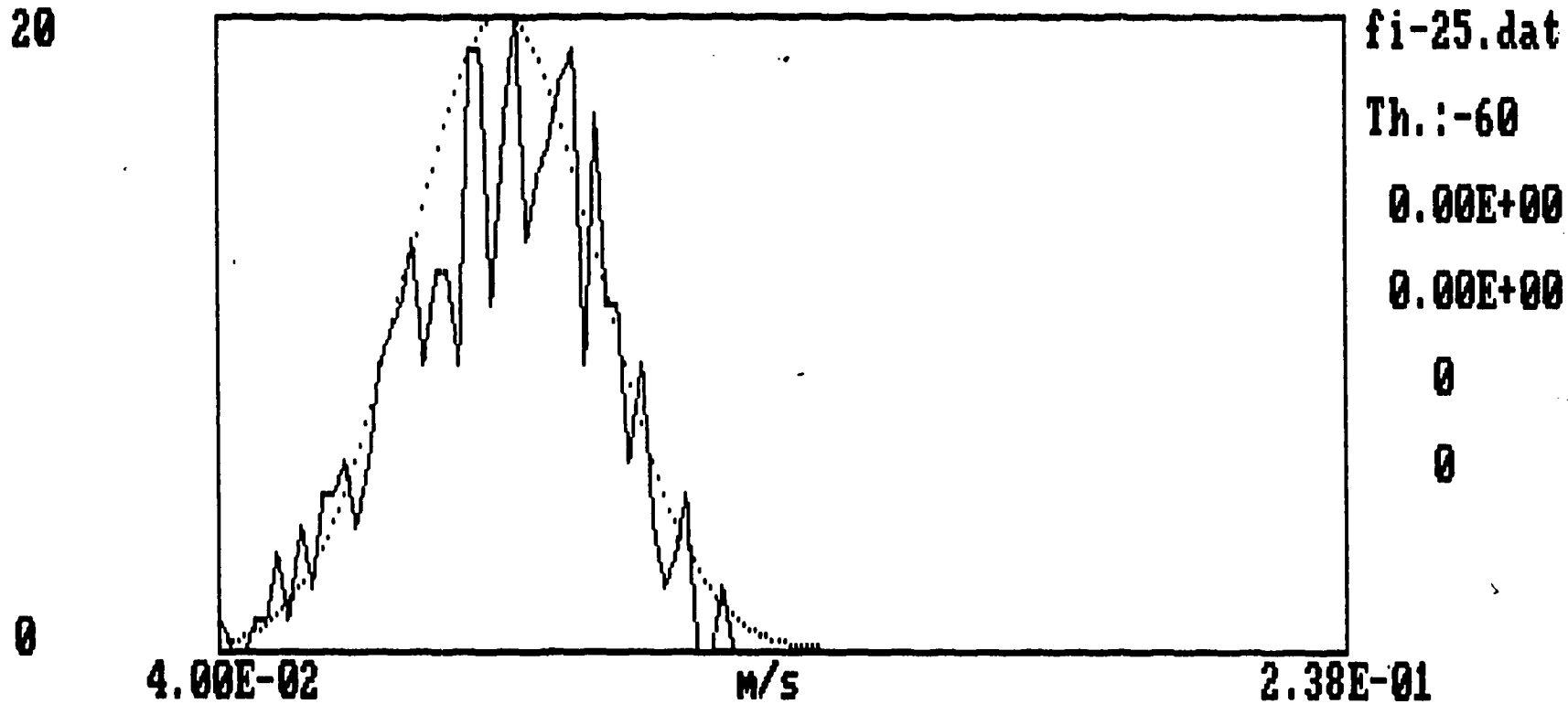

Velocity Distribution

Mean	: 9.002E-02 m/s	Dist. From Inlet	:	3.000E+01	cm
Stand. deviat.	: 1.688E-02 m/s	Radial Distance	:	1.400E+01	mm
Veloc. for max.	: 9.204E-02 m/s	Bulk velocity	:	1.180E-01	m/s
Skewness : -2.858E-01	Kurtosis : 2.569E+00	Re.	:	3.680E+03	

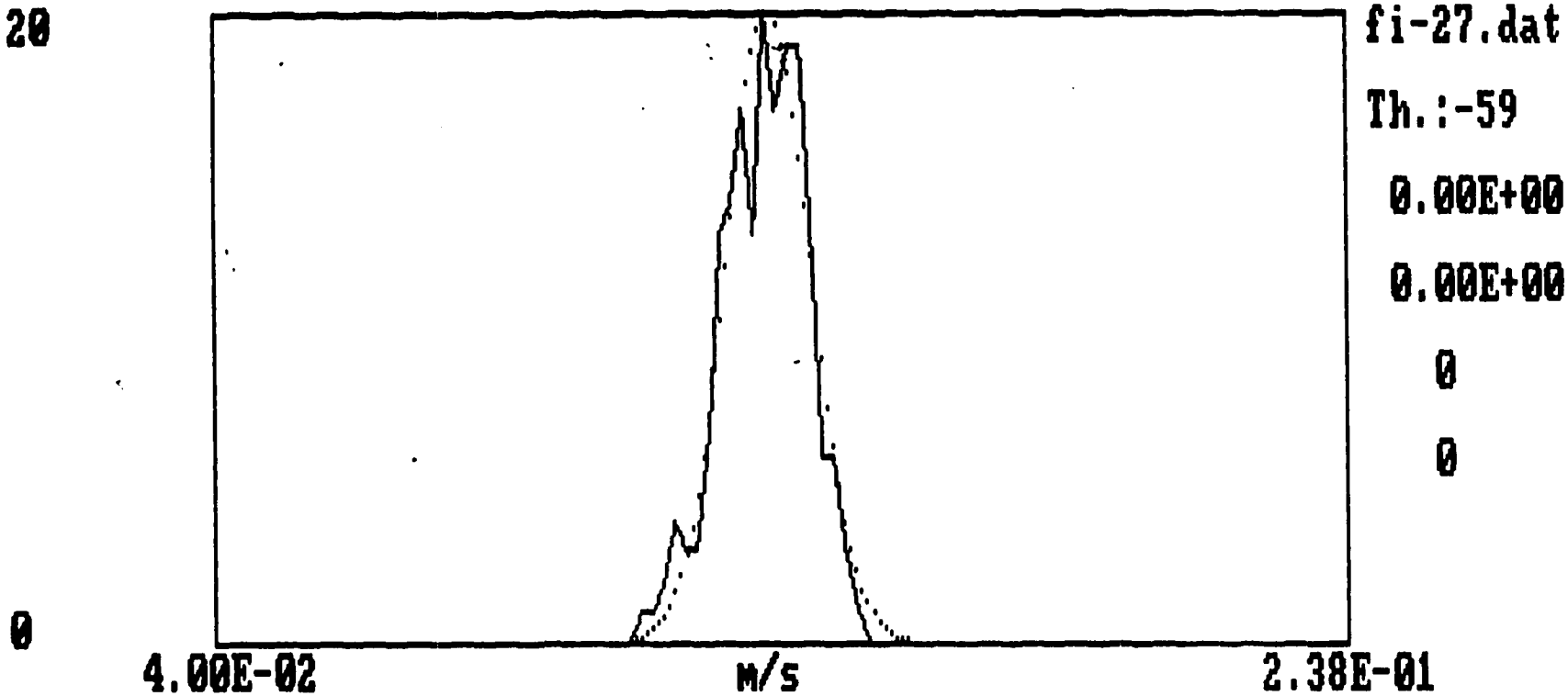

Velocity Distribution

Mean	: 1.367E-01 m/s	Dist. From Inlet	:	6.000E+01 cm
Stand. deviat.	: 7.395E-03 m/s	Radial Distance	:	0.000E+00 mm
Veloc. for max.	: 1.361E-01 m/s	Bulk velocity	:	1.180E-01 m/s
Skewness : -3.448E-01	Kurtosis : 2.784E+00	Re.	:	3.680E+03

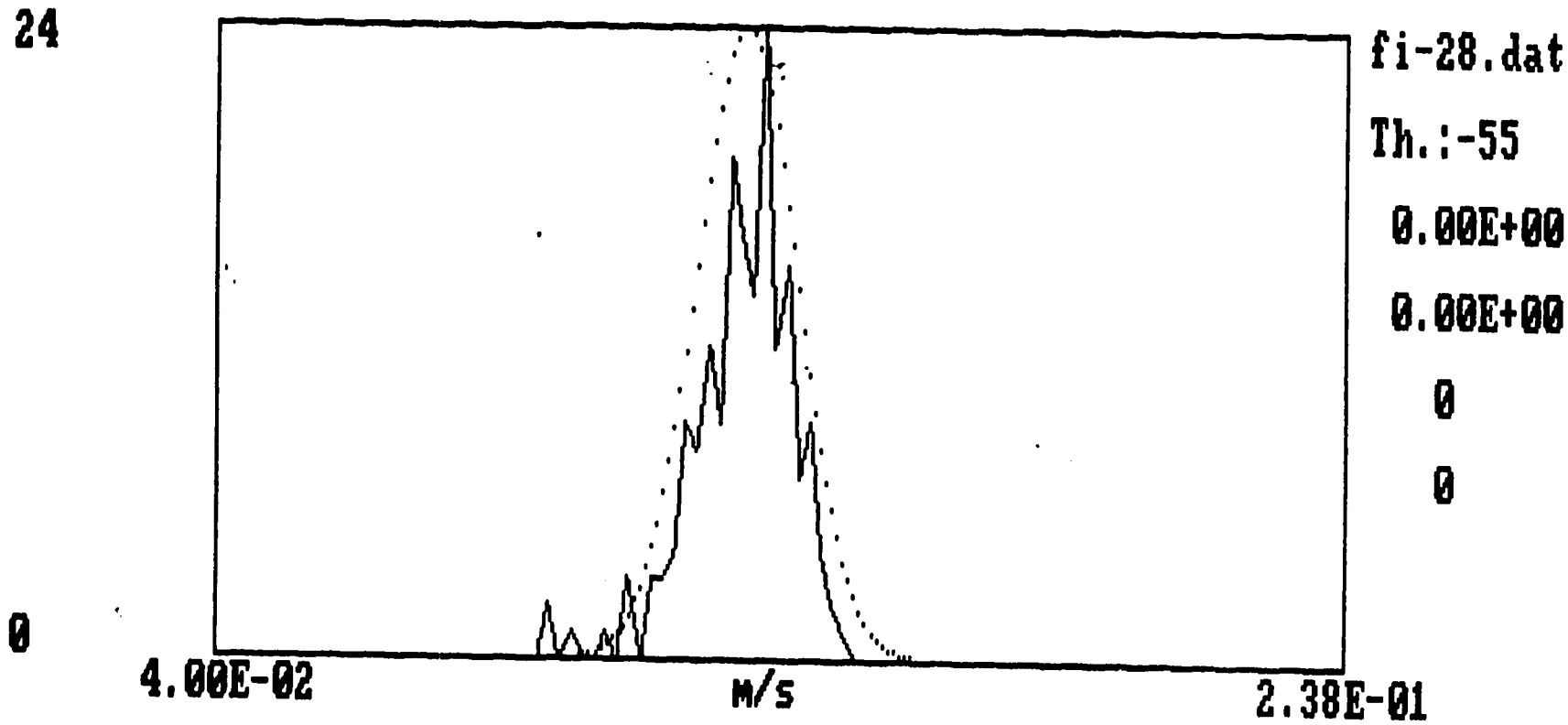

Velocity Distribution

Mean	: 1.328E-01 m/s	Dist. From Inlet		:	6.000E+01 cm
Stand. deviat.	: 8.909E-03 m/s	Radial Distance		:	5.000E+00 mm
Veloc. for max.	: 1.361E-01 m/s	Bulk velocity		:	1.180E-01 m/s
Skewness :	-9.746E-01	Kurtosis :	4.749E+00	Re. :	3.680E+03

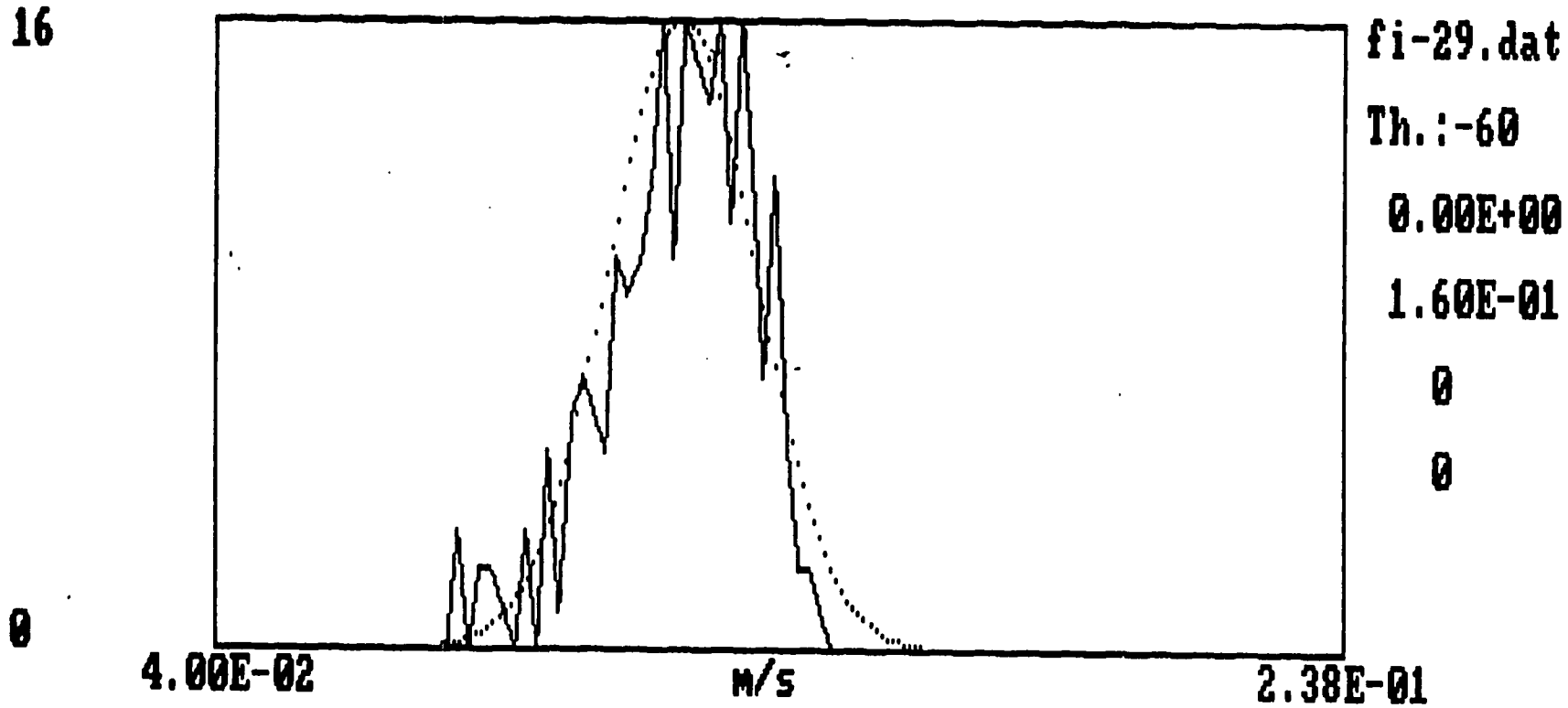

Velocity Distribution

Mean	: 1.217E-01 m/s	Dist. From Inlet	:	6.000E+01	cm
Stand. deviat.	: 1.306E-02 m/s	Radial Distance	:	1.000E+01	mm
Veloc. for max.	: 1.180E-01 m/s	Bulk velocity	:	1.180E-01	m/s
Skewness : -6.611E-01	Kurtosis : 3.229E+00	Re.	:	3.680E+03	

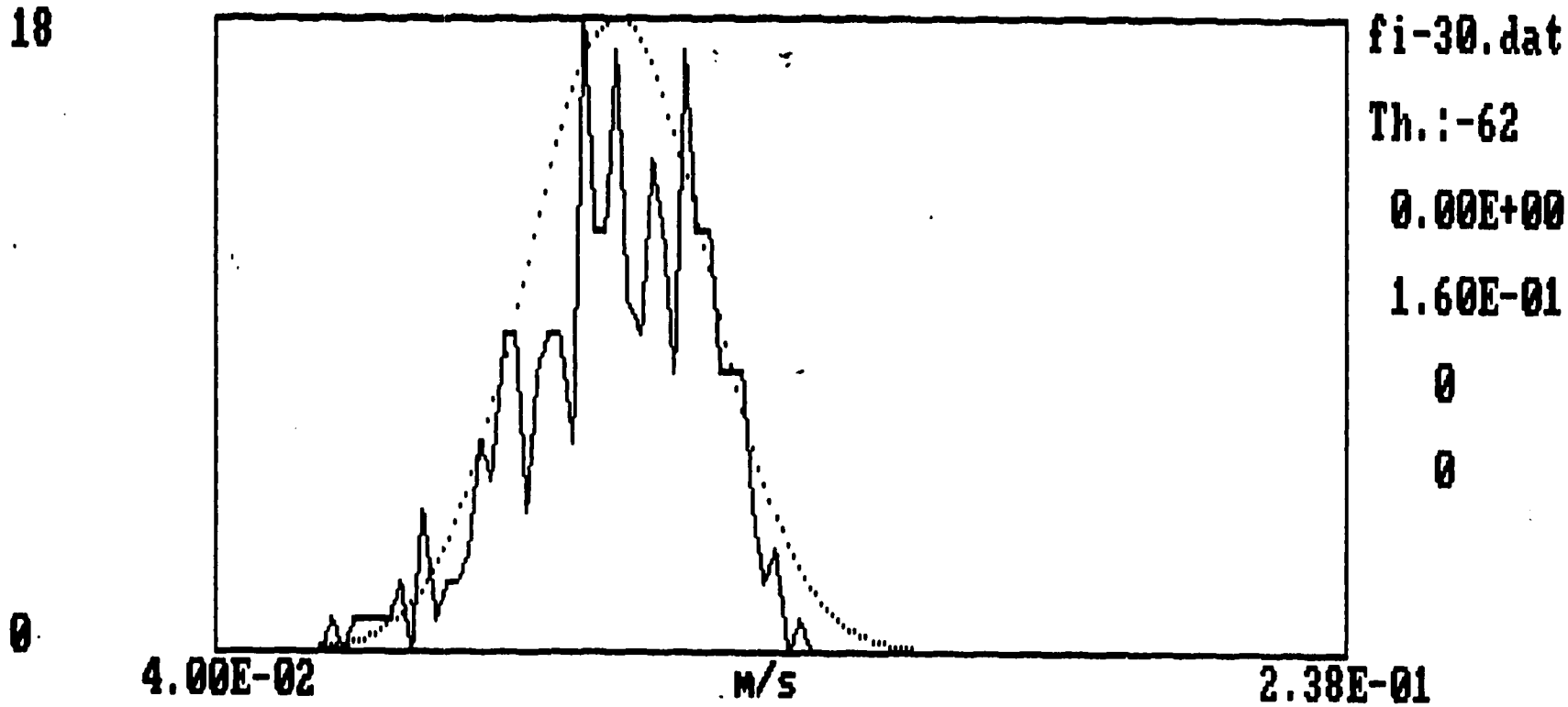

Velocity Distribution

Mean	: 1.101E-01 m/s	Dist. From Inlet	:	6.000E+01 cm
Stand. deviat.	: 1.597E-02 m/s	Radial Distance	:	1.200E+01 mm
Veloc. for max.	: 1.040E-01 m/s	Bulk velocity	:	1.180E-01 m/s
Skewness : -4.812E-01	Kurtosis : 2.795E+00	Re.	:	3.680E+03

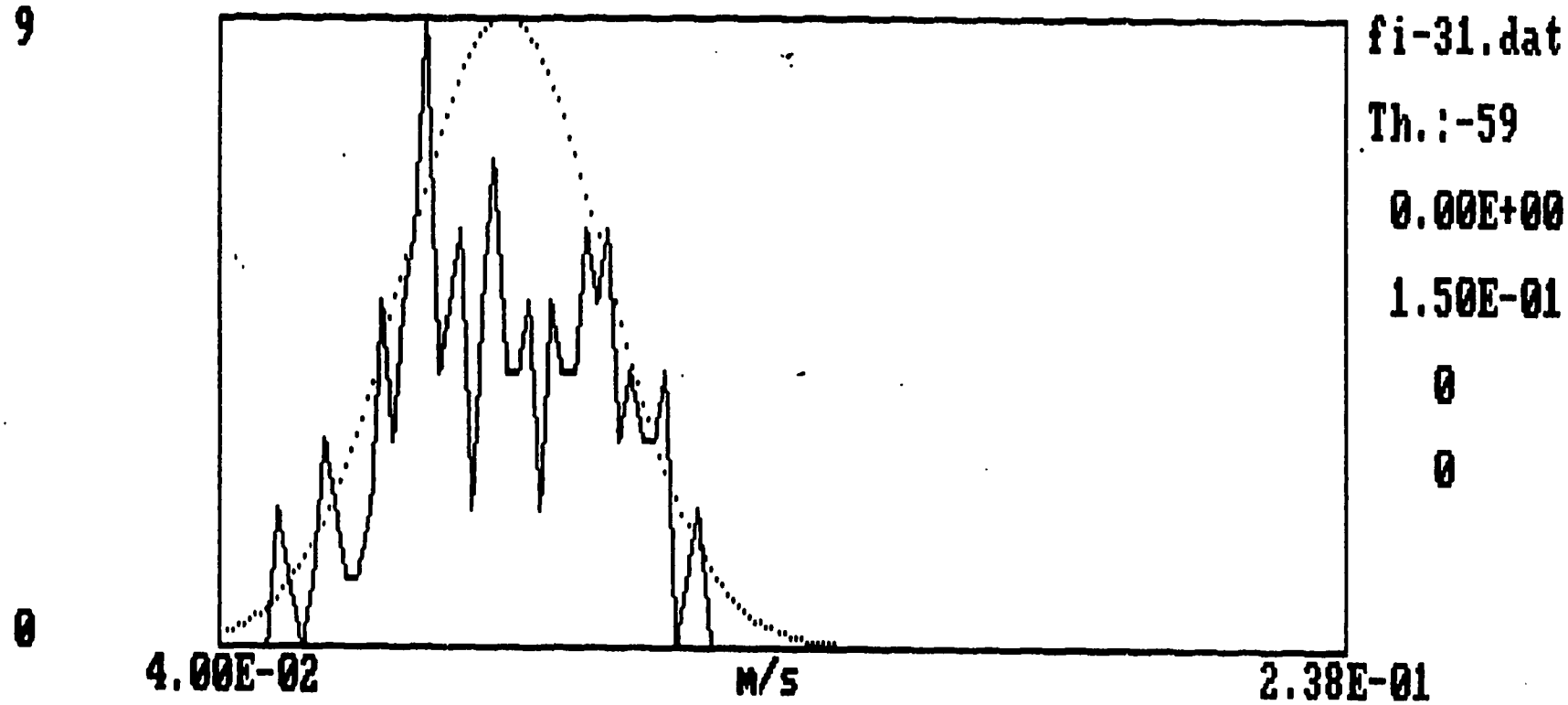

Velocity Distribution

Mean	: 8.994E-02 m/s	Dist. From Inlet	:	6.000E+01	cm
Stand. deviat.	: 1.786E-02 m/s	Radial Distance	:	1.400E+01	mm
Veloc. for max.	: 7.603E-02 m/s	Bulk velocity	:	1.180E-01	m/s
Skewness : -5.051E-02	Kurtosis : 2.126E+00	Re.	:	3.680E+03	

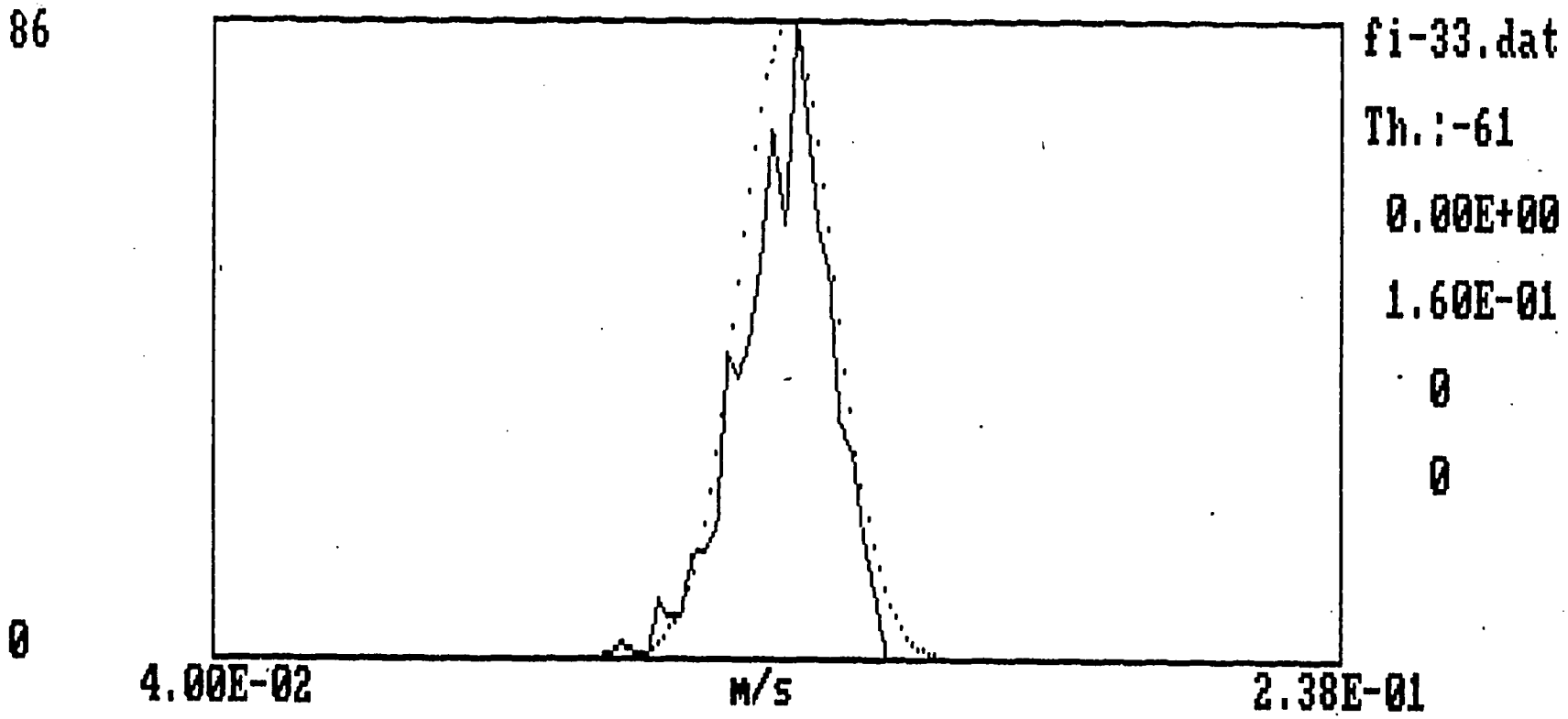

Velocity Distribution

Mean	: 1.406E-01 m/s	Dist. From Inlet	:	1.000E+02 cm	
Stand. deviat.	: 8.252E-03 m/s	Radial Distance	:	0.000E+00 mm	
Veloc. for max.	: 1.421E-01 m/s	Bulk velocity	:	1.180E-01 m/s	
Skewness : -5.154E-01	Kurtosis : 3.225E+00	Re.	:	3.680E+03	

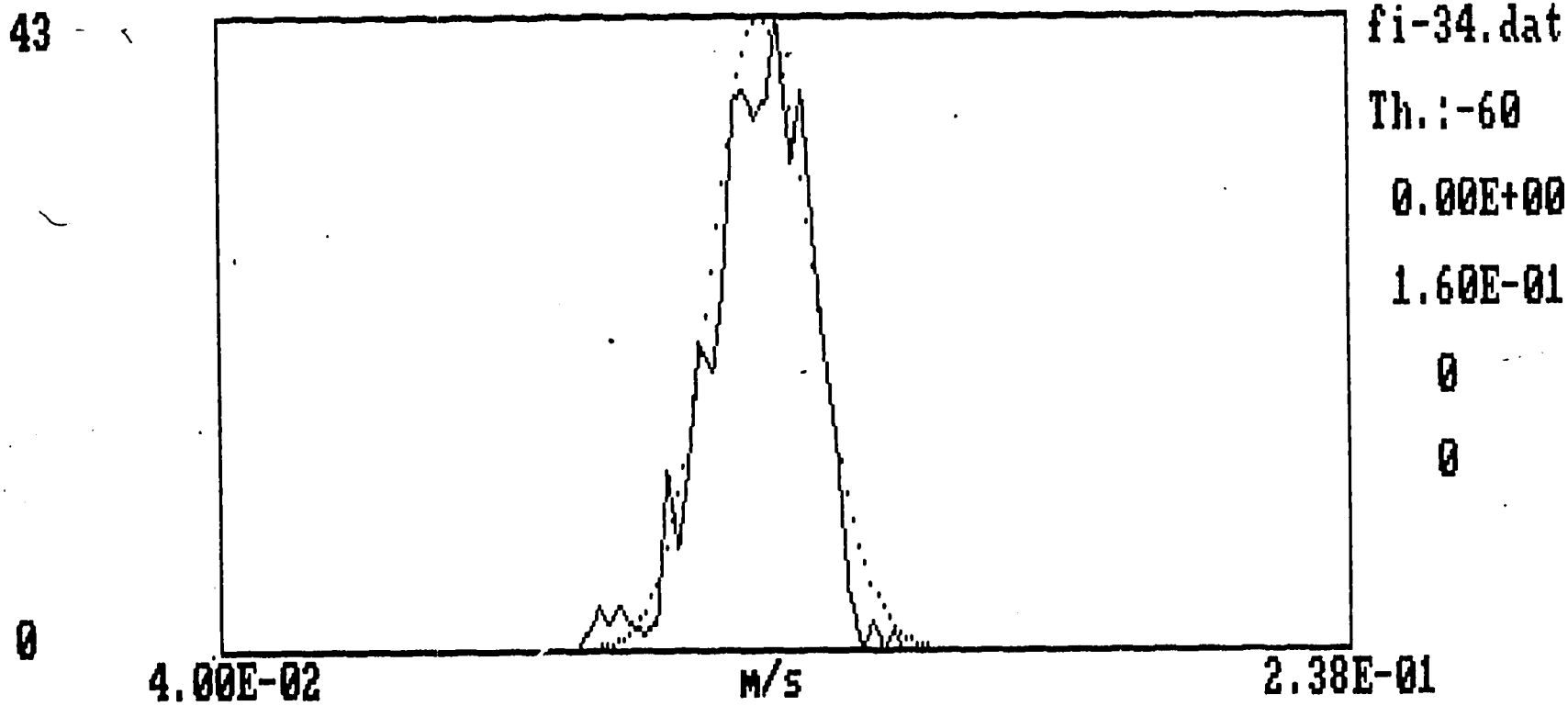

Velocity Distribution

Mean	: 1.351E-01 m/s	Dist. From Inlet	:	1.000E+02	cm
Stand. deviat.	: 8.872E-03 m/s	Radial Distance	:	5.000E+00	mm
Veloc. for max.	: 1.381E-01 m/s	Bulk velocity	:	1.180E-01	m/s
Skewness : -5.946E-01	Kurtosis : 3.516E+00	Re.	:	3.680E+03	

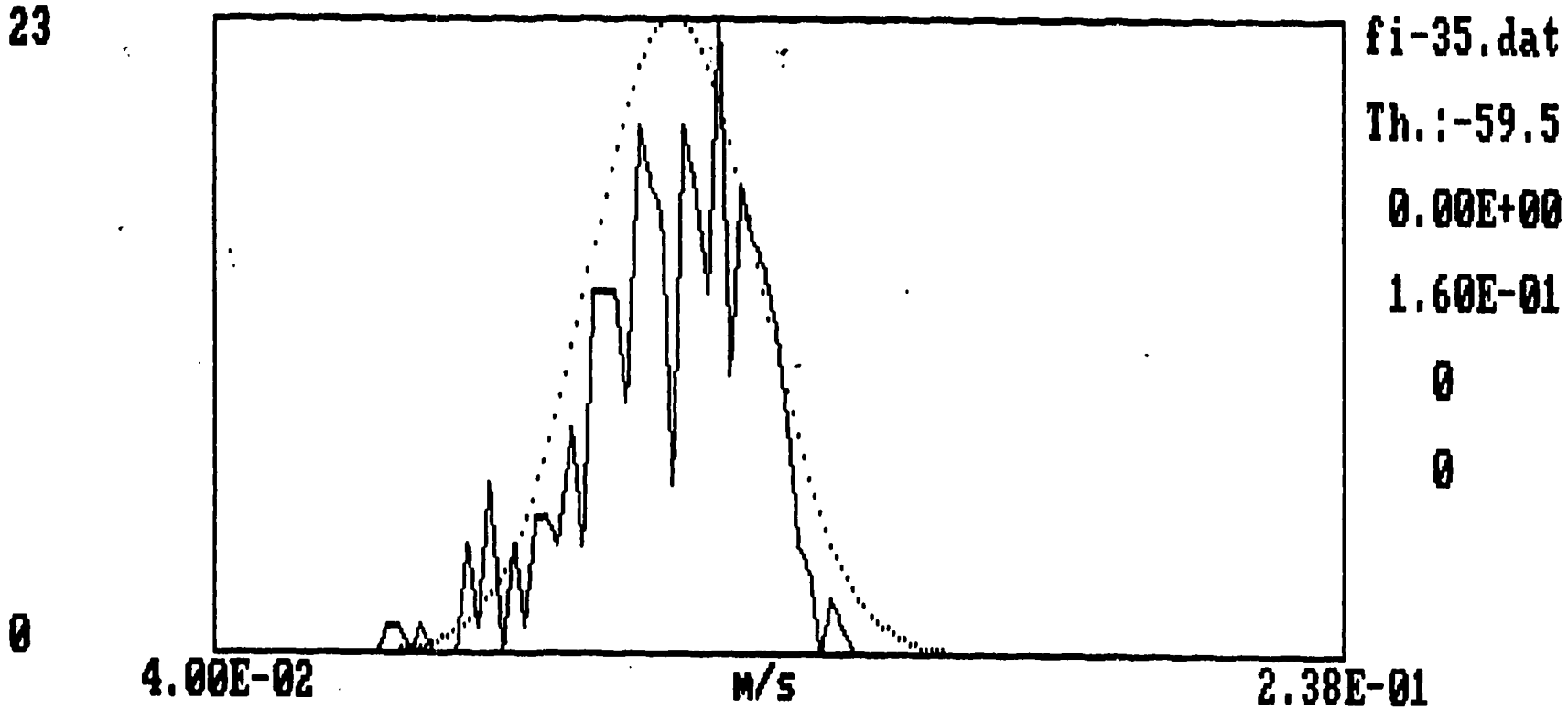

Velocity Distribution

Mean	: 1.203E-01 m/s	Dist. From Inlet	:	1.000E+02	cm
Stand. deviat.	: 1.474E-02 m/s	Radial Distance	:	1.000E+01	mm
Veloc. for max.	: 1.280E-01 m/s	Bulk velocity	:	1.180E-01	m/s
Skewness : -5.880E-01	Kurtosis : 3.135E+00	Re.	:	3.680E+03	

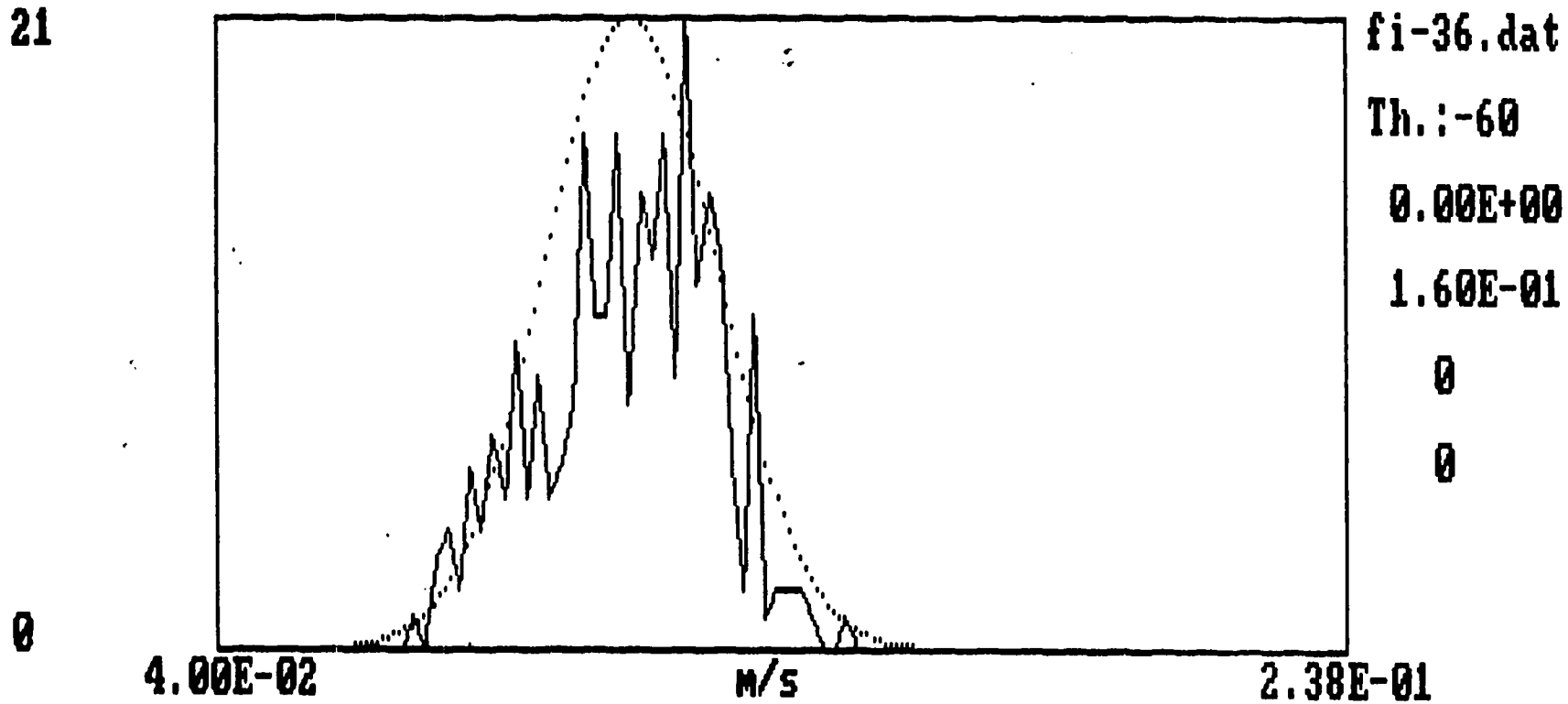

Velocity Distribution

Mean	: 1.124E-01 m/s	Dist. From Inlet	:	1.000E+02	cm
Stand. deviat.	: 1.509E-02 m/s	Radial Distance	:	1.200E+01	mm
Veloc. for max.	: 1.220E-01 m/s	Bulk velocity	:	1.180E-01	m/s
Skewness : -2.726E-01	Kurtosis : 2.471E+00	Re.	:	3.680E+03	

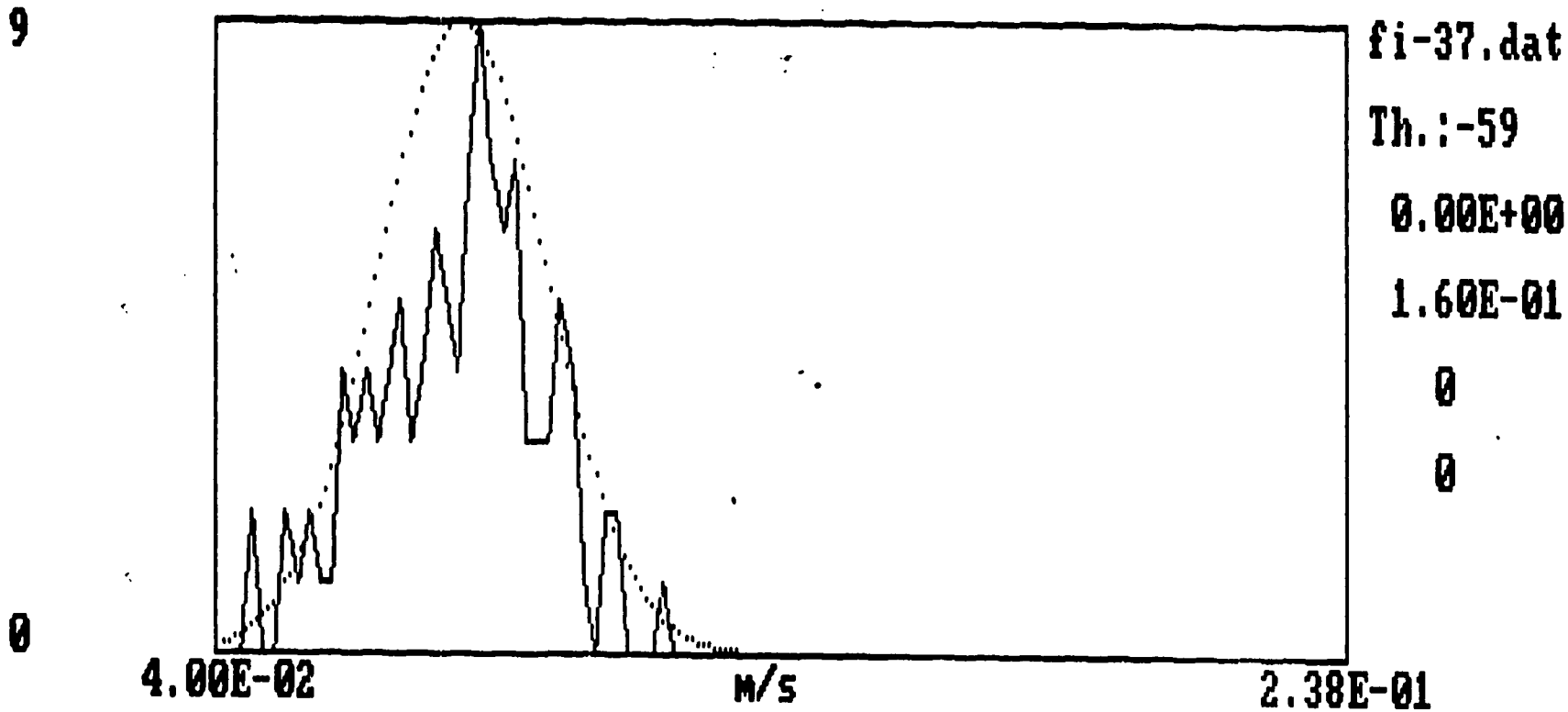

Velocity Distribution

Mean	: 8.292E-02 m/s	Dist. From Inlet	:	1.000E+02 cm	
Stand. deviat.	: 1.469E-02 m/s	Radial Distance	:	1.400E+01 mm	
Veloc. for max.	: 8.603E-02 m/s	Bulk velocity	:	1.180E-01 m/s	
Skewness : -2.102E-01	Kurtosis : 2.655E+00	Re.	:	3.680E+03	

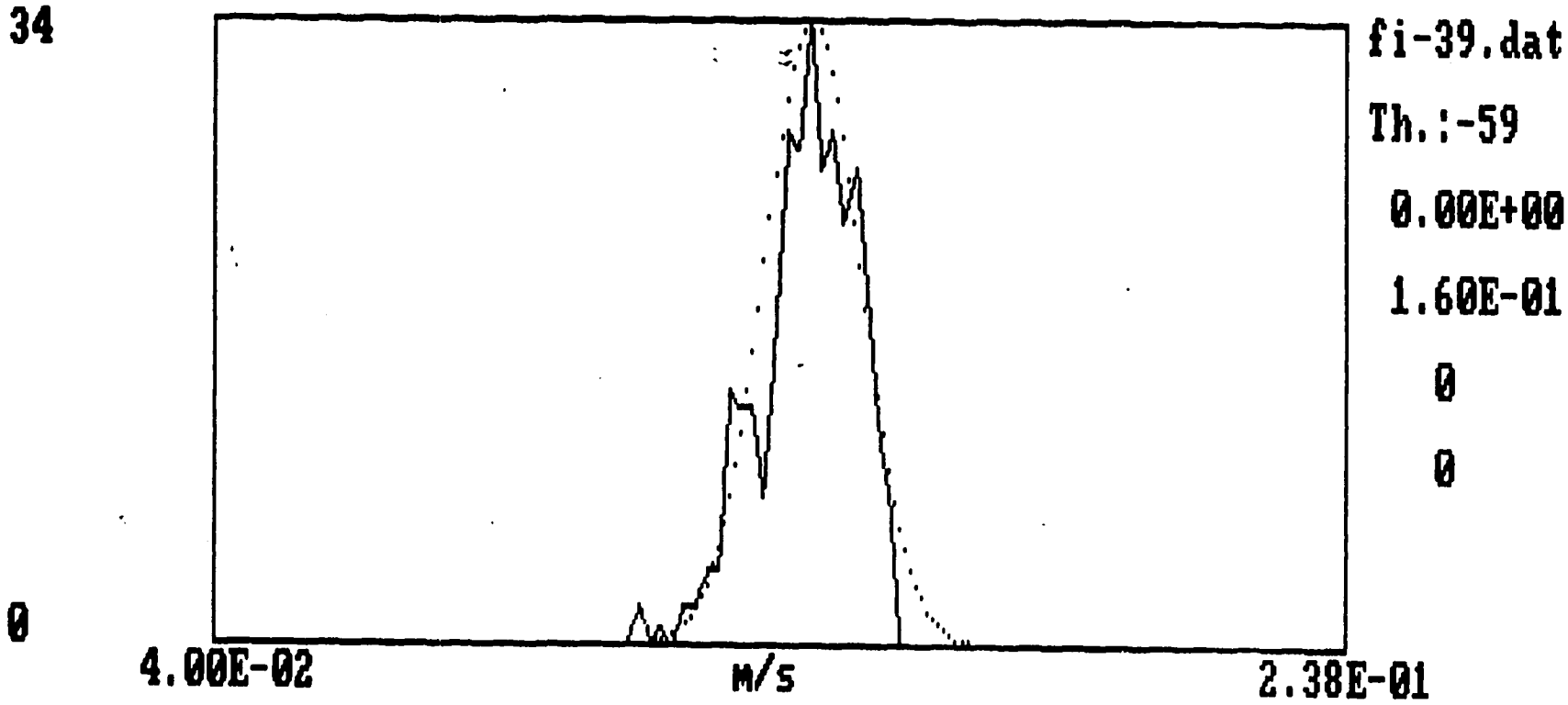

Velocity Distribution

Mean	: 1.445E-01 m/s	Dist. From Inlet	:	1.500E+02 cm
Stand. deviat.	: 8.462E-03 m/s	Radial Distance	:	0.000E+00 mm
Veloc. for max.	: 1.441E-01 m/s	Bulk velocity	:	1.180E-01 m/s
Skewness : -6.169E-01	Kurtosis : 3.227E+00	Re.	:	3.680E+03

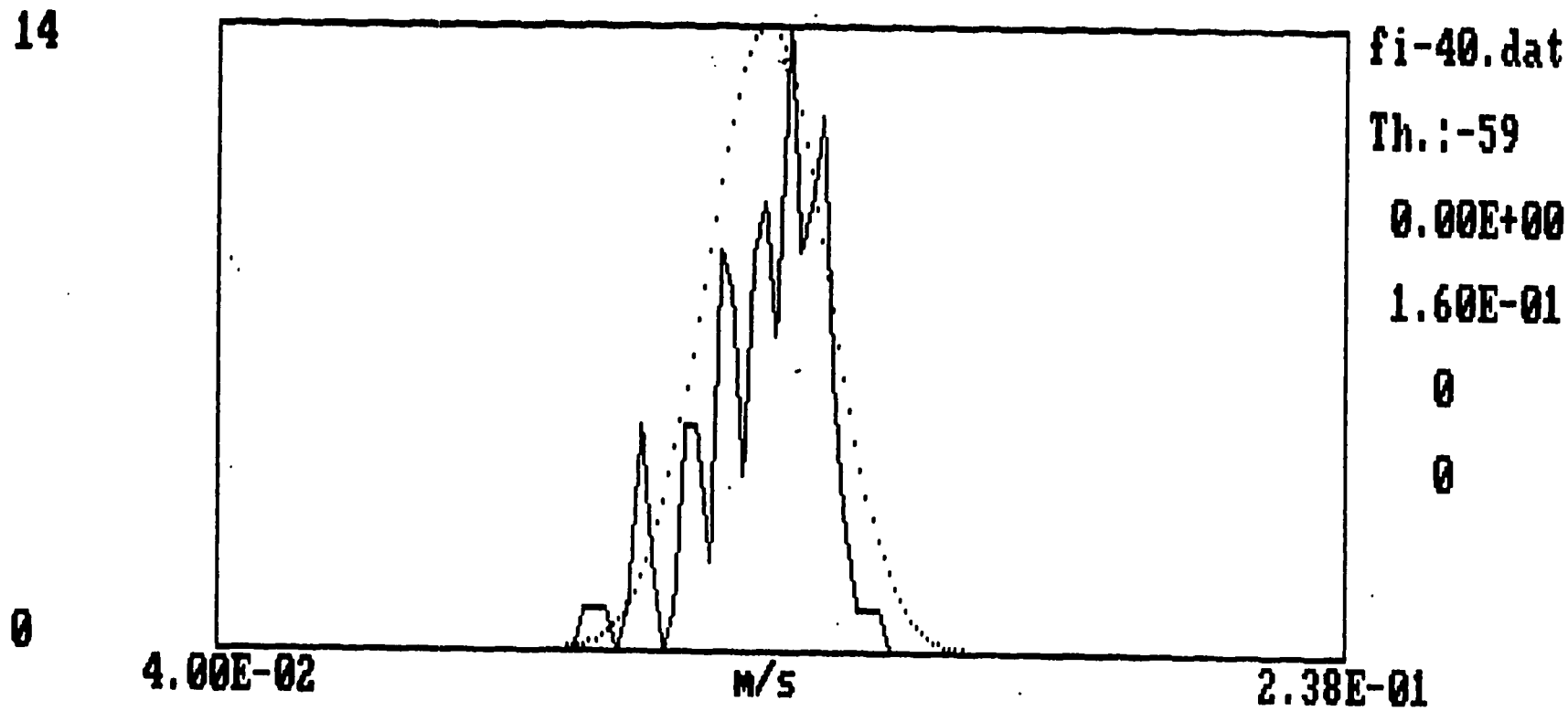

Velocity Distribution

Mean	: 1.362E-01 m/s	Dist. From Inlet		:	1.500E+02 cm
Stand. deviat.	: 1.062E-02 m/s	Radial Distance		:	5.000E+00 mm
Veloc. for max.	: 1.401E-01 m/s	Bulk velocity		:	1.180E-01 m/s
Skewness :	-6.910E-01	Kurtosis :	3.032E+00	Re. :	3.680E+03

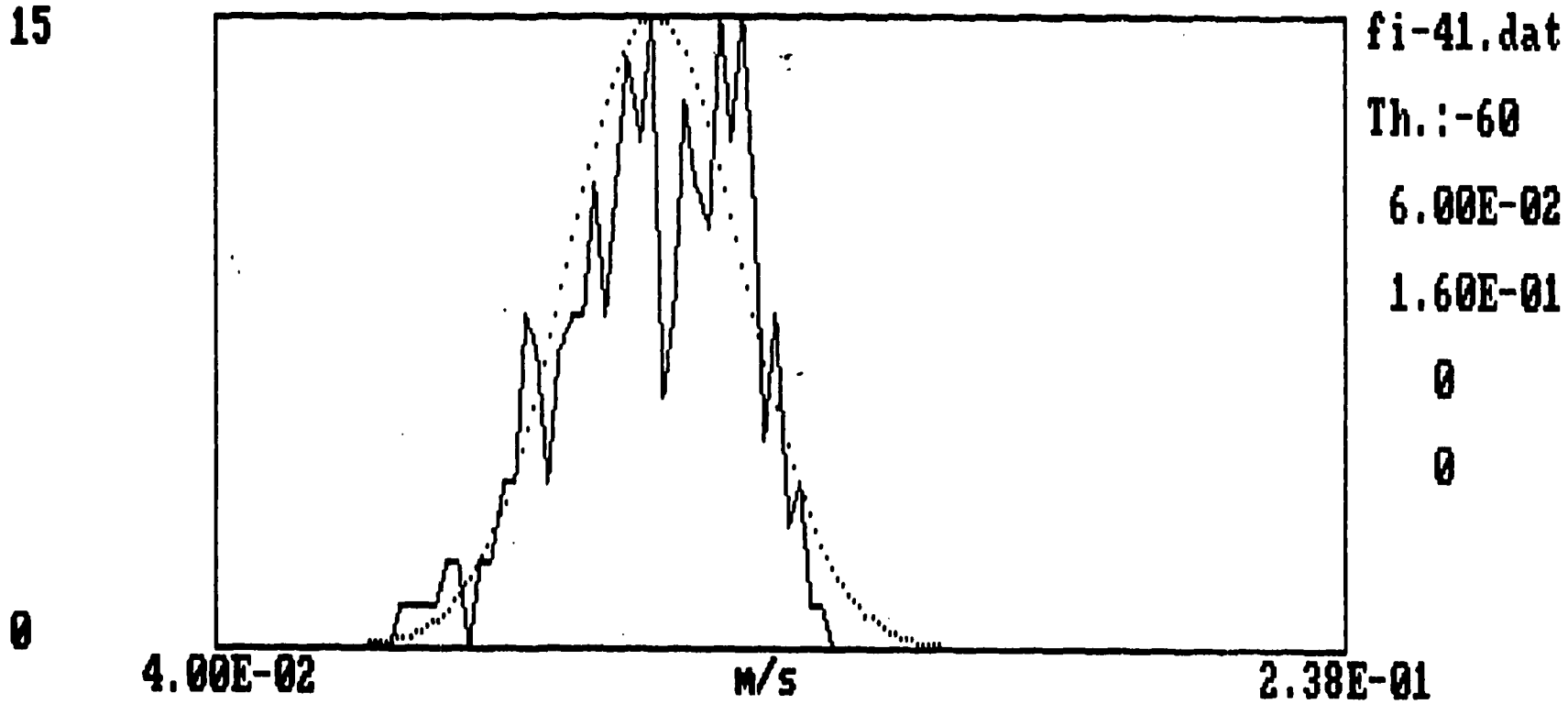

Velocity Distribution

Mean	: 1.168E-01 m/s	Dist. From Inlet	:	1.500E+02	cm
Stand. deviat.	: 1.543E-02 m/s	Radial Distance	:	1.000E+01	mm
Veloc. for max.	: 1.160E-01 m/s	Bulk velocity	:	1.180E-01	m/s
Skewness : -4.208E-01	Kurtosis : 2.592E+00	Re.	:	3.680E+03	

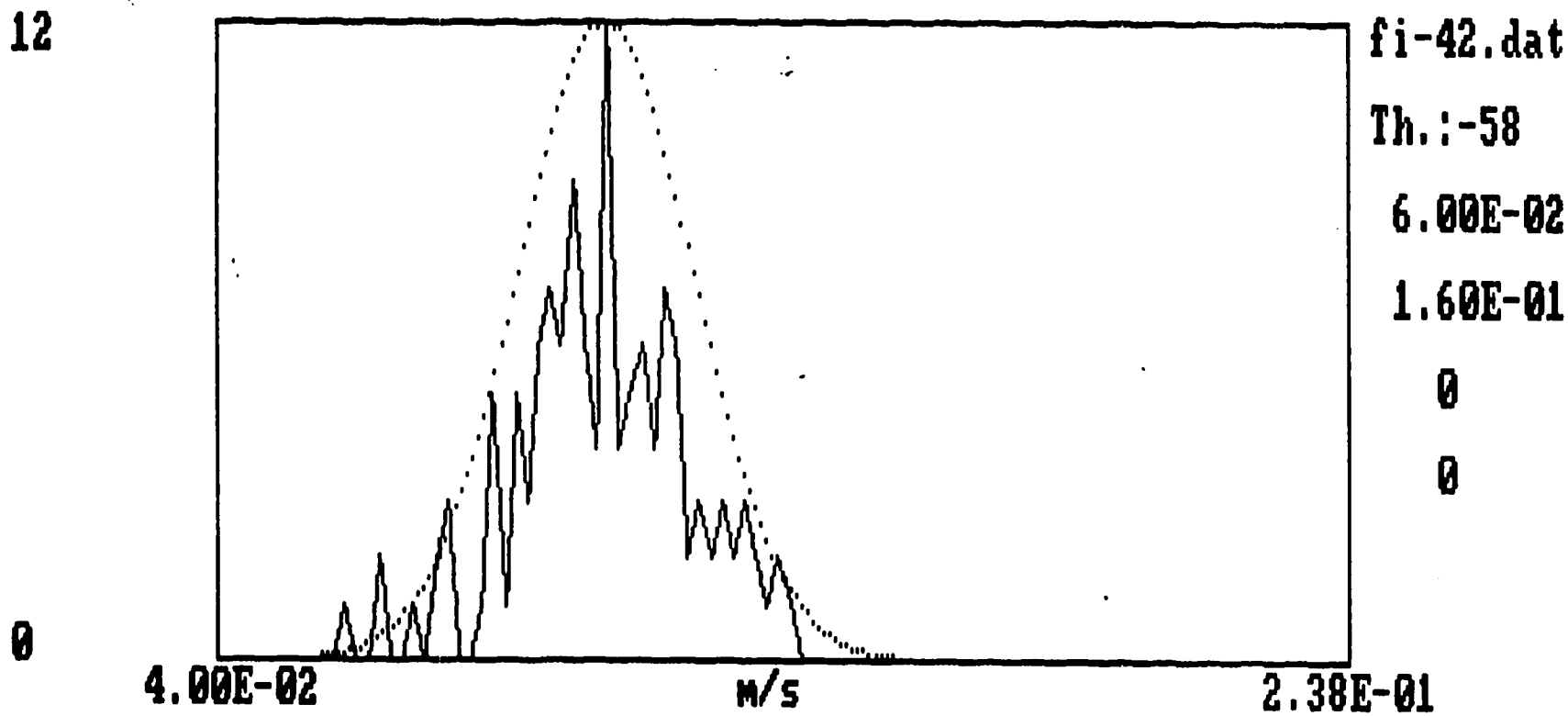

Velocity Distribution

Mean	: 1.079E-01 m/s	Dist. From Inlet	:	1.500E+02	cm
Stand. deviat.	: 1.543E-02 m/s	Radial Distance	:	1.200E+01	mm
Veloc. for max.	: 1.080E-01 m/s	Bulk velocity	:	1.180E-01	m/s
Skewness : -2.328E-01	Kurtosis : 3.024E+00	Re.	:	3.680E+03	

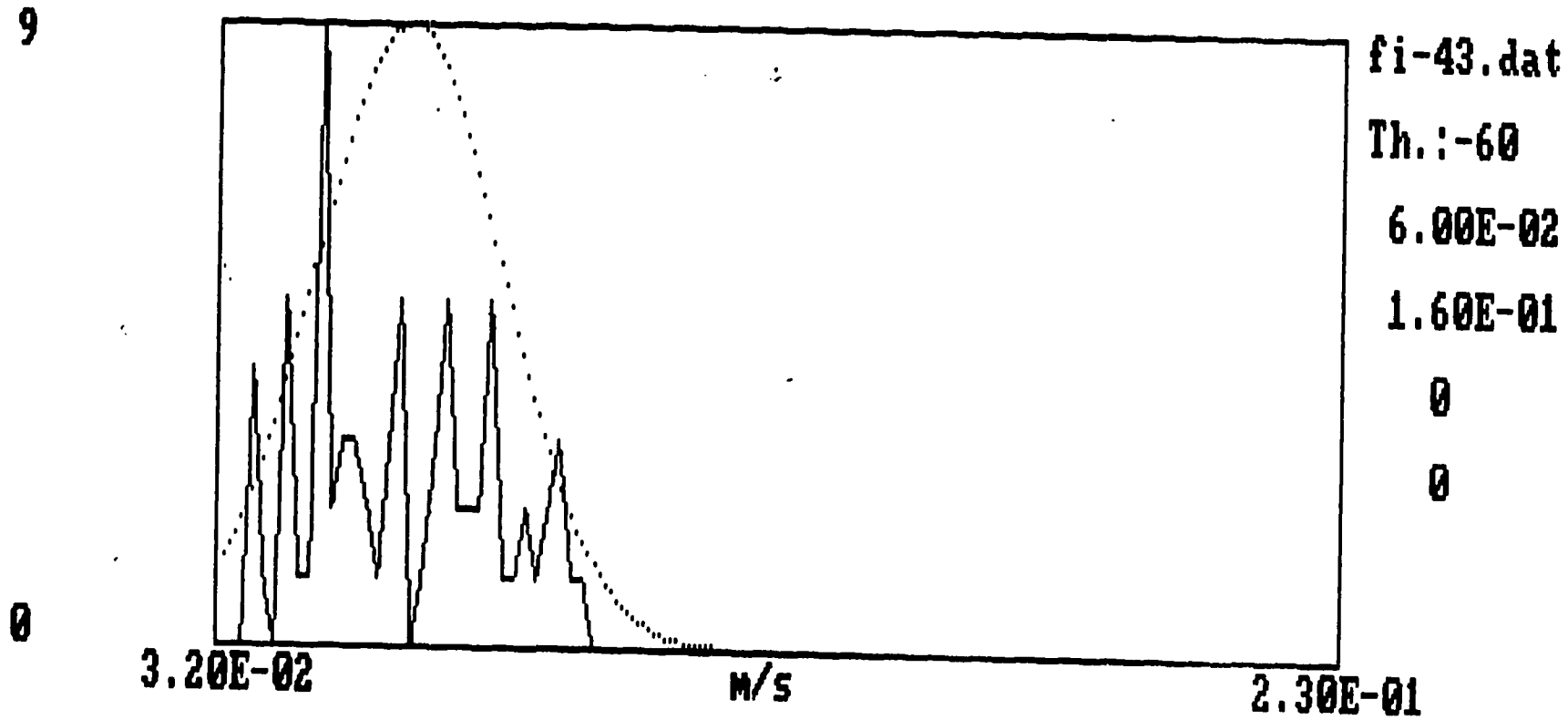

Velocity Distribution

Mean	: 6.537E-02 M/S	Dist. From Inlet		:	1.500E+02 CM
Stand. deviat.	: 1.644E-02 M/S	Radial Distance		:	1.400E+01 MM
Veloc. for max.	: 5.002E-02 M/S	Bulk velocity		:	1.180E-01 M/S
Skewness : 1.844E-01	Kurtosis : 1.878E+00		Re.	:	3.680E+03

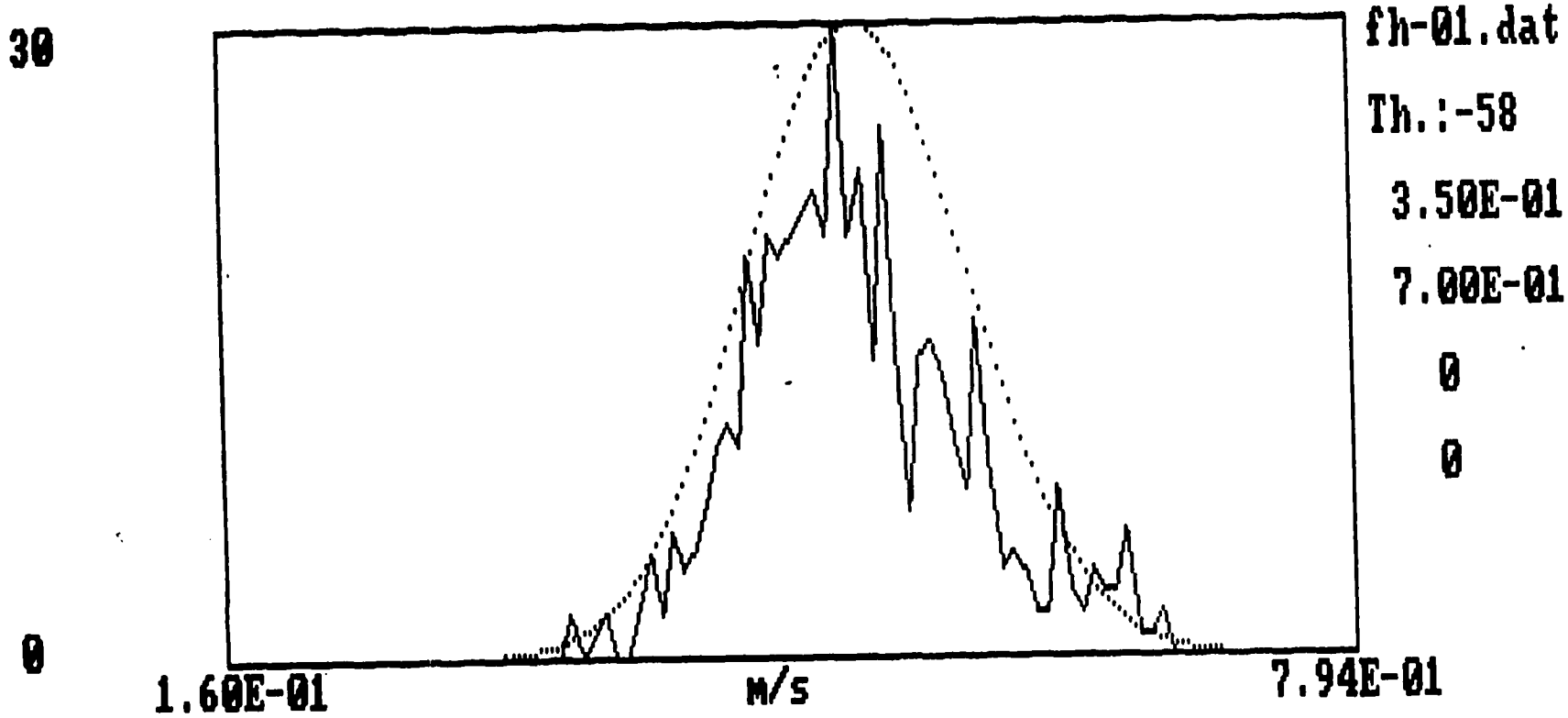

Velocity Distribution

Mean	: 5.163E-01 m/s	Dist. From Inlet		:	-1.000E+00 cm
Stand. deviat.	: 6.208E-02 m/s	Radial Distance		:	0.000E+00 mm
Veloc. for max.	: 5.058E-01 m/s	Bulk velocity		:	5.160E-01 m/s
Skewness :	3.813E-01	Kurtosis : 3.071E+00	Re.	:	1.670E+04

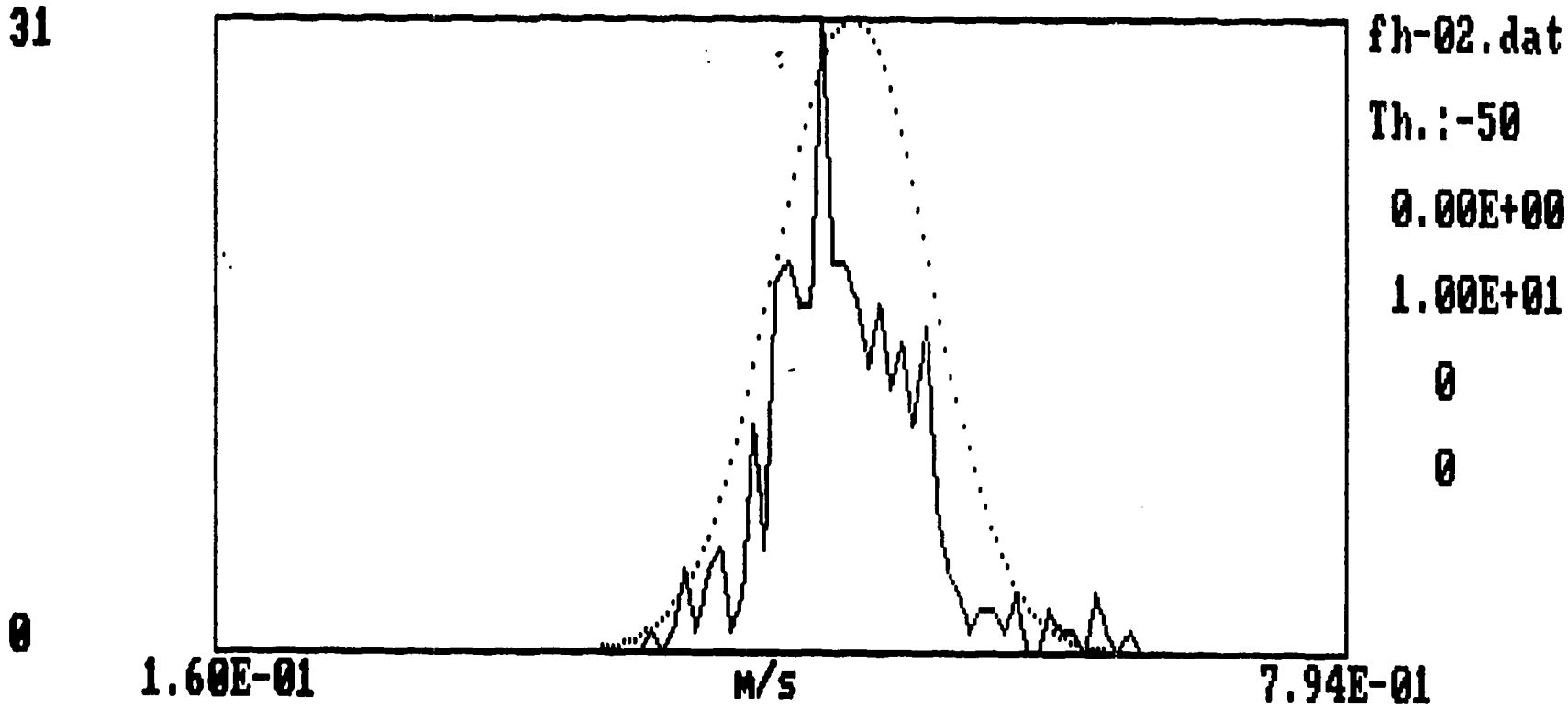

Velocity Distribution

Mean	: 5.161E-01 m/s	Dist. From Inlet	:	2.000E+00 cm	
Stand. deviat.	: 4.358E-02 m/s	Radial Distance	:	0.000E+00 mm	
Veloc. for max.	: 4.994E-01 m/s	Bulk velocity	:	5.160E-01 m/s	
Skewness : 6.907E-01	Kurtosis : 4.360E+00	Re.	:	1.670E+04	

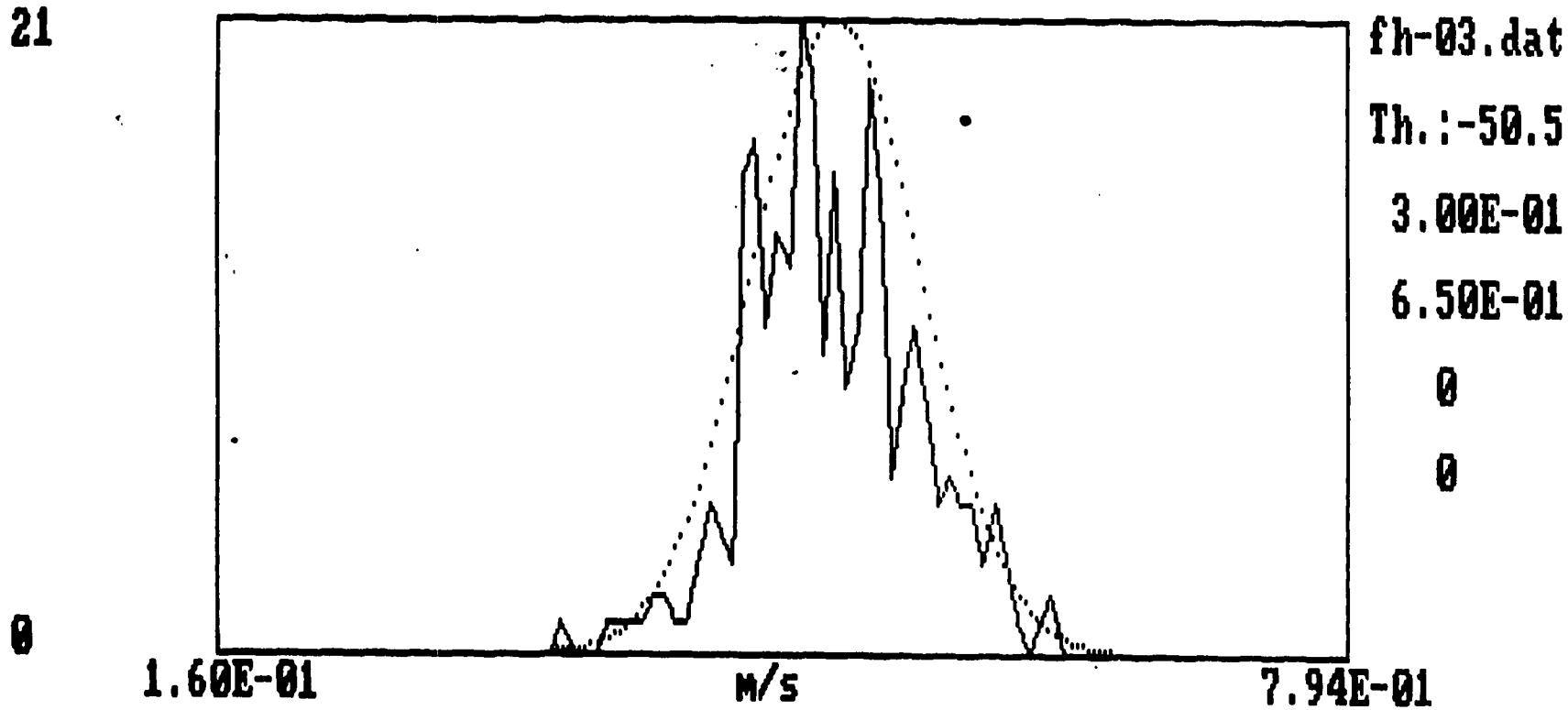

Velocity Distribution

Mean	: 5.067E-01 m/s	Dist. From Inlet		:	2.000E+00 cm
Stand. deviat.	: 4.762E-02 m/s	Radial Distance		:	5.000E+00 mm
Veloc. for max.	: 4.866E-01 m/s	Bulk velocity		:	5.160E-01 m/s
Skewness : 3.813E-02	Kurtosis	: 3.021E+00	Re.	:	1.670E+04

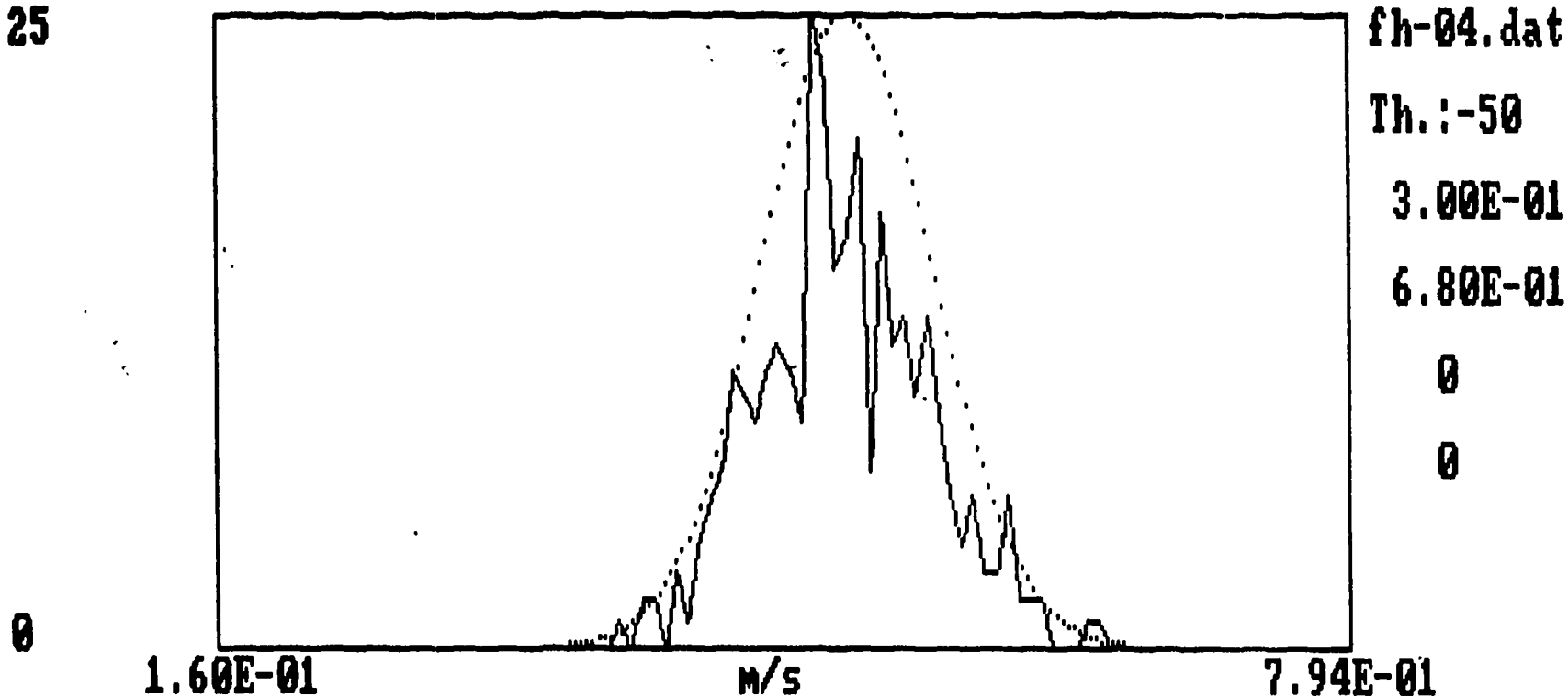

Velocity Distribution

Mean	: 5.124E-01 m/s	Dist. From Inlet	:	2.000E+00	cm
Stand. deviat.	: 4.784E-02 m/s	Radial Distance	:	1.000E+01	mm
Veloc. for max.	: 4.930E-01 m/s	Bulk velocity	:	5.160E-01	m/s
Skewness : 1.446E-01	Kurtosis : 2.867E+00	Re.	:	1.670E+04	

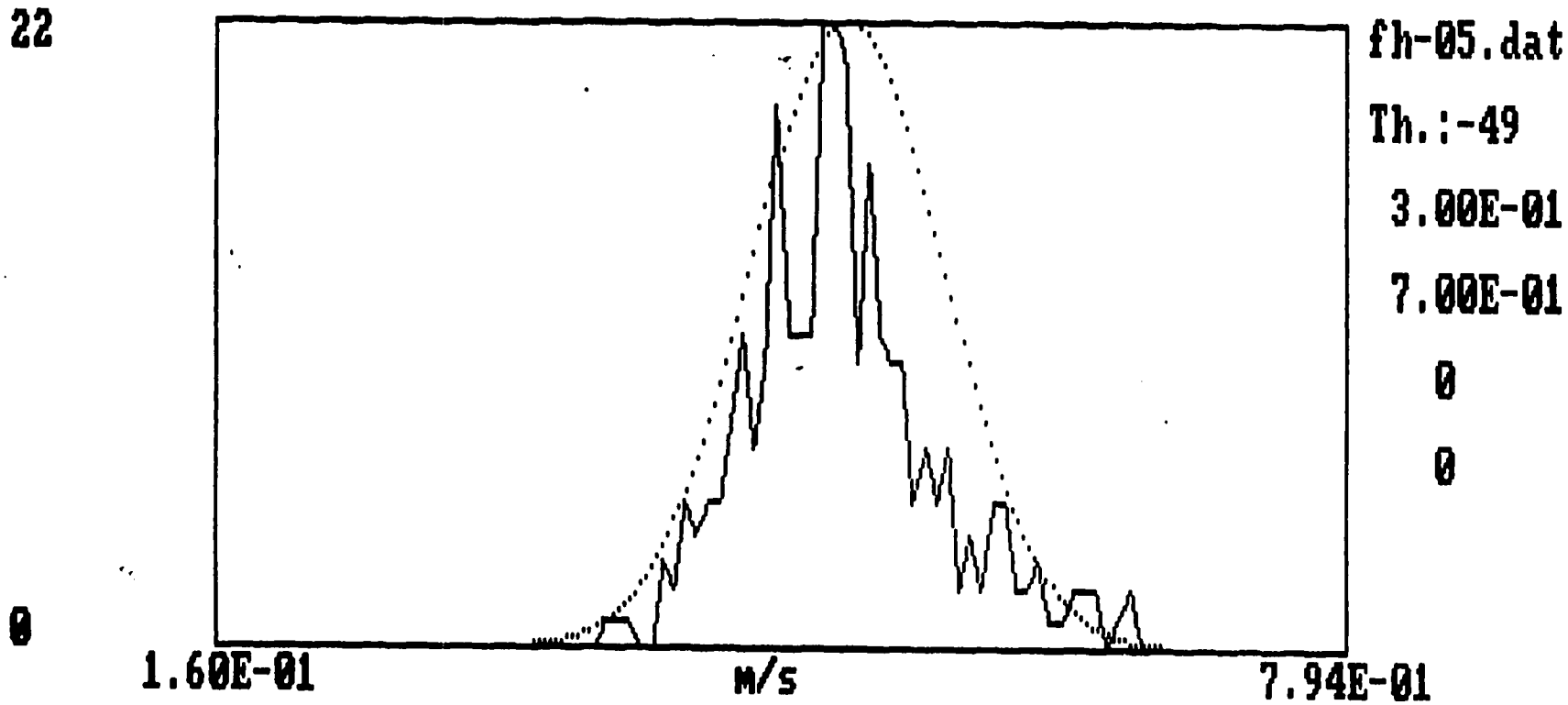

Velocity Distribution

Mean	: 5.133E-01 m/s	Dist. From Inlet	:	2.000E+00	cm
Stand. deviat.	: 5.408E-02 m/s	Radial Distance	:	1.200E+01	mm
Veloc. for max.	: 4.994E-01 m/s	Bulk velocity	:	5.160E-01	m/s
Skewness : 5.365E-01	Kurtosis : 3.447E+00	Re.	:	1.670E+04	

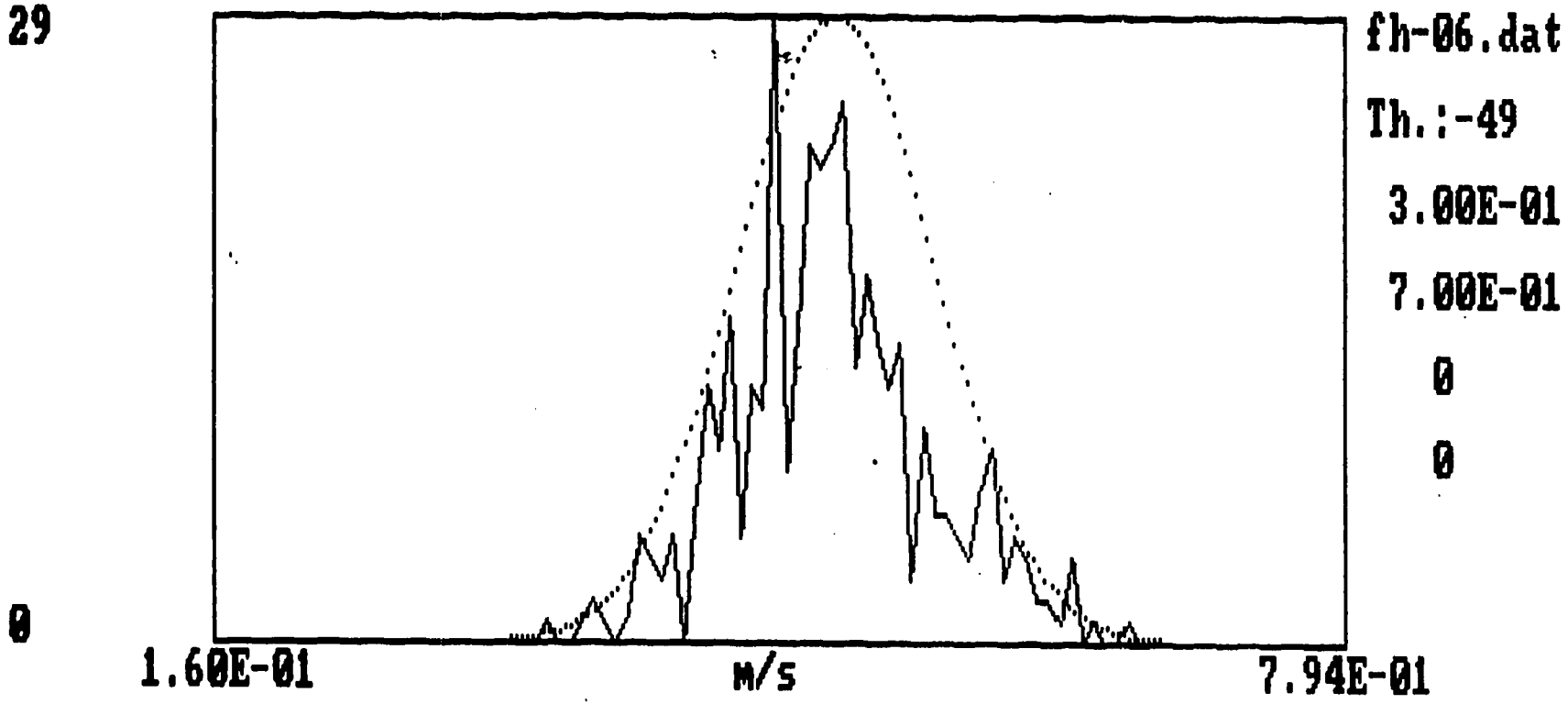

Velocity Distribution

Mean	: 5.078E-01 m/s	Dist. From Inlet	:	2.000E+00	cm
Stand. deviat.	: 5.569E-02 m/s	Radial Distance	:	1.400E+01	mm
Veloc. for max.	: 4.738E-01 m/s	Bulk velocity	:	5.160E-01	m/s
Skewness : 2.160E-01	Kurtosis : 3.087E+00	Re.	:	1.670E+04	

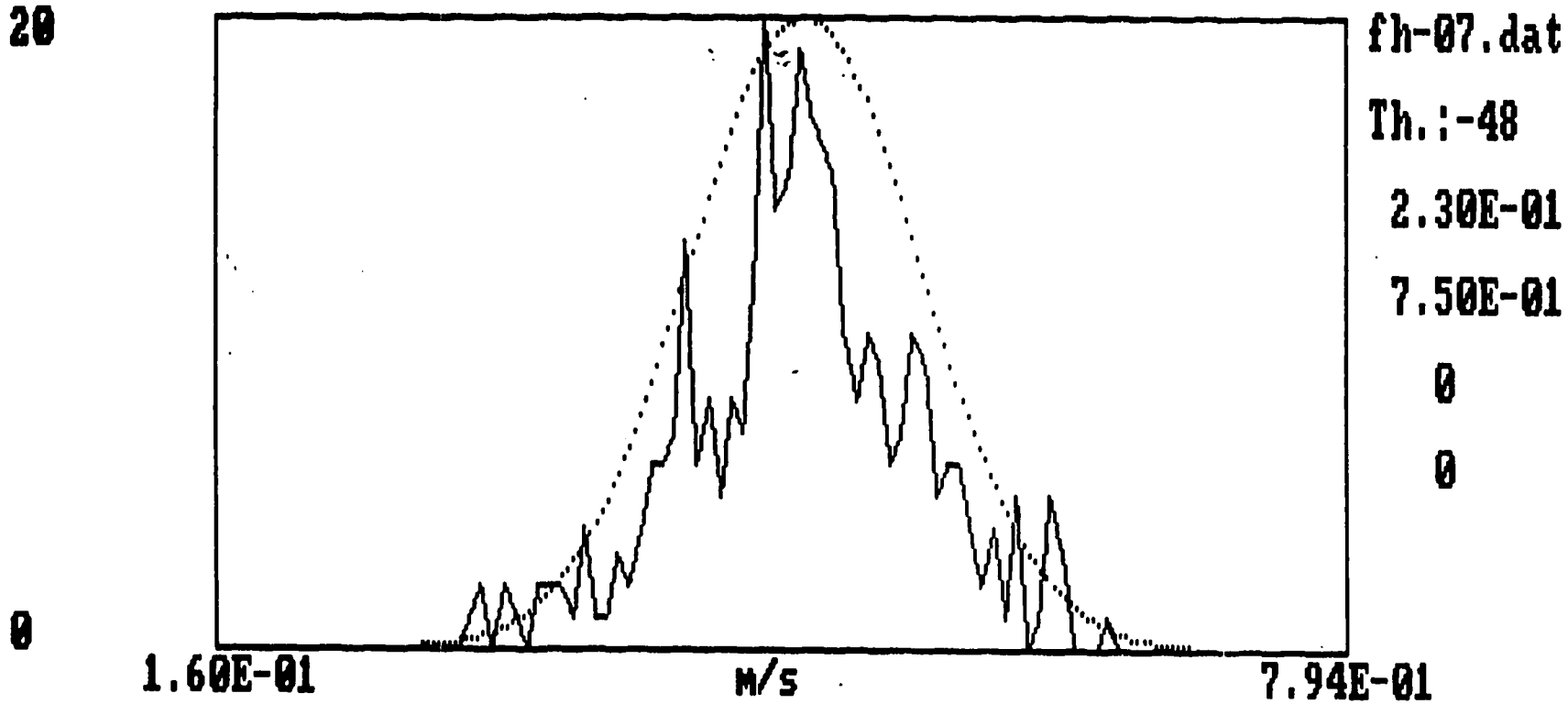

Velocity Distribution

Mean	: 4.896E-01 m/s	Dist. From Inlet		:	2.000E+00 cm
Stand. deviat.	: 6.577E-02 m/s	Radial Distance		:	1.500E+01 mm
Veloc. for max.	: 4.674E-01 m/s	Bulk velocity		:	5.160E-01 m/s
Skewness : -1.517E-01	Kurtosis : 3.148E+00		Re.	:	1.670E+04

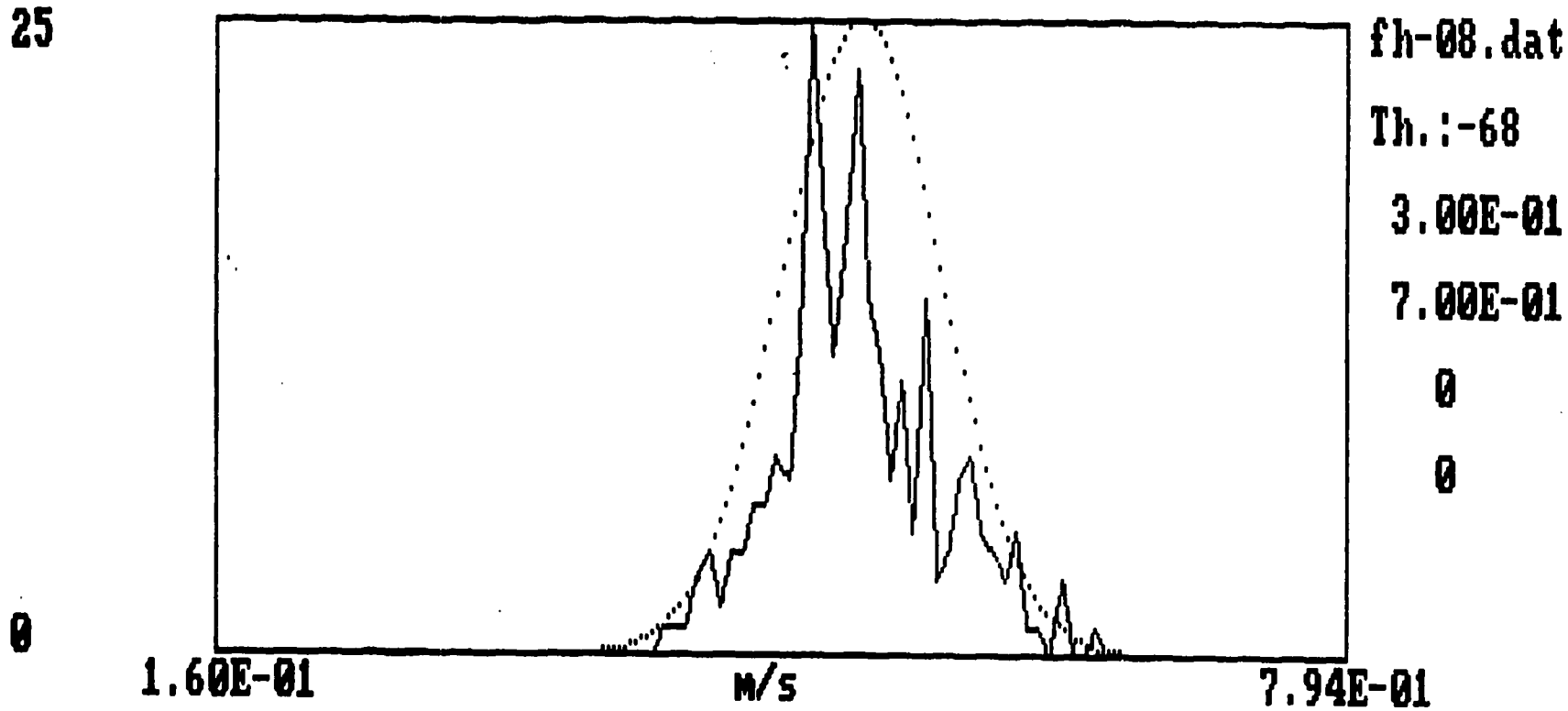

Velocity Distribution

Mean	: 5.215E-01 m/s	Dist. From Inlet	:	6.000E+00 cm	
Stand. deviat.	: 4.495E-02 m/s	Radial Distance	:	0.000E+00 mm	
Veloc. for max.	: 4.930E-01 m/s	Bulk velocity	:	5.160E-01 m/s	
Skewness : 2.906E-01	Kurtosis : 2.957E+00	Re.	:	1.670E+04	

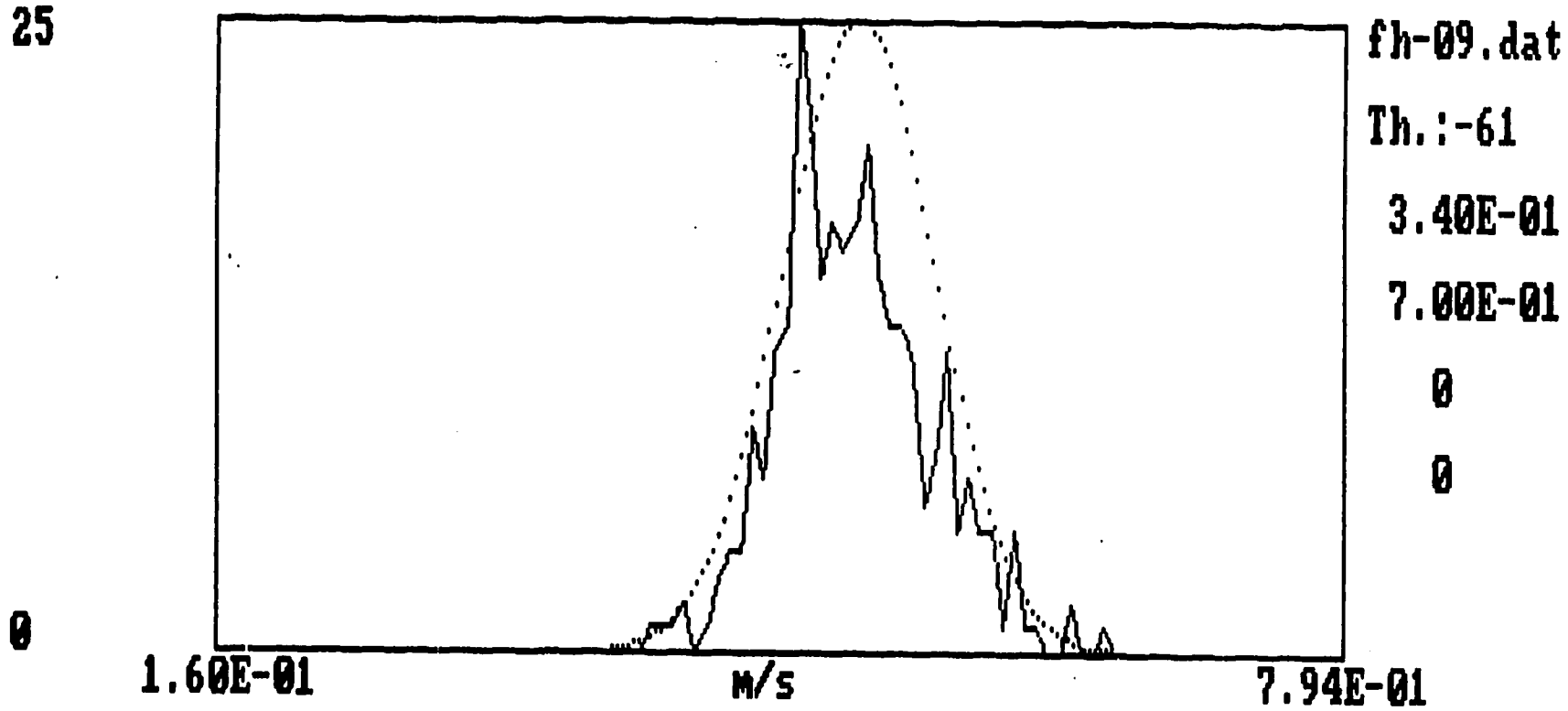

Velocity Distribution

Mean	: 5.206E-01 m/s	Dist. From Inlet	:	6.000E+00 cm	
Stand. deviat.	: 4.314E-02 m/s	Radial Distance	:	5.000E+00 mm	
Veloc. for max.	: 4.866E-01 m/s	Bulk velocity	:	5.160E-01 m/s	
Skewness : 3.204E-01	Kurtosis : 3.147E+00	Re.	:	1.670E+04	

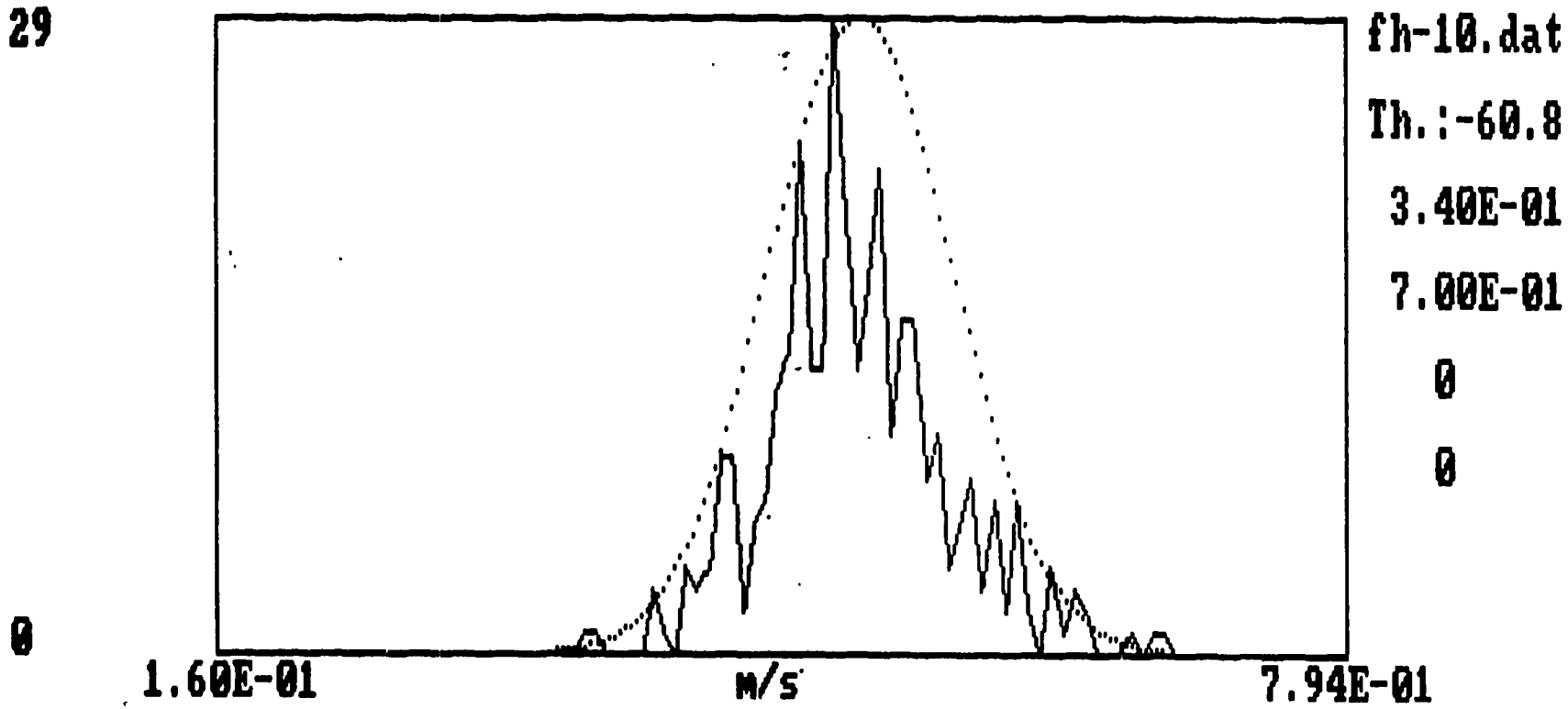

Velocity Distribution

Mean	: 5.207E-01 m/s	Dist. From Inlet	:	6.000E+00	cm
Stand. deviat.	: 5.199E-02 m/s	Radial Distance	:	1.000E+01	mm
Veloc. for max.	: 5.058E-01 m/s	Bulk velocity	:	5.160E-01	m/s
Skewness : 3.329E-01	Kurtosis : 3.571E+00	Re.	:	1.670E+04	

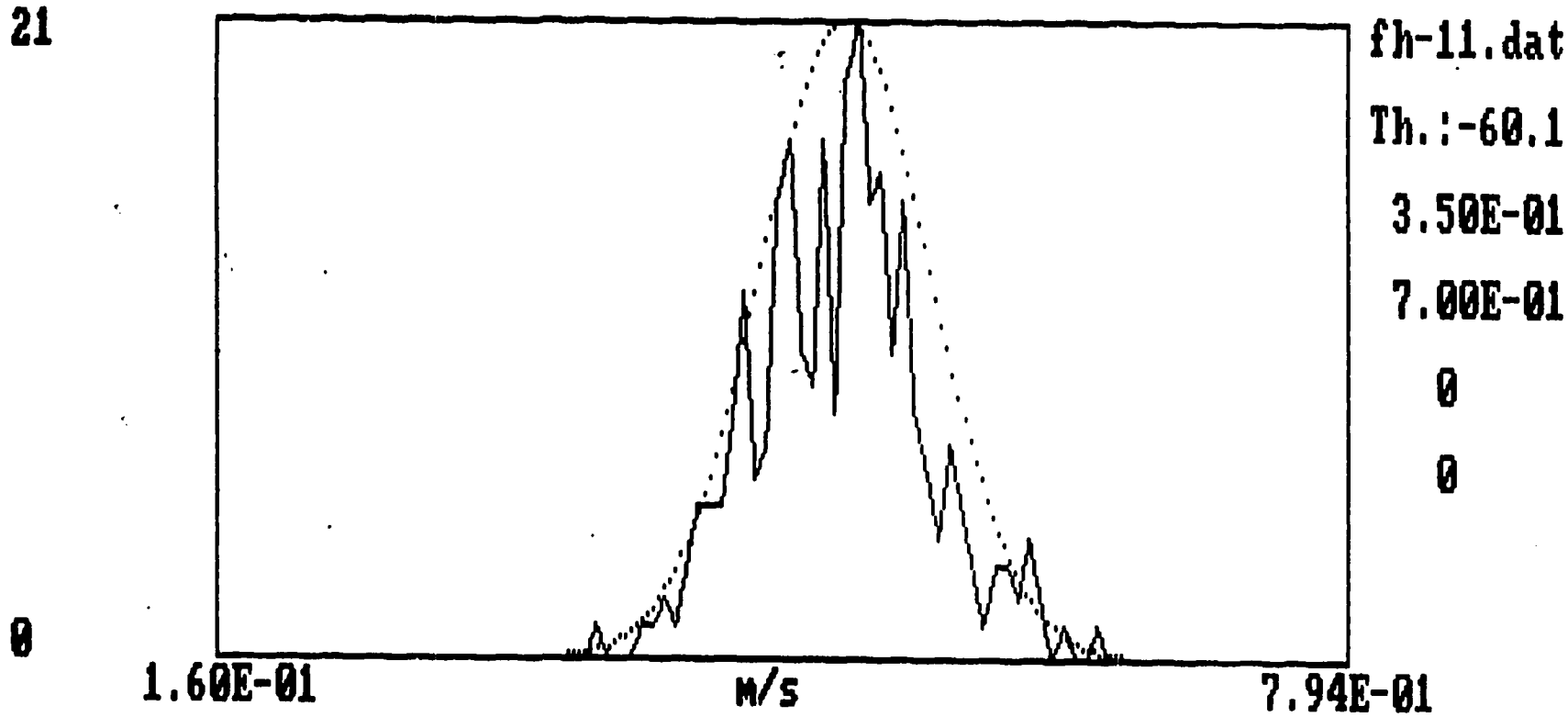

Velocity Distribution

Mean	: 5.115E-01 m/s	Dist. From Inlet	:	6.000E+00 cm	
Stand. deviat.	: 4.784E-02 m/s	Radial Distance	:	1.200E+01 mm	
Veloc. for max.	: 5.186E-01 m/s	Bulk velocity	:	5.160E-01 m/s	
Skewness : 1.693E-01	Kurtosis : 3.008E+00	Re.	:	1.670E+04	

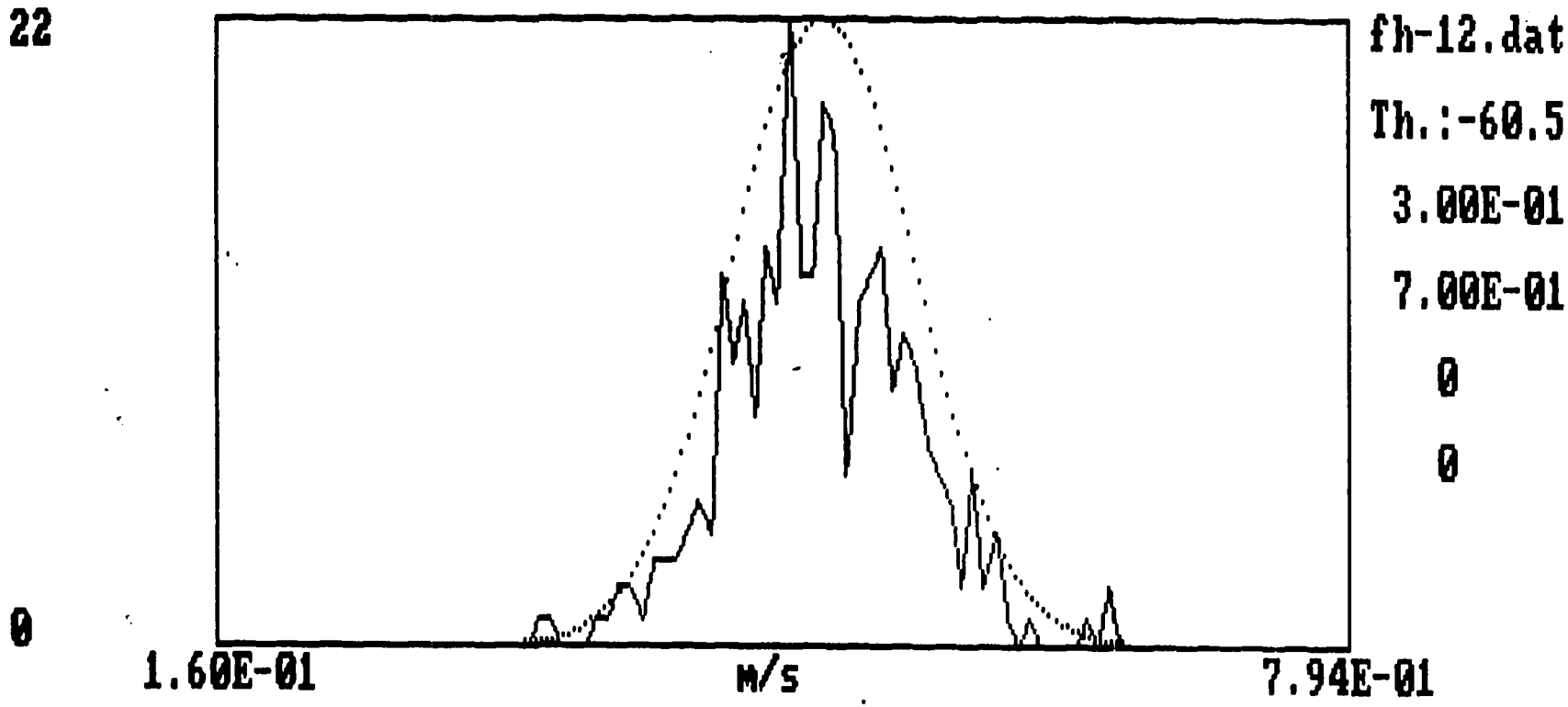

Velocity Distribution

Mean	: 4.993E-01 m/s	Dist. From Inlet	:	6.000E+00	cm
Stand. deviat.	: 5.154E-02 m/s	Radial Distance	:	1.400E+01	mm
Veloc. for max.	: 4.802E-01 m/s	Bulk velocity	:	5.160E-01	m/s
Skewness : 4.804E-02	Kurtosis : 3.377E+00	Re.	:	1.670E+04	

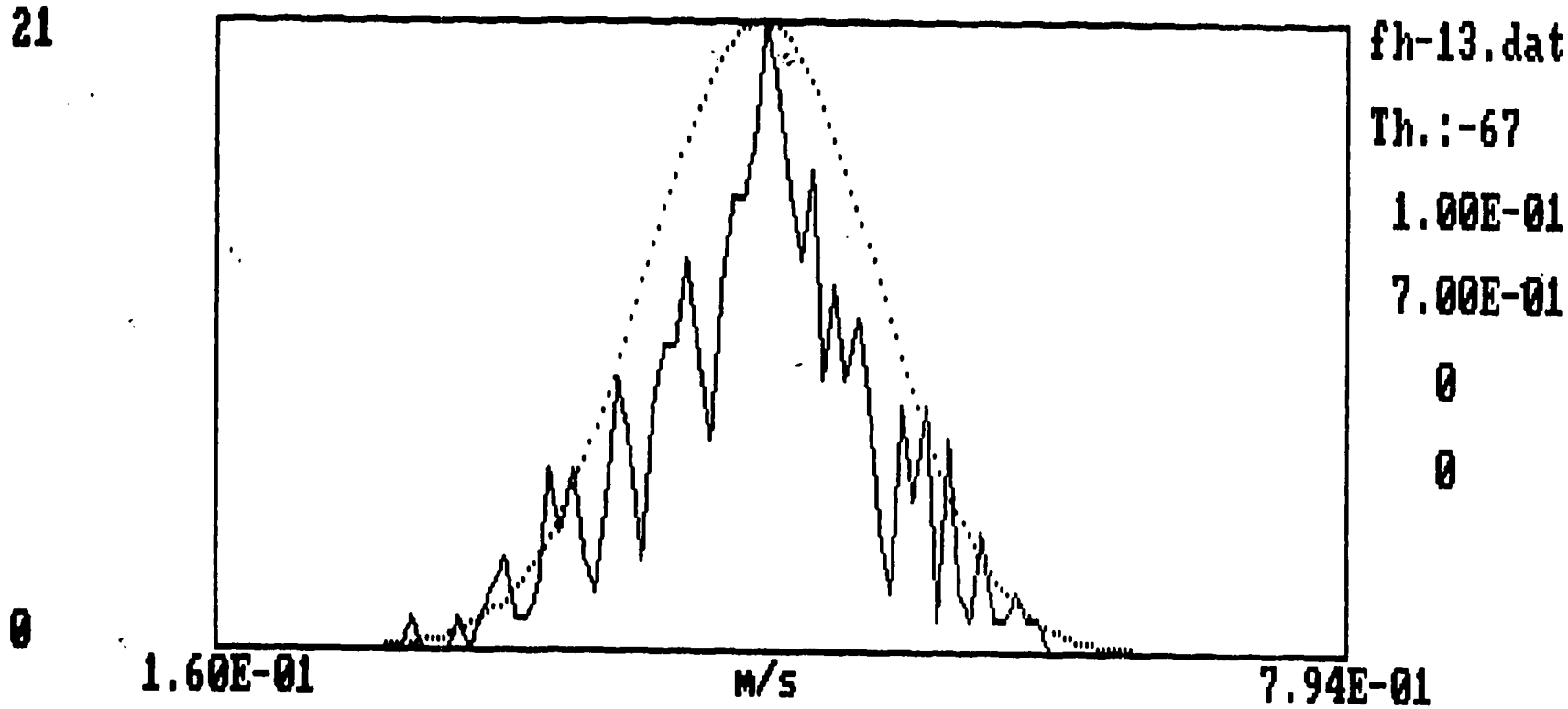

Velocity Distribution

Mean	: 4.645E-01 m/s	Dist. From Inlet		:	6.000E+00 cm
Stand. deviat.	: 6.372E-02 m/s	Radial Distance		:	1.500E+01 mm
Veloc. for max.	: 4.674E-01 m/s	Bulk velocity		:	5.160E-01 m/s
Skewness :	-1.428E-01	Kurtosis :	2.950E+00	Re. :	1.670E+04

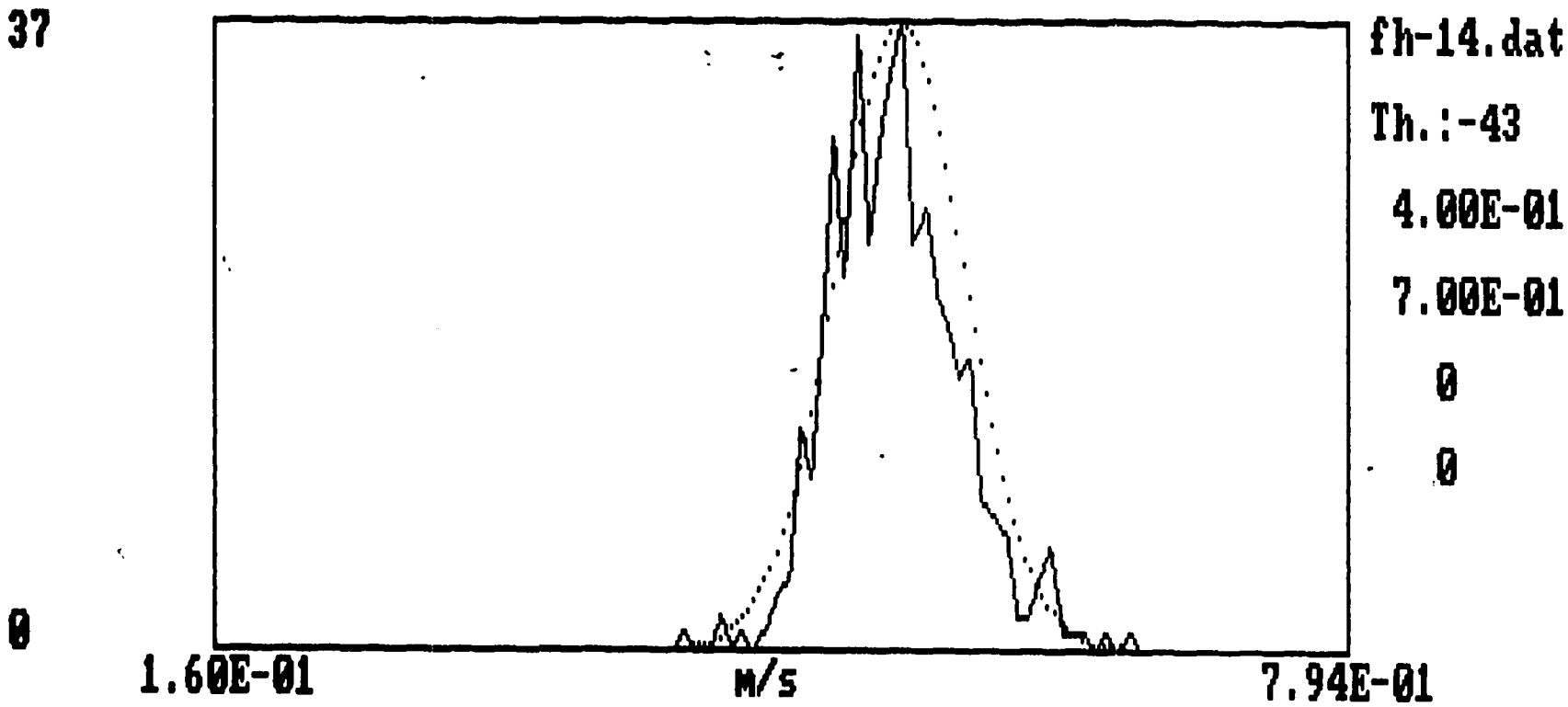

Velocity Distribution

Mean	: 5.431E-01 m/s	Dist. From Inlet	:	1.200E+01 cm	
Stand. deviat.	: 3.593E-02 m/s	Radial Distance	:	0.000E+00 mm	
Veloc. for max.	: 5.442E-01 m/s	Bulk velocity	:	5.160E-01 m/s	
Skewness : 4.072E-01	Kurtosis : 3.603E+00	Re.	:	1.670E+04	

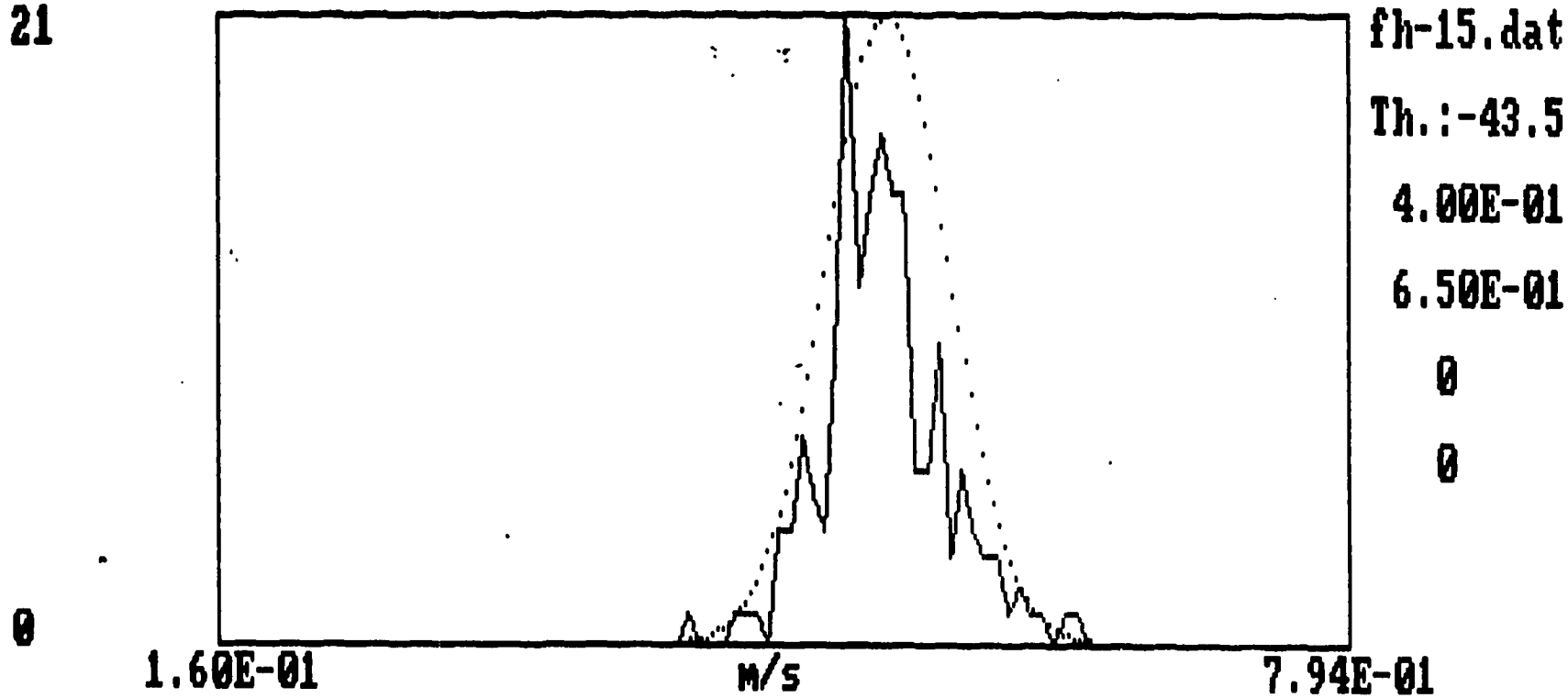

Velocity Distribution

Mean	: 5.347E-01 m/s	Dist. From Inlet	:	1.200E+01 cm
Stand. deviat.	: 3.464E-02 m/s	Radial Distance	:	5.000E+00 mm
Veloc. for max.	: 5.122E-01 m/s	Bulk velocity	:	5.160E-01 m/s
Skewness : 2.912E-01	Kurtosis : 3.729E+00	Re.	:	1.670E+04

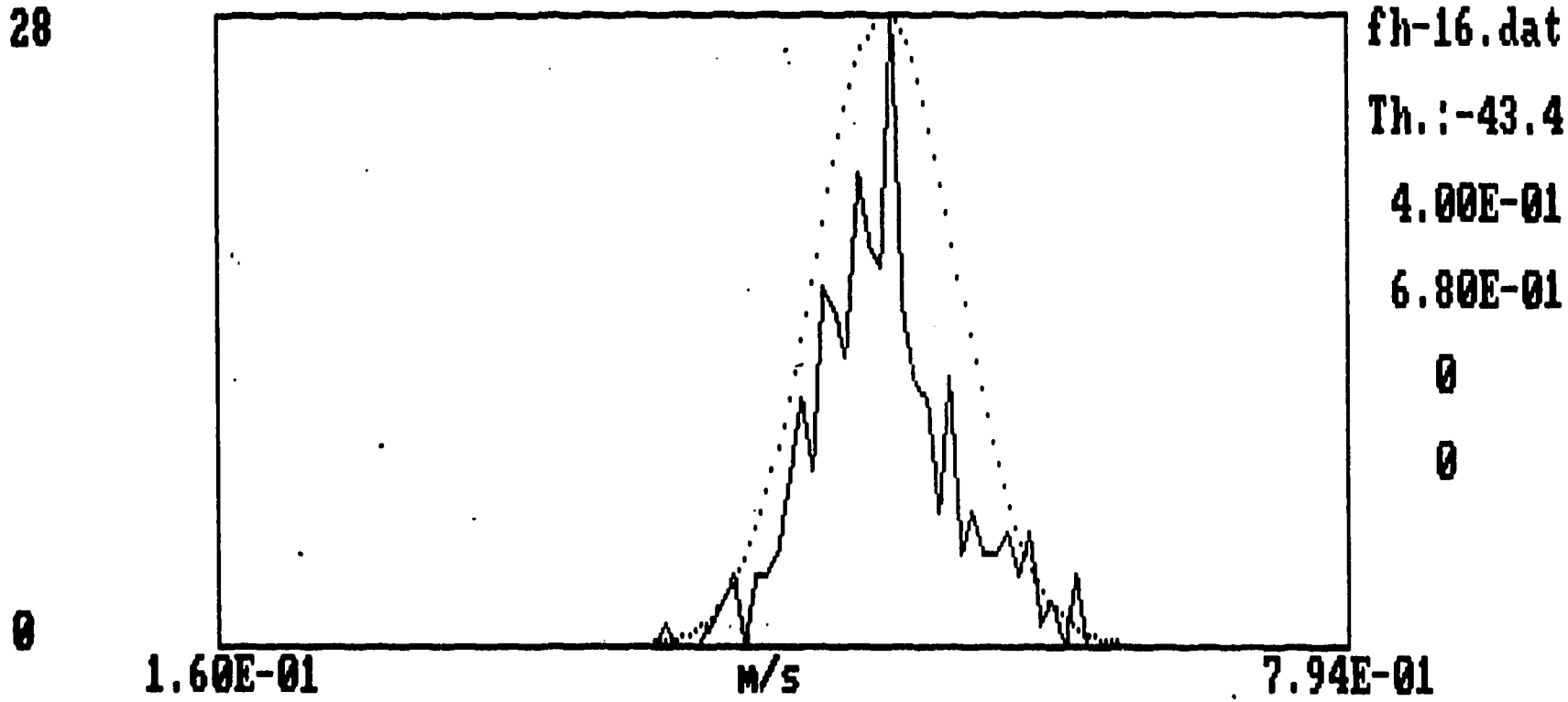

Velocity Distribution

Mean	: 5.345E-01 m/s	Dist. From Inlet	:	1.200E+01	cm
Stand. deviat.	: 3.989E-02 m/s	Radial Distance	:	1.000E+01	mm
Veloc. for max.	: 5.378E-01 m/s	Bulk velocity	:	5.160E-01	m/s
Skewness : 2.454E-01	Kurtosis : 3.244E+00	Re.	:	1.670E+04	

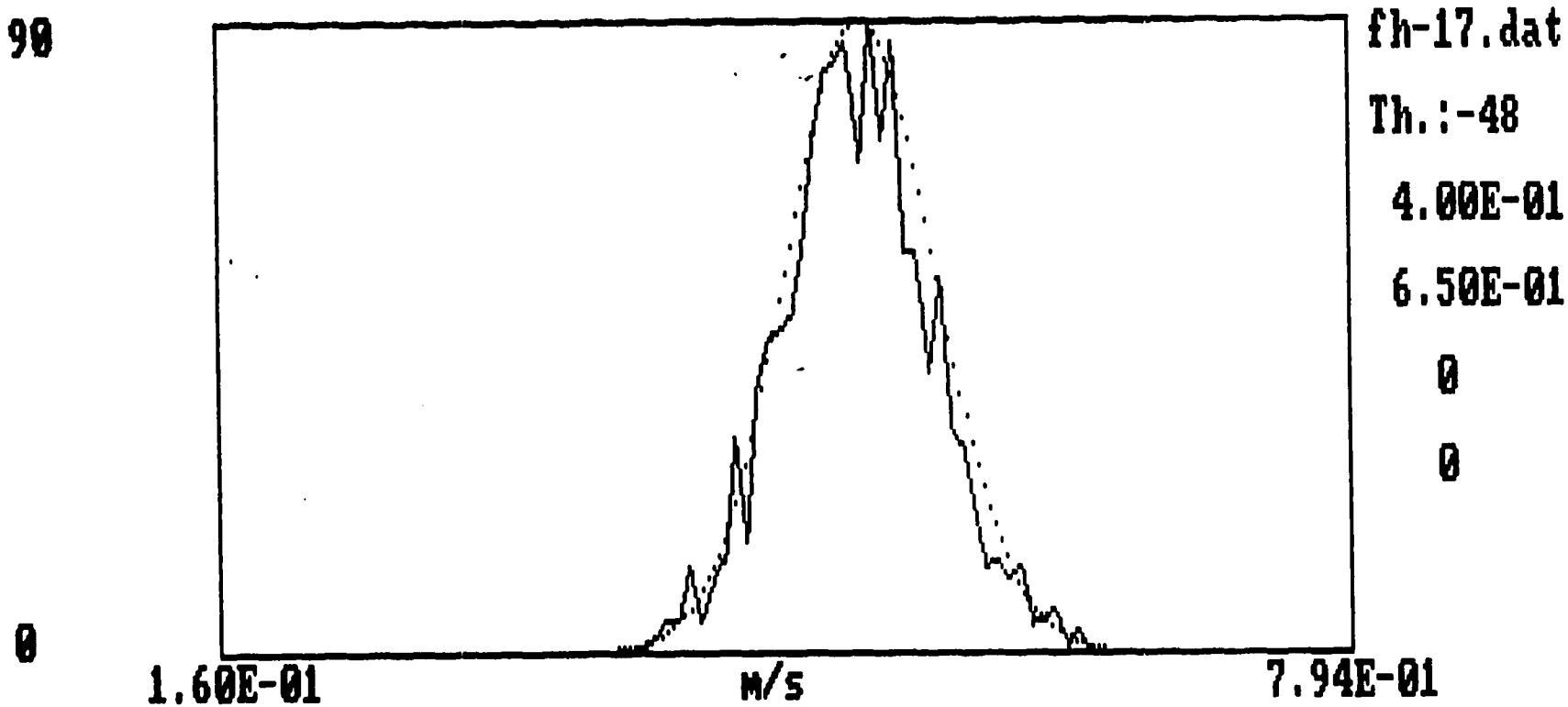

Velocity Distribution

Mean	: 5.195E-01 m/s	Dist. From Inlet	:	1.200E+01 cm	
Stand. deviat.	: 4.189E-02 m/s	Radial Distance	:	1.200E+01 mm	
Veloc. for max.	: 5.250E-01 m/s	Bulk velocity	:	5.160E-01 m/s	
Skewness : 6.316E-02	Kurtosis : 3.006E+00	Re.	:	1.670E+04	

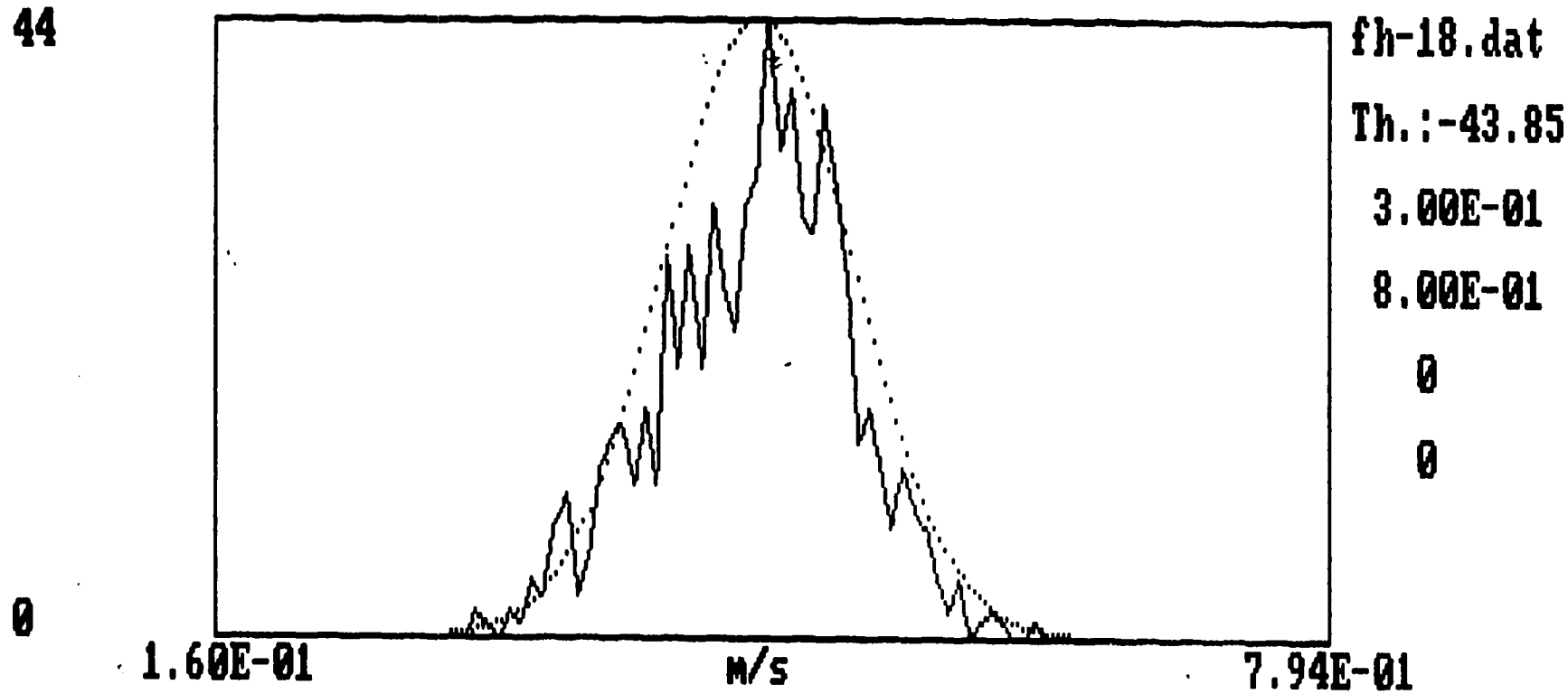

Velocity Distribution

Mean	: 4.684E-01 m/s	Dist. From Inlet	:	1.200E+01 cm	
Stand. deviat.	: 5.416E-02 m/s	Radial Distance	:	1.400E+01 mm	
Veloc. for max.	: 4.738E-01 m/s	Bulk velocity	:	5.160E-01 m/s	
Skewness : -2.387E-01	Kurtosis : 2.844E+00	Re.	:	1.670E+04	

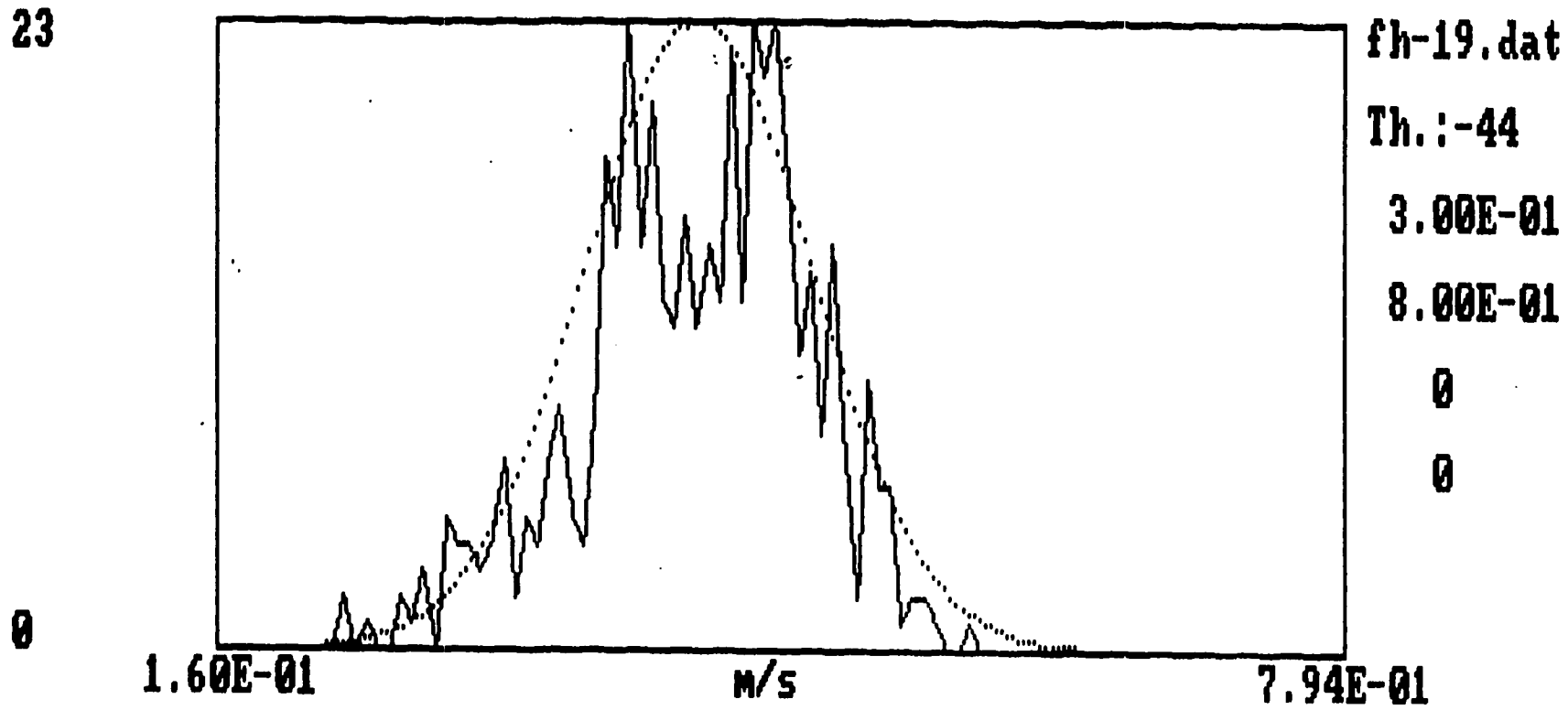

Velocity Distribution

Mean	: 4.302E-01 m/s	Dist. From Inlet	:	1.200E+01 cm
Stand. deviat.	: 6.450E-02 m/s	Radial Distance	:	1.500E+01 mm
Veloc. for max.	: 3.905E-01 m/s	Bulk velocity	:	5.160E-01 m/s
Skewness : -4.251E-01	Kurtosis : 2.897E+00	Re.	:	1.670E+04

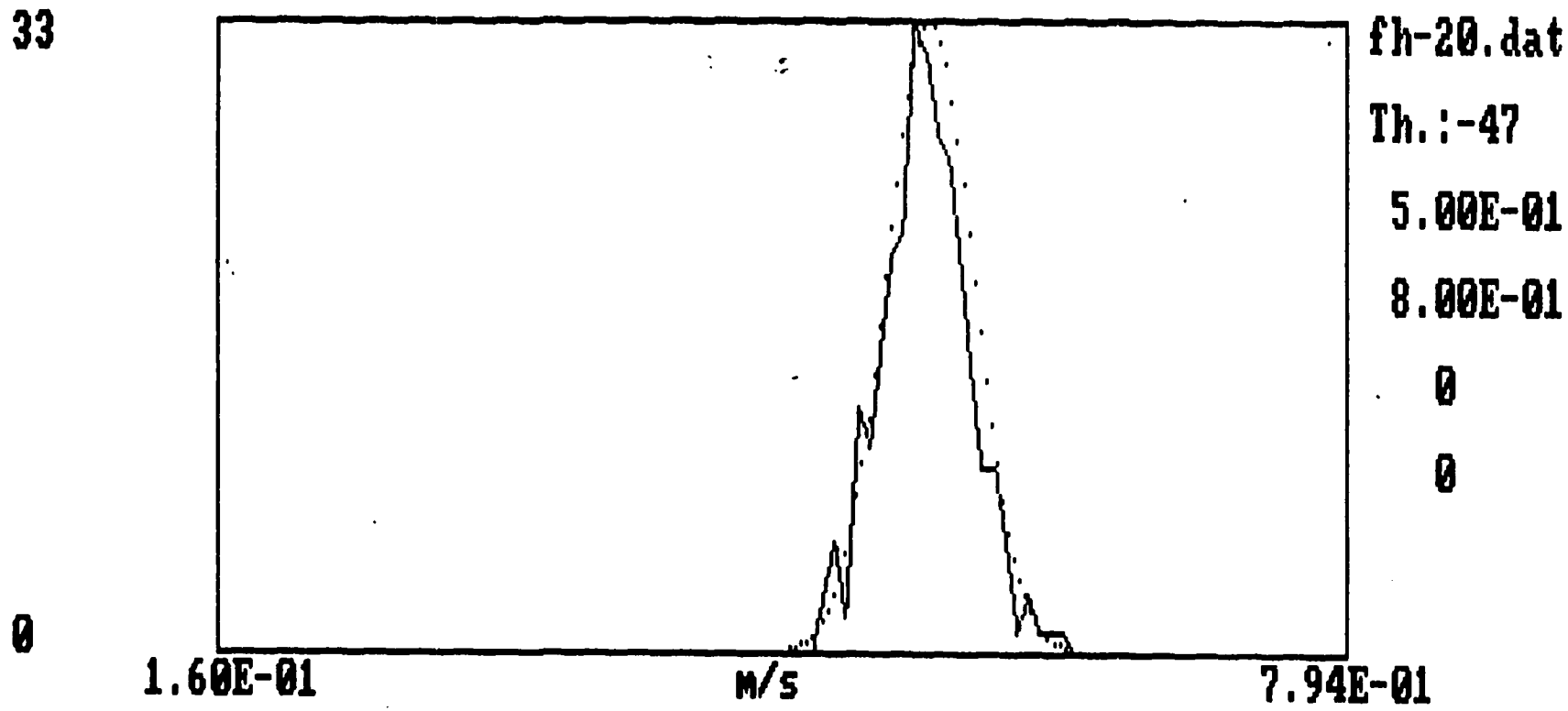

Velocity Distribution

Mean	: 5.593E-01 m/s	Dist. From Inlet	:	3.000E+01 cm
Stand. deviat.	: 2.480E-02 m/s	Radial Distance	:	0.000E+00 mm
Veloc. for max.	: 5.506E-01 m/s	Bulk velocity	:	5.160E-01 m/s
Skewness : 1.429E-01	Kurtosis : 3.025E+00	Re.	:	1.670E+04

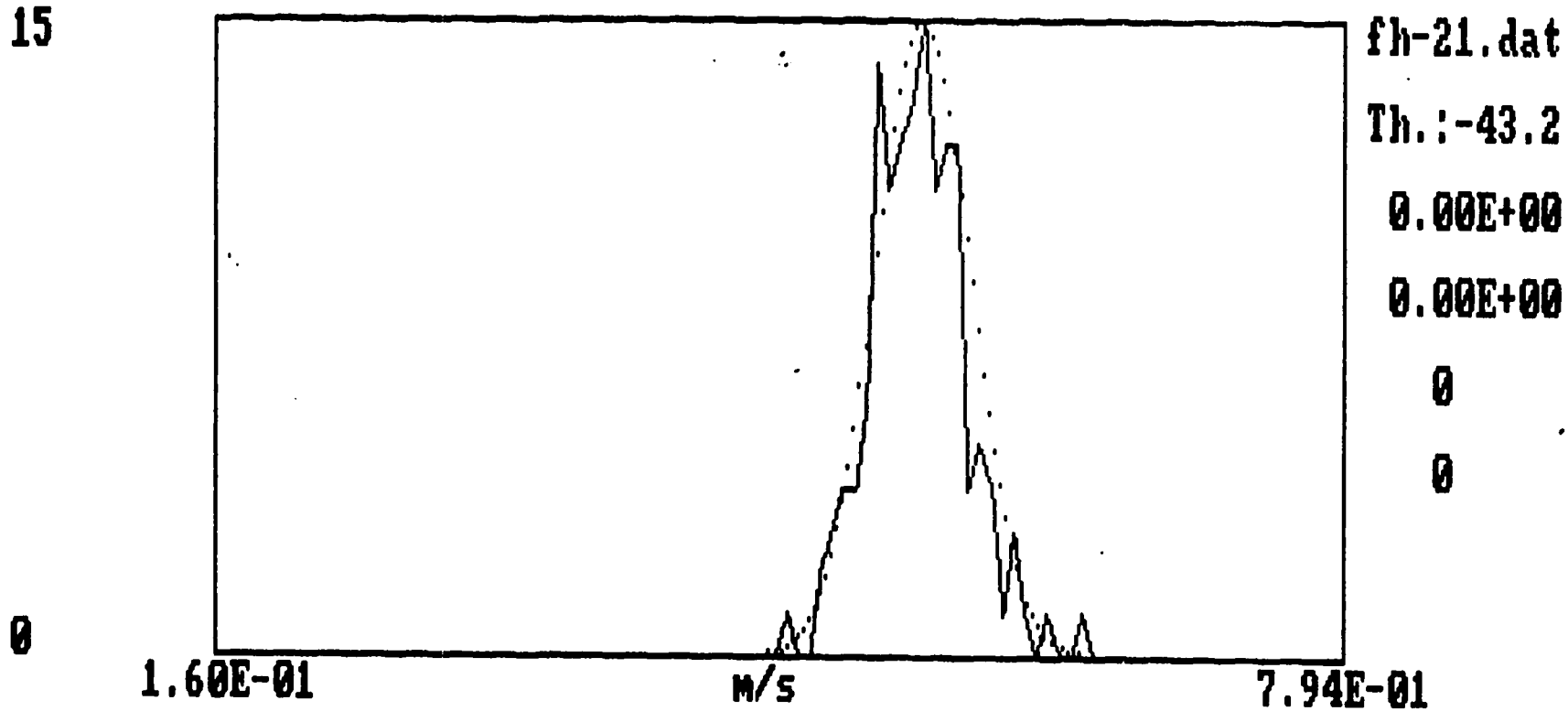

Velocity Distribution

Mean	: 5.568E-01 m/s	Dist. From Inlet	:	3.000E+01 cm	
Stand. deviat.	: 2.706E-02 m/s	Radial Distance	:	5.000E+00 mm	
Veloc. for max.	: 5.570E-01 m/s	Bulk velocity	:	5.160E-01 m/s	
Skewness : 2.845E-01	Kurtosis : 3.671E+00	Re.	:	1.670E+04	

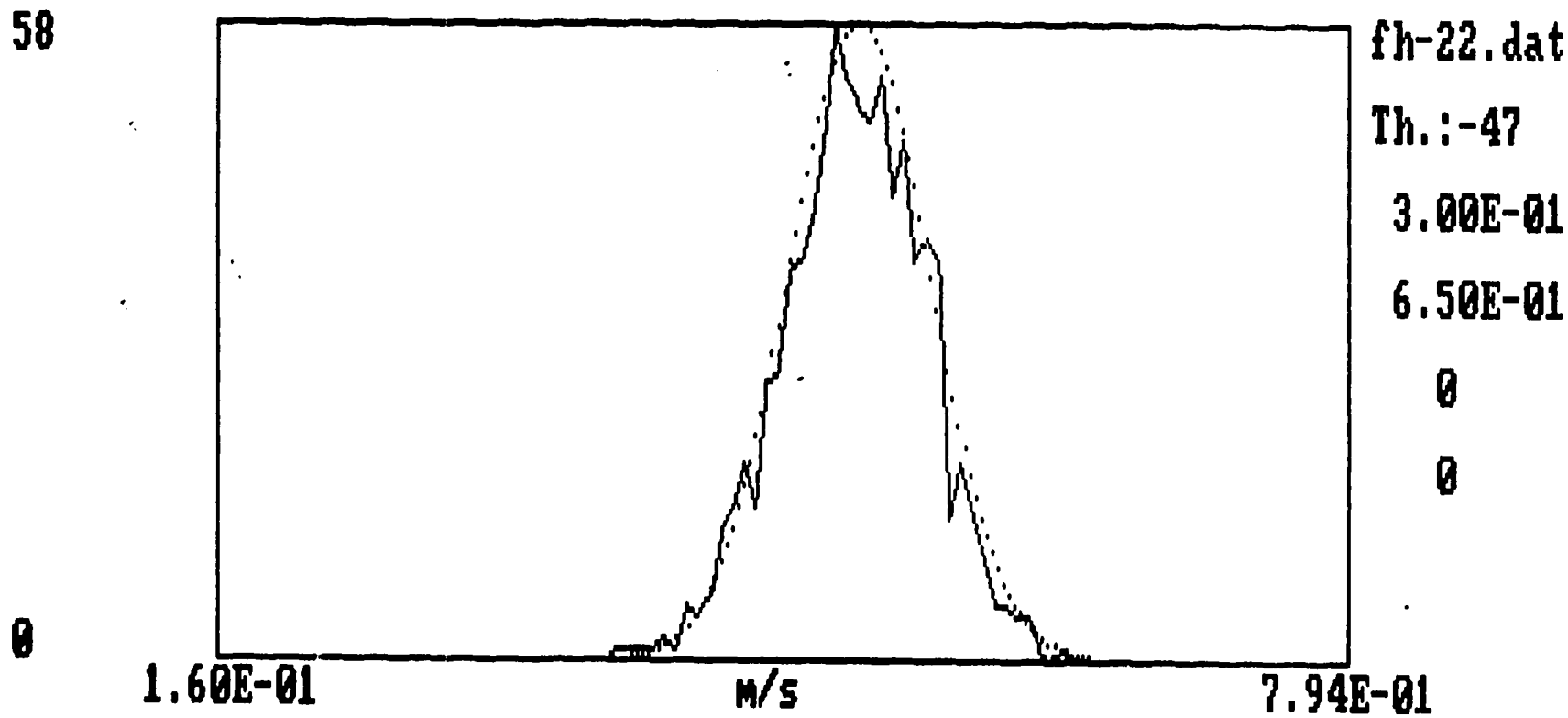

Velocity Distribution

Mean	: 5.191E-01 m/s	Dist. From Inlet	:	3.000E+01	cm
Stand. deviat.	: 3.981E-02 m/s	Radial Distance	:	1.000E+01	mm
Veloc. for max.	: 5.058E-01 m/s	Bulk velocity	:	5.160E-01	m/s
Skewness : -1.359E-01	Kurtosis : 2.980E+00	Re.	:	1.670E+04	

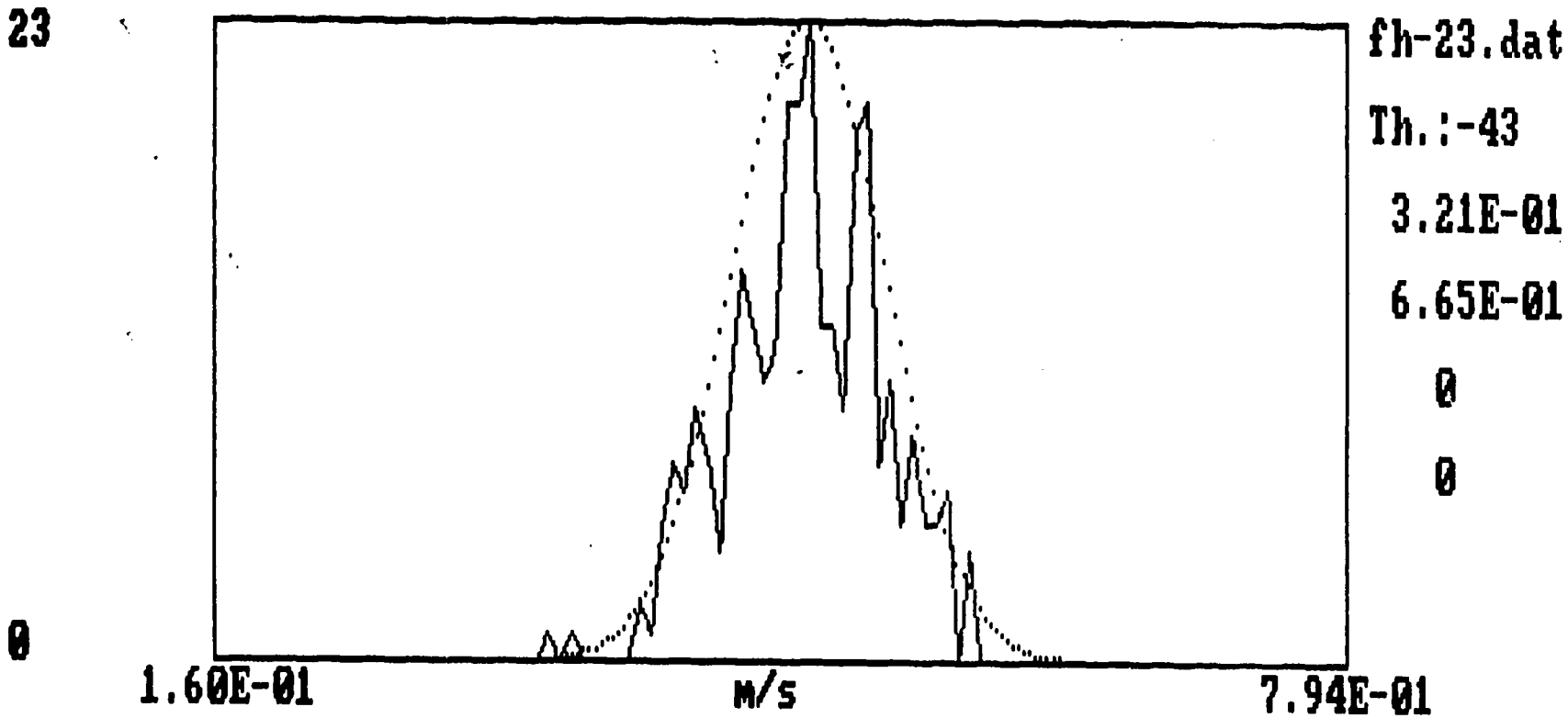

Velocity Distribution

Mean	: 4.922E-01 m/s	Dist. From Inlet	:	3.000E+01	cm
Stand. deviat.	: 4.312E-02 m/s	Radial Distance	:	1.200E+01	mm
Veloc. for max.	: 4.930E-01 m/s	Bulk velocity	:	5.160E-01	m/s
Skewness : -2.122E-01	Kurtosis : 2.818E+00	Re.	:	1.670E+04	

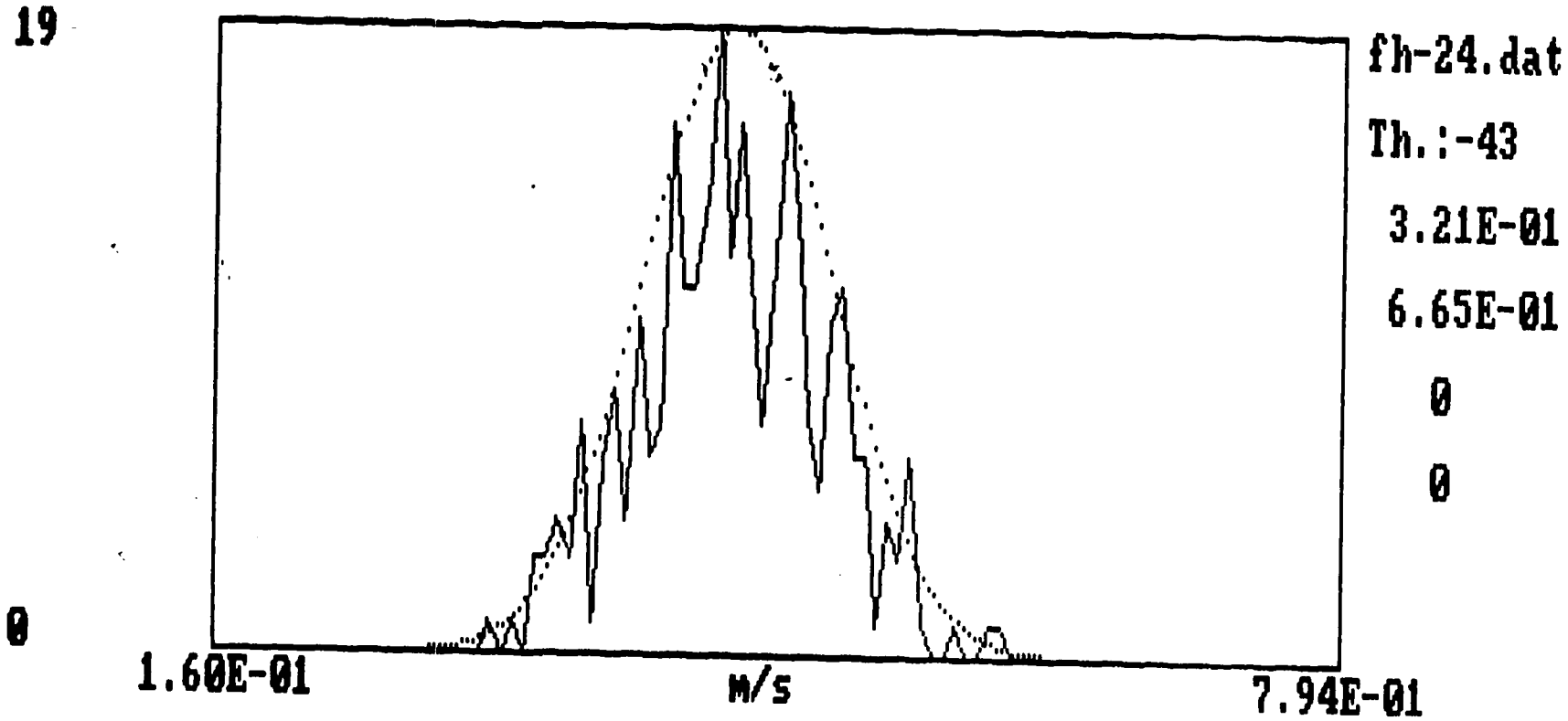

Velocity Distribution

Mean	: 4.527E-01 M/S	Dist. From Inlet		:	3.000E+01 CM
Stand. deviat.	: 5.286E-02 M/S	Radial Distance		:	1.400E+01 MM
Veloc. for max.	: 4.418E-01 M/S	Bulk velocity		:	5.160E-01 M/S
Skewness :	6.860E-03	Kurtosis :	2.752E+00	Re. :	1.670E+04

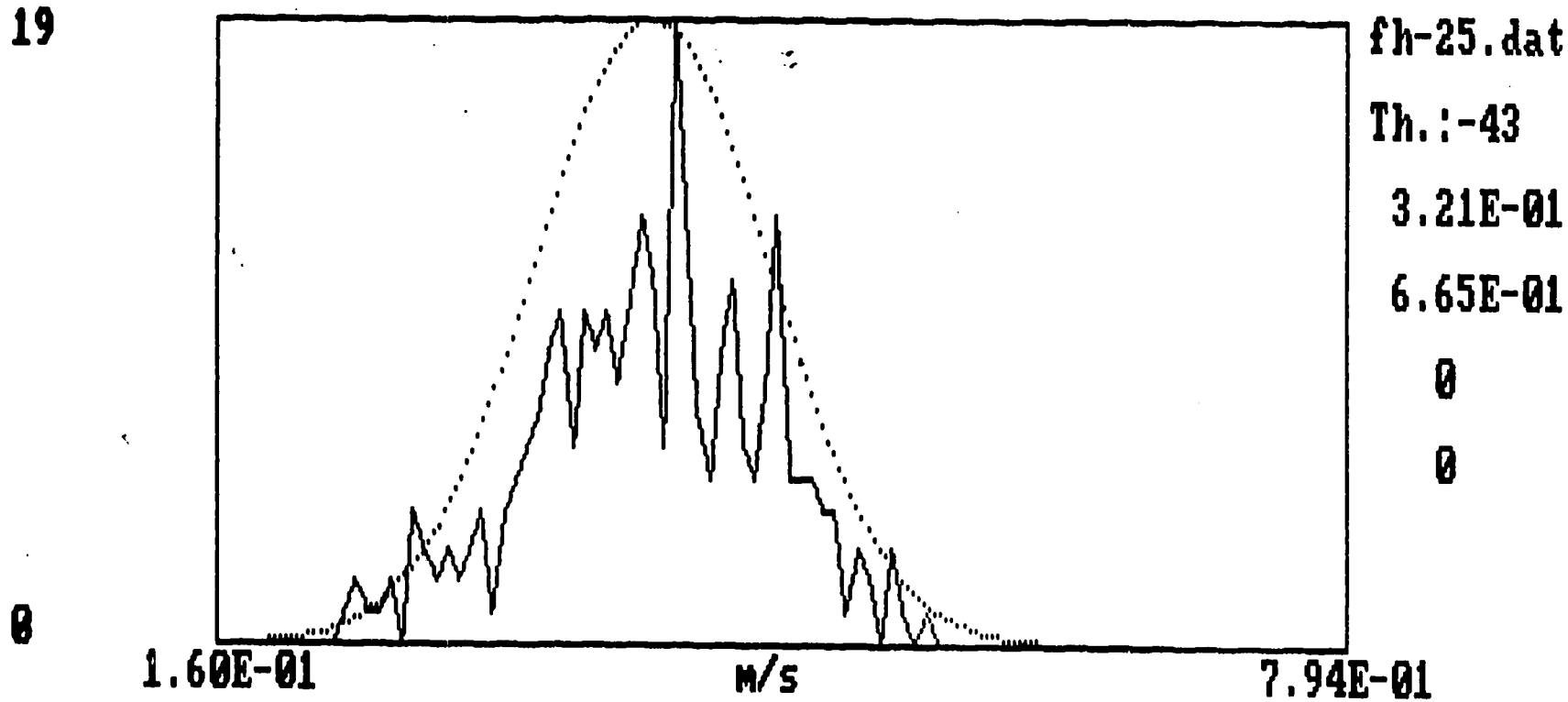

Velocity Distribution

Mean	: 4.037E-01 m/s	Dist. From Inlet	:	3.000E+01	cm
Stand. deviat.	: 6.611E-02 m/s	Radial Distance	:	1.500E+01	mm
Veloc. for max.	: 4.162E-01 m/s	Bulk velocity	:	5.160E-01	m/s
Skewness : -2.138E-01	Kurtosis : 2.696E+00	Re.	:	1.670E+04	

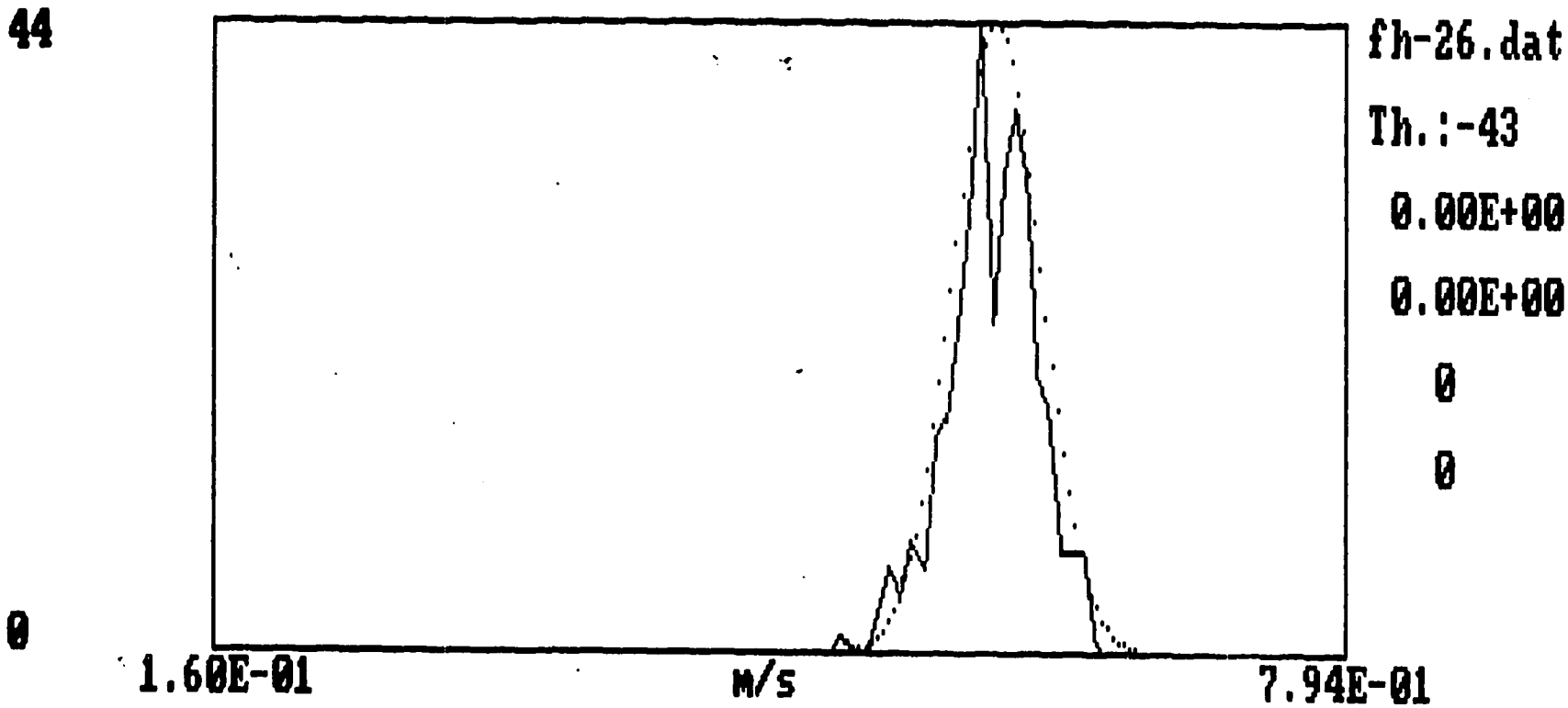

Velocity Distribution

Mean	: 5.980E-01 m/s	Dist. From Inlet		:	6.000E+01 cm
Stand. deviat.	: 2.471E-02 m/s	Radial Distance		:	0.000E+00 mm
Veloc. for max.	: 5.890E-01 m/s	Bulk velocity		:	5.160E-01 m/s
Skewness :	-3.183E-01	Kurtosis : 3.013E+00	Re.	:	1.670E+04

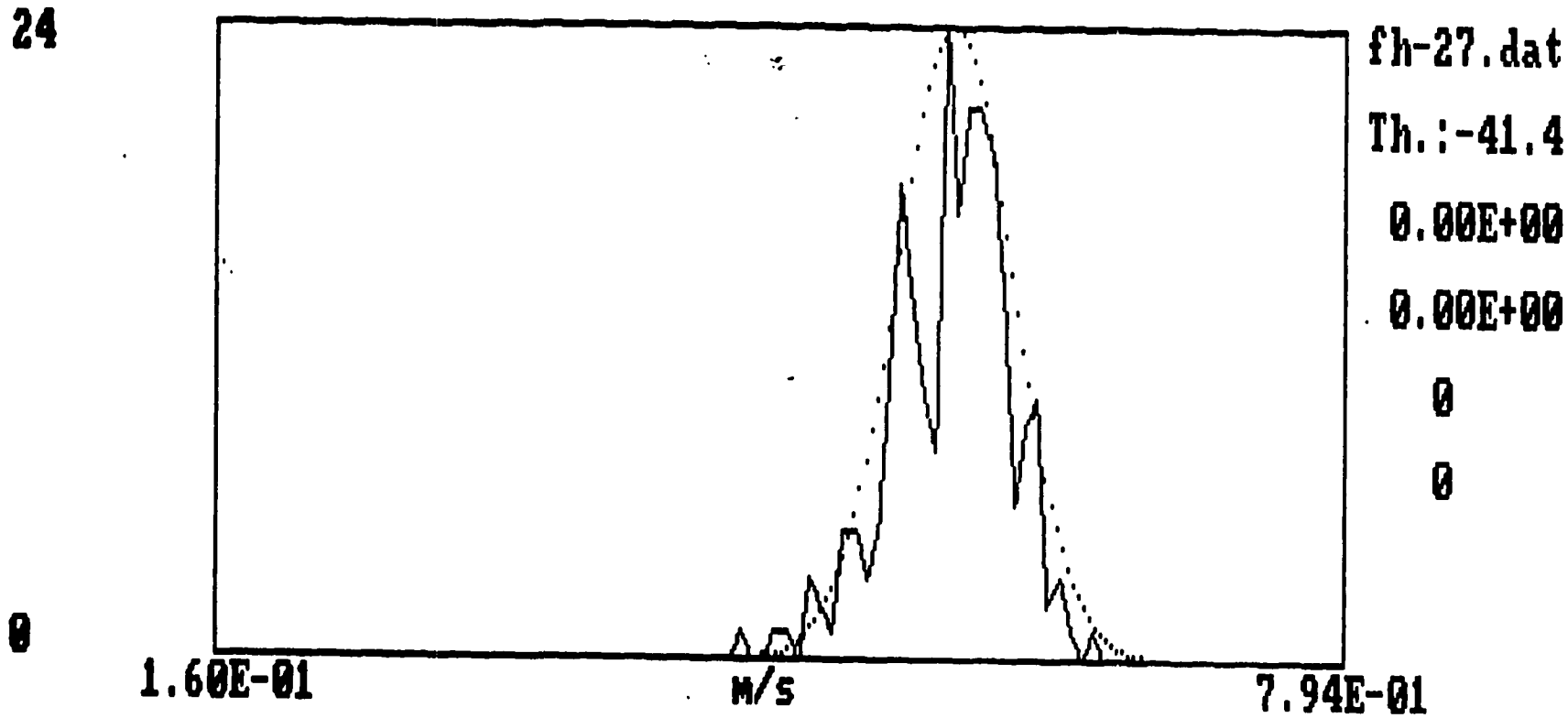

Velocity Distribution

Mean	: 5.743E-01 m/s	Dist. From Inlet	:	6.000E+01 cm
Stand. deviat.	: 3.298E-02 m/s	Radial Distance	:	5.000E+00 mm
Veloc. for max.	: 5.698E-01 m/s	Bulk velocity	:	5.160E-01 m/s
Skewness : -5.054E-01	Kurtosis : 3.344E+00	Re.	:	1.670E+04

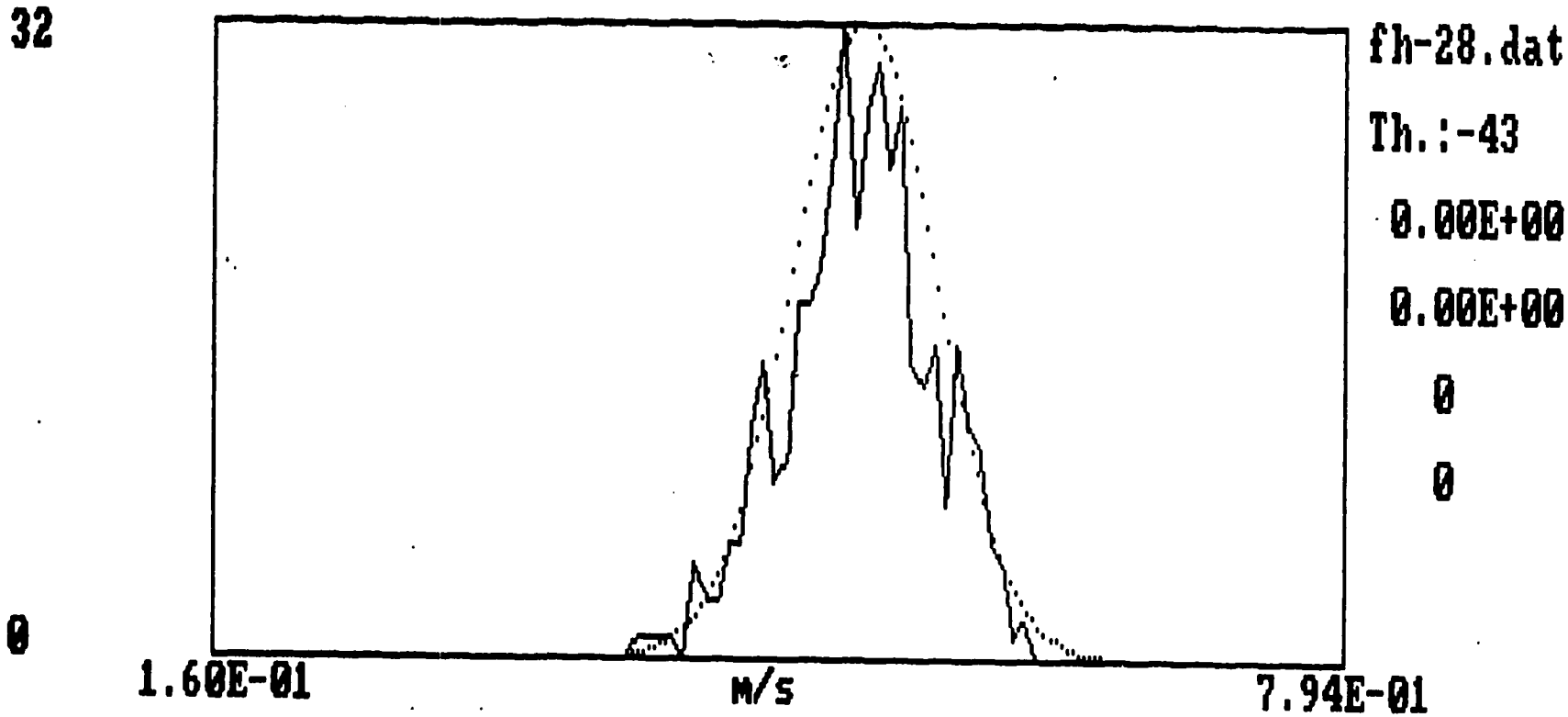

Velocity Distribution

Mean	: 5.238E-01 M/S	Dist. From Inlet		:	6.000E+01 CM
Stand. deviat.	: 4.101E-02 M/S	Radial Distance		:	1.000E+01 MM
Veloc. for max.	: 5.122E-01 M/S	Bulk velocity		:	5.160E-01 M/S
Skewness :	-2.051E-01	Kurtosis : 2.784E+00	Re.	:	1.670E+04

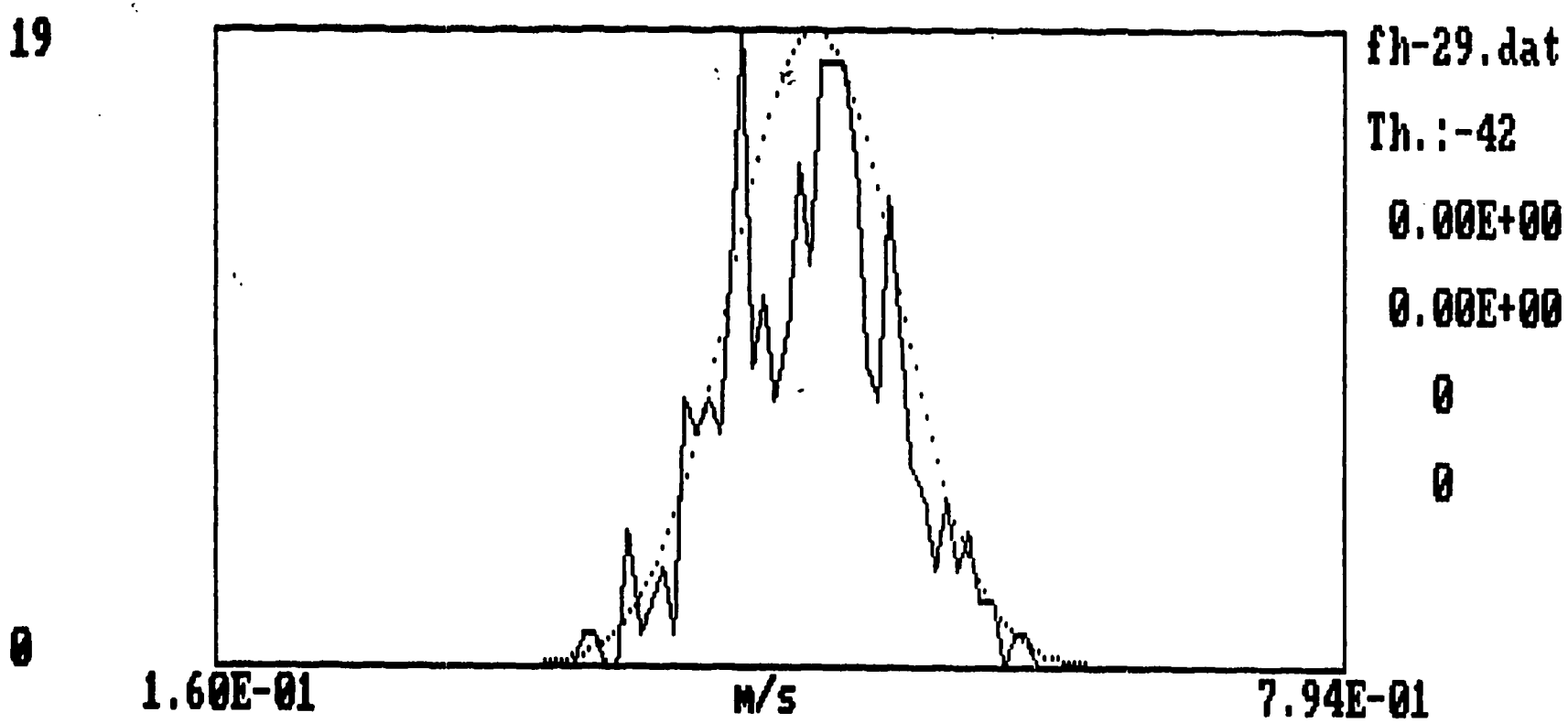

Velocity Distribution

Mean	: 4.957E-01 m/s	Dist. From Inlet	:	6.000E+01	cm
Stand. deviat.	: 4.660E-02 m/s	Radial Distance	:	1.200E+01	mm
Veloc. for max.	: 4.546E-01 m/s	Bulk velocity	:	5.160E-01	m/s
Skewness : -5.515E-02	Kurtosis : 2.694E+00	Re.	:	1.670E+04	

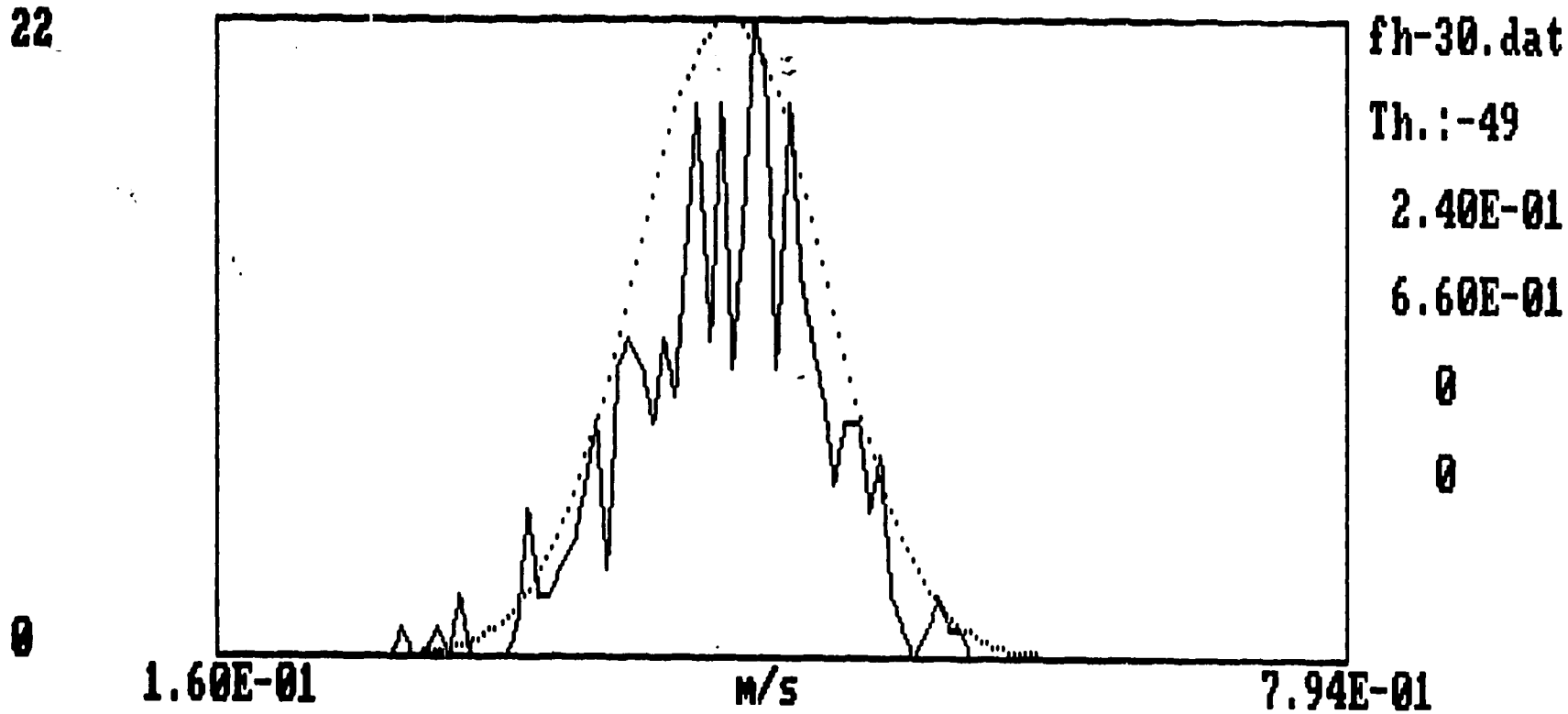

Velocity Distribution

Mean	: 4.469E-01 m/s	Dist. From Inlet	:	6.000E+01 cm	
Stand. deviat.	: 5.298E-02 m/s	Radial Distance	:	1.400E+01 mm	
Veloc. for max.	: 4.610E-01 m/s	Bulk velocity	:	5.160E-01 m/s	
Skewness : -3.434E-01	Kurtosis : 3.148E+00	Re.	:	1.670E+04	

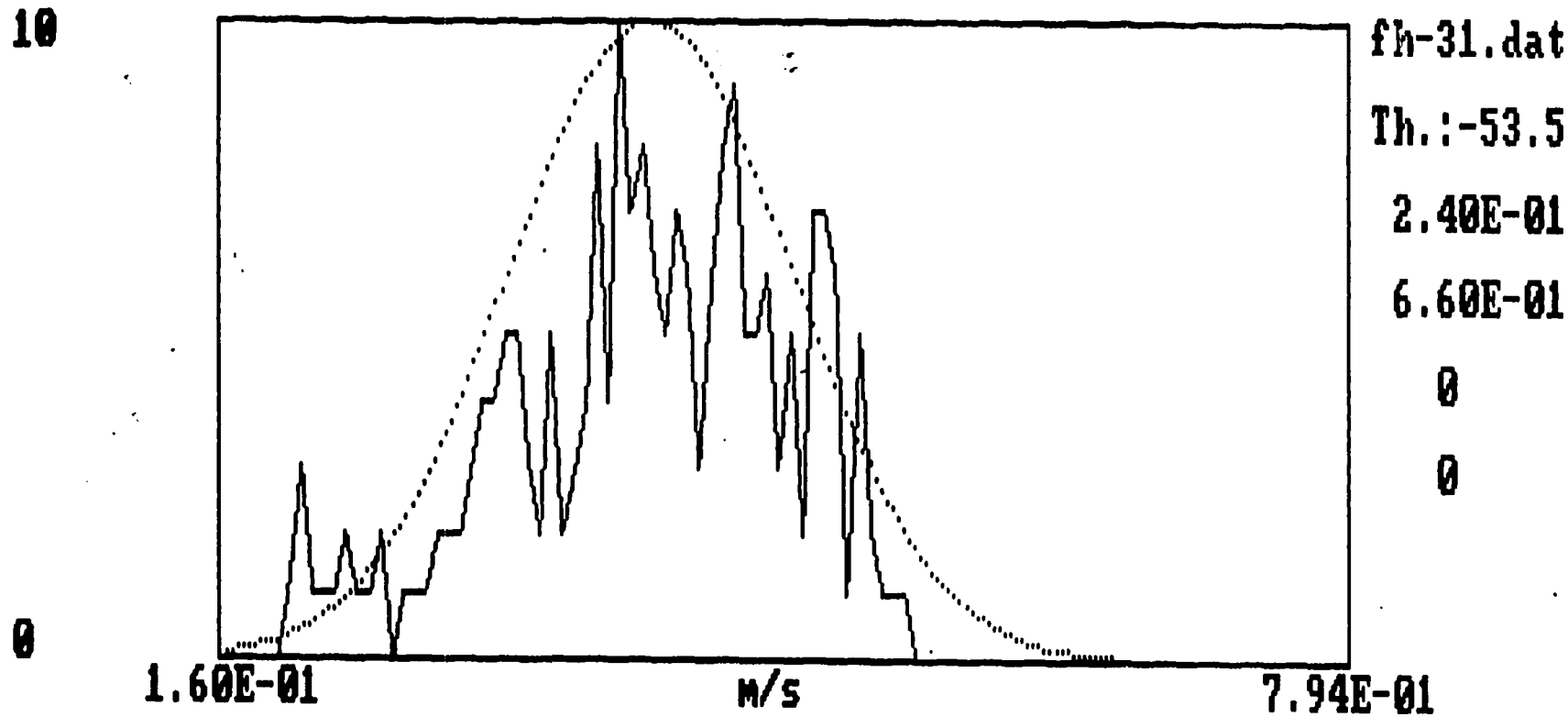

Velocity Distribution

Mean	: 4.020E-01 m/s	Dist. From Inlet		:	6.000E+01 cm
Stand. deviat.	: 7.945E-02 m/s	Radial Distance		:	1.600E+01 mm
Veloc. for max.	: 3.841E-01 m/s	Bulk velocity		:	5.160E-01 m/s
Skewness :	-4.838E-01	Kurtosis :	2.654E+00	Re. :	1.670E+04

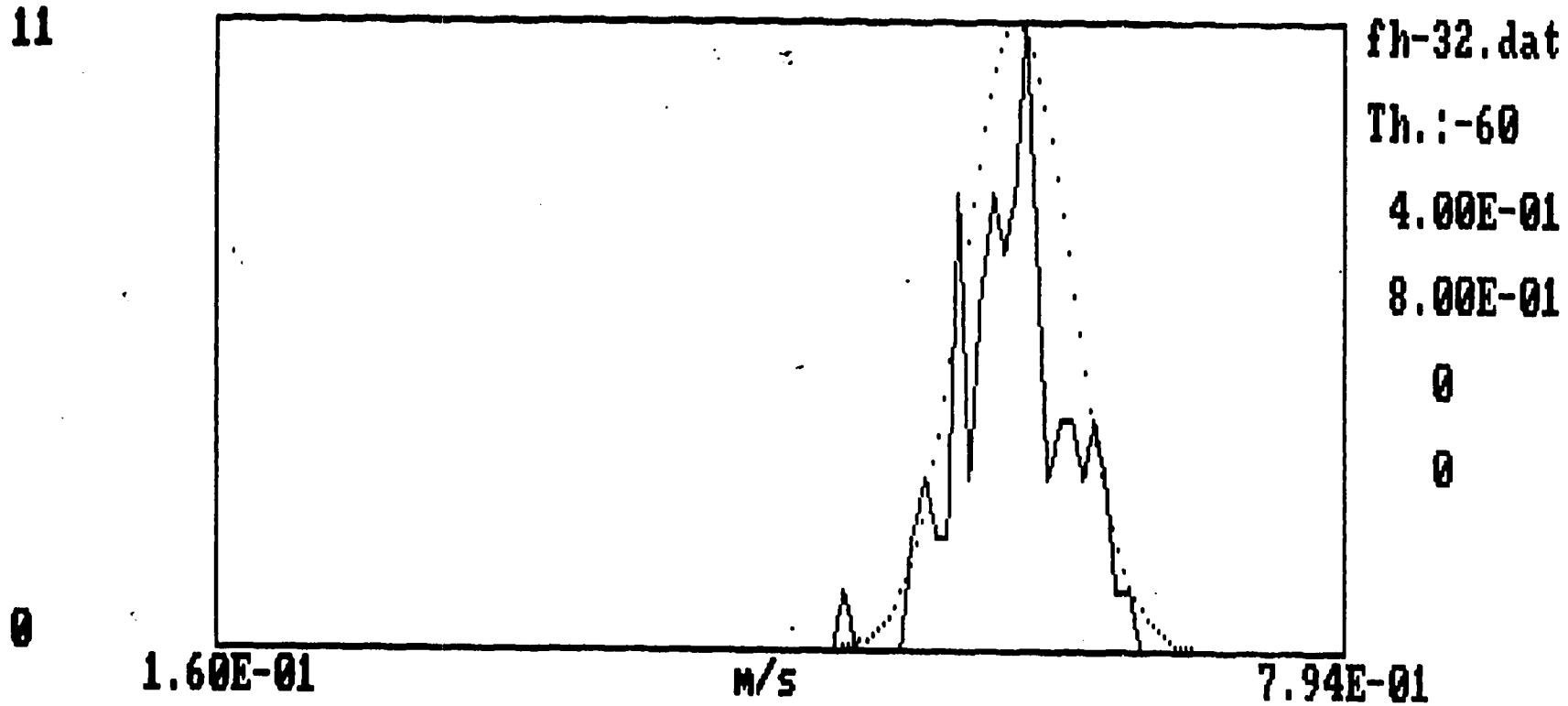

Velocity Distribution

Mean	: 6.096E-01 m/s	Dist. From Inlet		:	1.000E+02 cm
Stand. deviat.	: 3.015E-02 m/s	Radial Distance		:	0.000E+00 mm
Veloc. for max.	: 6.146E-01 m/s	Bulk velocity		:	5.160E-01 m/s
Skewness : -2.069E-01	Kurtosis : 3.077E+00		Re.	:	1.670E+04

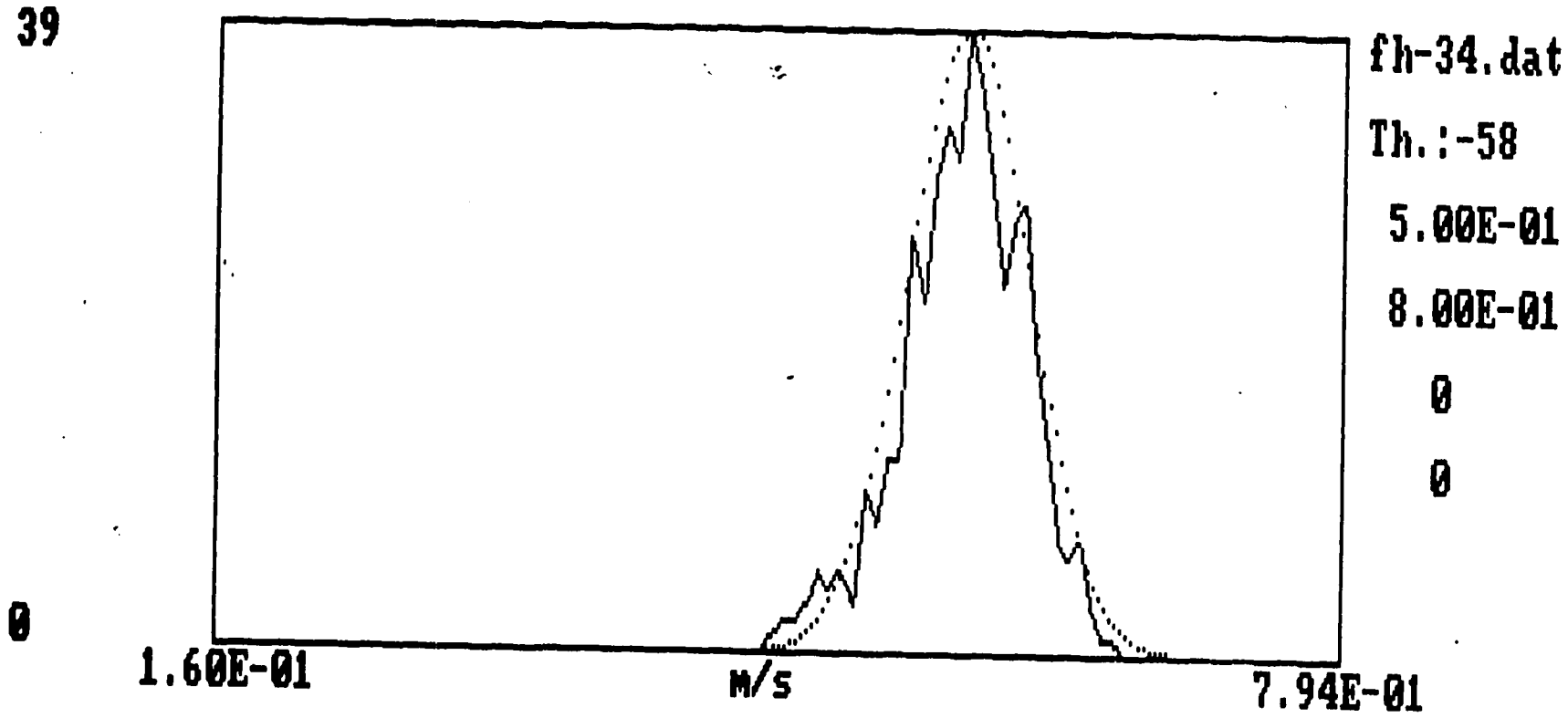

Velocity Distribution

Mean	: 5.827E-01 M/S	Dist. From Inlet		:	1.000E+02 CM
Stand. deviat.	: 3.455E-02 M/S	Radial Distance		:	5.000E+00 MM
Veloc. for max.	: 5.826E-01 M/S	Bulk velocity		:	5.160E-01 M/S
Skewness : -3.665E-01	Kurtosis : 3.150E+00		Re.	:	1.670E+04

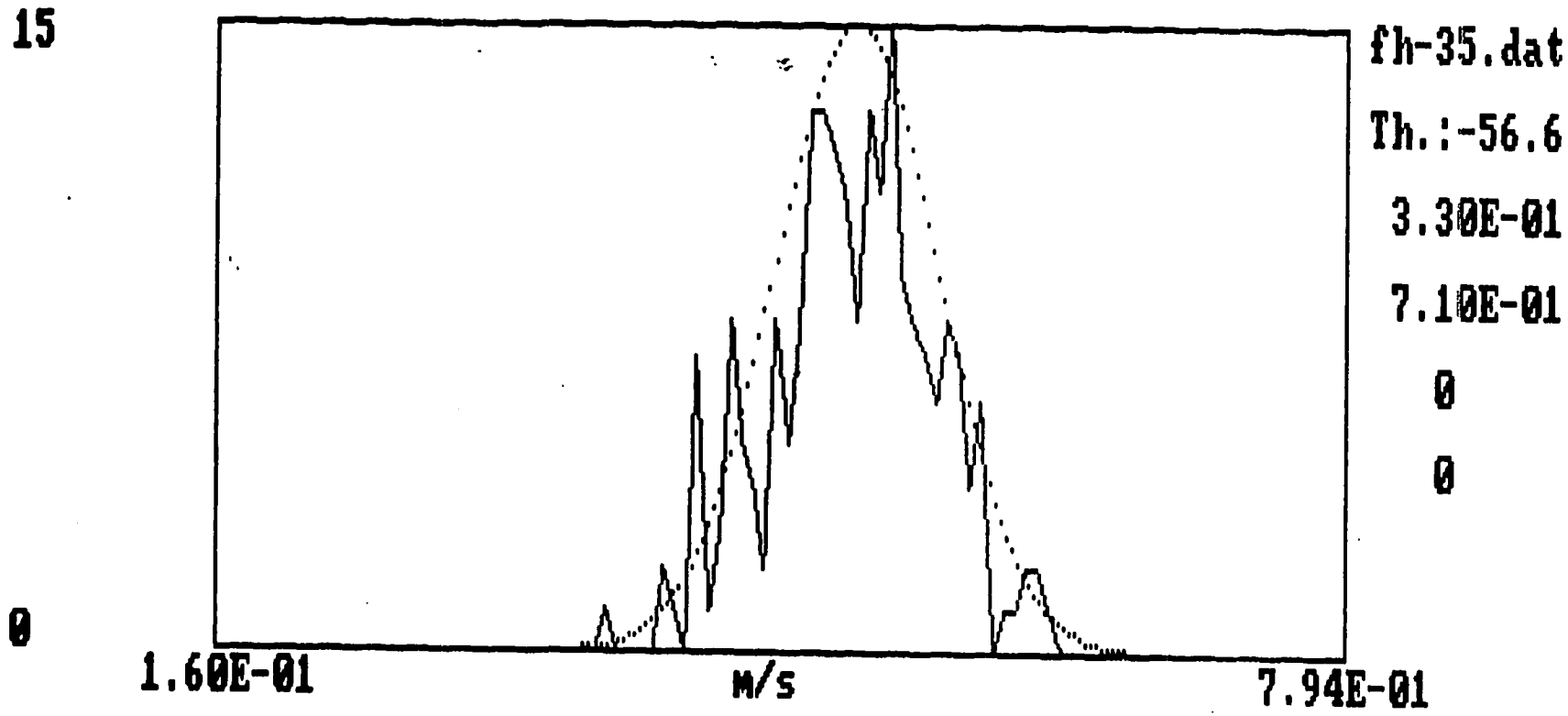

Velocity Distribution

Mean	: 5.188E-01 m/s	Dist. From Inlet		:	1.000E+02 cm
Stand. deviat.	: 4.656E-02 m/s	Radial Distance		:	1.000E+01 mm
Veloc. for max.	: 5.378E-01 m/s	Bulk velocity		:	5.160E-01 m/s
Skewness :	-1.553E-01	Kurtosis :	2.774E+00	Re. :	1.670E+04

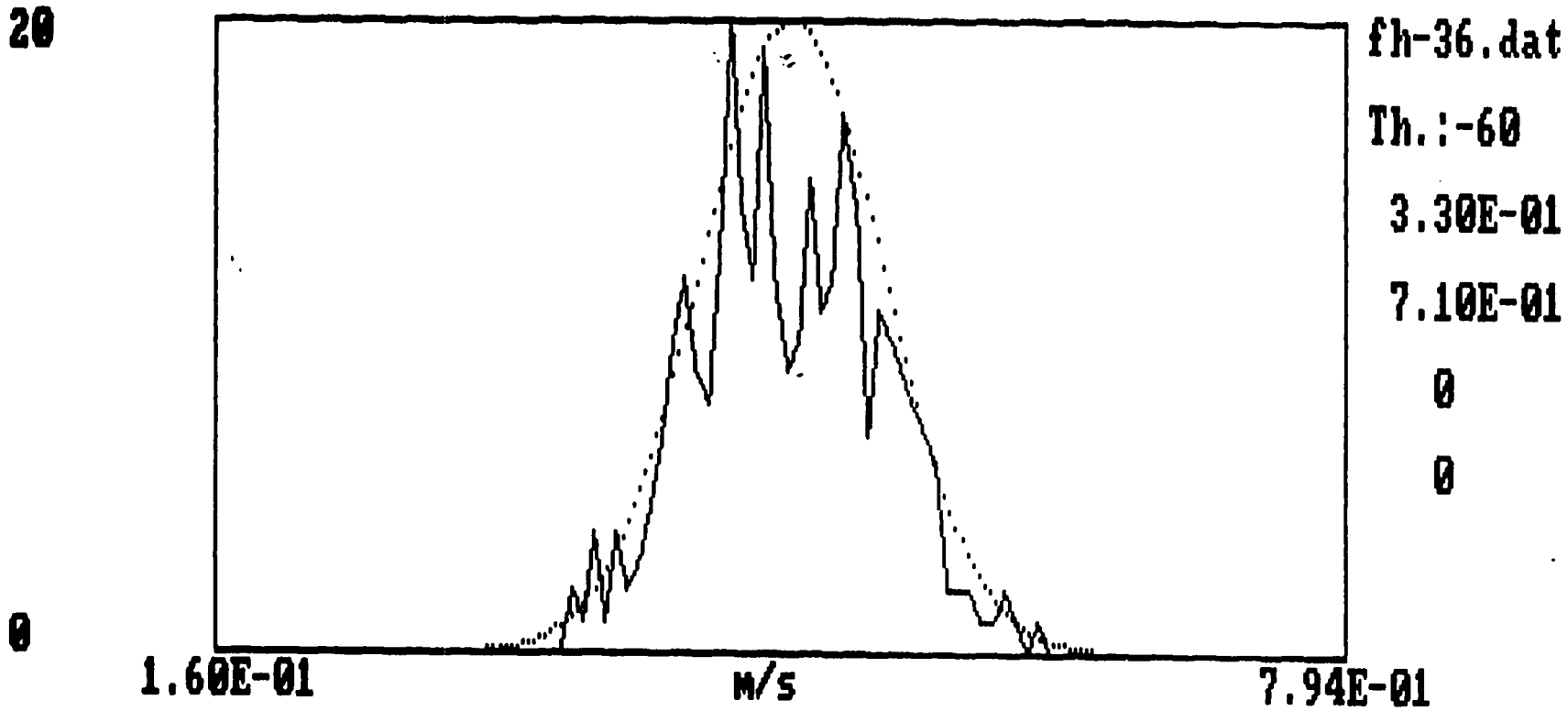

Velocity Distribution

Mean	: 4.829E-01 m/s	Dist. From Inlet	:	1.000E+02 cm
Stand. deviat.	: 5.208E-02 m/s	Radial Distance	:	1.200E+01 mm
Veloc. for max.	: 4.482E-01 m/s	Bulk velocity	:	5.160E-01 m/s
Skewness : 5.467E-02	Kurtosis : 2.488E+00	Re.	:	1.670E+04

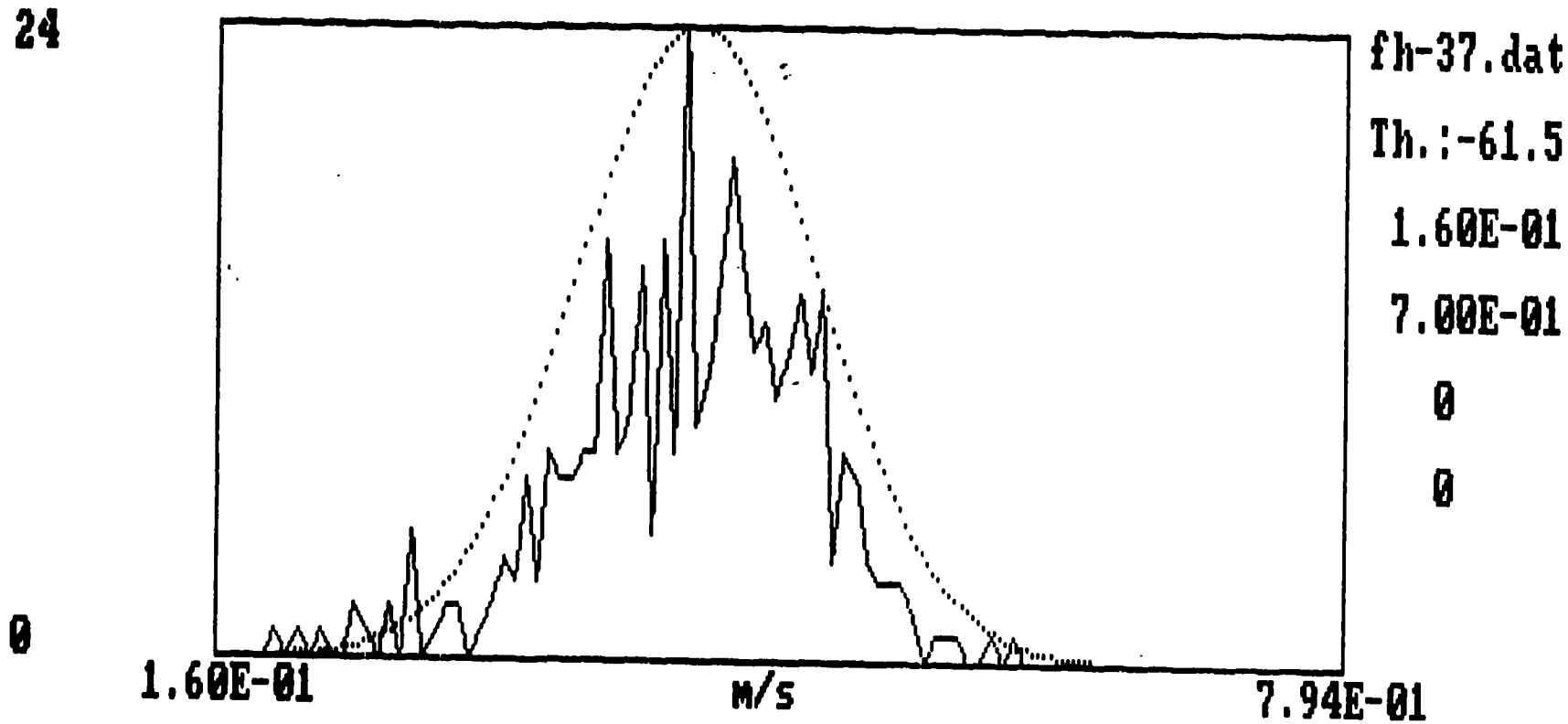

Velocity Distribution

Mean	: 4.287E-01 m/s	Dist. From Inlet		:	1.000E+02 cm
Stand. deviat.	: 6.837E-02 m/s	Radial Distance		:	1.500E+01 mm
Veloc. for max.	: 4.226E-01 m/s	Bulk velocity		:	5.160E-01 m/s
Skewness :	-5.102E-01	Kurtosis :	3.502E+00	Re. :	1.670E+04

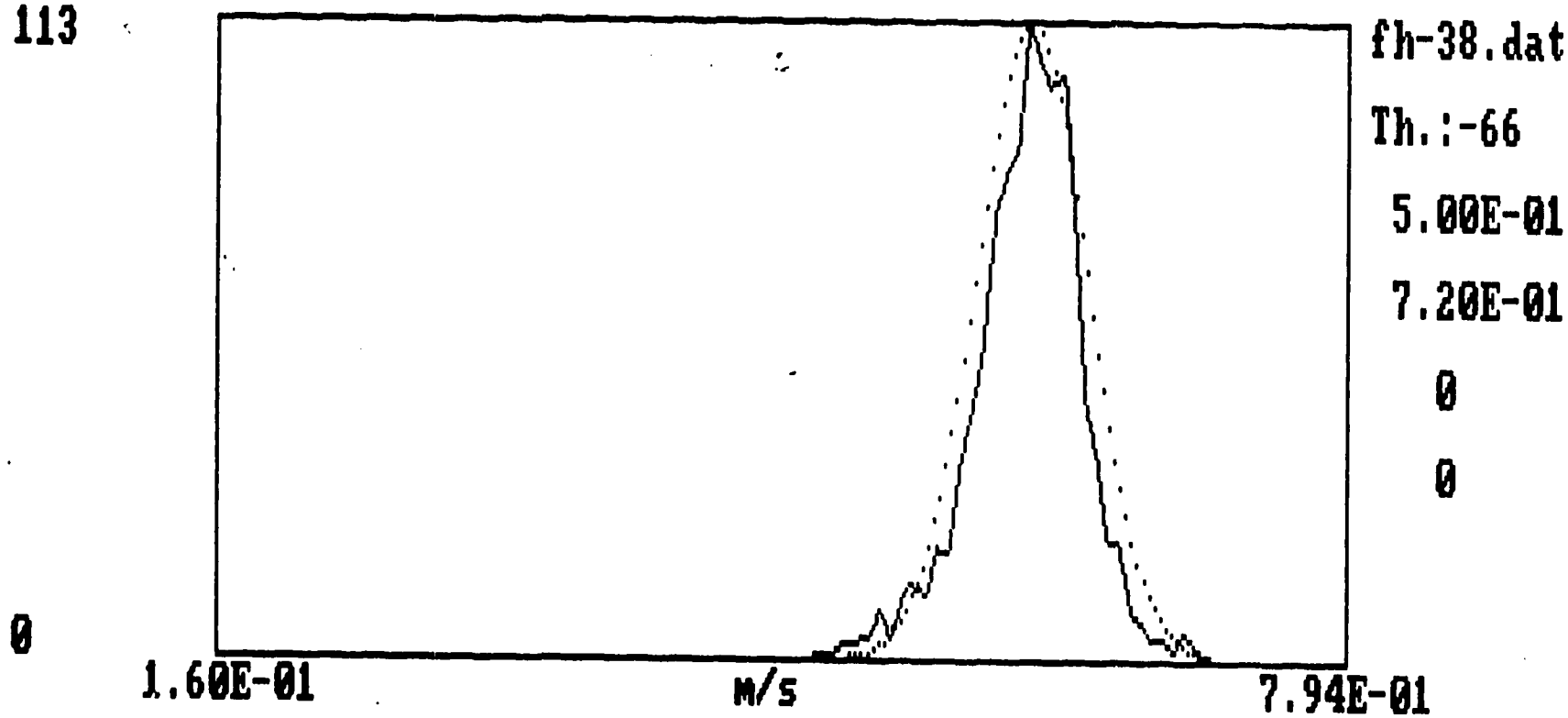

Velocity Distribution

Mean	: 6.168E-01 m/s	Dist. From Inlet		:	1.500E+02 cm
Stand. deviat.	: 3.110E-02 m/s	Radial Distance		:	0.000E+00 mm
Veloc. for max.	: 6.146E-01 m/s	Bulk velocity		:	5.160E-01 m/s
Skewness :	-3.409E-01	Kurtosis :	3.975E+00	Re. :	1.670E+04

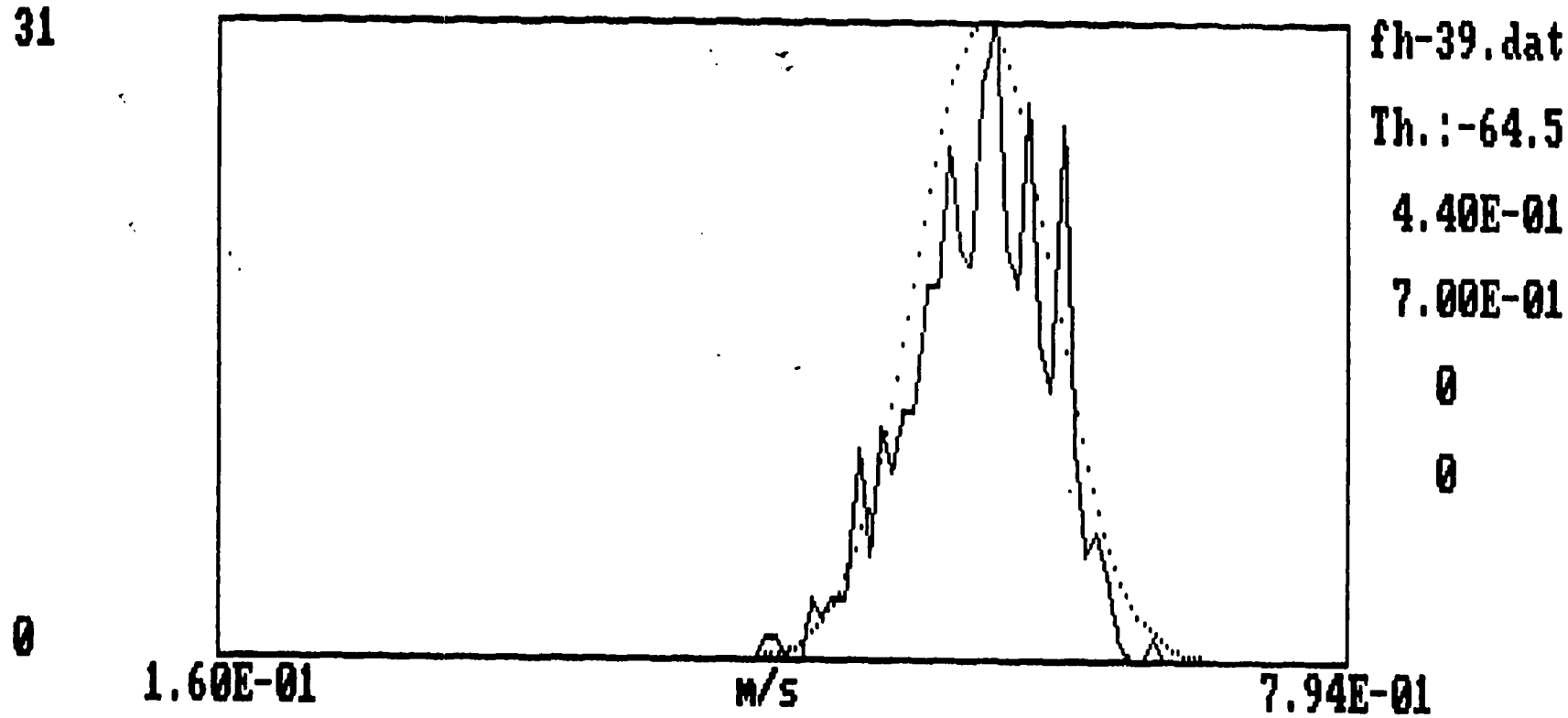

Velocity Distribution

Mean	: 5.893E-01 m/s	Dist. From Inlet	:	1.500E+02 cm	
Stand. deviat.	: 3.805E-02 m/s	Radial Distance	:	5.000E+00 mm	
Veloc. for max.	: 5.954E-01 m/s	Bulk velocity	:	5.160E-01 m/s	
Skewness : -3.108E-01	Kurtosis : 2.773E+00	Re.	:	1.670E+04	

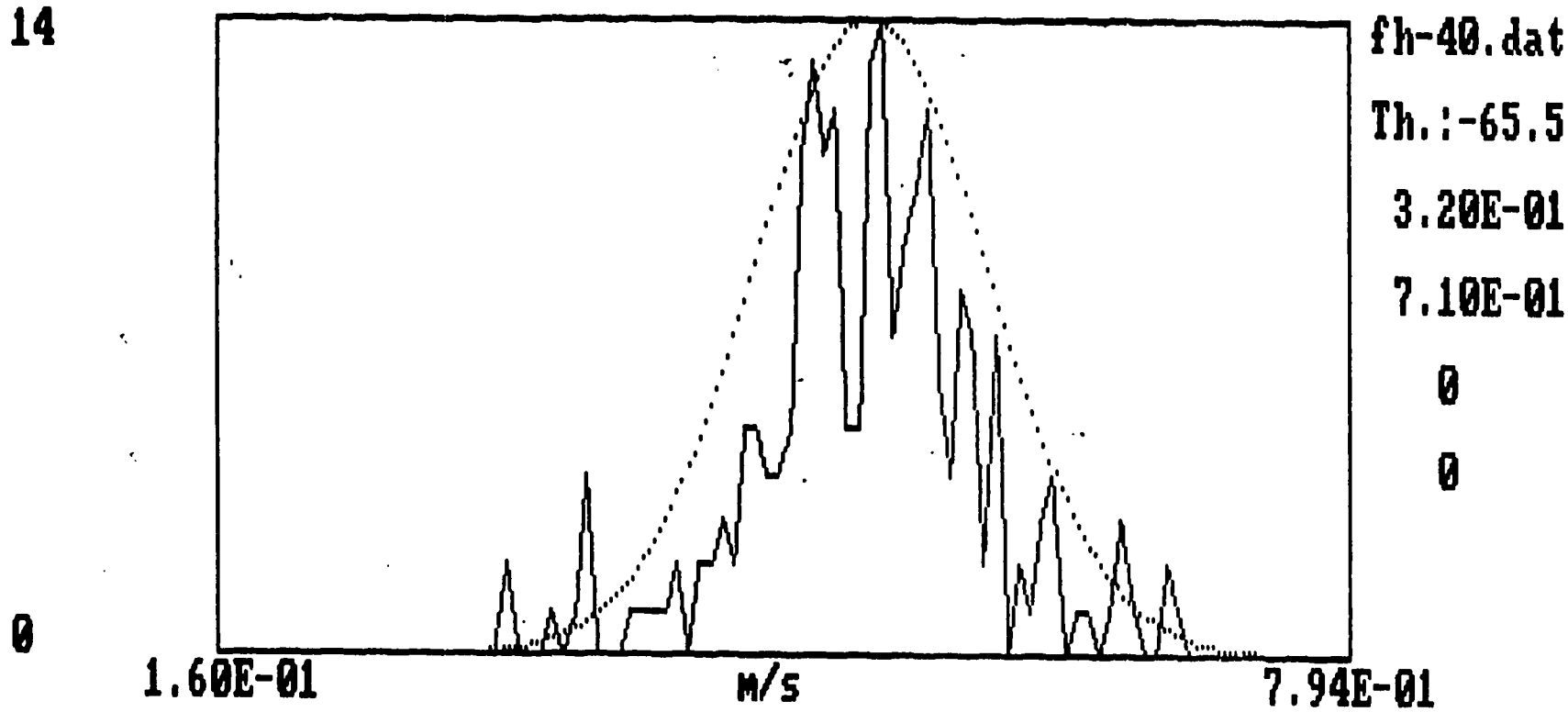

Velocity Distribution

Mean	: 5.255E-01 m/s	Dist. From Inlet		:	1.500E+02 cm
Stand. deviat.	: 6.561E-02 m/s	Radial Distance		:	1.000E+01 mm
Veloc. for max.	: 5.314E-01 m/s	Bulk velocity		:	5.160E-01 m/s
Skewness :	-2.204E-01	Kurtosis :	3.873E+00	Re. :	1.670E+04

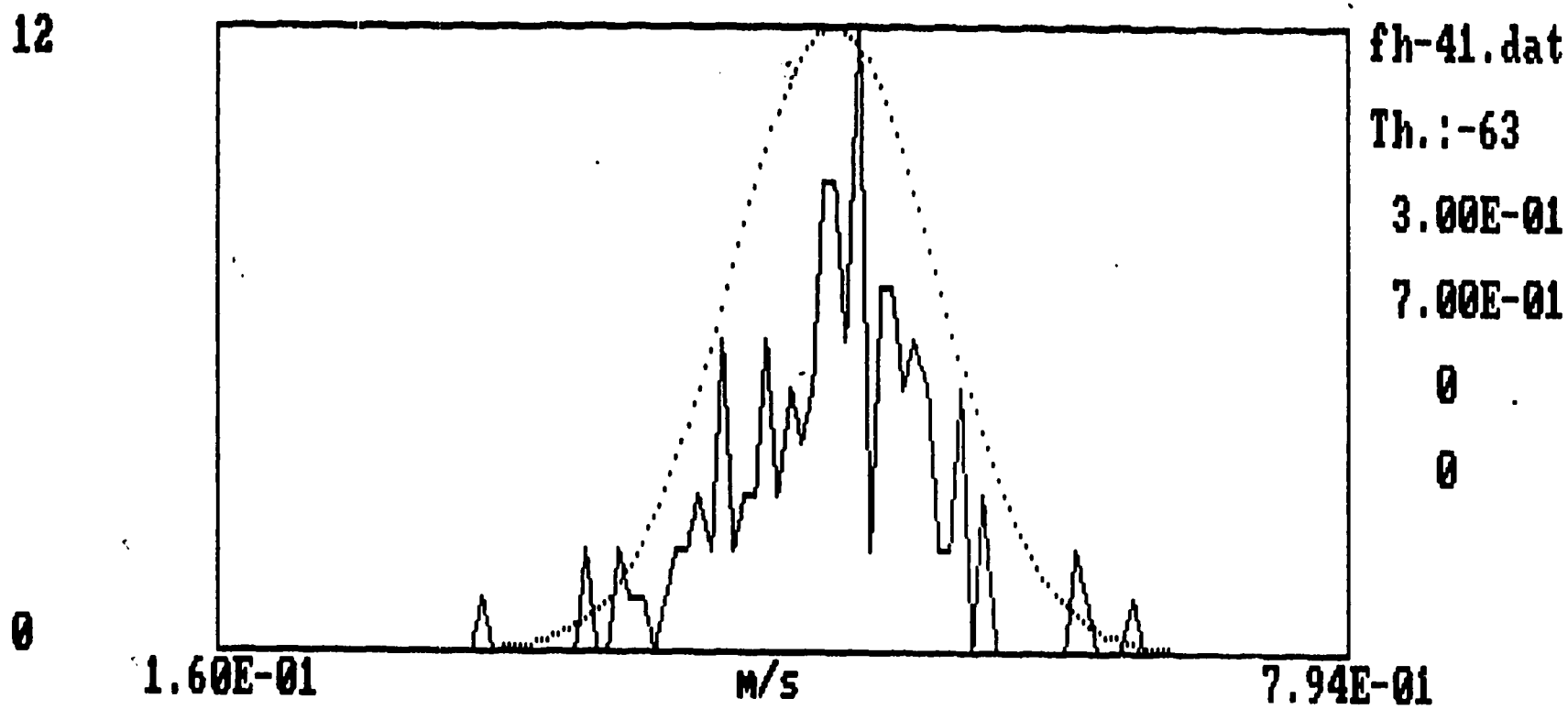

Velocity Distribution

Mean	: 5.051E-01 m/s	Dist. From Inlet	:	1.500E+02 cm	
Stand. deviat.	: 5.740E-02 m/s	Radial Distance	:	1.200E+01 mm	
Veloc. for max.	: 5.186E-01 m/s	Bulk velocity	:	5.160E-01 m/s	
Skewness : -2.493E-01	Kurtosis : 3.882E+00	Re.	:	1.670E+04	

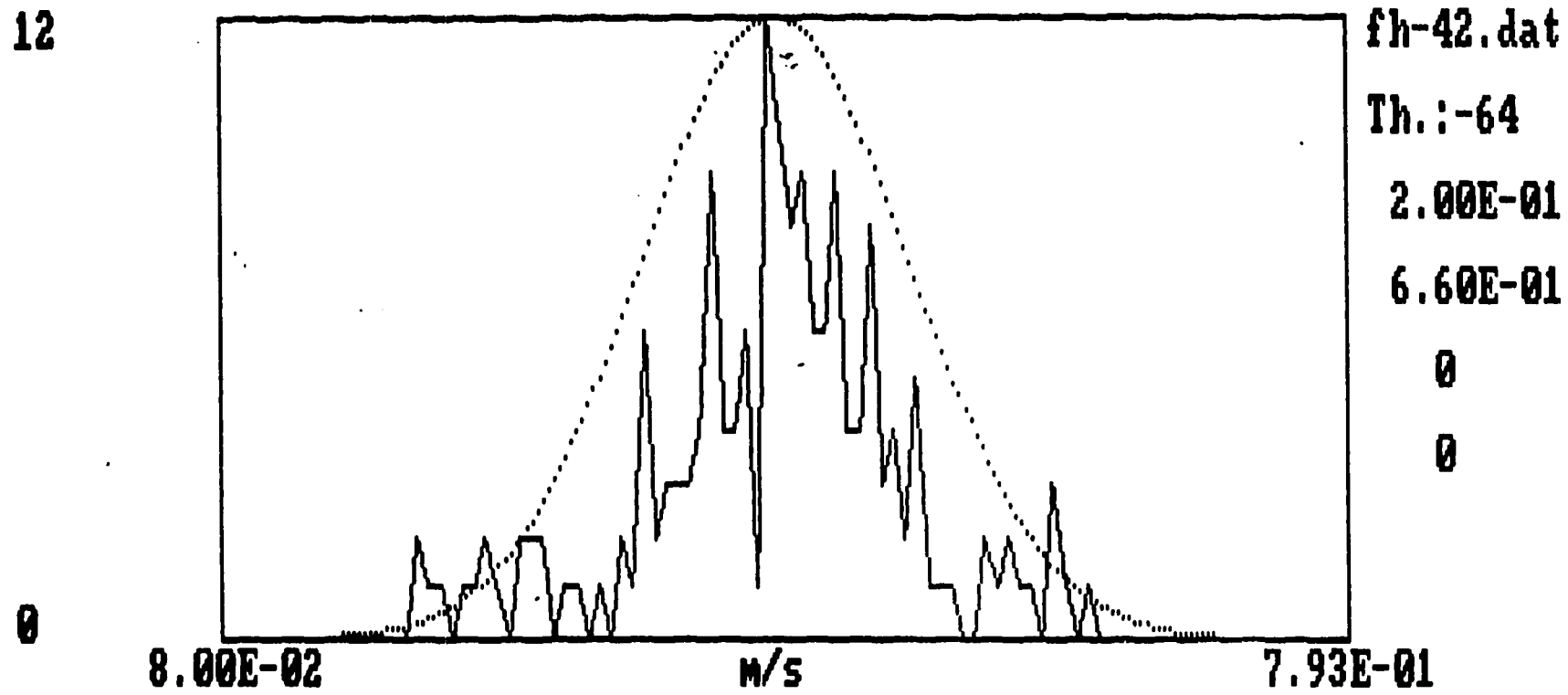

Velocity Distribution

Mean	: 4.306E-01 m/s	Dist. From Inlet	:	1.500E+02 cm	
Stand. deviat.	: 8.492E-02 m/s	Radial Distance	:	1.400E+01 mm	
Veloc. for max.	: 4.258E-01 m/s	Bulk velocity	:	5.160E-01 m/s	
Skewness : -3.951E-01	Kurtosis : 3.444E+00	Re.	:	1.670E+04	

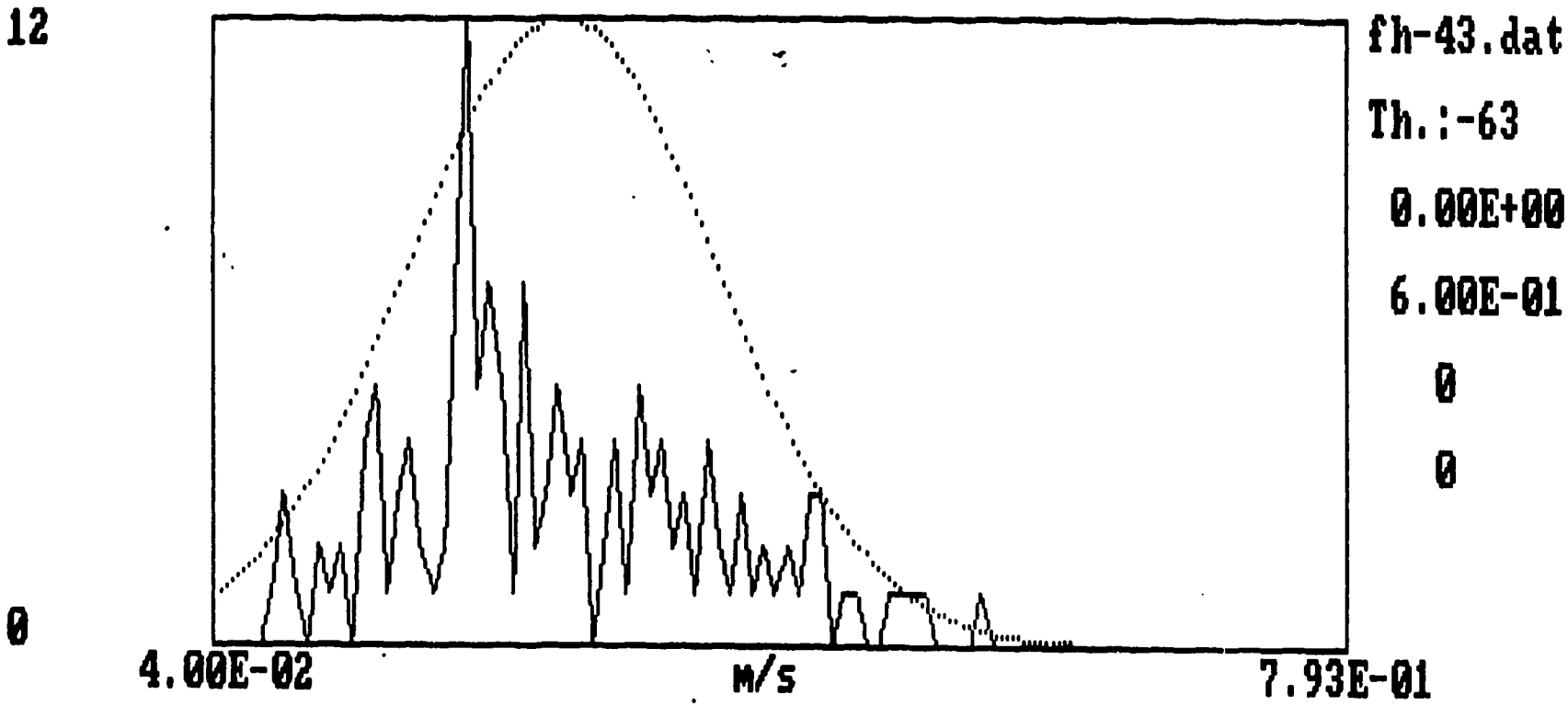

Velocity Distribution

Mean	: 2.715E-01 m/s	Dist. From Inlet	:	1.500E+02	cm
Stand. deviat.	: 1.033E-01 m/s	Radial Distance	:	1.500E+01	mm
Veloc. for max.	: 2.073E-01 m/s	Bulk velocity	:	5.160E-01	m/s
Skewness : 4.544E-01	Kurtosis : 2.556E+00	Re.	:	1.670E+04	

REFERENCES

1. Benidict, R., ***Fundamentals Of Pipe Flow*** , John Wiley & Sons, New York (1980)
2. Schiller, V. L., and H. Kirsten, ***E. Tech. Phys.*** , Vol. 10, 1929, pp. 268-274
3. Nikurdse J., ***Gesetzmassigkeit der turbulenten Stromung in glatten Rohern*** , Forschg. Arb. Ing.-Wes. No. 356 (1932).
4. Latsko, H. E., ***Heat transfer in a turbulent liquid or gas stream*** , NACA TM 1068, October 1944
5. Barbin A. R., and J. B. Jones, ***Turbulent flow in the inlet region of a smooth pipe*** , ASME Trans. J. Basic Eng., Vol. 85, n1, 1973, pp 29-34.
6. Bowlus, D. A. and J. A. Brighton, ***Incompressible turbulent flow in the inlet region of pipe*** , J. of Basic Eng., Trans. ASME, September 1968, pp. 431-433.
7. Wang, J., ***Turbulent flow in a pipe inlet region*** , Ph.D. dissertation, Colorado State University, 1972.
8. Klein, A., ***Review of turbulent developing pipe flow*** , ASME J. Fluid Eng., Vol. 103, n. 2, 1981, pp. 243-249.
9. Salami, L., A., ***An Investigation of turbulent developing flow at the entrance to a smooth pipe*** , Int. J. Heat & Fluid Flow, Vol. 7, n 4, 1986, pp. 247-256.
10. Janna, W., S., ***Introduction To Fluid Mechanics*** , PWS Publishers, 2nd ed., Boston (1987).

11. Schlichting, H., ***Boundary Layer Theory*** , McGraw-Hill, 7th ed., New York (1979).

12. Narasimha, R., and K. R. Sreenivasan, ***Relaminarization of fluid flows*** , Adv. Appl. Mech., Vol. 19, 1979, pp. 221-309.

13. Laufer, J., ***Decay of non-isotropic turbulent field*** in "Miszellaneen de angewandte Mechanik, Festschrift Walter Tollmein", Academie-Verlag, Berlin (1962).

14. Sibulkin, M., ***Transition from turbulent to laminar flow*** , Phys. Fluids, Vol. 5, n 3, 1962, pp. 280-284.

15. Patel, V. C., and M. R. Head, ***Reversion of turbulent to laminar flow*** , J. Fluid Mech., Vol. 34, 1968, pp. 371-391.

16. Badri Nrarayanan, M. A., ***An experimental study of reverse transition in a two dimensional channel flow*** , J. Fluid Mech., Vol. 31, 1968, pp. 609-623.

17. Sreenivasan, K. R., ***Laminarscent, relaminarizing and retranslational flows*** , Acta Mechanica, Vol. 44, 1982, pp. 1-48.

18. Laser Velocimeter Techniques, Technical Data, TSI Inc., St. Paul, USA.

19. Yeh, Y., and H. Z. Cummins, ***Localized fluid flow measurements with an He-Ne Laser Spectrometer*** , J. Applied Physics Letters, Vol 4, n 10, 1964, pp 176-178.

20. Rudd, M. J., ***A new theoretical model for laser dopplermeter*** , J. Phys. E., Vol. 2, 1969, pp. 55-58.

21. Drain, L., ***The Laser Doppler Technique*** , John Wiley & Sons, Chichester 1981.

22. Durst, F. , E. Melling and J. Whitelaw, ***Principles And Practice of Laser Doppler Anemometry*** , Academic Press, 2nd ed., London 1981.

23. Durst, F. and J. H. Whitelaw, ***Optimization of optical anemometers*** , Proc. Roy. Soc., Vol. A 324, 1971, pp. 157-181.

24. Stevenson, W. ***Laser Doppler Velocimetry : A status report*** , Proceedings of the IEEE, Vol 70, n 6, 1982, pp 652-658.

25. Emrich, R. J. (Editor), ***Methods Of Experimental Physics*** , Vol 18, Part A, Fluid Dynamics, Academic Press, New York 1981.

26. U. K. A. Klein, F. A. Jamjoom, H. A. Al-Juwair , I. Oksuz, R. Stuff and A. A. Al-Suwayyan, ***Molecular Approach To Laminar-Turbulent Transition of Flow By Laser Technique*** , Final Report, KACST Project N0. AR-7-156, 1989.

27. Miller, D., ***Performance of straight diffusers*** , Part II of "Internal Flow. A guide to Losses in Pipe and Duct Systems", B.H.R.A.-Fluid Engineering, Cranfield/Bedford, 1971.

28. Cockrell, D. J. and E. Markland, ***The effect of inlet conditions on incompressible fluid flow through conical diffusers*** , J. Roy. Aeronautical Soc., Vol. 66, n 1, 1962, pp. 51-52.

29. Senecal, V. E. and R. R. Ruthfus, ***Transition flow of fluids in smooth tubes*** , Chem. Eng. Prog., Vol. 49, n 10, 1953, pp. 533-538.

30. Press, W. H., B. P. Flannery, S. A. Teukolsky and W. T. Vetterling, ***Numerical Recipes: The Art of Scientific Computing*** , Cambridge Univ. Press, Cambridge U.K., 1986.

31. Ribeiro, M. M. and J. H. Whitelaw, ***Statistical characteristics of a turbulent jet***, J. Fluid Mech., Vol. 70, 1975, pp. 1-15.